University of Alberta

Insights into the Transcriptional Regulation and Physiological Importance of Phosphatidylethanolamine *N*-Methyltransferase

by

Laura Kathleen Cole

A thesis submitted to the Faculty of Graduate Studies and Research
in partial fulfillment of the requirements for the degree of

Doctor of Philosophy

Department of Biochemistry

Spring 2010
Edmonton, Alberta

Examining Committee

Dennis E. Vance, Biochemistry

Jason R.B. Dyck, Pediatrics/Pharmacology

Rosaline Godbout, Oncology/Biochemistry

Michael C. Schultz, Biochemistry

Hei Sook Sul, Nutritional Science and Toxicology, University of California, Berkley, CA

DEDICATION

To my parents Ron and Bonnie Cole

and my husband Vern Dolinsky

ABSTRACT

Phosphatidylcholine (PC) is made in all nucleated mammalian cells via the CDP-choline pathway. Another major pathway for PC biosynthesis in liver is catalyzed by phosphatidylethanolamine *N*-methyltransferase (PEMT). We have identified 3T3-L1 adipocytes as a cell culture model that expresses PEMT endogenously. Analysis of the proximal PEMT promoter in 3T3-L1 adipocytes revealed an important regulatory region. Sp1 binds to a GC-rich site within this section of the promoter and inhibits PEMT transcriptional activity. Tamoxifen is an anti-estrogen drug widely used for the treatment of hormone-responsive breast cancer but has a frequent side-effect of increasing accumulation of lipid in the liver (hepatic steatosis). Tamoxifen represses PEMT gene expression by promoting Sp1 binding to the promoter. However, decreased catalytic activity of PEMT was not a major initial contributor to tamoxifen-mediated hepatic steatosis. We found that increased *de novo* fatty acid synthesis is the primary event which leads to tamoxifen-induced steatosis in mouse liver. Tamoxifen did not significantly alter hepatic fatty acid uptake, triacylglycerol secretion or fatty acid oxidation. Finally, we provide evidence that deletion of the PEMT gene in a well-established mouse model of atherosclerosis (apolipoprotein E deficient) reduces the formation of aortic lesions and prevents the associated development of dilated cardiomyopathy. This beneficial effect is likely due a reduction of atherogenic lipoproteins. These results indicate that treatment strategies aimed at the

inhibition of PEMT could prevent the development of atherosclerosis that predisposes individuals to heart failure.

ACKNOWLEDGEMENTS

First and foremost, I thank my supervisor Dr. Dennis Vance for providing me with the opportunity and resources to take on three very different research projects. It has been both a challenging and rewarding experience.

I thank my supervisory and examining committee for providing experimental advice through out the graduate program and for helpful comments during examination of this document.

There are several people who were central in developing the research contained in this document and to whom I owe a debt of gratitude. Dr. Claudia Banchio and Dr. Chieko Aoyama were instrumental during my first few years in the lab. Their contribution of time and advice made the transcriptional work possible. I thank Dr. René Jacobs for encouraging a molecular biologist to pursue lipid biochemistry. I am also very appreciative for the east coast humour which made difficult days tolerable. And of course I thank Dr. Vernon Dolinsky who has been an invaluable source for constructive criticism and constant encouragement during the many years it took to finish this degree.

I would like to thank Susanne Lingrell, Sandra Kelly, Donna Beker, Audric Moses, Russ Watts and Laura Hargreaves for excellent technical assistance.

I am also grateful for the encouragement, support and friendship of Lorissa Niebergall and Dr. Jelske van der Veen.

Finally, I thank all the past and present members of the Vance lab and MCBL group who have made my time here a wonderful experience.

Table of Contents

CHAPTER 1: Introduction

CHAPTER 5: Conclusions and future directions

List of Tables

List of Figures

Abbreviations

ACE	acetylcholinesterase
ACC	acetyl CoA carboxylase
AdoHcy	*S*-adenosyl-homocysteine
AdoMet	*S*-adenosyl-L-homocysteine
AMP	adenosine monophosphate
AMPK	AMP-activated protein kinase
AP	activating protein
ApoB	apolipoprotein B
ApoE	apolipoprotein E
ATP	adenosine triphosphate
AV	aortic valve
BADH	betaine aldehyde dehydrogenase
BAT	brown adipose tissue
BHMT	betaine-homocysteine methyltransferase
bp	base pair
cAMP	cyclic adenosine monophosphate
CD	choline deficient
cDNA	complementary deoxyribonucleic acid
CAT	choline acetyltransferase
CE	cholesteryl ester
C/EBP	CAAT element binding protein
CHDH	choline dehydrogenase

ChIP	chromatin immunoprecipitation
CoA	coenzyme A
CPT	CDP-choline:1,2-diacylglycerol choline phosphotransferase
CPT1	carnitine: palmitolytransferase 1
CK	choline kinase
CT	CTP:phosphocholine cytidylyltransferase
CTP	cytidine triphosphate
CMP	cytidine monophosphate
CO	cardiac output
CYC	cyclophilin
DAP	diastolic arterial pressure
DG	diacylglycerol
DGAT	diacylglycerol acetyltransferase
DMEM	Dulbecco’s modified Eagle’s medium
DMG	dimethylglycine
DMSO	dimethylsulfoxide
DNA	deoxyribonucleic acid
ECG	electrocardiograph
ECL	enhanced chemiluminescence
EDTA	ethylene diaminetetraacetic acid
EMSA	electrophoretic mobility shift assay
ER	endoplasmic reticulum
ESR	estrogen receptor

FABP	fatty acid binding protein
FAS	fatty acid synthase
FBS	fetal bovine serum
g	gram
h	human
Hcy	homocysteine
HDL	high density lipoprotein
HMG	hydroxylmethylglutaryl
HNF	hepatocyte nuclear factor
HR	heart rate
IDL	intermediate density lipoprotein
IgG	immunoglobulin gamma
IVCT	isoventricular contraction time
IVRT	isoventricular relaxation time
IVS	intraventricular septum thickness
KB	kilobases
kDa	kilodalton
KO	knock-out
LA	left atrium
LCAD	long chain acyl-CoA dehydrogenase
LDL	low density lipoprotein
LDLr	low density lipoprotein receptor
LVPW	left ventricle posterior wall

Lyso-PC	lysophosphatidylcholine
LV	left ventricle
LXR	liver X receptor
m	mouse
MAM	mitochondria-associated membrane
MAP	mean arterial pressure
MCD	malonyl-CoA decarboxylase
MEM	minimum essential medium
MDR	multiple-drug resistance protein
MHz	mega herz
mRNA	messenger RNA
NAFLD	non-alcoholic fatty liver disease
NTC	non-template control
PAGE	polyacrylamine gel electrophoresis
PBS	phosphate buffered saline
PC	phosphatidylcholine
PCR	polymerase chain reaction
PDI	protein disulphide isomerase
PDME	phosphatidyldimethylethanolamine
PE	phosphatidylethanolamine
PEMT	phosphatidylethanolamine *N*-methyltransferase
PFIC	progressive familial intrahepatic cholestasis
PI	phosphatidylinositol

PL	phospholipid
PLA	phospholipase A
PLC	phospholipase C
PLD	phospholipase D
PMME	phosphatidylmonomethylethanolamine
PPAR	peroxisome proliferator activated receptor
PPi	pyrophosphate
PS	phosphatidylserine
PVDF	polyvinylidene fluoride
RIPA	radioimmunoprecipitation assay
RNA	ribonucleic acid
RT-PCR	reverse transcription PCR
SAP	systolic arterial pressure
SCD1	stearoyl-CoA desaturase 1
SEM	standard error mean
SDS	sodium dodecyl sulphate
SRB1	scavenger receptor B1
SREBP	sterol response element binding protein
SV	stroke volume
TBP	TATA-box binding protein
TG	triacylglycerol
TGH	triacylglycerol hydrolase
TMX	tamoxifen

T-TBS	tween-tris buffered saline
UCP	uncoupling protein
VLDL	very low density lipoprotein
WAT	white adipose tissue
WT	wild type
YY1	yin yang protein 1

Chapter 1

Introduction

1.1 Phosphatidylcholine: the molecule

Phosphatidylcholine (PC) was originally described in 1847 as a constituent of egg yolk and named lecithin based on the Greek equivalent *lekithos* (1). Shortly thereafter, Diakonow and Strecker demonstrated that PC contained two fatty acids esterified to a glycerol backbone with a phosphodiester linkage connecting the third hydroxyl group to choline (Figure 1.1) (2-4). The diversity of PC molecules is based on differences in the fatty acid species which vary in length, as well as the number and position of double bonds (5). In the liver, PC typically contains a saturated fatty acid at the sn-1 position (e.g., 16:0 palmitic acid) and a polyunsaturated fatty acid at the sn-2 position (e.g., 20:4, arachidonic acid) (5). More than 20 different PC species have been detected in mammalian cells facilitating the various physiological roles carried out by this molecule (5).

1.2 Physiological importance of PC

PC is physiologically important as the principal component of eukaryotic cellular membranes, a precursor of signalling molecules and a key element of lipoproteins, bile and lung surfactant.

1.2.1 PC as a Component of Cellular Membranes

A primary function of PC is as a structural component of eukaryotic cellular membranes (6). PC is the major lipid component of eukaryotic

cellular membranes although the exact amount depends on cell type, organelle and leaflet of the lipid bilayer (6,7). Specific transport pathways facilitate and maintain the intracellular distribution of PC (8-11). Presumably, the appropriate distribution of PC has important consequences for cellular and organelle function (12). Physical properties of the membrane such as fluidity and permeability (integrity) are altered with phospholipid composition (13,14). It is becoming clear that a direct link exists between the lipid environment and the function of some integral membrane proteins (15).

1.2.2 PC as a Precursor of Signalling Molecules

The integration of PC into cellular membranes serves as a precursor for essential signalling molecules. In response to a variety of physiological and pathophysiological stimuli (hormones, cytokines, growth factors, adhesion molecules) lipid second messengers are rapidly released from the membrane by phospholipases (16,17) (Figure 1.2). PC-derived signals are chemically diverse including lysophosphatidylcholine (lyso-PC), lysophosphatic acid, phosphatidic acid, diacylglycerol (DAG), and eicosanoids produced from long chain fatty acids (18,19). The generation and release of specific lipid signalling molecules is dependent on the extracellular stimuli and cell type particularly in the case of eicosanoid formation. Lipid metabolites derived from PC are considered important in a wide range of cellular events

including inflammatory responses (20,21), membrane vesicle trafficking (22-24), cytoskeleton reorganization (25,26), cell proliferation (27), differentiation (28,29) and apoptosis (30). Recent publications suggest that targeted suppression of PC-derived signals may be effective for the treatment of various immune diseases (29), post-ischemic brain injury (31) and cancer (32).

1.2.3 PC as a Component of Lung Surfactant

The lung surfactant which coats alveoli is predominately composed of PC (~70%) (33,34). The surfactant is critical for lung function as it intersperses between water molecules to reduce surface tension and prevent alveolar collapse (33,34). The unique biophysical properties of pulmonary surfactant are largely attributable to a specific PC species dipalmitoylphophatidylcholine (33,34).

1.2.4 PC as a Component of Bile

The components of bile (bile acids, cholesterol, phospholipid) are produced by the liver and function in the intestinal tract to facilitate the digestion and absorption of lipids and fat soluble vitamins (35). The phospholipid portion of bile is ~95% PC (36) and represents a significant physiological fate of hepatic PC. In mice, the total amount of PC secreted into bile within a 24 h period is equivalent to the entire amount of PC present in the liver (37).

As a component of bile, PC is required to neutralize the detergent action of bile acids and maintain the solubility of cholesterol (35,38). A PC-specific transport protein (flippase), multiple-drug resistance protein 3 (MDR3 also called ABCB4) actively translocates PC across the hepatocyte canalicular membrane into bile (39,40). The importance of PC in bile was underscored when mutations in the *MDR3* gene were associated with progressive familial intrahepatic cholestasis 3 (PFIC3) (40). This rare childhood disease is characterized by persistent blockage of bile ducts (cholestasis) that progresses to irreversible liver damage and failure (41). Since establishing a link between this disease and MDR3, a growing number of genetic mutations have been reported (42-44). Recently, it was shown in cell culture that one naturally occurring mutation causes intracellular retention of MDR3 which can be rescued by low temperature treatment (27ºC) (45).

1.2.5 PC as a Component of Lipoproteins

The other major fate of hepatic PC is as a component of lipoproteins. Lipoproteins are responsible for transporting hydrophobic lipid in an aqueous circulatory system (46). Structurally, phospholipids and cholesterol form a monolayer on the surface of the lipoprotein surrounding the hydrophobic core of triacylglycerol (TAG) and cholesteryl esters (CE) (46). The different types of lipoproteins are classified on the basis of their density. Very low density lipoprotein (VLDL) has the

greatest buoyancy as a result of the TAG-rich core. Low density lipoprotein (LDL) and high density lipoprotein (HDL) are both more dense and carries a higher proportion of cholesterol (46). Each lipoprotein class carries characteristic protein components referred to as apolipoproteins (46). For example, apolipoprotein B is the major protein component of VLDL and LDL and apolipoprotein E is a minor protein component of all the lipoprotein classes (46).

PC is by far the major phospholipid component of all the lipoprotein classes with levels ranging from 60-80% (47). The other phospholipid components are sphingomyelin, lyso-PC, phosphatidylethanolamine (PE), phosphatidylserine, and phosphatidylinositol (47). In general, the total PL component and thus PC content of lipoproteins increases with lipoprotein density and surface area (47). As a result the PC component of HDL can constitute up to 40% of the total lipoprotein lipid (47). In addition to the structural role of PC in lipoproteins, the enzyme lecithin:cholesterol acyltransferase acts on HDL particles to esterify free cholesterol with fatty acids derived from PC (48).

1.2.6 The Biosynthesis of PC

In mammalian species there are two pathways which synthesize PC *de novo.* The major pathway which occurs in all nucleated cells is the cytidine diphosphate (CDP)-choline pathway (Figure 1.3, Table 1.1). This pathway was first described in the 1950s by Eugene Kennedy and

therefore is occasionally referred to as the Kennedy pathway (49). The CDP-pathway requires dietary choline and consists of three enzymatic steps: choline kinase catalyzes the phosphorylation of choline using adenosine triphosphate (ATP) 2) CTP:phosphocholine cytidylyltransferase (CT) catalyzes the reaction of phosphocholine with cytidine triphosphate (CTP) to form CDP-choline and 3) CDP-choline:1,2-diacylglycerol cholinephosphotransferase (CPT) catalyzes the exchange of cytidine monophosphate (CMP) for DAG to form PC.

In a second pathway PC can be generated endogenously via three sequential methylations of PE by phosphatidylethanolamine *N*-methyltransferase (PEMT) (Figure 1.3, Table 1.1)(6). The PEMT pathway is quantitatively significant only in the liver where it contributes approximately 30% of total hepatic PC synthesis (50). Production of PC may also occur through base-exchange of the choline head group (51) or by the reacylation of lyso-PC (52); however, these pathways are considered quantitatively insignificant.

1.3 Biosynthesis of PC: the CDP-choline pathway

1.3.1 Choline

The nutritional importance of choline was first described by Charles Best in 1932 (53). It is now recognized that choline is an essential nutrient with an Adequate intake (AI) set at 550 mg/day for men and 425 mg/day

for women (54). Since choline is present in most food, sufficient dietary choline is easily attained except during periods of starvation (55,56). Rich sources of choline include lettuce, peanuts, liver, coffee, and cauliflower (57). Individuals that should be closely monitored for choline deficiency are pregnant and lactating women (58). Maternal choline pools can become diminished due to the demand of the growing fetus and neonate (59,60). Human (61) and animal studies (62,63) have indicated that early brain development is particularly sensitive to the availability of maternal choline. In latter life, the major phenotype of choline deficiency (<50 mg/d) is the accumulation of hepatic TG (liver steatosis) (64-66) which can lead to liver dysfunction (64). Skeletal muscle damage has also been reported in a few individuals consuming a low-choline diet (64,67).

Excess choline undergoes irreversible oxidation to yield betaine in the kidney and liver (68) (Figure 1.3) This is completed during a two step oxidation process catalyzed by choline dehydogenase and betaine aldehyde dehydrogenase in the mitochondria (69,70). The principal roles of betaine are as an organic osmolyte and a methyl donor (71) (Figure 1.3). Betaine provides methyl groups to covert homocysteine to methionine as part of the methionine cycle in the liver (Figure 1.4) (71).

A small fraction of dietary choline is acetylated in cholinergic neurons to form the neurotransmitter acetylcholine (Figure 1.3) (72). Choline may be acetylated immediately after uptake by the neuron or

converted to a storage pool for later use (PC, phosphocholine) (72). Choline derived from the degradation of PC may be particularly important for sustained acetylcholine release or during choline deficiency (73,74).

Other choline derived phospholipids are lyso-PC, sphingomyelin, sphingosylphosphorylcholine and platelet-activating factor (18).

1.3.2 Choline Transport

Choline carries a positive charge and thus requires protein-mediated transport across the plasma membrane. Many organs use one or more of the following choline transport mechanisms: (1) facilitated diffusion, (2) sodium and energy-dependent transport and (3) sodium-independent, energy-dependent transport (75). In murine liver, choline uptake is primarily accomplished by the energy-dependent organic cation transporter (OCT1) (76,77). This process may occur in combination with facilitated diffusion at specific membrane sites (e.g., cannicular membrane) (76). Recently, a choline transporter (SLC44A1) has been localized to the mitochondria membrane and functions in part to supply choline for oxidation to betaine (78).

1.3.3 Choline Kinase

Choline kinase (CK) catalyzes the first reaction in the CDP-choline pathway, the phosphorylation of choline to yield phosphocholine (79) (Figure 1.3). The enzyme was first detected in yeast extracts by

Wittenberg and Kornberg in the 1950s (80). In mammalian cells, CK exists as three isoforms (CKα1, CKα2, CKβ) which are expressed from two separate genes (81-83) (Table 1.1). The *ckα* gene on chromosome 19 in mice encodes two proteins CKα1 (50 kDa) and CKα2 (52 kDa) by alternative splicing of exon II'' (82). Currently the functional difference between the two CKα enzymes is unknown due in part to the lack of a discriminating antibody. A separate gene encodes *ckβ* (42 kDa) found on chromosome 15 in mice (82).

Both CKβ and CKα (1 and 2) are ubiquitously expressed in all mouse tissues with relatively high levels in the liver (84). The active enzyme consists of either a homo- or hetero-dimer form (84,85). In most tissues, the majority of the activity is due to α/β hetero-dimers (50-80 %) with the remaining activity split between α/α and β/β homo-dimers (84). The enzymatic activity of CK appears to be dependent on the type of dimer complex generated (86,87).

In addition, CKα is induced at the transcriptional level by a distal activating protein-1 (AP-1) element (-875/-867) upon binding of c-Jun (88). Other putative transcription factors which may regulate CKα include Sp1 and GATA-1 (88). It is now clear that the activity of CK in the cell is more complicated than initially expected; varying with both the expression level of each isoform and the specific dimer generated.

Although CK catalyzes the first committed step in the biosynthesis of PC, the enzyme is generally not considered rate-limiting in the pathway. The generation of CK deficient mice have begun to reveal specific physiological roles for each isoform (89,90). The absence of CKα in mice resulted in embryonic lethality at day 7.5, indicating that CKα is crucial for early development (89). It remains unclear however whether this result is due to impaired PC biosynthesis. Adult mice heterozygous for CKα maintained normal levels of PC in all tissues tested despite a 30 % reduction in total enzyme activity (89). Instead CKα heterozygous mice had significantly lower levels of the product of CK, phosphocholine (89). Phosphocholine may act as an intracellular second messenger (91,92) in response to certain growth factors (e.g., platelet-derived growth factor, basic fibroblast growth factor, insulin-like growth factor, epidermal growth factor) (91,93-95) and other mitogenic factors (e.g., prolactin, estrogen) (96,97). Recently, a direct link has been found between CKα expression and cell cycle regulation (98).

Due to the relationship between CKα and cell growth, the enzyme has been the subject of intense research regarding carcinogenic growth. CKα protein and phosphocholine were shown to be drastically elevated in human tumours (breast, bladder, lung) (99-102). CK inhibitors with anti-tumour activity have been developed and are in pre-clinical development (103).

CKβ is essential for maintaining normal PC levels in skeletal muscle (89,90,104). A spontaneous occurring genomic deletion in CKβ results in muscular dystrophy and neonatal bone deformity in mice (104). This is due to attenuated PC biosynthesis combined with enhanced PC catabolism (89,90). The muscle damage can be reversed by injection of CDP-choline, the substrate for the final step of the CDP-choline pathway (90).

1.3.4 CTP:phosphocholine cytidylyltransferase

CTP:phosphocholine cytidylyltransferase (CT) catalyzes the rate limiting step in the CDP-choline pathway (105,106) (Figure 1.3). The formation of CDP-choline from phosphocholine and CTP was first described by Kennedy and Weiss in the 1950s (49,107). In mammalian cells, CT exists as three isoforms which are expressed from two separate genes (*Pcyt1a*, *Pcyt1b*) (108-113) (Table 1.1). The predominant form in most tissues is CTα encoded by *Pcyt1a* (111,113). One unique feature of CTα is the presence of a nuclear localization signal sequence which directs the enzyme to the nucleus in many cell types (114). *Pcyt1b* is located on the X-chromosome and encodes two isoforms: CTβ1 and β2 in humans, and CTβ2 and CTβ3 in mice (109,110,113) The expression of CTβ isoforms is low in most tissues with enrichment in the brain and reproductive organs (113).

CT is predominately regulated by the reversible translocation from a soluble, inactive form to a membrane-associated form that is activated (115-118). Translocation is mediated by the lipid binding domain; a structural feature common to all CT isoforms (119). Several lipid ligands including fatty acids (120), DAG (121), oxysterols (122) and low levels of membrane PC (123,124) stimulate the translocation and activation of CT. Thus, allowing for rapid modulation of PC biosynthesis in response to the availability of lipid precursors and alterations in membrane composition. Nuclear export of CTα is also regulated by the membrane binding domain in response to lipid activators (122,125). Activation of nuclear CTα results in translocation to the nuclear envelope (126) as well as export to cytoplasmic membranes (120,127,128). CTβ is constitutively found in the cytoplasm (128), the same localization as CTα in cells with increased demand for PC, such as hepatocytes (129).

CT activity is further modulated by phosphorylation. This mode of regulation remains poorly understood but in general dephosphorylation of CT correlates with membrane association (130-132). The first crystal structure of CT is now available and should provide further insight into the covalent and allosteric regulation of enzymatic activity (133).

Regulation of CT activity also occurs at the level of transcription (134-136). Transcriptional regulation of CTα is controlled by cell replication and growth (137-140). An increase in PC synthesis during the cell cycle is

required to generate adequate membrane (139). CTα transcription increases early in the cell cycle (G1 phase) in preparation for maximal CT activity and PC accumulation at a later phase (S phase) (139). The temporal expression of CTα is controlled by cyclin-dependent kinase 2 (CDK2) mediated phosphorylation of Sp1; phosphorylated Sp1 binds within the CTα proximal promoter and enhances gene transcription (139,141,142). In addition, repression of CTα gene expression in quiescent cells is mediated in part by the formation of Sp1 inhibitory complexes (143,144).

CTα gene expression during the cell cycle is further modulated by the retinoblastoma (Rb) protein and E2F (143,144) There is evidence that TEF-4, Ets-1 and Net may regulate CTα transcription during rapid cell proliferation and embryogenesis (77,145,146). Investigation of the regulatory mechanisms involved in gene expression of CTβ2 and CTβ3 are still in early stages (136).

The generation of CT deficient mice has begun to reveal specific physiological roles of each isoform. Due to the strict requirement of CTα during embryogenesis, global disruption of *Pcyt1a* results in cell death immediately following fertilization (day 3.5) (147). Thus, the Cre-lox system has been utilized to specifically disrupt CTα in several cell types. The absence of CTα in macrophages increases sensitivity to cholesterol loading (148) and reduces the secretion of some cytokines (tumour

necrosis factor alpha and interleukin -6) (149). The importance of CTα in the lung was illustrated when severe respiratory failure developed in mice lacking CTα in lung epithelial cells. These mice suffered from a significant decrease in the major lung surfactant phospholipid, dipalmitoyl-PC (150). Liver-specific deletion of CTα in mice indicated its requirement in lipoprotein homeostasis (151). Hepatic deficiency of CTα significantly reduced plasma levels of both HDL and VLDL. The levels of both lipoproteins could be normalized upon restoration of CTα expression levels in the liver using adenovirus (152).

The most notable phenotype of CTβ2$^{-/-}$ mice is infertility accompanied by either lack of ovarian follicles or testicular degeneration (153,154). Enhanced expression of CTβ isoforms in the brain suggests an important role for neuronal development. However, CTβ2 deficient mice do not have gross neurological defects (153). Recent studies have revealed that CTβ2 activity accompanies neurite outgrowth and branching from axons in cultured neuron-like cells (155,156). When CTβ2 was silenced in cell culture, neurite branching was reduced despite the presence of CTα (155). Subtle defects in learning, memory and motor coordination are currently being investigated in CTβ2 deficient mice (155).

1.3.5. Cholinephosphotransferase

In the terminal reaction of the CDP-choline pathway, CDP-choline:1,2-diacylglycerol cholinephosphotransferase (CPT) catalyzes the transfer of the phosphocholine moiety from CDP-choline to DAG resulting in the formation of PC and CMP (Figure 1.3) (157). As the ultimate step in the Kennedy pathway, the intracellular localization of CPT defines the site from which *de novo* PC is generated. Membrane fractionation studies have determined that the majority of CPT activity is associated with the endoplasmic reticulum (ER) (127,158,159). However, the precise intracellular location is unclear and may additionally include the Golgi, mitochondrial and nuclear membranes (127,159-162) (Table 1.1). The CPT protein has not been successfully purified from any source delaying the generation of antibodies for immunofluorescence or electron microscopy. Purification is extremely difficult because CPT is an integral membrane-bound protein whose activity is destroyed upon solubilisation with detergents (163,164).

One CPT gene (*CPT1*) isolated from the yeast *Saccharomyces cerevisiae* was found to be responsible for 95% of PC biosynthesis (165,166). Based on similarity to the yeast *CPT1* gene, three human CPT cDNAs (CEPT1, CHPT1, CHPT1β) were identified from NCBI expressed sequence tag databases (167,168). The human CHPT1 gene has been mapped to chromosome 12q and CEPT1 located on chromosome 1

(167,168). The most notable difference between human isoforms is substrate specificity. CHPT1 specifically uses CDP-choline as a substrate (167-169) whereas CEPT1 utilizes CDP-choline and -ethanolamine resulting in both PC and PE (168).

Nothing is known about the transcriptional regulation or post-translational modifications of CPT. It is accepted that the enzymatic activity of CPT is regulated *in vivo* by substrate supply (169,170). Additional studies have demonstrated that CPT activity is inhibited by ceramide (171) and farnesol (172).

1.4 Biosynthesis of PC: the PE methylation pathway

1.4.1 Discovery of the PE methylation pathway

In the early 1940s, heavy isotope methodology revealed that ethanolamine and methionine were utilized in the biosynthesis of choline (173,174). Twenty-years later Bremer and Greenberg showed that PE accepted methyl groups from *S*-adenosylmethionine (AdoMet) to generate PC and *S*-adenosylhomocysteine (AdoHcy) (175-177) (Figure 1.3). They subsequently determined that the methylation of PE occurred by three stepwise reactions which took place in a concerted fashion (175,178). Incorporation of the first methyl group was identified as the rate-limiting step since the reaction intermediates phosphatidylmonomethylethanolamine (PMME) and

phosphatidyldimethylethanolamine (PDME) did not accumulate when rat-liver microsomes were incubated with [Me-^{14}C]AdoMet (177). These predictions were later confirmed by kinetic analysis of the purified PEMT protein (179,180).

Bremer and Greenberg additionally discovered that the liver is the only organ capable of any significant amount of PE methylation (177). In all other tissues tested (testis, kidney, heart, brain, intestine) the conversion of PE to PC was less then 10% of that detected in the liver (177). Using isolated rat hepatocytes, formation of PC via PE was estimated to be 20-40% of the total rate of PC biosynthesis (50). In general it is accepted that ~30% of newly synthesized PC in the liver is due to the PEMT pathway (6,181). The remainder is generated by the CDP-choline pathway.

1.4.2 Purification and Kinetic Analysis of PEMT

As is the case with all intrinsic membrane proteins PEMT was extremely difficult to purify. In 1987 Ridgeway and Vance purified PEMT to homogeneity from rat liver by taking advantage of the non-ionic detergent Triton X-100 (180). Triton X-100 solubilised PEMT without inhibiting activity provided phosphate buffers were used (180,182,183). Analysis by electrophoresis and silver staining indicated that PEMT is a single protein of 19 kDa (180). The purified enzyme catalyzed the conversion of PE to PC with specific activities of 0.63, 8.59 and 3.75 μmol/min/mg protein for

PE, PMME and PDME substrates, respectively (180). Kinetic studies revealed that the phospholipid substrates bind at a single active site (179). Once the active site of PEMT is occupied by a phospholipid substrate, AdoMet binds, a methylgroup is transferred to the phospholipid and AdoHcy is released (179). The reaction intermediates (PMME, PDME) do not diffuse away from the active site but instead are sequentially methylated to generate PC (179,180,184). PEMT does not appear to have preference for a specific PE substrate (179,185-187).

1.4.3 Cloning of PEMT

Oligonucleotide probes based on the N-terminal sequence of the purified rat PEMT were used to screen a rat liver cDNA library (188). One cDNA was recognized which consisted of 913 nucleotides and a predicted molecular weight of 22 kDa (188). The cloned cDNA was expressed in three different cell lines resulting in a 5-12 fold increase in PEMT activity (188). The kinetic parameters of the expressed enzyme matched the purified PEMT thus indicating that the cDNA cloned encoded PEMT (188).

Rat PEMT cDNA was subsequently used as a radio-labelled probe to screen a mouse genomic DNA library (189) and a human liver cDNA library (190). For each species the open reading frame of PEMT encodes a 199-amino acid protein with a molecular weight of 22 kDa (188-190). The amino acid sequence of mouse and human PEMT are 93.5% and

80.4% identical, respectively, to the rat protein, suggesting strong conservation among species (189,190).

The human *PEMT* gene is comprised of 9 exons and 8 introns on chromosome 17p11.2. (Figure 1.5A) (190,191). Alternative splicing results in three human PEMT splice forms (190). All three cDNAs encode the same amino acid sequence (exons 4-9) but differ in the specific 5'untranslated region (either exon 1, 2 or 3) (190,191). In the human liver each of the three splice variants could be detected by polymerase chain reaction (191). However, the PEMT splice form containing exon 2 was by far the most abundant and was the only mRNA detected in Northern blot experiments (191).

Genomic characterization of mouse *Pemt* demonstrated that the gene spans 35 kb on chromosome 11 (Figure 1.6) (189). The *Pemt* gene generated a single isoform containing 7 exons which was in contrast to 9 exons identified in humans (189). Additional exons were not identified in the mouse *Pemt* gene when human sequences were used as radio-labelled probes (191). However, two additional transcription start sites (referred to as A and C) have been identified from NCBI expressed sequence tag databases (192). This result suggests that alternative splicing of *PEMT* may be conserved between mice and humans. In mice, the PEMT transcript originally published (referred to as B) was found to be the most abundantly expressed in liver (~75%) (192). The predominance

of one mouse PEMT transcript may explain why a single transcription start site was previously detected experimentally (189).

1.4.4 Sub-cellular Localization and Topography

Historically PEMT activity has been localized to the microsomal fraction of liver homogenates (177,193). Sub-cellular fractionation revealed that PEMT activity resides primarily on the ER, and also in the mitochondria-associated membrane (MAM) (127,188,194,195). The MAM is a sub-domain of ER that co-isolates with mitochondria (195-197). The sub-cellular localization of PEMT is determined by an ER retrieval signal composed of an essential lysine (x<u>K</u>x*x)* residue (198) (Figure 1.5B). Unexpectedly, the antibody raised against the C-terminal of PEMT detects protein in MAM but not the ER fraction of rat liver (188). Immunocytochemistry using electron microscopy confirms this sub-cellular localization (188). This has led to the identification of two PEMT isoforms: PEMT 1 localized to the ER and catalyzing the majority of PE methylation and PEMT 2, localized to the MAM (188). The physiological importance of two PEMT isoforms with differential sub-cellular locations is not known. However, this finding may be confined to rodents since PEMT protein was successfully detected by immunoblot in both ER and MAM fractions of human liver (194).

Localization of PEMT to the ER/MAM places it at one of the major lipid biosynthesis sites within the cell. Other lipid biosynthetic enzymes at this location are CPT (195), CDP-ethanolamine:1,2-diacylglycerolethanolamine-phosphotransferase (195), phosphatidylserine synthase (195,199,200), acyl-CoA:diacylglycerol acyltransferase (199,201), acyl-CoA synthetase (202), and acyl-CoA:cholesterol acyltransferase (199).

Purification of PEMT confirmed that it is a membrane bound protein (180). Bioinformatic analysis of PEMT predicted four significant stretches of hydrophobicity which were likely transmembrane segments (188,190) (Figure 1.5B). The exact topographical orientation of PEMT on microsomes has been determined by endoproteinase-protection analysis of epitope tagged recombinant protein (194). These results confirmed the presence of four transmembrane regions and demonstrated that PEMT is orientated in the microsomal membrane such that the N and C termini are exposed to the cytosol (Figure 1.5B) (194). Earlier studies suggested that the active site of PEMT was also located on the cytoplasmic side (203,204). Indeed, the binding site of AdoMet has been identified on the external surface of PEMT (205). Two required amino acid motifs ^{98}GXG^{100} and ^{180}EE^{181} are located on the external portion of the third and fourth transmembrane helices, respectively (Figure 1.5B) (205). This would predictably provide optimal access to the AdoMet pool in the cytosol.

1.4.5 Regulation of PEMT Activity

(a) Substrate Supply

One of the major mechanisms for regulating PEMT activity is the supply of substrates (50,206). Each of the metabolites in the PEMT pathway has been shown to stimulate PE methylation. Addition of ethanolamine, to primary cultured hepatocytes increased the level of PE by 50% and doubled the rate of PE conversion to PC (206). Similarly, increasing the level of PMME and PDME by adding *N*-monomethylethanolamine or *N,N*–dimethylethanolamine, respectively to hepatocytes increased the formation of PC via PE methylation (50).

The cellular ratio of AdoMet to AdoHcy regulates methylation reactions including PEMT (207-209). The rate of PC formation from PE doubled in primary hepatocytes when the intracellular concentration of AdoMet was raised using exogenous L-methionine (50,207). The reverse is also true, increases in the cellular AdoHcy concentration decreases the AdoMet/AdoHcy ratio and inhibits PEMT activity (207). PE methylation decreased by more than 99% when the hepatic AdoMet/AdoHcy ratio was reduced experimentally from a normal value of 5.6 to 0.3 (207-211).

(b) Hormonal Effects

In the 1980s there were numerous studies on the regulation of PEMT activity in response to various hormones (212-220). In general, the effects were small and inconsistent between publications. For example, treatment of isolated rat hepatocytes with 100 nM glucagon inhibited the conversion of PE to PC by 25% (213) in one study and activated PE methylation by 100% in another (216). Conflicting results were also obtained when the purified PEMT enzyme was studied. PEMT was phosphorylated *in vitro* by the glucagon activated cAMP-dependent protein kinase (218). However, an associated change in PEMT activity did not result (214,218). Furthermore, attempts to promote phosphorylation of PEMT with addition of exogenous cAMP to intact hepatocytes failed (218). Due to the number of conflicting results a consensus regarding cAMP/glucagon mediated regulation of PEMT has not been reached.

Preliminary reports indicated that PEMT activity increased in response to vasopressin (221), angiotensin (221), epidermal growth factor (219), estradiol (222), and calmodulin (223). These effects have not been revisited since the purification and characterization of PEMT (184). Thus, it remains unclear whether these hormones have any direct effects on PEMT activity.

(c) Tissue Specific Expression

As previously mentioned, Bremer and Greenberg initially reported that the liver is the site of highest PEMT activity (177). Tissue specific expression of PEMT was later confirmed by immunoblot. PEMT protein was present in rat liver but undetectable in brain, heart, kidney, lung, muscle, spleen, intestine and testis (188). Immunocytochemical studies localized rat PEMT specifically to hepatocytes and not in non-parenchymal hepatic cell types such as Kupffer and endothelial cells (188). In human tissues, PEMT mRNA was only detectable in liver (191). However, low levels of PEMT transcripts could be detected by polymerase chain reaction amplification in human testes, muscle, heart and brain (191). These results agree with previous studies that detected low levels of PEMT activity in various rat tissues (testes, muscle, heart, brain) albeit at less then 6% of the activity measured in liver homogenate (1238 pmol/min/mg protein) (188).

Whether PEMT has any physiologically relevant role in non-hepatic tissues is not known. There is some evidence that even very low levels of PEMT activity may be important for normal development of the fetal brain (224,225). There are also reports that PEMT activity may become elevated in adipose (226) and decreased in heart (227,228) during disease states in rats. These studies typically relied on *in vitro* PEMT activity assays in whole tissue homogenates and/or sub-cellular fractions

(224-228). Therefore, more extensive experimentation in an intact cell model is necessary to show a direct relationship between the PEMT protein/activity level, amount of PC produced and the subsequent physiological effect. Currently, it is accepted that PEMT is a quantitatively significant source of PC only in the liver (6).

(d) Regulation of PEMT expression during development and growth

In general, PEMT is primarily expressed in quiescent differentiated hepatocytes. For example, PEMT mRNA, protein and activity levels are very low in the rodent prenatal liver when growth is rapid and tissue specification has not been completed (140,229). At birth, proliferation of fetal hepatocytes declines and differentiation occurs (230). It is during this period that hepatic PEMT mRNA and protein expression commences (140,229,231).

Liver regeneration is another model of hepatic growth and differentiation associated with PEMT expression. When two-thirds of the liver is removed the remaining hepatocytes de-differentiate and proliferate to restore original liver mass (232,233). PEMT mRNA and protein levels are drastically reduced (90%) during the period of maximal growth that initially follows the procedure (234). As liver size is restored, tissue specification begins (~48 h post hepatectomy) and PEMT protein expression increases (234). The amount of PEMT protein and mRNA

returns to normal values at the same time that liver regeneration is complete (~8 days) (234).

The de-differentiation of primary hepatocytes in culture also results in decreased expression of PEMT (235). It is well established that as the time after isolation increases so does the disparity of gene expression with that of whole liver (235-237). PEMT mRNA is undetectable in primary rat hepatocytes after 50 h in cell culture (238). This result is consistent with microarray analysis indicating that PEMT transcripts are significantly reduced within 12 h of isolation (235). PEMT is also not expressed in immortalized hepatoma cell lines which typically increase expression of genes for growth and decrease those which support liver-specific function (188,237,239-241).

In comparison to whole liver, more than 500 genes may be differentially expressed in hepatoma cell lines (240), in primary hepatocytes during prolonged culture (235,240) and throughout liver regeneration (242,243). Thus, *Pemt* appears to be one of many genes which are regulated as part of a global hepatic response to promote de-differentiation and growth. In these situations the CDP-choline pathway appears to be the preferred pathway for generating PC (140,234,244,245).

(e) Transcriptional Regulation

Characterization of the mouse and human PEMT genes provided the information required to study transcriptional regulation (189,191). The most active mouse *Pemt* promoter is 50% identical to the promoter region of the major human PEMT transcript (Figure 1.7). A TATA box does not precede the transcription start site for either the mouse or human promoters (189,191). Analysis of the major *Pemt* gene promoter from each species revealed several conserved putative transcription factor binding sites including those for hepatic nuclear factor (HNF), activating protein-1 (AP-1), yin yang protein 1 (YY1), GATA and SP1 (189,191). However, the ability of these specific factors to mediate *Pemt* gene expression has not been examined (189,191).

One recent study by Ressigue et al., demonstrated that estrogen may activate *Pemt* gene expression in primary cultures of mouse and human hepatocytes (192). However, caution must be used when examining the data. One problem is that primary hepatocyte cultures were incubated for >50 h prior to estrogen treatment for an additional 24 h (72 h total). As previously mentioned PEMT mRNA levels are undetectable in hepatocytes when cultured for extended periods of time (238). Ressigue et al. likely had the same difficulty since PEMT immunoblots and activity assays were performed with large amounts of membrane enriched

fractions (50 μg protein) (192). Therefore, the changes in the level of PEMT may be exaggerated and/or physiologically irrelevant.

A second problem was that PEMT mRNA, protein and activity levels prior to estrogen treatment were not provided ($t \cong 50$ h) (192). Thus, it is uncertain whether estrogen increased *Pemt* gene expression during the 24 h treatment or prevented mRNA levels from decreasing further. Finally, a direct link between estrogen and *Pemt* gene expression was not established. Classical promoter analysis using luciferase activity assays with promoter deletion constructs and/or expression of the proposed transcription factor (estrogen receptor) were not preformed (192). More experimental data are required to determine whether estrogen and its nuclear receptor regulate gene expression of PEMT.

1.4.6 Physiological Function and importance of PEMT

The *Pemt* gene was disrupted in mice to determine the physiological relevance of the enzyme (246). A targeting vector was designed to replace the majority of exon 2 which encodes the translation initiation codon (189,246). The resulting *Pemt*$^{-/-}$ mice lacked all *in vivo* PE methylation activity assessed after [L-methyl-^{3}H]methionine injection (246). Gene ablation of PEMT marked the first time in which an intact animal lacked an enzyme for phospholipid biosynthesis.

(a) Non-alcoholic Fatty Liver Disease

Non-alcoholic fatty liver disease (NAFLD) includes a wide range of chronic hepatic pathology which occurs in the absence of alcohol abuse (247). The disease typically progresses from simple fatty liver (steatosis), to steatohepatitis (lipid accumulation with inflammation), and eventually liver failure (247,248). It is not fully understood why the disease progresses from steatosis into steatohepatitis in some individuals (12-40%) and not others (247). The current consensus is that hepatic steatosis sensitizes the liver to a variety of metabolic injuries such as oxidative stress and cytokines which promote inflammation (249). A link between the absence of PEMT activity and the development of steatohepatitis has been established in two separate diet-induced animal models: (1) choline-deficiency (37,250,251) and (2) high-fat (Jacobs, R., unpublished results).

Choline-deficient Diet

In mammals, a choline-deficient (CD) diet eliminates the choline substrate required to synthesize PC via the CDP-choline pathway. This diet was initially prepared for *Pemt*$^{-/-}$ mice to determine the evolutionary significance of PEMT. On a standard chow diet there was no obvious difference between *Pemt*$^{-/-}$ and wild-type mice due to compensation by the CDP-choline pathway (246). When *Pemt*$^{-/-}$ mice were placed on a CD diet a dramatic phenotype was induced: the animals developed severe liver pathology and died within 5 days (37,252). This result was accompanied

by a 50% decrease in hepatic PC in CD *Pemt*$^{-/-}$ animals compared to the controls (37). Thus, it is clear that PEMT had been evolutionary conserved to provide PC when dietary choline is insufficient (e.g., starvation).

The severe liver failure indentified in CD *Pemt*$^{-/-}$ mice was identified as steatohepatitis (250,251). Histological examination of livers from CD *Pemt*$^{-/-}$ mice indicated an increase in TG levels accompanied by inflammation (37,251). It was found that the severe liver failure was a result of hepatic PC secretion into bile (250,251). In a pivotal study, *Pemt*$^{-/-}$ mice were bred with mice lacking MDR2 (the mouse ortholog of human MDR3) that actively translocates PC across the hepatocyte canalicular membrane into bile (39,40,250). Remarkably, the *Pemt*$^{-/-}$/*Mdr2*$^{-/-}$ mice did not develop liver failure and lived for at least 90 days when fed a CD diet (251).

The *Pemt*$^{-/-}$/*Mdr2*$^{-/-}$ mice are protected because the liver can adapt to reductions in hepatic PC when biliary loss is negligible. The liver adapts by recycling the available hepatic PC via membrane degradation and resynthesis (250,251). Interestingly, increased membrane degradation also results in less hepatic PE (251). Thus, *Pemt*$^{-/-}$/*Mdr2*$^{-/-}$ have two advantages over *Pemt*$^{-/-}$ mice on a CD diet (1) PC can be reused for basic hepatocyte function, (2) the hepatic PC/PE ratio, which is important for membrane integrity, is maintained.

A reduced PC/PE ratio results in imperfect packing of the plasma membrane and allows pro-inflammatory molecules (e.g., cytokines) to leak into the hepatocyte (251). It was shown that *Pemt*$^{-/-}$/*Mdr2*$^{-/-}$ mice are able to maintain the hepatic PC/PE ratio at a normal level (1.6-1.8) regardless of the amount of dietary choline provided (251). In contrast, the PC/PE ratio was decreased to 0.8 in CD *Pemt*$^{-/-}$ animals (251). The CD *Pemt*$^{-/-}$/*Mdr2*$^{-/-}$ mice continued to accumulate TG in the liver, indicating that maintaining a normal PC/PE ratio does not prevent steatosis but instead prevents the molecular insult required for the progression to steatohepatitis (250,251).

High Fat Diet

Pemt$^{-/-}$ mice also develop steatosis and steatohepatitis when challenged with a high-fat diet (253)(Jacobs, R., unpublished results). The hepatic TG content of *Pemt*$^{-/-}$ mice was ~5-fold higher after 3 weeks of a high fat/high cholesterol diet compared to wild-type animals (253). These results are consistent with reports that the absence of either the CDP-choline or PE methylation pathway results in the accumulation of TG in both cell (254,255) and animal models (151,152,256-258). Inadequate levels of hepatic PC impair the secretion of TG-rich VLDL particles from the liver (259-261).

It has recently been demonstrated that feeding PEMT deficient mice a high-fat diet for 10 weeks results in the progression of steatosis to steatohepatitis (Jacobs, R., unpublished results). The development of steatohepatitis was due to a reduced hepatic PC level and a low PC/PE ratio in the liver of *Pemt*$^{-/-}$ mice compared to wild-type controls (Jacobs, R., unpublished results). Severe liver damage was prevented in the absence of PEMT when the high-fat diet (1.3 g choline/kg diet) was supplemented with additional choline (4 g choline /kg diet) (Jacobs, R., unpublished results). Normalization of hepatic PC levels with additional dietary choline prevented steatohepatitis but not steatosis in *Pemt*$^{-/-}$ mice (Jacobs, R., unpublished results). These results indicate that PEMT deficiency increases the susceptibility to steatohepatitis even when normal amounts of dietary choline are consumed. Furthermore, PEMT activity may regulate hepatic TG metabolism independently of total PC levels. Preliminary evidence has shown that surgical disruption of the neuronal connection (vagal nerve) between the liver and brain prevents steatosis from occurring in *Pemt*$^{-/-}$ mice on a high-fat diet (Jacobs, R., unpublished results). The underlying mechanism is currently being investigated.

Interestingly, PEMT activity may be an important predictor of NAFLD in humans (251,262-265). A genetic variant of human *PEMT* has been identified that results in partial loss of activity due to a single amino acid substitution (V175M) (262). This polymorphism occurred more frequently (1.7-fold) in humans with NAFLD then in normal controls (262,265). The

strength of the relationship between the sequence variation (V175) of PEMT and hepatic triglyceride content appears to be dependent on the ethnicity of the population studied (263,265,266). It was additionally shown that patients with steatohepatitis had significantly lower hepatic PC/PE ratios (~1.2) compared to the control group (~2.5) (251). Thus, diminished PEMT activity may increase the susceptibility to NAFLD.

(b) Cardiovascular disease

It is estimated that ~33% of North Americans adults have cardiovascular disease which continues to be the leading cause of mortality in both men and women (267). Several established risk factors for cardiovascular disease are (1) elevated plasma levels of VLDL, (2) elevated plasma homocysteine and (3) reduced plasma HDL (267,268). PEMT activity has been shown to regulate the amounts of circulating VLDL, HDL and homocysteine and thus may be an important pharmaceutical target.

Plasma VLDL Metabolism and Atherosclerosis

Elevated plasma levels of VLDL is a well established risk factor for atherosclerosis (268). Vascular lesions are initiated by accumulation of lipoprotein-derived lipid within artery walls (268). As previously mentioned, inadequate levels of hepatic PC impair the secretion of TG-rich VLDL particles from the liver. A specific role for PEMT in VLDL-TG secretion

has been demonstrated *in vivo* (253) *Pemt*$^{-/-}$ mice challenged with a high fat/cholesterol diet for 3 weeks secreted 50% less VLDL-TG than the wild-type controls (253). Subsequently, the fasting plasma TG level was reduced (50%) in the absence of PEMT (253).

The hypolipidemic effect of PEMT deficiency was recently shown to attenuate plaque formation in a well-known animal model of atherosclerosis, the LDL receptor deficient (*Ldlr*$^{-/-}$) mouse (269) After 16 weeks of a high fat/high cholesterol diet the atherosclerotic lesion area was 80% smaller in *Pemt*$^{-/-}$/*Ldlr*$^{-/-}$ mice compared to *Pemt*$^{+/+}$/*Ldlr*$^{-/-}$ controls (269). This effect was accompanied by a significant decrease in plasma VLDL-TG (~65%) (269). The hypolipidemic effect was due in part to reduced hepatic PC levels and inhibition of VLDL-TG secretion (30%) (269). However, the predominant effect of PEMT deficiency was increased VLDL clearance from the plasma. Inadequate levels of hepatic PC significantly reduced the amount of PC on the surface of nascent VLDL particles by 50% in *Pemt*$^{-/-}$/*Ldlr*$^{-/-}$ mice compared to *Pemt*$^{+/+}$/*Ldlr*$^{-/-}$ controls (269). Radio-labelled VLDL ([^{3}H]-TG, [^{125}I]-apolipoprotein B) derived from *Pemt*$^{-/-}$/*Ldlr*$^{-/-}$ animals were preferentially removed from circulation *in vivo* compared to those particles isolated from *Pemt*$^{+/+}$/*Ldlr*$^{-/-}$ mice (269).

Plasma Homocysteine

Elevated plasma homocysteine is an independent risk factor for cardiovascular disease and atherosclerosis (270,271). It is known that PEMT activity influences the amount of homocysteine in the plasma (Figure 1.4). AdoHcy molecules generated during PE methylation are subsequently hydrolysed to form homocysteine (272). In *Pemt*$^{-/-}$ mice, the level of homocysteine in the plasma was 50% lower than in wild-type mice (273). Furthermore, when PEMT activity was elevated in cellular (198,273) and animal models (274), plasma homocysteine levels increased accordingly. The reduction in atherosclerotic lesions in *Pemt*$^{-/-}$/*Ldlr*$^{-/-}$ animals also coincided with a significant decrease in homocysteine levels (~30-50%) (269). Thus, the absence of PEMT may mediate cardioprotective effects in part by reducing plasma homocysteine levels (269).

Plasma HDL Metabolism

PEMT also plays an important role in high density lipoprotein (HDL) metabolism. HDL protects against cardiovascular disease by transporting cholesterol from extra-hepatic tissues to the liver for breakdown (275-277). In wild-type mice HDL particles are responsible for carrying the majority of PC and cholesterol in the plasma. The levels of both HDL-PC and -cholesterol were lower (25-45%) in *Pemt*$^{-/-}$ mice compared to wild-type controls (253). Hepatic uptake of radio-labelled HDL particles ([^{3}H]-

cholesterol, [^{3}H]-PC) was increased in mice lacking PEMT (278). This was caused by increased expression of a receptor for HDL, scavenger receptor Class B, type 1 (SR-B1) in the liver of *Pemt*$^{-/-}$ mice compared to the wild-type controls (278). The exact mechanism linking PEMT activity to SR-B1 protein levels has not yet been elucidated.

It is unclear whether the risk of cardiovascular disease will be affected when plasma HDL levels are reduced in the absence of PEMT. In general, reductions in plasma HDL increases the risk for cardiovascular disease (268). In contrast, elevated hepatic uptake of HDL indicates greater transport of cholesterol from extra-hepatic tissues to the liver where it can be excreted from the body (276,277). The plasma HDL levels were similar between *Pemt*$^{+/+}$/*Ldlr*$^{-/-}$ and *Pemt*$^{-/-}$/*Ldlr*$^{-/-}$ animal groups suggesting that HDL metabolism may not be a major atheroprotective effect of PEMT deficiency (269).

1.5 Thesis Objectives

The liver is a unique tissue because substantial amounts of PC can be synthesized endogenously by PEMT (6). PC derived from PEMT has been shown to contribute to hepatic lipid metabolism and lipoprotein secretion (251,253,269,278). The physiological importance of PEMT has been recently underscored in *Pemt*$^{-/-}$ mice which develop NAFLD (238,251) and are protected from cardiovascular disease (269).

Thesis Objective 1:

Despite the important role that PEMT plays in hepatic lipid metabolism, little is known about its transcriptional regulation. **Our first objective was to identify transcription factors which regulate the gene expression of PEMT.** In order to investigate transcriptional regulation of PEMT it was first necessary to identify a cell culture model in which PEMT was expressed endogenously. We then examined the *Pemt* promoter using classical promoter analysis techniques including promoter deletion-reporter gene constructs and electrophoretic mobility shift assays. We also used RNA silencing and recombinant cDNA strategies to either "knock-down" or over-express transcription factors to determine their contribution to transcriptional activation/ repression.

Thesis Objective 2:

Tamoxifen is an anti-estrogen drug widely used for the treatment of hormone-sensitive breast cancer (279,280). Approximately 43% of breast cancer patients treated with tamoxifen develop hepatic steatosis (248,281-283). The mechanism(s) by which tamoxifen induces lipid accumulation in the liver is unclear. We hypothesized that inhibition of PEMT may contribute to the development of hepatic steatosis in response to tamoxifen. **Our second objective was to elucidate the effects of tamoxifen on hepatic lipid metabolism.** We evaluated lipid metabolism in primary hepatocytes isolated from mice treated with vehicle or tamoxifen. Lipid synthesis, uptake and secretion were examined using radio-labelled precursors of TG, cholesterol and PC. These studies were complemented with measurements of hepatic lipid biosynthetic enzymes.

Thesis Objective 3:

It is known that PEMT activity influences the development of cardiovascular disease (269). The absence of PEMT reduced the size of atherosclerotic lesions in mice lacking the LDL receptor (269). Another animal model which spontaneously develops atherosclerosis is the apolipoprotein E receptor (apoE) deficient mouse (284). $Apoe^{-/-}$ mice develop changes in left ventricle structure and function as a result of plaque formation (285). **Our third objective was to investigate the contribution of PEMT to atherosclerotic lesion formation and heart**

dysfunction in apoE deficient mice. We examined the distribution of lipid in the liver, plasma and aorta of *Pemt*$^{+/+}$/*Apoe*$^{-/-}$ and *Pemt*$^{-/-}$/*Apoe*$^{-/-}$ mice. Quantitation of atherosclerotic lesion formation was combined with *in vivo* measurements of heart function using echocardiography.

Combined these studies will greatly enhance our understanding of *Pemt* gene expression and the role of PE methylation in the progression of liver and heart disease.

Enzyme	Gene	Tissue Expression	Subcellular Location	Regulation
CK	*Chka* *Chkb*	Ubiquitous	Cytosol	Transcription, Dimer complexes
CT	*Pcyt1α* *Pcyt1β*	Ubiquitous (α), Brain and Reproductive organs (β)	Nuclear (α), Cytoplasmic (α,β)	Transcription, Reversible membrane translocation
CPT	*Cept1* *Cpt1*	Ubiquitous	ER (Golgi, Mitochondria, Nucleus)	Substrate
PEMT	*Pemt*	Liver	ER (PEMT1) MAM (PEMT2)	Substrate

Table 1.1. Properties of PC biosynthetic enzymes

This table summarizes current information on PC biosynthetic enzymes including relevant gene(s), tissue expression, sub-cellular localization and regulation. CK, Choline kinase; CT, CTP: phosphocholine cytidylyltransferase; CPT, Choline phosphotransferase; PEMT, Phosphatidylethanolamine *N*-methyltransferase; ER, endoplasmic reticulum; MAM, mitochondria associated membrane.

Figure 1.1.Structure of phosphatidylcholine and phosphatidylethanolamine.

The molecular structure of a typical molecule of (**A**) PC (1-palmitoyl-2-arachidonyl-phosphatidylcholine) and (**B**) PE (1,2-dipalmitolyl-phosphatdylethanomaine) is shown. The choline and ethanolamine moieties are enclosed within blocks.

Figure 1.1

(A) Phosphatidylcholine

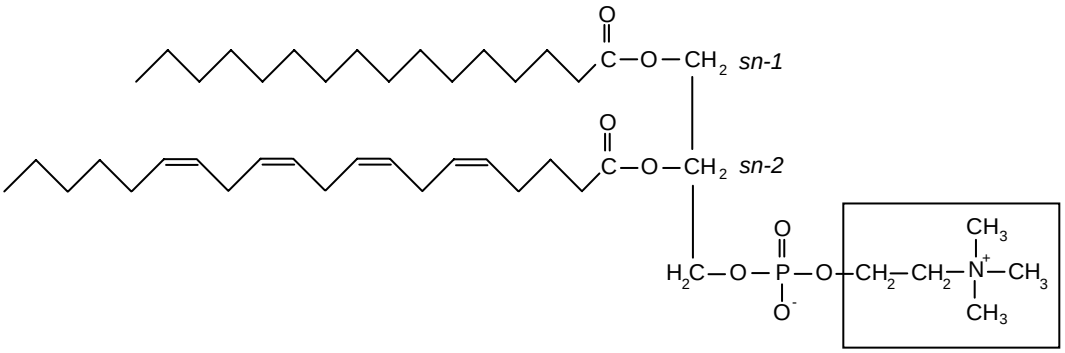

(B) Phosphatidylethanolamine

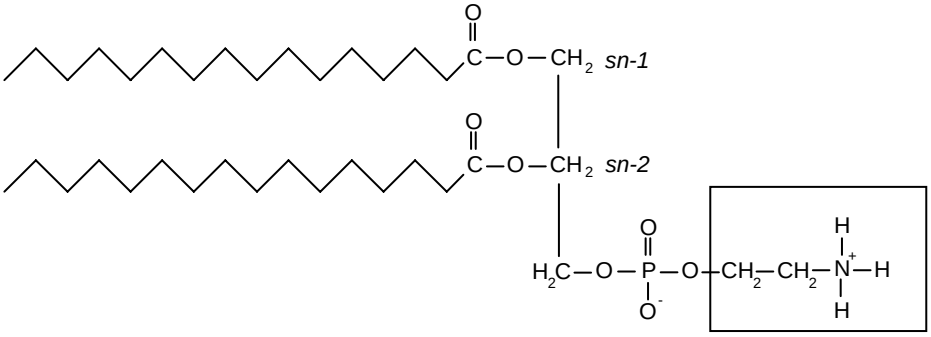

Figure 1.2. The PC-derived signalling molecules.

As a component of the plasma membrane PC is acted upon by several phospholipases (PL) to generate phospholipid-derived second messengers. PLA hydrolyses the acyl ester bond at either the *sn-1* (PLA_1) or *sn-2* (PLA_2) position. The action of PLA_2 releases lyso-PC and arachidonic acid which can be converted to eicosanoids. Phospholipase C (PLC) catalyzes the release of diacylglycerol and phosphocholine. Phosphatidic acid and choline are generated as a result of phospholipase D activity.

Figure 1.2

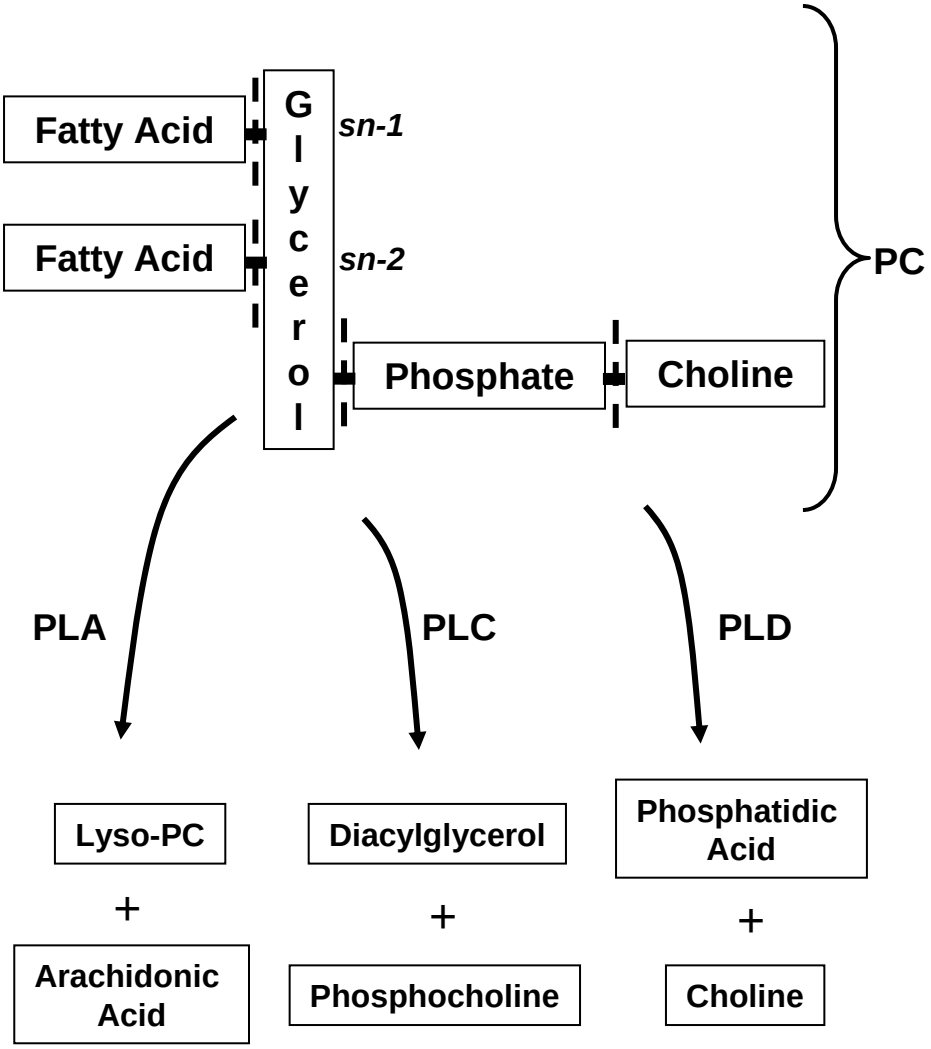
Fatty Acid
Fatty Acid
Glycerol
sn-1
sn-2
Phosphate
Choline
PC
PLA
PLC
PLD
Lyso-PC
+
Arachidonic Acid
Diacylglycerol
+
Phosphocholine
Phosphatidic Acid
+
Choline

Figure 1.3. Pathways involved in phosphatidylcholine biosynthesis.

The enzymes involved are as follows, with mammalian tissue distribution in parentheses:

CAT Choline acetyltransferase (cholinergic neurons)

ACE Acetylcholinesterase (cholinergic neurons)

CHDH Choline dehydrogenase (liver and kidney)

BADH Betaine aldehyde dehydrogenase (liver and kidney)

CK Choline kinase (all tissues)

CT CTP: phosphotransferase cytidylyltransferase (all tissues)

CPT Choline phosphotransferase (all tissues)

PEMT Phosphatidylethanolamine *N*-methyltransferase (liver)

The reaction intermediates of PEMT enzymatic activity are phosphatidylmonomethylethanolamine (PMME) and phosphatidyldimethylethanolamine (PDME). Other abbreviations include: ATP, adenosine triphosphate; ADP, adenosine diphosphate; CTP, cytidine triphosphate; CDP, cytidine diphosphate; CMP, cytidine monophosphate; CoA, coenzyme A; DAG, diacylglycerol; AdoMet, *S*-adenosylmethionine; AdoHcy, *S*-adenosylhomocysteine; PPi, pyrophosphate.

Figure 1.3

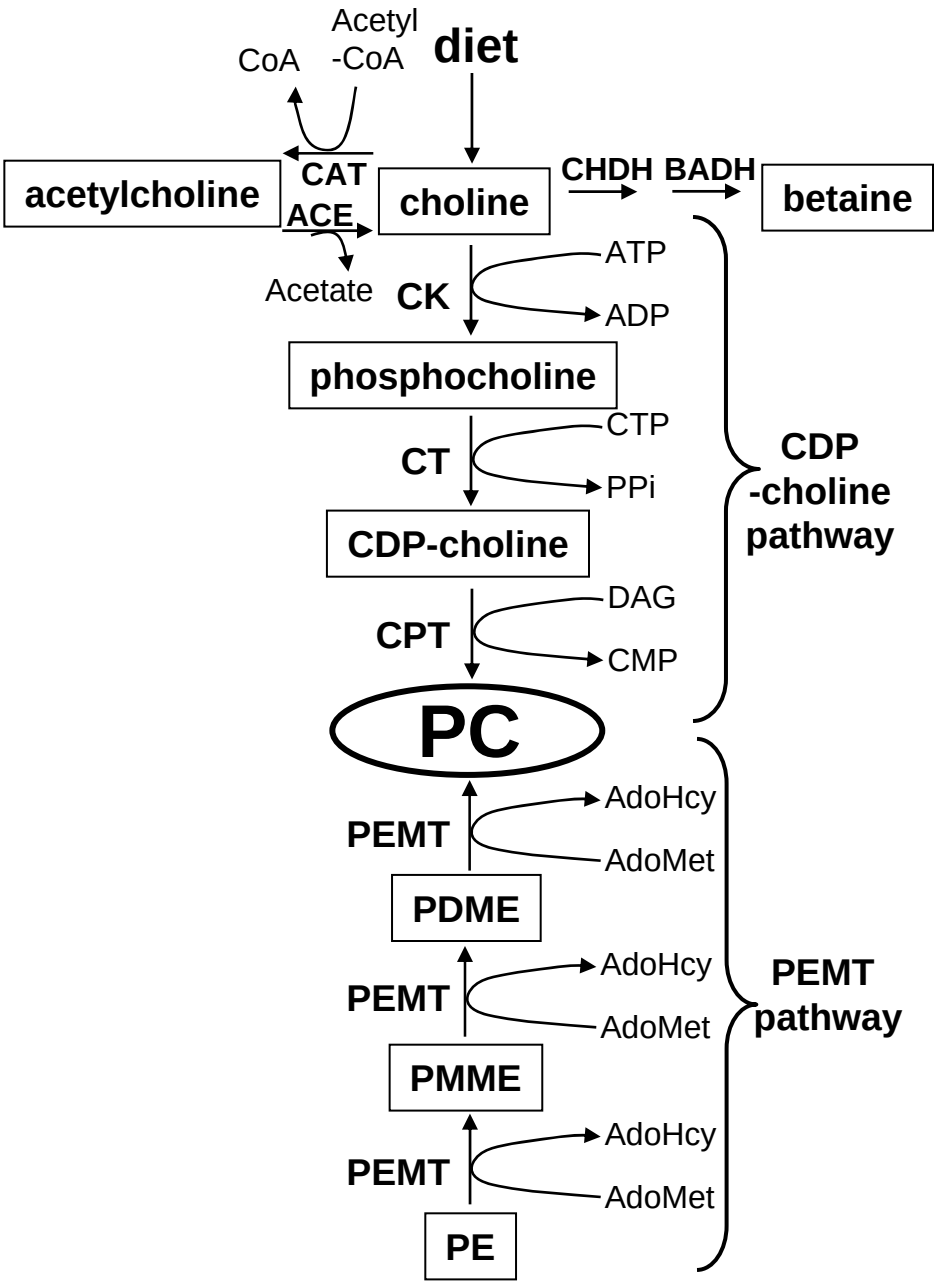
Acetyl
-CoA
CoA
diet
CAT
ACE
acetylcholine
choline
CHDH
BADH
betaine
Acetate
CK
ATP
ADP
phosphocholine
CT
CTP
PPi
CDP-choline
CPT
DAG
CMP
CDP
-choline
pathway
PC
PEMT
AdoHcy
AdoMet
PDME
PEMT
AdoHcy
AdoMet
PMME
PEMT
AdoHcy
AdoMet
PE
PEMT
pathway

Figure 1.4. Relationship between hepatic methionine and phosphatidylcholine metabolism.

S-adenosylmethionine (AdoMet) is a methyl donor for numerous methyltransferases, including phosphatidylethanolamine *N*-methyltransferase (PEMT). When a methyl group is removed from AdoMet, *S*-adenosylhomocysteine (AdoHcy) is formed and subsequently cleaved by AdoHcy hydrolase to generate homocysteine. Betaine-homocysteine methyltransferase (BHMT) uses betaine as a methyl donor to remethylate homocysteine and form dimethylglycine (DMG). Choline can be converted to betaine in a two step oxidation reaction catalyzed by choline dehydrogenase (CHDH) and betaine aldehyde dehydrogenase (BADH). Modified from Stead, *et al.* 2006. Am. J. Clin. Nutr. **83**:5-10.

Figure 1.4

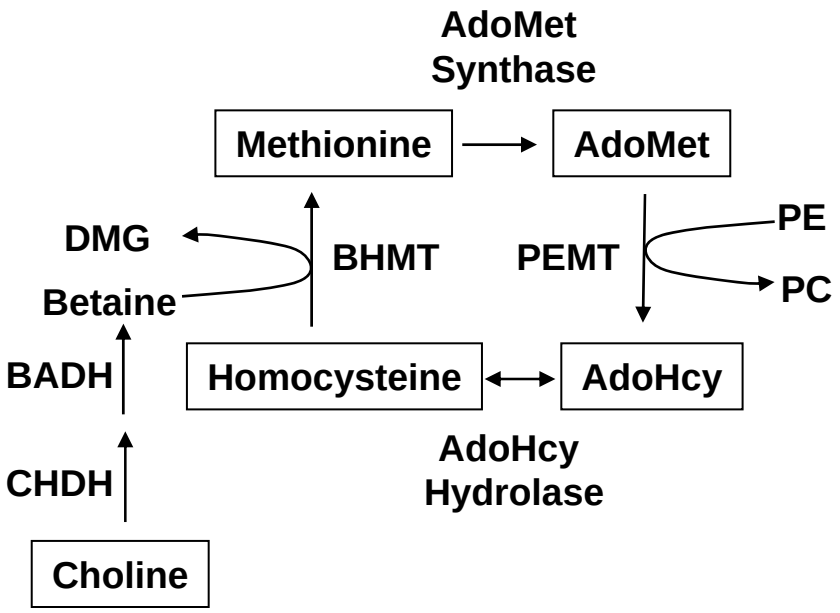
AdoMet
Synthase
Methionine
AdoMet
DMG
Betaine
BHMT
PEMT
PE
PC
BADH
Homocysteine
AdoHcy
AdoHcy
Hydrolase
CHDH
Choline

Figure 1.5. Genomic organization and topology of human *PEMT*.

(A) Schematic representation of the exon-intron organization of human *PEMT*. The introns are numbered with their corresponding sizes (kb). The exons, shown as boxes are aligned with the corresponding cDNA. The filled and unfilled boxes indicate untranslated and translated DNA regions, respectively. The three alternative transcriptional start sites and their accompanying cDNA transcripts are shown. The most abundant transcript in the liver contains exon II. (B) Membrane topology of PEMT. Four transmembrane domains span the ER membrane such that both the N and C termini are in the cytosol. Hydrophilic connecting loops are labelled A, B and C. The position of the AdoMet binding site (GXG, EE) and ER retrieval motif (xKxx) are as indicated. Modified from Shields *et al.,* 2001, Biochim. Biophys Acta, **1532:**105-114. and Shields *et al.,* 2003, JBC. **278**:2956-2962.

Figure 1.5

(A) Human *PEMT*

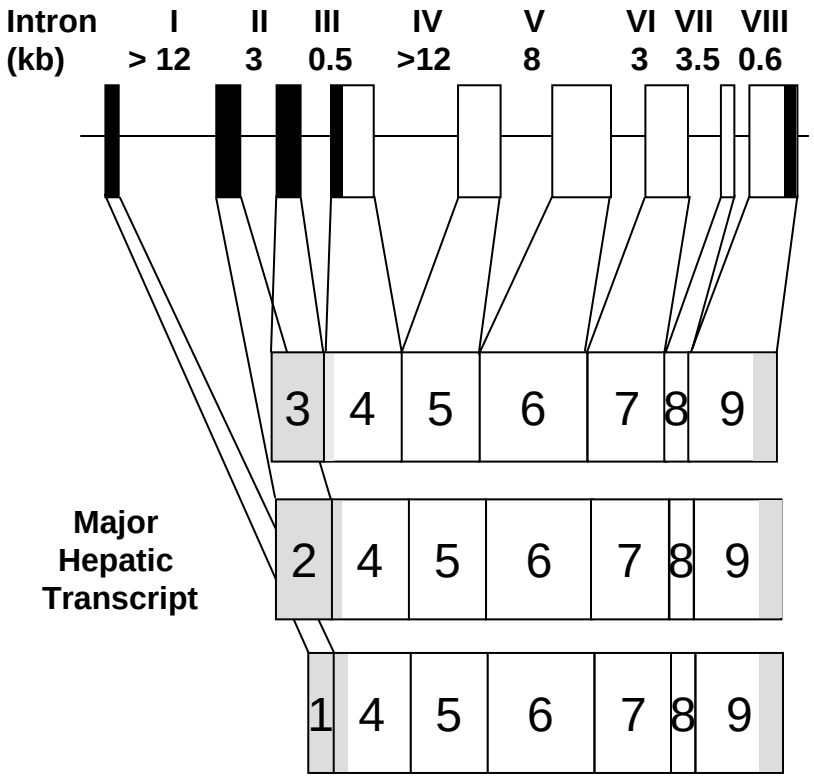

(B)

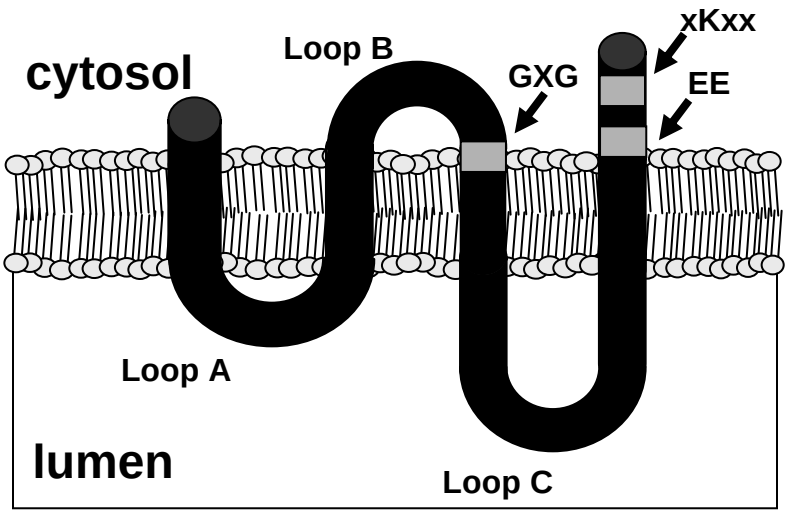

Figure 1.6. Genomic organization of mouse *Pemt*.

Schematic representation of the exon-intron organization of mouse *Pemt*. The introns are numbered with their corresponding sizes (kb). The exons, shown as boxes are aligned with the corresponding cDNA. The filled and unfilled boxes indicate untranslated and translated DNA regions, respectively. The transcript expressed predominantly in the liver is B. Two alternative transcriptional start sites have been predicted (striped boxes) and their accompanying transcripts are shown (transcript A and C). Modified from Walkey, *et al.* 1996. J. Lipid Res. **37**:2341-2350.

Figure 1.6

Mouse *Pemt*

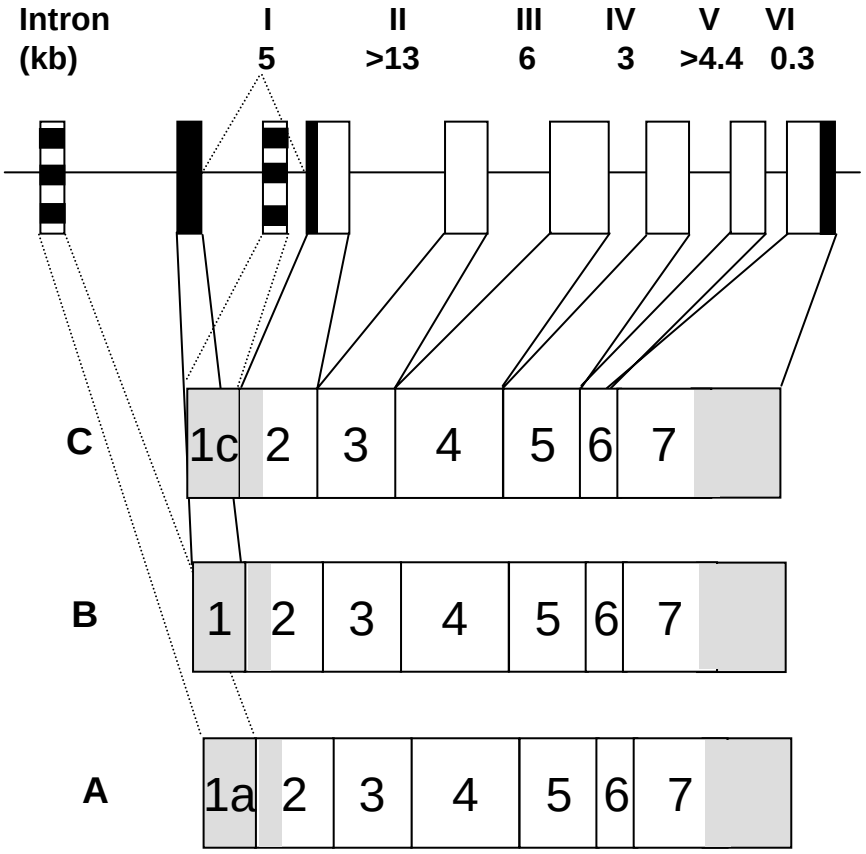

Figure 1.7. *PEMT* promoter alignment.

The mouse (m) and human (h) *PEMT* promoters shown are those which generate the major hepatic transcript for each species. The sequences are upstream of exon 1 (transcript B) for mice and exon 2 for humans. For each species the numbering refers to the transcriptional start site as number 1 (denoted with an asterix *). The nucleotides conserved between species are within shaded boxes. Analysis of the *PEMT* promoter revealed several conserved putative transcription factor binding sites including those for hepatic nuclear factor (HNF), activating protein-1 (AP-1), yin yang protein 1 (YY1), GATA and SP1.

Figure 1.7

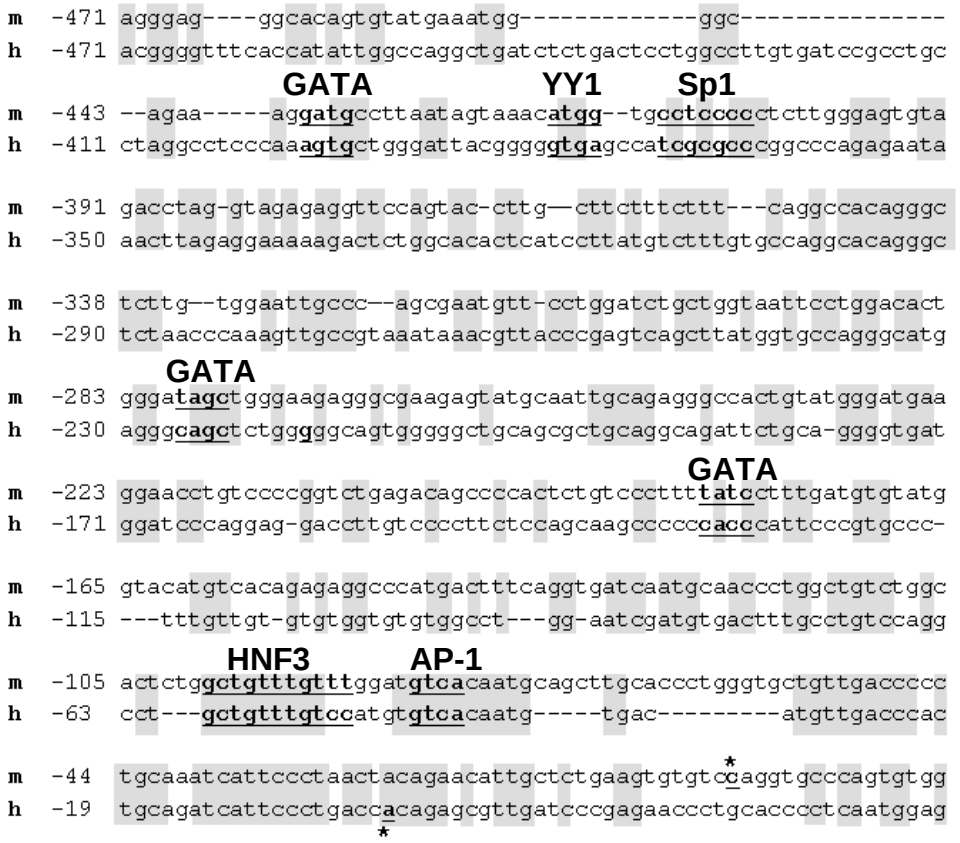

1.5 References

1. Gobley, M. (1850) *J. Pharm. Chim.* **17**, 401-407
2. Diakonow, C. (1868) *Zbl. Med. Wiss.* **2**, 434-435
3. Strecker, A. (1868) *Ann. Chem. Pharm.* **148**, 77-90
4. Baer, E., and Kates, M. (1950) *The Journal of biological chemistry* **185**(2), 615-623
5. Yamashita, A., Sugiura, T., and Waku, K. (1997) *Journal of biochemistry* **122**(1), 1-16
6. Vance, D. E. (2008) Phospholipid biosynthesis in eukaryotes. In: Vance, D. E., & Vance, J.E. (ed). *Biochemistry of Lipids, Lipoproteins and Membranes (pp. 214-244)*, 5 Ed., Elsevier, New York
7. Zachowski, A. (1993) *The Biochemical journal* **294 (Pt 1)**, 1-14
8. Kaplan, M. R., and Simoni, R. D. (1985) *The Journal of cell biology* **101**(2), 441-445
9. Sleight, R. G., and Pagano, R. E. (1984) *The Journal of cell biology* **99**(2), 742-751
10. van Helvoort, A., Smith, A. J., Sprong, H., Fritzsche, I., Schinkel, A. H., Borst, P., and van Meer, G. (1996) *Cell* **87**(3), 507-517
11. Kanno, K., Wu, M. K., Scapa, E. F., Roderick, S. L., and Cohen, D. E. (2007) *Biochimica et biophysica acta* **1771**(6), 654-662

12. Testerink, N., van der Sanden, M. M., Houweling, M., Helms, J. B., and Vaandrager, A. B. (2009) *Journal of lipid research* **50**(11), 2182-2192

13. Cribier, S., Morrot, G., Neumann, J. M., and Devaux, P. F. (1990) *Eur Biophys J* **18**(1), 33-41

14. Kumar, V. V. (1991) *Proceedings of the National Academy of Sciences of the United States of America* **88**(2), 444-448

15. Phillips, R., Ursell, T., Wiggins, P., and Sens, P. (2009) *Nature* **459**(7245), 379-385

16. Jenkins, G. M., and Frohman, M. A. (2005) *Cell Mol Life Sci* **62**(19-20), 2305-2316

17. Shimizu, T., Ohto, T., and Kita, Y. (2006) *IUBMB life* **58**(5-6), 328-333

18. van Meer, G., Voelker, D. R., and Feigenson, G. W. (2008) *Nature reviews* **9**(2), 112-124

19. Robinson, B. S., Yao, Z. M., Baisted, D. J., and Vance, D. E. (1989) *The Biochemical journal* **260**(1), 207-214

20. Houard, X., Ollivier, V., Louedec, L., Michel, J. B., and Back, M. (2009) *Faseb J* **23**(5), 1376-1383

21. Andrei, C., Margiocco, P., Poggi, A., Lotti, L. V., Torrisi, M. R., and Rubartelli, A. (2004) *Proceedings of the National Academy of Sciences of the United States of America* **101**(26), 9745-9750

22. Huang, P., Altshuller, Y. M., Hou, J. C., Pessin, J. E., and Frohman, M. A. (2005) *Molecular biology of the cell* **16**(6), 2614-2623

23. Kristiansen, S., Nielsen, J. N., Bourgoin, S., Klip, A., Franco, M., and Richter, E. A. (2001) *American journal of physiology* **281**(3), E608-618

24. Yea, K., Kim, J., Yoon, J. H., Kwon, T., Kim, J. H., Lee, B. D., Lee, H. J., Lee, S., Kim, J. I., Lee, T. G., Baek, M. C., Park, H. S., Park, K. S., Ohba, M., Suh, P. G., and Ryu, S. H. (2009) *The Journal of biological chemistry* **284**(49), 33833-33840

25. Colley, W. C., Sung, T. C., Roll, R., Jenco, J., Hammond, S. M., Altshuller, Y., Bar-Sagi, D., Morris, A. J., and Frohman, M. A. (1997) *Curr Biol* **7**(3), 191-201

26. Lehman, N., Di Fulvio, M., McCray, N., Campos, I., Tabatabaian, F., and Gomez-Cambronero, J. (2006) *Blood* **108**(10), 3564-3572

27. Spadaro, F., Ramoni, C., Mezzanzanica, D., Miotti, S., Alberti, P., Cecchetti, S., Iorio, E., Dolo, V., Canevari, S., and Podo, F. (2008) *Cancer research* **68**(16), 6541-6549

28. Zhao, J., Zhao, B., Wang, W., Huang, B., Zhang, S., and Miao, J. (2007) *Journal of cellular biochemistry* **102**(2), 421-428

29. Yao, C., Sakata, D., Esaki, Y., Li, Y., Matsuoka, T., Kuroiwa, K., Sugimoto, Y., and Narumiya, S. (2009) *Nature medicine* **15**(6), 633-640

30. Cheng, Y., Zhao, Q., Liu, X., Araki, S., Zhang, S., and Miao, J. (2006) *FEBS letters* **580**(20), 4911-4915

31. Saleem, S., Kim, Y. T., Maruyama, T., Narumiya, S., and Dore, S. (2009) *Journal of neuroimmunology* **208**(1-2), 87-93

32. Toschi, A., Lee, E., Xu, L., Garcia, A., Gadir, N., and Foster, D. A. (2009) *Molecular and cellular biology* **29**(6), 1411-1420

33. Perez-Gil, J. (2008) *Biochimica et biophysica acta* **1778**(7-8), 1676-1695

34. Goerke, J. (1998) *Biochimica et biophysica acta* **1408**(2-3), 79-89

35. Sherwood, L. (2001) The digestive system. In: Sherwood, L. (ed). *Human physiology from cells to humans (pp. 546-600)*, 4 Ed., Brooks/Cole a divsion of Thomson Learning, Pacific Grove, CA

36. Alvaro, D., Cantafora, A., Attili, A. F., Ginanni Corradini, S., De Luca, C., Minervini, G., Di Biase, A., and Angelico, M. (1986) *Comparative biochemistry and physiology* **83**(3), 551-554

37. Walkey, C. J., Yu, L., Agellon, L. B., and Vance, D. E. (1998) *The Journal of biological chemistry* **273**(42), 27043-27046

38. Rosmorduc, O., and Poupon, R. (2007) *Orphanet journal of rare diseases* **2**, 29

39. Smit, J. J., Schinkel, A. H., Oude Elferink, R. P., Groen, A. K., Wagenaar, E., van Deemter, L., Mol, C. A., Ottenhoff, R., van der Lugt, N. M., van Roon, M. A., and et al. (1993) *Cell* **75**(3), 451-462

40. de Vree, J. M., Jacquemin, E., Sturm, E., Cresteil, D., Bosma, P. J., Aten, J., Deleuze, J. F., Desrochers, M., Burdelski, M., Bernard, O., Oude Elferink, R. P., and Hadchouel, M. (1998) *Proceedings of the National Academy of Sciences of the United States of America* **95**(1), 282-287

41. Jacquemin, E., De Vree, J. M., Cresteil, D., Sokal, E. M., Sturm, E., Dumont, M., Scheffer, G. L., Paul, M., Burdelski, M., Bosma, P. J., Bernard, O., Hadchouel, M., and Elferink, R. P. (2001) *Gastroenterology* **120**(6), 1448-1458

42. Ziol, M., Barbu, V., Rosmorduc, O., Frassati-Biaggi, A., Barget, N., Hermelin, B., Scheffer, G. L., Bennouna, S., Trinchet, J. C., Beaugrand, M., and Ganne-Carrie, N. (2008) *Gastroenterology* **135**(1), 131-141

43. Degiorgio, D., Colombo, C., Seia, M., Porcaro, L., Costantino, L., Zazzeron, L., Bordo, D., and Coviello, D. A. (2007) *Eur J Hum Genet* **15**(12), 1230-1238

44. Rosmorduc, O., Hermelin, B., and Poupon, R. (2001) *Gastroenterology* **120**(6), 1459-1467

45. Delaunay, J. L., Durand-Schneider, A. M., Delautier, D., Rada, A., Gautherot, J., Jacquemin, E., Ait-Slimane, T., and Maurice, M. (2009) *Hepatology (Baltimore, Md* **49**(4), 1218-1227

46. Jonas, A., Phillips, M.A.,. (2008) Lipoprotein structure. In: Vance, D. E., and Vance, J.E. (ed). *Biochemistry of Lipids, Lipoproteins and Membranes (pp. 485-506)*, 5 Ed., Elsevier, New York

47. Skipski, V. P., Barclay, M., Barclay, R. K., Fetzer, V. A., Good, J. J., and Archibald, F. M. (1967) *The Biochemical journal* **104**(2), 340-352

48. Rousset, X., Vaisman, B., Amar, M., Sethi, A. A., and Remaley, A. T. (2009) *Current opinion in endocrinology, diabetes, and obesity* **16**(2), 163-171

49. Kennedy, E. P., and Weiss, S. B. (1956) *The Journal of biological chemistry* **222**(1), 193-214

50. Sundler, R., and Akesson, B. (1975) *The Journal of biological chemistry* **250**(9), 3359-3367

51. Vance, J. E. (2008) *Journal of lipid research* **49**(7), 1377-1387

52. Shindou, H., and Shimizu, T. (2009) *The Journal of biological chemistry* **284**(1), 1-5

53. Best, C. H., and Huntsman, M. E. (1932) *The Journal of physiology* **75**(4), 405-412

54. Inst. Med., N. A. S. U. C. *Washington, DC:Natl. Acad. Press*, 390-422

55. Fischer, L. M., Scearce, J. A., Mar, M. H., Patel, J. R., Blanchard, R. T., Macintosh, B. A., Busby, M. G., and Zeisel, S. H. (2005) *The Journal of nutrition* **135**(4), 826-829

56. Savendahl, L., Mar, M. H., Underwood, L. E., and Zeisel, S. H. (1997) *The American journal of clinical nutrition* **66**(3), 622-625

57. Wardlaw, G. M. (1999) The water-soluble vitamins. In: Wardlaw, G. M. (ed). *Perpectives in nutrition (pp. 413-462)*, 4 Ed., McGraw-Hill, New York

58. Blusztajn, J. K. (1998) *Science (New York, N.Y* **281**(5378), 794-795

59. Garner, S. C., Mar, M. H., and Zeisel, S. H. (1995) *The Journal of nutrition* **125**(11), 2851-2858

60. McMahon, K. E., and Farrell, P. M. (1985) *Clinica chimica acta; international journal of clinical chemistry* **149**(1), 1-12

61. Shaw, G. M., Carmichael, S. L., Yang, W., Selvin, S., and Schaffer, D. M. (2004) *American journal of epidemiology* **160**(2), 102-109

62. Craciunescu, C. N., Albright, C. D., Mar, M. H., Song, J., and Zeisel, S. H. (2003) *The Journal of nutrition* **133**(11), 3614-3618

63. Cheng, R. K., MacDonald, C. J., Williams, C. L., and Meck, W. H. (2008) *Learning & memory (Cold Spring Harbor, N.Y* **15**(3), 153-162

64. Fischer, L. M., daCosta, K. A., Kwock, L., Stewart, P. W., Lu, T. S., Stabler, S. P., Allen, R. H., and Zeisel, S. H. (2007) *The American journal of clinical nutrition* **85**(5), 1275-1285

65. Buchman, A. L., Ament, M. E., Sohel, M., Dubin, M., Jenden, D. J., Roch, M., Pownall, H., Farley, W., Awal, M., and Ahn, C. (2001) *Jpen* **25**(5), 260-268

66. Buchman, A. L., Dubin, M. D., Moukarzel, A. A., Jenden, D. J., Roch, M., Rice, K. M., Gornbein, J., and Ament, M. E. (1995) *Hepatology (Baltimore, Md* **22**(5), 1399-1403

67. da Costa, K. A., Badea, M., Fischer, L. M., and Zeisel, S. H. (2004) *The American journal of clinical nutrition* **80**(1), 163-170

68. Bianchi, G., and Azzone, G. F. (1964) *The Journal of biological chemistry* **239**, 3947-3955

69. Tsuge, H., Nakano, Y., Onishi, H., Futamura, Y., and Ohashi, K. (1980) *Biochimica et biophysica acta* **614**(2), 274-284

70. Kaiser, W., and Bygrave, F. L. (1968) *European journal of biochemistry / FEBS* **4**(4), 582-585

71. Craig, S. A. (2004) *The American journal of clinical nutrition* **80**(3), 539-549

72. Bussiere, M., Vance, J. E., Campenot, R. B., and Vance, D. E. (2001) *Journal of biochemistry* **130**(4), 561-568

73. Blusztajn, J. K., Holbrook, P. G., Lakher, M., Liscovitch, M., Maire, J. C., Mauron, C., Richardson, U. I., Tacconi, M., and Wurtman, R. J. (1986) *Psychopharmacology bulletin* **22**(3), 781-786

74. Blusztajn, J. K., Liscovitch, M., and Richardson, U. I. (1987) *Proceedings of the National Academy of Sciences of the United States of America* **84**(15), 5474-5477

75. Michel, V., Yuan, Z., Ramsubir, S., and Bakovic, M. (2006) *Experimental biology and medicine (Maywood, N.J* **231**(5), 490-504

76. Kwon, Y., Lee, R. D., and Morris, M. E. (1996) *The Journal of pharmacology and experimental therapeutics* **279**(2), 774-781

77. Sinclair, C. J., Chi, K. D., Subramanian, V., Ward, K. L., and Green, R. M. (2000) *Journal of lipid research* **41**(11), 1841-1848

78. Michel, V., and Bakovic, M. (2009) *Faseb J* **23**(8), 2749-2758

79. Aoyama, C., Liao, H., and Ishidate, K. (2004) *Progress in lipid research* **43**(3), 266-281

80. Wittenberg, J., and Kornberg, A. (1953) *The Journal of biological chemistry* **202**(1), 431-444

81. Aoyama, C., Nakashima, K., Matsui, M., and Ishidate, K. (1998) *Biochimica et biophysica acta* **1390**(1), 1-7

82. Aoyama, C., Yamazaki, N., Terada, H., and Ishidate, K. (2000) *Journal of lipid research* **41**(3), 452-464

83. Aoyama, C., Nakashima, K., and Ishidate, K. (1998) *Biochimica et biophysica acta* **1393**(1), 179-185

84. Aoyama, C., Ohtani, A., and Ishidate, K. (2002) *The Biochemical journal* **363**(Pt 3), 777-784

85. Liao, H., Aoyama, C., Ishidate, K., and Teraoka, H. (2006) *Biochimica et biophysica acta* **1761**(1), 111-120

86. Porter, T. J., and Kent, C. (1990) *The Journal of biological chemistry* **265**(1), 414-422

87. Ishidate, K., Furusawa, K., and Nakazawa, Y. (1985) *Biochimica et biophysica acta* **836**(1), 119-124

88. Aoyama, C., Ishidate, K., Sugimoto, H., and Vance, D. E. (2007) *Biochimica et biophysica acta* **1771**(9), 1148-1155

89. Wu, G., Aoyama, C., Young, S. G., and Vance, D. E. (2008) *The Journal of biological chemistry* **283**(3), 1456-1462

90. Wu, G., Sher, R. B., Cox, G. A., and Vance, D. E. (2009) *Biochimica et biophysica acta* **1791**(5), 347-356

91. Crilly, K. S., Tomono, M., and Kiss, Z. (1998) *Archives of biochemistry and biophysics* **352**(1), 137-143

92. Ramirez de Molina, A., Penalva, V., Lucas, L., and Lacal, J. C. (2002) *Oncogene* **21**(6), 937-946

93. Chung, T., Huang, J. S., Mukherjee, J. J., Crilly, K. S., and Kiss, Z. (2000) *Cellular signalling* **12**(5), 279-288

94. Jimenez, B., del Peso, L., Montaner, S., Esteve, P., and Lacal, J. C. (1995) *Journal of cellular biochemistry* **57**(1), 141-149

95. Cuadrado, A., Carnero, A., Dolfi, F., Jimenez, B., and Lacal, J. C. (1993) *Oncogene* **8**(11), 2959-2968

96. Ko, K. W., Cook, H. W., and Vance, D. E. (1986) *The Journal of biological chemistry* **261**(17), 7846-7852

97. Vigo, C., and Vance, D. E. (1981) *The Biochemical journal* **200**(2), 321-326

98. Ramirez de Molina, A., Gallego-Ortega, D., Sarmentero-Estrada, J., Lagares, D., Gomez Del Pulgar, T., Bandres, E., Garcia-Foncillas,

J., and Lacal, J. C. (2008) *The international journal of biochemistry & cell biology* **40**(9), 1753-1763

99. Smith, T. A., Bush, C., Jameson, C., Titley, J. C., Leach, M. O., Wilman, D. E., and McCready, V. R. (1993) *NMR in biomedicine* **6**(5), 318-323

100. Ramirez de Molina, A., Banez-Coronel, M., Gutierrez, R., Rodriguez-Gonzalez, A., Olmeda, D., Megias, D., and Lacal, J. C. (2004) *Cancer research* **64**(18), 6732-6739

101. Ramirez de Molina, A., Sarmentero-Estrada, J., Belda-Iniesta, C., Taron, M., Ramirez de Molina, V., Cejas, P., Skrzypski, M., Gallego-Ortega, D., de Castro, J., Casado, E., Garcia-Cabezas, M. A., Sanchez, J. J., Nistal, M., Rosell, R., Gonzalez-Baron, M., and Lacal, J. C. (2007) *The lancet oncology* **8**(10), 889-897

102. Hernando, E., Sarmentero-Estrada, J., Koppie, T., Belda-Iniesta, C., Ramirez de Molina, V., Cejas, P., Ozu, C., Le, C., Sanchez, J. J., Gonzalez-Baron, M., Koutcher, J., Cordon-Cardo, C., Bochner, B. H., Lacal, J. C., and Ramirez de Molina, A. (2009) *Oncogene* **28**(26), 2425-2435

103. Al-Saffar, N. M., Troy, H., Ramirez de Molina, A., Jackson, L. E., Madhu, B., Griffiths, J. R., Leach, M. O., Workman, P., Lacal, J. C., Judson, I. R., and Chung, Y. L. (2006) *Cancer research* **66**(1), 427-434

104. Sher, R. B., Aoyama, C., Huebsch, K. A., Ji, S., Kerner, J., Yang, Y., Frankel, W. N., Hoppel, C. L., Wood, P. A., Vance, D. E., and Cox, G. A. (2006) *The Journal of biological chemistry* **281**(8), 4938-4948

105. Sundler, R., Arvidson, G., and Akesson, B. (1972) *Biochimica et biophysica acta* **280**(4), 559-568

106. Vance, D. E., Trip, E. M., and Paddon, H. B. (1980) *The Journal of biological chemistry* **255**(3), 1064-1069

107. Kennedy, E. P. (1956) *The Journal of biological chemistry* **222**(1), 185-191

108. Kalmar, G. B., Kay, R. J., Lachance, A., Aebersold, R., and Cornell, R. B. (1990) *Proceedings of the National Academy of Sciences of the United States of America* **87**(16), 6029-6033

109. Lykidis, A., Murti, K. G., and Jackowski, S. (1998) *The Journal of biological chemistry* **273**(22), 14022-14029

110. Lykidis, A., Baburina, I., and Jackowski, S. (1999) *The Journal of biological chemistry* **274**(38), 26992-27001

111. Tang, W., Keesler, G. A., and Tabas, I. (1997) *The Journal of biological chemistry* **272**(20), 13146-13151

112. Rutherford, M. S., Rock, C. O., Jenkins, N. A., Gilbert, D. J., Tessner, T. G., Copeland, N. G., and Jackowski, S. (1993) *Genomics* **18**(3), 698-701

113. Karim, M., Jackson, P., and Jackowski, S. (2003) *Biochimica et biophysica acta* **1633**(1), 1-12

114. Wang, Y., MacDonald, J. I., and Kent, C. (1995) *The Journal of biological chemistry* **270**(1), 354-360

115. Sleight, R., and Kent, C. (1980) *The Journal of biological chemistry* **255**(22), 10644-10650

116. Pelech, S. L., Pritchard, P. H., Brindley, D. N., and Vance, D. E. (1983) *The Biochemical journal* **216**(1), 129-136

117. Pelech, S. L., Paddon, H. B., and Vance, D. E. (1984) *Biochimica et biophysica acta* **795**(3), 447-451

118. Pelech, S. L., Cook, H. W., Paddon, H. B., and Vance, D. E. (1984) *Biochimica et biophysica acta* **795**(3), 433-440

119. Dunne, S. J., Cornell, R. B., Johnson, J. E., Glover, N. R., and Tracey, A. S. (1996) *Biochemistry* **35**(37), 11975-11984

120. Pelech, S. L., Pritchard, P. H., Brindley, D. N., and Vance, D. E. (1983) *The Journal of biological chemistry* **258**(11), 6782-6788

121. Utal, A. K., Jamil, H., and Vance, D. E. (1991) *The Journal of biological chemistry* **266**(35), 24084-24091

122. Gehrig, K., Lagace, T. A., and Ridgway, N. D. (2009) *The Biochemical journal* **418**(1), 209-217

123. Cornell, R. B. (1991) *Biochemistry* **30**(24), 5873-5880

124. Davies, S. M., Epand, R. M., Kraayenhof, R., and Cornell, R. B. (2001) *Biochemistry* **40**(35), 10522-10531

125. Gehrig, K., Morton, C. C., and Ridgway, N. D. (2009) *Journal of lipid research* **50**(5), 966-976

126. Watkins, J. D., and Kent, C. (1992) *The Journal of biological chemistry* **267**(8), 5686-5692

127. Vance, J. E., and Vance, D. E. (1988) *The Journal of biological chemistry* **263**(12), 5898-5909

128. Northwood, I. C., Tong, A. H., Crawford, B., Drobnies, A. E., and Cornell, R. B. (1999) *The Journal of biological chemistry* **274**(37), 26240-26248

129. Houweling, M., Cui, Z., Anfuso, C. D., Bussiere, M., Chen, M. H., and Vance, D. E. (1996) *European journal of cell biology* **69**(1), 55-63

130. Yang, W., and Jackowski, S. (1995) *The Journal of biological chemistry* **270**(28), 16503-16506

131. Wang, Y., and Kent, C. (1995) *The Journal of biological chemistry* **270**(30), 17843-17849

132. Shiratori, Y., Houweling, M., Zha, X., and Tabas, I. (1995) *The Journal of biological chemistry* **270**(50), 29894-29903

133. Lee, J., Johnson, J. E., Ding, Z., Paetzel, M., and Cornell, R. B. (2009) *The Journal of biological chemistry* **284**(48), 33535-33548

134. Bakovic, M., Waite, K., Tang, W., Tabas, I., and Vance, D. E. (1999) *Biochimica et biophysica acta* **1438**(1), 147-165

135. Bakovic, M., Waite, K., and Vance, D. E. (2003) *The Journal of biological chemistry* **278**(17), 14753-14761

136. Marcucci, H., Elena, C., Gilardoni, P., and Banchio, C. (2008) *Biochimica et biophysica acta* **1781**(5), 254-262

137. McCoy, D. M., Fisher, K., Robichaud, J., Ryan, A. J., and Mallampalli, R. K. (2006) *American journal of respiratory cell and molecular biology* **35**(3), 394-402

138. Banchio, C., Schang, L. M., and Vance, D. E. (2003) *The Journal of biological chemistry* **278**(34), 32457-32464

139. Golfman, L. S., Bakovic, M., and Vance, D. E. (2001) *The Journal of biological chemistry* **276**(47), 43688-43692

140. Sesca, E., Perletti, G. P., Binasco, V., Chiara, M., and Tessitore, L. (1996) *Biochemical and biophysical research communications* **229**(1), 158-162

141. Banchio, C., Schang, L. M., and Vance, D. E. (2004) *The Journal of biological chemistry* **279**(38), 40220-40226

142. Bakovic, M., Waite, K. A., and Vance, D. E. (2000) *Journal of lipid research* **41**(4), 583-594

143. Banchio, C., Lingrell, S., and Vance, D. E. (2006) *The Journal of biological chemistry* **281**(15), 10010-10015

144. Banchio, C., Lingrell, S., and Vance, D. E. (2007) *The Journal of biological chemistry* **282**(20), 14827-14835

145. Sugimoto, H., Sugimoto, S., Tatei, K., Obinata, H., Bakovic, M., Izumi, T., and Vance, D. E. (2003) *The Journal of biological chemistry* **278**(22), 19716-19722

146. Sugimoto, H., Bakovic, M., Yamashita, S., and Vance, D. E. (2001) *The Journal of biological chemistry* **276**(15), 12338-12344

147. Wang, L., Magdaleno, S., Tabas, I., and Jackowski, S. (2005) *Molecular and cellular biology* **25**(8), 3357-3363

148. Zhang, D., Tang, W., Yao, P. M., Yang, C., Xie, B., Jackowski, S., and Tabas, I. (2000) *The Journal of biological chemistry* **275**(45), 35368-35376

149. Tian, Y., Pate, C., Andreolotti, A., Wang, L., Tuomanen, E., Boyd, K., Claro, E., and Jackowski, S. (2008) *The Journal of cell biology* **181**(6), 945-957

150. Tian, Y., Zhou, R., Rehg, J. E., and Jackowski, S. (2007) *Molecular and cellular biology* **27**(3), 975-982

151. Jacobs, R. L., Devlin, C., Tabas, I., and Vance, D. E. (2004) *The Journal of biological chemistry* **279**(45), 47402-47410

152. Jacobs, R. L., Lingrell, S., Zhao, Y., Francis, G. A., and Vance, D. E. (2008) *The Journal of biological chemistry* **283**(4), 2147-2155

153. Jackowski, S., Rehg, J. E., Zhang, Y. M., Wang, J., Miller, K., Jackson, P., and Karim, M. A. (2004) *Molecular and cellular biology* **24**(11), 4720-4733

154. Gunter, C., Frank, M., Tian, Y., Murti, K. G., Rehg, J. E., and Jackowski, S. (2007) *Biochimica et biophysica acta* **1771**(7), 845-852

155. Carter, J. M., Demizieux, L., Campenot, R. B., Vance, D. E., and Vance, J. E. (2008) *The Journal of biological chemistry* **283**(1), 202-212

156. Carter, J. M., Waite, K. A., Campenot, R. B., Vance, J. E., and Vance, D. E. (2003) *The Journal of biological chemistry* **278**(45), 44988-44994

157. Weiss, S. B., Smith, S. W., and Kennedy, E. P. (1958) *The Journal of biological chemistry* **231**(1), 53-64

158. Wilgram, G. F., and Kennedy, E. P. (1963) *The Journal of biological chemistry* **238**, 2615-2619

159. Jelsema, C. L., and Morre, D. J. (1978) *The Journal of biological chemistry* **253**(21), 7960-7971

160. McMaster, C. R., and Bell, R. M. (1997) *Biochimica et biophysica acta* **1348**(1-2), 100-110

161. Higgins, J. A., and Fieldsend, J. K. (1987) *Journal of lipid research* **28**(3), 268-278

162. Henneberry, A. L., Wright, M. M., and McMaster, C. R. (2002) *Molecular biology of the cell* **13**(9), 3148-3161

163. Mancini, A., Roberti, R., Binaglia, L., el Missiri, A., and Freysz, L. (1993) *Membrane biochemistry* **10**(1), 43-52

164. Ishidate, K., Matsuo, R., and Nakazawa, Y. (1993) *Lipids* **28**(2), 89-96

165. McMaster, C. R., and Bell, R. M. (1994) *The Journal of biological chemistry* **269**(45), 28010-28016

166. Hjelmstad, R. H., and Bell, R. M. (1990) *The Journal of biological chemistry* **265**(3), 1755-1764

167. Henneberry, A. L., and McMaster, C. R. (1999) *The Biochemical journal* **339 (Pt 2)**, 291-298

168. Henneberry, A. L., Wistow, G., and McMaster, C. R. (2000) *The Journal of biological chemistry* **275**(38), 29808-29815

169. Wright, M. M., and McMaster, C. R. (2002) *Lipids* **37**(7), 663-672

170. Jamil, H., Utal, A. K., and Vance, D. E. (1992) *The Journal of biological chemistry* **267**(3), 1752-1760

171. Sinha Roy, S., Mukherjee, S., Kabir, S., Rajaratnam, V., Smith, M., and Das, S. K. (2005) *Journal of biochemical and molecular toxicology* **19**(5), 289-297

172. Voziyan, P. A., Goldner, C. M., and Melnykovych, G. (1993) *The Biochemical journal* **295 (Pt 3)**, 757-762

173. Stetten, D. (1941) *The Journal of biological chemistry* **138**, 437-438

174. Du Vigneaud, V., Cohn, M. (1941) *The Journal of biological chemistry* **140**, 625-641

175. Bremer, J., and Greenberg, D. M. (1959) *Biochimica et biophysica acta* **35**, 287-288

176. Bremer, J., and Greenberg, D. M. (1960) *Biochimica et biophysica acta* **37**, 173-175

177. Bremer, J., and Greenberg, D. M. (1961) *Biochimica et biophysica acta* **46**, 205-216

178. Gibson, K. D., Wilson, J. D., and Udenfriend, S. (1961) *The Journal of biological chemistry* **236**, 673-679

179. Ridgway, N. D., and Vance, D. E. (1988) *The Journal of biological chemistry* **263**(32), 16864-16871

180. Ridgway, N. D., and Vance, D. E. (1987) *The Journal of biological chemistry* **262**(35), 17231-17239

181. Reo, N. V., Adinehzadeh, M., and Foy, B. D. (2002) *Biochimica et biophysica acta* **1580**(2-3), 171-188

182. Schneider, W. J., and Vance, D. E. (1979) *The Journal of biological chemistry* **254**(10), 3886-3891

183. Tanaka, Y., Doi, O., and Akamatsu, Y. (1979) *Biochemical and biophysical research communications* **87**(4), 1109-1115

184. Vance, D. E., and Ridgway, N. D. (1988) *Progress in lipid research* **27**(1), 61-79

185. Ridgway, N. D., and Vance, D. E. (1988) *The Journal of biological chemistry* **263**(32), 16856-16863

186. Samborski, R. W., Ridgway, N. D., and Vance, D. E. (1990) *The Journal of biological chemistry* **265**(30), 18322-18329

187. DeLong, C. J., Shen, Y. J., Thomas, M. J., and Cui, Z. (1999) *The Journal of biological chemistry* **274**(42), 29683-29688

188. Cui, Z., Vance, J. E., Chen, M. H., Voelker, D. R., and Vance, D. E. (1993) *The Journal of biological chemistry* **268**(22), 16655-16663

189. Walkey, C. J., Cui, Z., Agellon, L. B., and Vance, D. E. (1996) *Journal of lipid research* **37**(11), 2341-2350

190. Walkey, C. J., Shields, D. J., and Vance, D. E. (1999) *Biochimica et biophysica acta* **1436**(3), 405-412

191. Shields, D. J., Agellon, L. B., and Vance, D. E. (2001) *Biochimica et biophysica acta* **1532**(1-2), 105-114

192. Resseguie, M., Song, J., Niculescu, M. D., da Costa, K. A., Randall, T. A., and Zeisel, S. H. (2007) *Faseb J* **21**(10), 2622-2632

193. van Golde, L. M., Raben, J., Batenburg, J. J., Fleischer, B., Zambrano, F., and Fleischer, S. (1974) *Biochimica et biophysica acta* **360**(2), 179-192

194. Shields, D. J., Lehner, R., Agellon, L. B., and Vance, D. E. (2003) *The Journal of biological chemistry* **278**(5), 2956-2962

195. Vance, J. E. (1990) *The Journal of biological chemistry* **265**(13), 7248-7256

196. Hayashi, T., Rizzuto, R., Hajnoczky, G., and Su, T. P. (2009) *Trends in cell biology* **19**(2), 81-88

197. Voelker, D. R. (2005) *Trends in biochemical sciences* **30**(7), 396-404

198. Shields, D. J., Lingrell, S., Agellon, L. B., Brosnan, J. T., and Vance, D. E. (2005) *The Journal of biological chemistry* **280**(29), 27339-27344

199. Rusinol, A. E., Cui, Z., Chen, M. H., and Vance, J. E. (1994) *The Journal of biological chemistry* **269**(44), 27494-27502

200. Stone, S. J., and Vance, J. E. (2000) *The Journal of biological chemistry* **275**(44), 34534-34540

201. Stone, S. J., Levin, M. C., Zhou, P., Han, J., Walther, T. C., and Farese, R. V., Jr. (2009) *The Journal of biological chemistry* **284**(8), 5352-5361

202. Lewin, T. M., Kim, J. H., Granger, D. A., Vance, J. E., and Coleman, R. A. (2001) *The Journal of biological chemistry* **276**(27), 24674-24679

203. Vance, D. E., Choy, P. C., Farren, S. B., Lim, P. H., and Schneider, W. J. (1977) *Nature* **270**(5634), 268-269

204. Audubert, F., and Vance, D. E. (1984) *Biochimica et biophysica acta* **792**(3), 359-362

205. Shields, D. J., Altarejos, J. Y., Wang, X., Agellon, L. B., and Vance, D. E. (2003) *The Journal of biological chemistry* **278**(37), 35826-35836

206. Akesson, B. (1978) *FEBS letters* **92**(2), 177-180

207. Hoffman, D. R., Marion, D. W., Cornatzer, W. E., and Duerre, J. A. (1980) *The Journal of biological chemistry* **255**(22), 10822-10827

208. Chiang, P. K., and Cantoni, G. L. (1979) *Biochemical pharmacology* **28**(12), 1897-1902

209. Chiang, P. K., Richards, H. H., and Cantoni, G. L. (1977) *Molecular pharmacology* **13**(5), 939-947

210. Pritchard, P. H., Chiang, P. K., Cantoni, G. L., and Vance, D. E. (1982) *The Journal of biological chemistry* **257**(11), 6362-6367

211. Schanche, J. S., Schanche, T., and Ueland, P. M. (1982) *Biochimica et biophysica acta* **721**(4), 399-407

212. Geelen, M. J., Groener, J. E., De Haas, C. G., and Van Golde, L. M. (1979) *FEBS letters* **105**(1), 27-30

213. Pelech, S. L., Pritchard, P. H., Sommerman, E. F., Percival-Smith, A., and Vance, D. E. (1984) *Canadian journal of biochemistry and cell biology = Revue canadienne de biochimie et biologie cellulaire* **62**(4), 196-202

214. Pelech, S. L., Ozen, N., Audubert, F., and Vance, D. E. (1986) *Biochemistry and cell biology = Biochimie et biologie cellulaire* **64**(6), 565-574

215. Pritchard, P. H., Pelech, S. L., and Vance, D. E. (1981) *Biochimica et biophysica acta* **666**(2), 301-306

216. Castano, J. G., Alemany, S., Nieto, A., and Mato, J. M. (1980) *The Journal of biological chemistry* **255**(19), 9041-9043

217. Marin-Cao, D., Alvarez Chiva, V., and Mato, J. M. (1983) *The Biochemical journal* **216**(3), 675-680

218. Ridgway, N. D., and Vance, D. E. (1989) *Biochimica et biophysica acta* **1004**(2), 261-270

219. Chiva, V. A., Cao, D. M., and Mato, J. M. (1983) *FEBS letters* **160**(1-2), 101-104

220. Merida, I., and Mato, J. M. (1987) *Biochimica et biophysica acta* **928**(1), 92-97

221. Alemany, S., Varela, I., and Mato, J. M. (1981) *FEBS letters* **135**(1), 111-114

222. Young, D. L. (1971) *Journal of lipid research* **12**(5), 590-595

223. Alemany, S., Varela, I., Harper, J. F., and Mato, J. M. (1982) *The Journal of biological chemistry* **257**(16), 9249-9251

224. Blusztajn, J. K., Zeisel, S. H., and Wurtman, R. J. (1985) *The Biochemical journal* **232**(2), 505-511

225. Zhu, X., Mar, M. H., Song, J., and Zeisel, S. H. (2004) *Brain research* **149**(2), 121-129

226. Chiappe de Cingolani, G. E. (1992) *Molecular and cellular biochemistry* **115**(1), 97-103

227. Panagia, V., Taira, Y., Ganguly, P. K., Tung, S., and Dhalla, N. S. (1990) *The Journal of clinical investigation* **86**(3), 777-784

228. Persad, S., and Panagia, V. (1995) *Journal of molecular and cellular cardiology* **27**(1), 579-587

229. Cui, Z., Shen, Y. J., and Vance, D. E. (1997) *Biochimica et biophysica acta* **1346**(1), 10-16

230. Gruppuso, P. A., Awad, M., Bienieki, T. C., Boylan, J. M., Fernando, S., and Faris, R. A. (1997) *In vitro cellular & developmental biology* **33**(7), 562-568

231. Cornatzer, W. E., Hoffman, D. R., and Haning, J. A. (1984) *Lipids* **19**(1), 1-4

232. Michalopoulos, G. K. (2007) *Journal of cellular physiology* **213**(2), 286-300

233. Taub, R. (2004) *Nature reviews* **5**(10), 836-847

234. Houweling, M., Cui, Z., Tessitore, L., and Vance, D. E. (1997) *Biochimica et biophysica acta* **1346**(1), 1-9

235. Baker, T. K., Carfagna, M. A., Gao, H., Dow, E. R., Li, Q., Searfoss, G. H., and Ryan, T. P. (2001) *Chemical research in toxicology* **14**(9), 1218-1231

236. Clayton, D. F., and Darnell, J. E., Jr. (1983) *Molecular and cellular biology* **3**(9), 1552-1561

237. Clayton, D. F., Harrelson, A. L., and Darnell, J. E., Jr. (1985) *Molecular and cellular biology* **5**(10), 2623-2632

238. Walkey, C. J. (1998) Evolutionary and nutritional importance of phospholipid methylation. In. *Biochemistry*, University of Alberta, Edmonton

239. Cui, Z., Houweling, M., and Vance, D. E. (1994) *The Journal of biological chemistry* **269**(40), 24531-24533

240. Boess, F., Kamber, M., Romer, S., Gasser, R., Muller, D., Albertini, S., and Suter, L. (2003) *Toxicol Sci* **73**(2), 386-402

241. Guillouzo, A., Corlu, A., Aninat, C., Glaise, D., Morel, F., and Guguen-Guillouzo, C. (2007) *Chemico-biological interactions* **168**(1), 66-73

242. Xu, C. S., Chang, C. F., Yuan, J. Y., Li, W. Q., Han, H. P., Yang, K. J., Zhao, L. F., Li, Y. C., Zhang, H. Y., Rahman, S., and Zhang, J. B. (2005) *World J Gastroenterol* **11**(19), 2932-2940

243. Xu, C. S., Shao, H. Y., Liu, S. S., Qin, B., Sun, X. F., and Tian, L. (2009) *Scandinavian journal of gastroenterology* **44**(4), 462-470, 410 p following 470

244. Pelech, S. L., Power, E., and Vance, D. E. (1983) *Canadian journal of biochemistry and cell biology = Revue canadienne de biochimie et biologie cellulaire* **61**(11), 1147-1152

245. Houweling, M., Tijburg, L. B., Jamil, H., Vance, D. E., Nyathi, C. B., Vaartjes, W. J., and van Golde, L. M. (1991) *The Biochemical journal* **278 (Pt 2)**, 347-351

246. Walkey, C. J., Donohue, L. R., Bronson, R., Agellon, L. B., and Vance, D. E. (1997) *Proceedings of the National Academy of Sciences of the United States of America* **94**(24), 12880-12885

247. de Alwis, N. M., and Day, C. P. (2008) *Journal of hepatology* **48 Suppl 1**, S104-112

248. Saadeh, S. (2007) *Nutr Clin Pract* **22**(1), 1-10

249. James, O., and Day, C. (1999) *Lancet* **353**(9165), 1634-1636

250. Li, Z., Agellon, L. B., and Vance, D. E. (2005) *The Journal of biological chemistry* **280**(45), 37798-37802

251. Li, Z., Agellon, L. B., Allen, T. M., Umeda, M., Jewell, L., Mason, A., and Vance, D. E. (2006) *Cell metabolism* **3**(5), 321-331

252. Waite, K. A., Cabilio, N. R., and Vance, D. E. (2002) *The Journal of nutrition* **132**(1), 68-71

253. Noga, A. A., and Vance, D. E. (2003) *The Journal of biological chemistry* **278**(24), 21851-21859

254. Noga, A. A., Zhao, Y., and Vance, D. E. (2002) *The Journal of biological chemistry* **277**(44), 42358-42365

255. Yao, Z. M., and Vance, D. E. (1988) *The Journal of biological chemistry* **263**(6), 2998-3004

256. Yao, Z. M., and Vance, D. E. (1990) *Biochemistry and cell biology = Biochimie et biologie cellulaire* **68**(2), 552-558

257. Raubenheimer, P. J., Nyirenda, M. J., and Walker, B. R. (2006) *Diabetes* **55**(7), 2015-2020

258. Rinella, M. E., Elias, M. S., Smolak, R. R., Fu, T., Borensztajn, J., and Green, R. M. (2008) *Journal of lipid research* **49**(5), 1068-1076

259. Fast, D. G., and Vance, D. E. (1995) *Biochimica et biophysica acta* **1258**(2), 159-168

260. Verkade, H. J., Fast, D. G., Rusinol, A. E., Scraba, D. G., and Vance, D. E. (1993) *The Journal of biological chemistry* **268**(33), 24990-24996

261. Vermeulen, P. S., Lingrell, S., Yao, Z., and Vance, D. E. (1997) *Journal of lipid research* **38**(3), 447-458

262. Song, J., da Costa, K. A., Fischer, L. M., Kohlmeier, M., Kwock, L., Wang, S., and Zeisel, S. H. (2005) *Faseb J* **19**(10), 1266-1271

263. Jun, D. W., Han, J. H., Jang, E. C., Kim, S. H., Kim, S. H., Jo, Y. J., Park, Y. S., and Chae, J. D. (2009) *European journal of gastroenterology & hepatology* **21**(6), 667-672

264. da Costa, K. A., Kozyreva, O. G., Song, J., Galanko, J. A., Fischer, L. M., and Zeisel, S. H. (2006) *Faseb J* **20**(9), 1336-1344

265. Dong, H., Wang, J., Li, C., Hirose, A., Nozaki, Y., Takahashi, M., Ono, M., Akisawa, N., Iwasaki, S., Saibara, T., and Onishi, S. (2007) *Journal of hepatology* **46**(5), 915-920

266. Romeo, S., Cohen, J. C., and Hobbs, H. H. (2006) *Faseb J* **20**(12), 2180; author reply 2181-2182

267. Lloyd-Jones, D., Adams, R., Carnethon, M., De Simone, G., Ferguson, T. B., Flegal, K., Ford, E., Furie, K., Go, A., Greenlund, K., Haase, N., Hailpern, S., Ho, M., Howard, V., Kissela, B., Kittner, S., Lackland, D., Lisabeth, L., Marelli, A., McDermott, M., Meigs, J., Mozaffarian, D., Nichol, G., O'Donnell, C., Roger, V., Rosamond, W., Sacco, R., Sorlie, P., Stafford, R., Steinberger, J., Thom, T.,

Wasserthiel-Smoller, S., Wong, N., Wylie-Rosett, J., and Hong, Y. (2009) *Circulation* **119**(3), e21-181

268. Glass, C. K., and Witztum, J. L. (2001) *Cell* **104**(4), 503-516

269. Zhao, Y., Su, B., Jacobs, R. L., Kennedy, B., Francis, G. A., Waddington, E., Brosnan, J. T., Vance, J. E., and Vance, D. E. (2009) *Arteriosclerosis, thrombosis, and vascular biology* **29**(9), 1349-1355

270. Boushey, C. J., Beresford, S. A., Omenn, G. S., and Motulsky, A. G. (1995) *Jama* **274**(13), 1049-1057

271. Nygard, O., Nordrehaug, J. E., Refsum, H., Ueland, P. M., Farstad, M., and Vollset, S. E. (1997) *The New England journal of medicine* **337**(4), 230-236

272. Finkelstein, J. D. (1998) *European journal of pediatrics* **157 Suppl 2**, S40-44

273. Noga, A. A., Stead, L. M., Zhao, Y., Brosnan, M. E., Brosnan, J. T., and Vance, D. E. (2003) *The Journal of biological chemistry* **278**(8), 5952-5955

274. Jacobs, R. L., Stead, L. M., Devlin, C., Tabas, I., Brosnan, M. E., Brosnan, J. T., and Vance, D. E. (2005) *The Journal of biological chemistry* **280**(31), 28299-28305

275. Glomset, J. A. (1968) *Journal of lipid research* **9**(2), 155-167

276. Duffy, D., and Rader, D. J. (2009) *Nat Rev Cardiol* **6**(7), 455-463

277. Van Eck, M., Pennings, M., Hoekstra, M., Out, R., and Van Berkel, T. J. (2005) *Current opinion in lipidology* **16**(3), 307-315

278. Robichaud, J. C., Francis, G. A., and Vance, D. E. (2008) *The Journal of biological chemistry* **283**(51), 35496-35506

279. (1998) *Lancet* **351**(9114), 1451-1467

280. Singh, M. N., Martin-Hirsch, P. L., and Martin, F. L. (2008) *Med Sci Monit* **14**(9), RA144-148

281. Nishino, M., Hayakawa, K., Nakamura, Y., Morimoto, T., and Mukaihara, S. (2003) *Ajr* **180**(1), 129-134

282. Bruno, S., Maisonneuve, P., Castellana, P., Rotmensz, N., Rossi, S., Maggioni, M., Persico, M., Colombo, A., Monasterolo, F., Casadei-Giunchi, D., Desiderio, F., Stroffolini, T., Sacchini, V., Decensi, A., and Veronesi, U. (2005) *BMJ (Clinical research ed* **330**(7497), 932

283. Oien, K. A., Moffat, D., Curry, G. W., Dickson, J., Habeshaw, T., Mills, P. R., and MacSween, R. N. (1999) *Lancet* **353**(9146), 36-37

284. Reddick, R. L., Zhang, S. H., and Maeda, N. (1994) *Arterioscler Thromb* **14**(1), 141-147

285. Onozuka, H., Fujii, S., Mikami, T., Yamada, S., Ishimori, N., Shimizu, T., Furumoto, T., Nakai, Y., Komuro, K., Nishihara, K., Okamoto, H., and Kitabatake, A. (2002) *Circ J* **66**(3), 272-276

Chapter 2

A Role for Sp1 in Transcriptional Regulation of Phosphatidylethanolamine *N*-Methyltransferase in Liver and 3T3-L1 Adipocytes

2.1 Introduction

Phosphatidylcholine (PC) is the predominant phospholipid of all cell membranes and of the circulating blood lipoproteins (1). In mammalian species, there are two major pathways for PC synthesis. The majority of PC is formed by the CDP-choline pathway (1) which is regulated by the activity of CTP:phosphocholine cytidylyltransferase (CT) and for which a dietary source of choline is required. In the liver substantial amounts of PC can also be synthesized by phosphatidylethanolamine *N*-methyltransferase (PEMT) (2,3). PEMT is a small integral membrane protein (22 kDa) which catalyzes three sequential methylations of phosphatidylethanolamine (PE) using *S*-adenosylmethionine as a methyl donor (4,5). PEMT contributes approximately 30% of total hepatic PC synthesis whereas the enzymes of the CDP-choline pathway produce the remaining 70% (4,6-8).

Despite being the smaller contributor to hepatic PC production in the liver, the significance of the PEMT pathway was underscored when *Pemt*$^{-/-}$ mice were fed a choline-deficient diet which attenuated the CDP-choline pathway. The mice developed severe liver pathology and died within 5 days (9). PC derived from PEMT has been shown to have an important role in the secretion of hepatic triacylglycerols *in vivo* (10,11). It is well established that dyslipidemia is strongly associated with fatty liver and cardiovascular disease (12-14). Recently our lab has linked PEMT

expression with the development of steatohepatitis (15,16) and atherosclerosis (17). Thus, knowledge of the factors that regulate *Pemt* gene expression might be useful for designing new therapeutic regimens.

Even though PEMT plays an important role in hepatic lipid metabolism, the transcriptional regulation of *Pemt* gene expression is not well understood. The PEMT gene is localized to mouse chromosome 11 and spans 35 kb; it contains 7 exons and 6 introns (18). The promoter lacks a TATA box but contains a GC-rich region that is characteristic of many TATA-less gene promoters (19).

Pemt gene expression is regulated in both a tissue-dependent and developmental manner (4,20). It was previously shown that PEMT expression is activated during the perinatal period in rat liver (20). Recently, it has also been shown that *Pemt* gene expression is induced by estrogen in human and mouse primary hepatocytes (21). In the present study we have identified 3T3-L1 adipocytes as a cell culture model that expresses PEMT endogenously. Thus, the aim of the study was to elucidate transcription factors and respective cis-acting elements that regulate gene expression of *Pemt* in 3T3-L1 adipocytes.

2.2 Experimental Procedures

2.2.1 Materials

Dexamethasone, 3-isobutyl-1-methylxanthine, bovine insulin, tamoxifen and mithramycin A were purchased from Sigma (St. Louis, MO, USA). The luciferase vectors, pGL3 Basic, and pGL3 Control vectors containing the cDNA for *Photinus pyralis*, the pSV-β-galactosidase vector, the dual luciferase reporter assay system and the β- galactosidase assay system were obtained from Promega (Madison, WI). The pBK-CMV vector was purchased from Stratagene (La Jolla, CA), pCL-ECO was purchased from IMGENEX (San Diego, CA) and pBabe-puro obtained from Addgene (Cambridge, MA). Lipofectamine™ Plus, lipofectamine™ 2000, DMEM (Dulbecco's modified Eagle's Medium), alpha MEM (Minimum Essential Medium), and fetal bovine serum (FBS) were from Invitrogen (Carlsbad, California).

Anti-Sp1 antibody, anti-Sp3 antibody, anti-SREBP-1 and anti-IgG antibodies were purchased from Santa Cruz biotechnology, anti-protein disulfide isomerase (PDI) antibody was purchased from Stressgen Biotechnologies (Victoria, B.C., Canada), anti-YY1 antibody was from Cedarlane Laboratories Ltd. (Burlington, ON., Canada) and anti-TBP antibody was obtained from Upstate Biotechnology (Lake Placid, NY). The polyclonal antibody directed against the C-terminal end of rat PEMT was raised in rabbit in our laboratory (4).

2.2.2 Cell Culture and Differentiation of NIH 3T3-L1 Fibroblasts

Cos-7 African green monkey kidney cells, C3H10T1/2 mouse embryonic fibroblasts, and NIH 3T3-L1 fibroblasts (A.T.C.C.) were cultured in high-glucose Dulbecco's Modified Eagles Medium (DMEM) supplemented with 10% (v/v) fetal bovine serum (FBS). Hepa-1c1c7 mouse hepatoma cells were cultured in Alpha-MEM, 10% (v/v) FBS and H2.35 mouse hepatocytes were cultured in high-glucose DMEM, 5% (v/v), FBS and 200 nM dexamethasone. All cell lines were obtained from A.T.C.C. and grown in medium supplemented with penicillin G (100 units/ml) and streptomycin (100 units/ml) in a 5% CO_2 humidified incubator at 37^{o}C.

To induce differentiation, NIH 3T3-L1 fibroblasts were cultivated in growth medium until confluent. Two days after reaching confluency, cells were induced to differentiate by the addition of 0.25 μM dexamethasone, 0.5 mM 3-isobutyl-1-methylxanthine and 3 μg/ml insulin for 3 days. Cells were then incubated in normal growth media until differentiated. Medium was replaced every 2 days**.** Cells were considered adipocytes when > 90 % had large cytoplasmic lipid droplets.

Adult mouse cultured primary hepatocytes were isolated from male *Pemt*$^{+/+}$ mice with a mixed genetic background of 129/J and C57B6 using the collagenase perfusion technique as previously described (22). The cells were plated at a density of 0.5 X 10^6 on collagen-coated 60-mm

dishes in DMEM supplemented with 4% FBS, 100 nM dexamethasone, and 1 nM insulin.

2.2.3 Animal Care

All animal procedures are performed in accordance with the University of Alberta Animal Policy and Welfare Committee, which adheres to the principles for biomedical research involving animals developed by the Council for International Organizations of Medical Sciences (CIOMS). Male C57Bl/6J mice (Jackson Laboratory, Bar Harbour, ME) were 8-12 weeks old and maintained on standard chow diet containing 6% (w/w) fat and 0.02% (w/w) cholesterol (LabDiet). Tamoxifen (Sigma) was dissolved at a concentration of 0.2 mg/mL in sesame oil containing 1% benzyl alcohol. The mice were injected subcutaneously with either tamoxifen 0.5 mg/kg of mouse weight or vehicle 2.5 μl (sesame oil, 1% benzyl alcohol)/g of mouse weight. The mice were injected at the same time on five consecutive days and anesthetized 4 h following the final injection.

2.2.4 Immunoblot Analyses

Cell lysates (50 μg) from NIH 3T3-L1 cells during differentiation were heated for 10 min at 90^0C in 62.5 mM Tris-HCl (pH 8.3), 10% glycerol, 5% (v/v) 2-mercaptoethanol, 1% SDS, and 0.004% bromophenol blue. The samples were electrophoresed on a 10% SDS-polyacrylamide gel in 25 mM Tris-HCl (pH 8.5), 192 mM glycine, and 0.1% SDS buffer.

The proteins were transferred to polyvinylidene fluoride (PVDF) by electroblotting in transfer buffer (125 mM Tris-HCl, pH 8.3), 960 mM glycine, 10% (v/v) methanol). Following transfer, the membrane was incubated overnight at 4^{o}C with 5% skim milk in 10 mM Tris-HCl (pH 7.4), 100 mM NaCl, 0.1% Tween 20 (T-TBS) followed by 1 h at room temperature or overnight at 4^{o}C with antibody raised against the protein indicated. Anti-PEMT, anti-Sp1, anti-Sp3 and anti-YY1 antibodies were diluted (1:5000) in 1% milk, T-TBS. Anti-PDI and anti-TBP antibodies were diluted (1:4000) in 4% bovine serum albumin, T-TBS. Immunoreactive proteins were detected using enhanced chemiluminescence system (Amersham Biosciences) according to the manufacturer's instructions.

2.2.5 RNA Isolation and PCR Analysis

Total RNA was isolated from liver tissue or cultured cells using the Trizol® reagent (Life Technologies, Inc.) according to the manufacturer's instructions. First-strand cDNA synthesis from 2 μg of total RNA was performed using SuperScript™ II reverse transcriptase (Invitrogen) primed by oligo(dT)$_{12\text{-}18.}$ PCR was performed using the indicated gene specific primers given in Table 2.1. Amplicons were visualized with ethidium bromide on an agarose gel or measured using real-time quantitative PCR using the Rotor-gene 3000 instrument (Montreal Biotech) and analysed with the Rotor-Gene 6.0.19 program (Montreal Biotech).

2.2.6 Plasmid Construction

The *Pemt* promoter region -1000 to +130 was obtained by PCR amplification using mouse liver genomic DNA as a template. We used a numbering system based on the transcriptional start site (+1) previously determined (18). The primers (forward 5'-CGGGGTACCCCGCAGCCTGCCACTTGGCACACC-3') and (reverse 5'-CCCAAGCTTGGGCAGAACCAGAAGGAAATGGGA-3') were designed to contain restriction enzyme sites for Hind-III and Kpn-I. The promoter region was purified from agarose gel using the Qiax II gel extraction kit (Qiagen Inc., Mississauga, Ontario Canada) according to the manufacturer's instructions, and directionally ligated into double digested (Hind-III, Kpn-I) pGL3 Basic to generate -1000 Luc. All other promoter sections were generated by PCR using -1000 Luc as a template and then double digested and ligated into pGL3 Basic as previously outlined. The reverse primer remained the same with various forward primers for -471 Luc (5'-CGGGGTACCCCGA-GGGAGGGCACAGTGTATGAAT-3'), -371 Luc (5'-CGGGGTACCCCGGTACCTT-GCTTCTTTCTT-3'), -271 Luc (5'-CGGGGTACCCCGAGAGGGCGAAGAGTATG-CAAT-3'), -171 Luc (5'-GGGGTACCCCGGTGTATGGTACATGTCAC-3') and -71 Luc (5'-CGGGGTACCCCGCTTGCACCCTGGGTGCTGTTG-3').

The cDNA for full length mouse Sp1 was obtained by RT-PCR. Briefly, total RNA was obtained from mouse liver and reverse transcribed with SuperScript™ II primed by oligo$(dT)_{12\text{-}18}$. Primers used in the subsequent PCR amplification of Sp1 cDNA were forward (5'-CCGGAATTCGGACAATGAGCGACCAAGATCACTCCATG-3') and reverse (5'-CCGGAATTCCGGTTAGAAACCATTGCCACTGATATT-3') containing restriction enzyme sites for Eco-RI. The PCR product was digested with Eco-RI and gel purified prior to being ligated into pBabe.puro.

DNA oligonucleotides for the synthesis of shRNA were synthesized by the University of Alberta DNA Core Facility. For each specific gene we designed DNA oligonucleotides which are predicted to form a stem-loop structure when transcribed to RNA. The sequence of the forward DNA oligonucleotide included the unique nucleotide target sequence in both the sense and antisense orientation, separated by a spacer sequence (5'-TTCAAGAGA-3') and flanked by Bgl-II and Hind-III restriction site overhangs. The target sequence specific for Sp1 was 5'-GGCTGCTACCCCAACTTAC-3'. As a negative control, we used a sequence that did not have homology with expressed genes and is referred to as Scrambled (5'-ACTACCGTTGTTATAGGTGGT-3') (23). After annealing, the double-stranded DNA was directionally cloned into pSuper.retro.puro (OligoEngine, Seattle, WA) double digested with Bgl-II and Hind-III.

Site-directed mutagenesis was applied to introduce a mutation of the Sp1 binding element in the -471 Luc plasmid. For that purpose, the core sequence of the Sp1-element (5'-GGGAGG-3") was replaced with (5'-GGGAAA-3') using the QuickChange® site-directed mutagenesis kit (Stratagene, La Jolla, CA). The resulting construct was termed -471MSp1 Luc. The identity of the all generated plasmids was confirmed by sequencing.

2.2.7 Nuclear Extract Preparations and Electrophoretic Mobility Shift Assays (EMSAs)

Nuclear extracts from mouse liver and 3T3-L1 cells were prepared as described (24,25). Promoter-derived oligonucleotides (40 bp) were synthesized by the University of Alberta DNA Core Facility. Complementary oligonucleotides (1 nmol of each) containing 5' overhangs were heated at 90^{o}C for 10 min in 100 μl of annealing buffer (10 mM Tris-HCl, pH 7.5, 100 mM NaCl and 1 mM EDTA). The annealing mixtures were slowly cooled to room temperature and 50 pmol of double-stranded oligonucleotide were labeled by filling in end recessed 3' ends using Klenow fragment in the presence of [α-^{32}P]dCTP. For each binding reaction (40 μl), 2 μg of Poly(dI-dC)●Poly(dI-dC), 20 μl of a 2X binding buffer (12.5 mM HEPES, pH 7.9, 25 mM KCl, 2 mM MgCl, 0.07% Triton X, 13.3 % glycerol, 5 mM dithiothreitol), 20 μg of nuclear extract and labeled probe (150,000 cpm) were incubated for 1 h at 4^{o}C. For competitive

EMSAs, 100-fold molar excess of non-labeled double-stranded oligonucleotides were incubated with nuclear extracts for 15 min at 4°C before addition of labelled probe. Commercially available antibody (2 μg) was added to the binding reactions 15 min before the labeled probe for super-shift assays. Binding reactions were terminated by the addition of 8 μl of gel loading buffer (30%, v/v, glycerol, 0.25%, w/v, bromophenol blue, 0.25%, w/v, xylene cyanol). The protein-DNA complexes were separated on a 8% or 7% (for some competitive/super-shift assays) non-denaturing polyacrylamide gel electrophoresis with Tris borate-EDTA buffer system (89 mM Tris, 89 mM Borate, 2 mM EDTA, pH 8.3) at 4°C and detected by autoradiography of a dried gel.

2.2.8 Stable and Transient Transfections

3T3-L1 stable cell lines were generated by transfecting pre-adipocytes at 30% confluency in 100 mm dishes with 10 μg luciferase reporter construct and 1 μg pBK-CMV containing the neomycin cassette, using the calcium phosphate precipitation method (26). Stable cell lines were selected with Geneticin® (G-418 sulfate, Invitrogen) and confirmed by PCR amplification using commercially available primers RVP3 and GLP3 (Promega, Corp.) which flank the multiple cloning site. The copy number and level of differentiation of each clone was determined by PCR. To measure luciferase activity samples were collected from 3T3-L1 stable cell lines at various time points during the differentiation period.

Luciferase activity was assayed using commercial kits on a microbeta liquid scintillation counter (PerkinElmer) and normalized to protein concentration.

Cultured cell lines (H2.35, Hepa-1c1c7, Cos-7 and C3H10T1/2 (2 x 10^5/60 mm dish) and freshly isolated adult mouse cultured primary hepatocytes (5 X 10^5, 60 mm dish), were transiently transfected with 1 μg luciferase reporter construct and 1 μg pSV-β-galactosidase using Lipofectamine™ 2000 (hepatocytes) or Lipofectamine™ Plus reagent (cell lines). After 20-48 h, cell extracts were assayed for luciferase activity and normalized to β-galactosidase activity to adjust for transfection efficiency.

2.2.9 Retroviruses

The packaging human renal epithelium cell line 293T/17 was transiently transfected with the murine leukemia virus (MLV) packaging vector (pCL-ECO), an expression retroviral vector (pBabe.puro, or pSuper.retro.puro) using Lipofectamine™ Plus reagent. After a 24 h incubation at 37ºC, the conditioned medium was filtered (0.45 μm filters), supplemented with polybrene (8 μg/ml) and used to infect 3T3-L1 cells stably transfected with -471 Luc. Transduced 3T3-L1 cells were selected with medium containing 2.5 μg/ml of puromycin (Sigma) for 48 h. 3T3-L1 cells were then cultured and differentiated as described above.

2.2.10 Chromatin Immunoprecipitation (ChIP) Assays

3T3-L1 pre-adipocytes and adipocytes were fixed with 1% formaldehyde (27). Cells were washed with cold PBS twice and resuspended in 0.8 ml radioimmunoprecipitation assay (RIPA) buffer containing 0.1% SDS, 0.1% sodium deoxycholate, 1% Triton X-100, 1 mM EDTA, 0.5 mM EGTA, 140 mM NaCl, 10 mM Tris-HCl, pH 8, supplemented with protease inhibitor cocktail (Sigma)). The cells were sonicated (30 sec x 4) using a Sonicator Ultrasonic Processor XL (Misonix Farmingdale, NY) followed by centrifugation at 10,000 x g for 10 min at 4^0C. The supernatants were collected and diluted with RIPA buffer to 0.2 μg/ul DNA. Protein G-Sepharose beads (Sigma) were pre-treated with 0.1 mg/ml sonicated salmon sperm and 1 mg/ml BSA for 2 h at 4^oC.

Immunoprecipitation was performed by incubating 1 ml of diluted supernatant (200 μg DNA) with 4 μg anti-Sp1, anti-YY1 or anti-IgG antibodies for 30 min at room temperature. Then the pre-treated protein G-Sepharose beads (50 μl, 50% with 1X RIPA), 5 μg sonicated salmon sperm and 10 μg BSA were added and the immunoprecipitation was continued for 16 h at 4^oC. The protein G Sepharose beads were washed 3 times with 1X RIPA, 3 times with 1X RIPA supplemented with 1 M NaCl, 2 times with LiCl buffer (0.25 M LiCl, 1% Nonidet P-40, 1% sodium deoxycholate, 1 mM EDTA, 10 mM Tris-HCl, 500 mM NaCl, pH 8) and twice with TE buffer (20 mM Tris-HCl, pH 8, 1 mM EDTA). The protein-

DNA complexes were eluted from the beads at room temperature for 15 min each with 200 μl 1.5% SDS for 15 min, followed by 150 μl 0.5% SDS. The fractions were combined and incubated at 68^{o}C for 16 h to reverse crosslinks. Protein was digested with proteinase K and DNA extracted by phenol/chloroform followed by ethanol precipitation. To detect the *Pemt* promoter, the following primers were used for standard PCR: forward: (5'-TTCGGTAAGGAACCTGACC-3') and reverse: (5'-GAACATTCGCTGGGCAATTC-3').

2.2.11 Statistical Analysis

Values are expressed as means ± standard error mean (SEM). A significant difference between means was determined using the unpaired Student's two-tailed t-test for most analyses. To compare differences between multiple groups one way analysis of variance (ANOVA) using Tukey post-hoc analysis or ANOVA on the ranks using Kruskal-Wallis post-hoc analysis were used where appropriate. A probability of <0.05 is considered significant.

2.3 Results

2.3.1 3T3-L1 Cells Express PEMT mRNA Upon Differentiation to Adipocytes

Despite the important role that PEMT plays in hepatic lipid metabolism, very little is known about its transcriptional regulation.

Therefore, the goal of this study was to identify promoter elements and *trans*-acting factors that regulate expression of the *Pemt* gene. Previous research on this topic was impeded by the lack of immortalized cell lines which express PEMT. We found very low levels of PEMT mRNA in several immortalized cell lines including the monkey kidney cell line Cos7, the mouse hepatoma cell lines H2.35, Hepa-1c1c7 and the mouse embryonic fibroblast cell line C3H10T1/2 (Figure 2.1A). PEMT is highly expressed in the liver making primary cultures of mouse hepatocytes an obvious choice for studies on gene expression. However, while PEMT mRNA levels are initially high in primary cultures of mouse hepatocytes (Figure 2.1A), expression decreases rapidly within 16 h of isolation. These results are consistent with the de-differentiation of hepatocytes that occurs in culture (28).

When each cell type was transiently transfected with luciferase reporter construct -471 Luc containing the mouse *Pemt* promoter (-471 to +130) the luciferase activity was lower than that from the promoter-less parent pGL3 basic (Empty) plasmid (Figure 2.1B). Since, luciferase activity was detected at high levels in each cell type when the reporter gene was under the control of a strong SV40 promoter (pGL3 control), the low level of luciferase activity was not due to inefficient transfection efficiency. Therefore, the low level of *Pemt* gene expression observed in both immortalized cell lines and primary cultures of mouse primary hepatocytes was not sufficient to investigate promoter function.

However, PEMT mRNA and protein are expressed in 3T3-L1 mouse embryonic fibroblasts following adipocyte differentiation (Figures 2.2A and B). Analysis of the level of PEMT mRNA by PCR before and after differentiation demonstrated that PEMT mRNA was barely detectable in pre-adipocytes and increased dramatically (~100 fold) following differentiation to adipocytes (Figure 2.2B). PEMT mRNA levels remained low during the early stages of differentiation and increased markedly by day 4 during the late stage of adipocyte differentiation. This process is characterized by the expression of Ap2/FABP4 and follows increased expression of mRNAs encoding PPARγ and C/EBPα (29) (Figure 2.2B).

Consistent with the increase in PEMT mRNA during 3T3-L1 differentiation, we found that luciferase activity from the *Pemt* promoter increased when 3T3-L1 fibroblasts stably expressing PEMT-luciferase constructs differentiated into adipocytes (Figure 2.2C). In contrast, luciferase activity was lower in adipocytes than pre-adipocytes when 3T3-L1 cells stably expressing pGL3 basic lacking a promoter upstream of the luciferase reporter gene were differentiated. These data establish that 3T3-L1 adipocytes provide a suitable cellular model for identification of elements in the *Pemt* gene using promoter-activity assays.

2.3.2 The Region -471/-371 Is Important for Activation of PEMT mRNA Expression

To identify section(s) of the mouse *Pemt* promoter which may be important for regulating activation of the *Pemt* gene, we generated 3T3-L1 clones which stably express different sections of the mouse *Pemt* promoter. Serial deletions from the 5' end of the *Pemt* promoter were constructed and ligated into the luciferase reporter gene pGL3 basic and stable cell lines were created. Luciferase activity was measured before (day -2), and after (day 7) differentiation to adipocytes. Two clones (clone -1, clone -2) were analyzed for each promoter length and normalized for cell protein, copy number and level of adipocyte differentiation. Compared to the promoter-less parent vector (pGL3-Basic), transfection of -471 Luc into pre-adipocytes resulted in no change in luciferase expression (Figure 2.3). Following differentiation of 3T3-L1 cells into adipocytes, the -471 Luc construct exhibited a 20- to 30-fold increase in luciferase expression. Deletion to -371 bp resulted in the absence of any measureable promoter activity, suggesting that transcription factor binding sites located in the region between -471 and -371 bp may be important for regulating the activation of *Pemt* gene expression. Since, this promoter region is more active in 3T3-L1 adipocytes than in pre-adipocytes, subsequent experiments focused on characterization of the sequence between -471 and -371 of the mouse *Pem*t promoter.

2.3.3 Identification of Sp and YY1 Binding Sites Within the Activation Region of the *Pemt* Promoter

In an attempt to identify the *cis*-elements responsible for regulating the activation of *Pemt* gene expression, we utilized electrophoretic mobility shift assays (EMSA). We used thirteen overlapping DNA oligonucleotides from the -471/-371 region to identify the sections which bind nuclear proteins. Each oligonucleotide was labelled with ^{32}P and incubated with nuclear extract isolated from 3T3-L1 adipocytes. Three different protein-DNA complexes were generated as indicated by the appearance of bands labelled “a” through “c” (Figure 2.4). DNA oligonucleotides which contained the *Pemt* promoter region -426 to -402 generated all three DNA-protein complexes.

Comparison of the binding patterns produced with nuclear extracts from mouse liver or 3T3-L1 cells revealed that mouse liver generates three protein-DNA complexes (d-f) which are not detected with nuclear extract from 3T3-L1 cells (Figure 2.5). When nuclear extract isolated from mouse liver was incubated with the thirteen overlapping DNA oligonucleotides, those which contained the *Pemt* promoter region -426 to -402 generated all six DNA-protein complexes. Together these results indicate that nuclear proteins which regulate the trans-activation of the *Pemt* gene expression might bind within the -426 to -402 promoter section (Figures 2.5 and 2.6). Comparison of the -426 to -402 sequence of the *Pemt*

promoter with the TRANSFAC database revealed that this region contains two candidate binding sites, one for the Sp family of transcription factors and one for YY1, a member of the gli-Kruppel class of zinc finger transcription factors (30).

2.3.4 The Transcription Factors Sp1, Sp3 and YY1 Bind to the Mouse *Pemt* Promoter

The Sp transcription factor family includes several members (Sp1, Sp2, Sp3 and Sp4) that share significant sequence homology and recognize GC boxes with similar specificity (31). To determine which of these proteins bind to the *Pemt* promoter, we performed super-shift assays with antibodies specific for individual Sp proteins. Antibodies specific for Sp1 were added to an EMSA reaction with the ^{32}P-labeled *Pemt* -441/-402 promoter fragment and nuclear extracts isolated from 3T3-L1 cells (Figure 2.6) and mouse liver (Figure 2.7).

In the absence of antibody, incubation of ^{32}P-labeled *Pemt* -441/-402 promoter fragment with nuclear extracts isolated from 3T3-L1 cells generates three different protein-DNA complexes (a-c) (lane 6 and 16, Figure 2.5). Upon addition of Sp1 specific antibody to the EMSA reaction the mobility of complex a was retarded such that a new upper band appeared in lane 2 (left panel, Figure 2.6). The accompanying decrease in the intensity of complex a in the presence of Sp1 antibody was detected when complexes were resolved using a 6% non-denaturing

polyacrylamide gel (lane 12, right panel, Figure 2.6). The addition of anti-Sp3 antibodies decreased the intensity of complexes a and b with an accompanying super-shifted complex (lane 4 and 14, Figure 2.6). The disappearance of more than one band is likely due to the different isoforms of Sp3 (115-kDa, 80-kDa and 78-kDa)(31) (Figure 2.11); the experimental conditions might be unable to resolve the protein-DNA complexes generated by Sp1 from those of full length Sp3.

We further illustrated that both complex a and b contain Sp family members by adding oligonucleotides corresponding to the consensus GC box (GGGGCGGGG) to EMSA reactions. In the presence of the consensus GC box, formation of both complexes was prevented (lane 1 and 11, Figure 2.6). Together, these results indicate the presence of Sp1 in complex a and Sp3 in complexes a and b. Antibodies raised against Sp2 did not alter the mobility or formation of any complex (lanes 3 and 13, Figure 2.6). Sp4 in the mouse is primarily in the brain and thus is not considered to regulate expression in the liver (31).

Next, we investigated whether the *Pemt* promoter interacted with the nuclear protein YY1. Addition of antibodies specific for YY1 to the EMSA reaction reduced the mobility of complex c so that it co-migrated with complex a (lane 7 and 17, Figure 2.6). The addition of the unlabeled competitor YY1 consensus sequence reduced the appearance of complexes c-f (lanes 9 and 19, Figures 2.5 and 2.6), indicating that the

YYI binding site is important for generating several complexes. However, the super-shift with anti-YY1 (lanes 7 and 17, Figures 2.5 and 2.6) suggests that only complex c contains the YY1 protein. Since similar DNA-transcription factor complexes containing Sp1, Sp3 and YY1 are formed with both 3T3-L1 (Figure 2.6) and liver (Figure 2.7) nuclear extracts, similar mechanisms may regulate the *Pemt* promoter in these cells.

2.3.5 Inhibition of Sp1 Binding to the Mouse *Pemt* Promoter Increases *Pemt* Reporter Activity

Next we determined whether Sp1 and/or YY1 protein bound to the *Pemt* promoter *in vivo*. We performed chromatin immunoprecipitation assays (ChIP) using pre-adipocytes and adipocytes to determine the temporal binding pattern of each transcription factor. Sp1 and YY1 were detected at the *Pemt* promoter before and after differentiation of 3T3-L1 cells (Figure 2.8A). Significantly fewer *Pemt* promoter fragments were pulled down by immunoprecipitation of Sp1 in 3T3-L1 adipocytes than in pre-adipocytes (Figure 2.8A), indicating that less Sp1 had bound to the *Pemt* promoter. In contrast, similar amounts of YY1 protein were present at the *Pemt* promoter in either pre-adipocytes or adipocytes (Figure 2.8B). The temporal binding pattern of Sp1 to the *Pemt* promoter is consistent with a regulatory role for Sp1 as an inhibitor of *Pemt* gene transcription.

To obtain further support for the proposal that reduction of Sp1 binding at the *Pemt* promoter increases promoter activity we used the cell

permeable agent mithramycin A to inhibit the binding of Sp1 to the DNA. Mithramycin A binds to GC-rich DNA sequences, thereby precluding the binding of nuclear proteins including Sp1 (32). When adipocytes stably expressing -471 Luc were treated with 10 μM mithramycin A for 24 h, luciferase activity was significantly increased compared to that in vehicle treated cells (Figure 2.9A). The mithramycin A-mediated increase in promoter activity was accompanied by reduced formation of the Sp1-*Pemt* promoter complex (complex a) in EMSA experiments (Figures 2.9B and C). In addition, significantly fewer *Pemt* promoter fragments were pulled down by immunoprecipitation of Sp1 in 3T3-L1 adipocytes treated with mithramycin A than with vehicle (Figure 2.9D and E), indicating that less Sp1 had bound to the *Pemt* promoter. Together these results suggest that decreased Sp1 binding promotes increased *Pemt* promoter activity.

2.3.6 Expression of the Mouse *Pemt* gene is regulated by Sp1 in 3T3-L1 Adipocytes

To determine whether Sp1 directly inhibits transcription from the mouse *Pemt* promoter, Sp1 was over-expressed using a retrovirus containing Sp1 cDNA in pre-adipocytes which stably express the *Pemt* promoter construct -471 Luc. Over-expression of Sp1 significantly reduced the ability of the *Pemt* promoter construct -471 Luc to drive luciferase activity in both 3T3-L1 pre-adipocytes and adipocytes (Figures 2.10A to C), indicating that Sp1 is a negative regulator of the *Pemt* promoter. To

investigate whether reduction of Sp1 protein increased *Pemt* promoter activity, we constructed retroviruses that contained short hairpin sequences corresponding to Sp1. A 50% decrease in Sp1 protein significantly increased luciferase activity from -471 Luc in 3T3-L1 adipocytes compared to the scrambled RNAi control (Figures 2.10D to F). Thus, Sp1 inhibits *Pemt* promoter activity independent of the differentiation status of the cells. However, the reduction of Sp1 was insufficient to induce *Pemt* gene transcription in pre-adipocytes.

To further address the functional significance of Sp1-mediated regulation of *Pemt* gene expression during 3T3-L1 differentiation, the temporal expression of Sp1 and PEMT were evaluated by immunoblot analysis (Figure 2.11). The amount of Sp1 protein decreased 24 h prior to detection of PEMT protein. The amount of YY1 and Sp3 protein also decreased during 3T3-L1 differentiation but not until after the expression of PEMT, suggesting that these factors may not be involved. The reduction of Sp1 protein levels during 3T3-L1 differentiation is consistent with release of Sp1-mediated inhibition of *Pemt* gene transcription and thus activation in adipocytes.

2.3.7 Inhibition of the Mouse *Pemt* Promoter by Tamoxifen is Mediated by Sp1

We next examined whether Sp1 binding regulates *Pemt* gene expression in response to an estrogen receptor modulator. It was recently

shown that tamoxifen, a common breast cancer treatment drug, inhibits expression of PEMT in rodents (33). To determine whether we could reproduce this tamoxifen-mediated effect in mice we injected animals for 5 consecutive days with either vehicle (sesame oil, 1% benzyl alcohol) or tamoxifen (0.5 mg/kg/day). Analysis of hepatic PEMT mRNA levels by qPCR revealed that following tamoxifen treatment the mRNA level of PEMT was significantly reduced compared to the vehicle (Figure 2.12A). When adipocytes stably expressing -471 Luc were treated with either 1 μM or 10 μM tamoxifen for 7 days, luciferase activity was significantly decreased compared to that in vehicle treated cells (Figure 2.12B).

The tamoxifen-mediated decrease in promoter activity was accompanied by increased formation of the Sp1-*Pemt* promoter complexes (complex a) in EMSA experiments (Figures 2.13A and B). The amount of Sp1-*Pemt* promoter complexes generated (complex a) was normalized to the amount of YY1-*Pemt* promoter complexes (complex c) in an attempt to account for variation in gel loading (Figure 2.13B). In addition, significantly more *Pemt* promoter fragments were pulled down by immunoprecipitation of Sp1 in 3T3-L1 adipocytes treated with tamoxifen than with vehicle (Figure 2.13C and D), indicating that more Sp1 had bound to the *Pemt* promoter.

To confirm that tamoxifen was inhibiting *Pemt* promoter activity via the Sp1 binding site, we mutated the GC-element (5'-GGGAGG-3') by replacing two guanine nucleotides with adenine (5'-GGGA**AA**-3'). We

demonstrated that this mutation prevented Sp1 binding to the *Pemt* promoter in EMSA experiments. The -441 to -402 section of the *Pemt* promoter was ^{32}P labelled and incubated with nuclear extract to generate the three different protein-DNA complexes previously observed (Figure 2.14A). When we ^{32}P labelled the -441 to -402 section of the *Pemt* promoter containing a mutation within the Sp1 binding site (MSp1) the formation of Sp-containing complexes was prevented, indicating the inability to bind Sp1 protein (Figure 2.14A). When adipocytes stably expressing -471MSp1 Luc were treated with tamoxifen there was no change in luciferase activity compared to the vehicle control (Figure 2.14B). Therefore, the tamoxifen-mediated decrease in *Pemt* promoter activity requires the Sp1 binding site. Together, these results indicate that tamoxifen inhibits *Pemt* gene expression by promoting Sp1 binding to the promoter.

2.4 Discussion

2.4.1 Sp1 is an inhibitor of *Pemt* Gene Transcription

Sp1 is responsible for recruiting basal transcriptional machinery to TATA-less promoters (34-36) as well as acting as an activator or an inhibitor at target promoters (37-40). We have found that Sp1 regulates *Pemt* gene expression in 3T3-L1 cells by acting as a transcriptional repressor. Sp1 has been previously shown to promote repression of target genes by recruiting histone deacetylases both directly (38) and

indirectly (37,41,42) to specific promoters. Typically Sp1 physically interacts with several nuclear proteins in a dynamic complex to perform transcriptional repression (43) as well as de-repression and activation (41).

The complexity of *Pemt* gene expression during 3T3-L1 adipogenesis was apparent from our observation that reduction in Sp1 protein was not sufficient to release repression of *Pemt* gene transcription in pre-adipocytes. It is likely that Sp1 is only part of the transcriptional machinery which cooperatively inhibits *Pemt* gene expression, thus modification of additional repressors might limit regulation by Sp1. This mechanism could potentially include the transcription factors YY1 and Sp3 since they physically interact with Sp1 in some cell types (44,45). However, we determined that the amount of YY1 binding at the *Pemt* promoter remained similar before and after activation of *Pemt* gene transcription. We also observed that both YY1 and Sp3 protein levels decreased primarily after the induction of *Pemt* gene expression in 3T3-L1 cells suggesting that YY1 and Sp3 contribute only minor inhibitory roles, at best. The activation of PEMT in 3T3-L1 adipocytes might also be promoted upon binding of an activation complex which is expressed during adipogenesis.

Although the decrease in Sp1 is required for *Pemt* gene expression during differentiation, the finding that this mechanism is not sufficient precludes the likelihood that decreasing Sp1 in other immortalized cell

models or primary mouse hepatocytes will promote *Pemt* gene expression. There is also evidence for additional regulation upstream of the -471 bp section of the mouse *Pemt* promoter. When we extended the length of PEMT promoter upstream of the luciferase reporter gene from -471 bp to -1000 bp (Figure 2.3) transcriptional activation was prevented suggesting additional repressor binding sites.

2.4.2 Implications for Transcriptional Regulation of the *Pemt* Gene in Mouse Liver

Our results demonstrate that elements of the transcriptional regulation of the *Pemt* promoter may be conserved between mouse liver and 3T3-L1 cells. In gel-shift assays Sp1, Sp3 and YY1 proteins from mouse liver nuclear extract bound to the *Pemt* promoter. Sp1 regulates the transcription of other genes involved in hepatic lipid metabolism (46) including PC metabolism (23,39). Sp1 regulates CT expression during the cell cycle, and another enzyme in the CDP-choline pathway, choline kinase may also be regulated by Sp1 because two putative binding sites have been recently identified (47).

The CDP-choline pathway is typically up-regulated in the liver when PEMT activity is repressed, for example during hepatic regeneration (48) and growth (20,49,50). The inverse transcriptional regulation of *Pemt* gene expression and the CDP-choline pathway could potentially be achieved with the contribution of Sp1. For example, such co-ordinate regulation

might promote the synthesis of PC via the CDP-choline pathway during growth and through the PEMT pathway in quiescent cells. We observed the highest levels of Sp1 protein during the early phase of 3T3-L1 differentiation (Figure 2.11) when pre-adipocytes undergo cell division (29). In adipocytes, which no longer divide, the Sp1 protein levels were low. These results are consistent with previous reports of cell-cycle-dependent regulation of Sp1 (51,52). Thus, Sp1-mediated repression of *Pemt* gene expression in 3T3-L1 pre-adipocytes may be part of a cellular response to promote growth.

We have observed three additional transcription factor-*Pemt* promoter complexes in the EMSAs with nuclear extract from liver but not with nuclear extract from 3T3-L1 cells, suggesting that liver specific expression of the *Pemt* gene might, in part, be controlled by these factors. We have been unable to identify these factors but have ruled out binding sites for NF1, Chop, C/EBP, GATA, SF1, MycMax, HNF1, HNF3/6, LXR, GR, STAT, PPAR, SMAD, CHREBP, NFKβ, NFAT, NKX2.5 and SREBP (data not shown). Since tamoxifen binds estrogen receptors (ESR) (53) and recent evidence has suggested that estrogen activates *Pemt* gene transcription (21), we introduced a double-stranded oligonucleotide containing the ESR element in gel mobility experiments but this also did not alter the binding pattern of nuclear factors to the *Pemt* promoter.

Alternatively, our data show that the Sp1 binding site was required for tamoxifen-mediated inhibition of *Pemt* promoter activity. In support of this finding it is known that estrogen and tamoxifen can affect expression from genes lacking a classical ESR element (54-56). Gene regulation by non-classical ESR signalling events is complex including physical interactions between ESR and other transcription factors (55,57), ESR-mediated changes in the expression levels of regulatory factors (58,59) and post-translational modification of nuclear proteins via intracellular signalling cascades (*e.g.* cAMP/PKA, MAPK/PI3K) (56,60,61). While the upstream signalling events remain to be elucidated our results clearly indicate that activation of ESR by tamoxifen promotes assembly of a Sp1 inhibitory complex at the *Pemt* promoter.

In conclusion, the present study demonstrates that the -471 to +130 bp section of the *Pemt* promoter is essential for *Pemt* gene expression in 3T3-L1 adipocytes, and that Sp1 transcriptionally regulates *Pemt* gene expression.

Gene	Forward Sequence	Reverse Sequence
Pemt	5'–CCGCTCGAGCTGTATGAGC TGGCTGCTGGGTTAC–3'	5'–CCTGTCAGCTTCT TTTGTGCA–3'
Cyc	5'–TTCAAAGACAGCAGAAAAC TTTCG-3'	5'–TCTTCTTGCTGGT CTTGCCATTCC–3'
C/ebpα	5'–TGGACAAGAACAGCAACGA G–3'	5'–TCACTGGTCAACT CCAGCAC–3'
Pparγ	5'–GAAAAGACAACGGACAAAT CAC–3'	5'–TACGGATCGAAA CTGGCAC–3'
Fabp4	5'–TGGAAGCTTGTCTCCAGTG A–3'	5'–AATCCCCATTTAC GCTGATG–
18S	5'–AGGACCGTCGTTCTATTTT GTTG–3'	–CGGGCCGGGTGAG GTTT–3'

Table 2.1 PCR primer sequences

The abbreviations for the mRNAs are: PEMT, phosphatidylethanolamine *N*-methyltransferase; CYC, cyclophilin; PPAR, peroxisome proliferator activated receptor; C/EBP, CAAT element binding protein; FABP4, fatty acid binding protein 4.

Figure 2.1. Expression of PEMT in various cell types.

(A) Total RNA was extracted from, COS-7 (COS), C3H10T1/2 (C3H), H2.35, Hepa-1c1c7 (Hepa) cells and primary mouse hepatocytes, reverse-transcribed to cDNA, and PEMT and cyclophilin (CYC) mRNAs were detected by PCR. Amplicons were visualized with ethidium bromide on a 2% agarose gel. Duplicate samples of isolated primary adult mouse hepatocytes were collected 4 and 16 h post isolation. Total RNA was isolated from the liver of adult male PEMT wild type (WT) and knock-out (KO) mice for positive and negative controls, respectively. A non-template control (NTC) represents a negative control for PCR in the absence of cDNA template. Results are from a single experiment which was repeated once with similar results. (**B)** Cells were transiently transfected in duplicate with -471 Luc, the empty pGL3 basic vector as a negative control (empty) or the pGL3 control vector containing the SV40 promoter upstream of luciferase cDNA (+ control) as a positive control for transfection efficiency. Luciferase activity was measured 20-48 h post-transfection and expressed relative to β-galactosidase activity. Values represent the means ± SEM of three independent experiments.

Figure 2.1

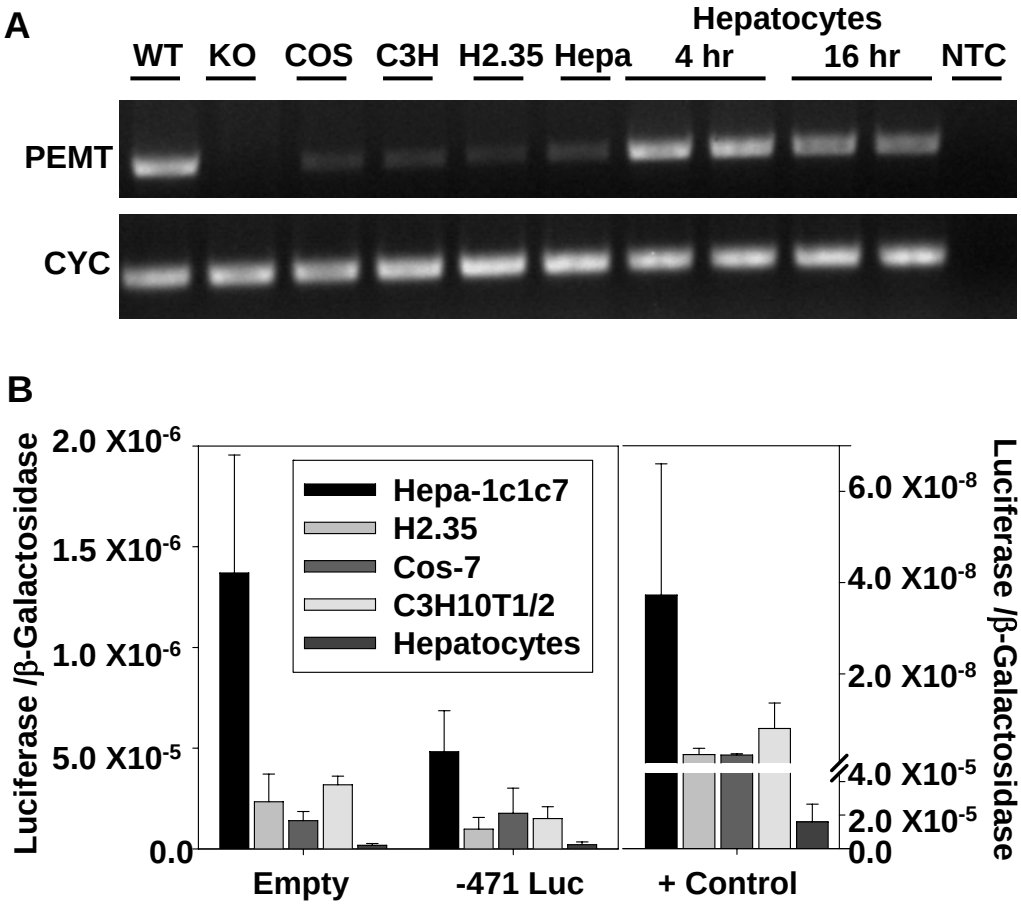
A
Hepatocytes
WT
KO
COS
C3H
H2.35
Hepa
4 hr
16 hr
NTC
PEMT
CYC
B
Luciferase /β-Galactosidase
2.0 X10-6
1.5 X10-6
1.0 X10-6
5.0 X10-5
0.0
Hepa-1c1c7
H2.35
Cos-7
C3H10T1/2
Hepatocytes
6.0 X10-8
4.0 X10-8
2.0 X10-8
4.0 X10-5
2.0 X10-5
0.0
Luciferase /β-Galactosidase
Empty
-471 Luc
+ Control

Figure 2.2. PEMT mRNA is increased during 3T3-L1 differentiation to adipocytes.

(A) Total RNA was extracted from triplicate cultures of 3T3-L1 pre-adipocytes and adipocytes, reverse-transcribed to cDNA, and *Pemt* and cyclophilin (CYC) mRNAs were detected by PCR. NTC is a non-template control (duplicate lanes). Amplicons were visualized with ethidium bromide on a 2% agarose gel. **(B)** 3T3-L1 fibroblasts were differentiated into adipocytes and cells were collected on the indicated days. Day 0 indicates two days post-confluence and the start of the differentiation protocol. Total RNA was isolated, reverse-transcribed to cDNA and *Pemt*, FABP4, PPARγ, and C/EBPα mRNA levels measured by qPCR. 18S RNA levels were measured by qPCR by generating a single stranded DNA template using the reverse primer. mRNA and 18s RNA levels were normalized to cyclophilin using a standard curve. All data are means ± SEM from three separate independent experiments. ND refers to non-detectable amplicon within the indicated sample. **(C)** 3T3-L1 fibroblasts were stably transfected with -471 Luc or the empty pGL3 basic vector (Empty) as a negative control. Luciferase activity was measured in pre-adipocytes and adipocytes and normalized to cellular protein. Values represent means ± SEM of three separate independent experiments (*, $P<0.05$).

Figure 2.2

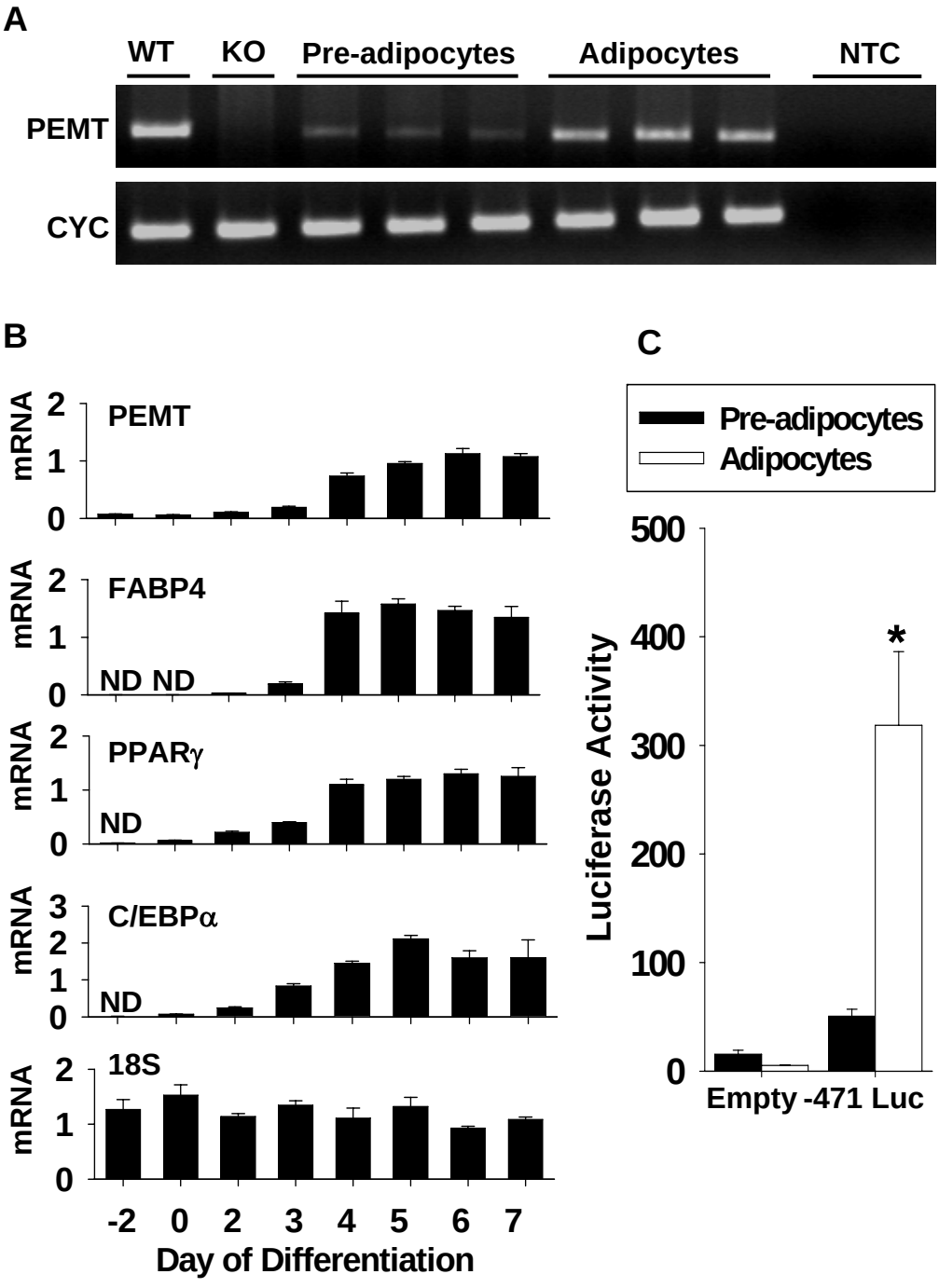
A
WT
KO
Pre-adipocytes
Adipocytes
NTC
PEMT
CYC
B
PEMT
FABP4
ND ND
PPARγ
ND
C/EBPα
ND
18S
mRNA
-2 0 2 3 4 5 6 7
Day of Differentiation
C
Pre-adipocytes
Adipocytes
Luciferase Activity
Empty -471 Luc
*

Figure 2.3. The mouse *Pemt* promoter region -471 /+130 bp is activated during 3T3-L1 differentiation.

3T3-L1 cells stably expressing various lengths of the *Pemt* promoter upstream of the luciferase reporter gene were generated and differentiated to adipocytes. Cells were collected before (-2) and following (+7) differentiation to adipocytes and luciferase activity was measured and normalized to cellular protein. The results are reported as fold induction at day 7 compared with luciferase activity at -2 day. Two stable cell lines (clone -1 and clone -2) are shown for each plasmid construct. The negative control was an empty pGL3 basic vector (Empty). Values represent means ± SEM of four independent experiments (*, $P<0.05$).

Figure 2.3

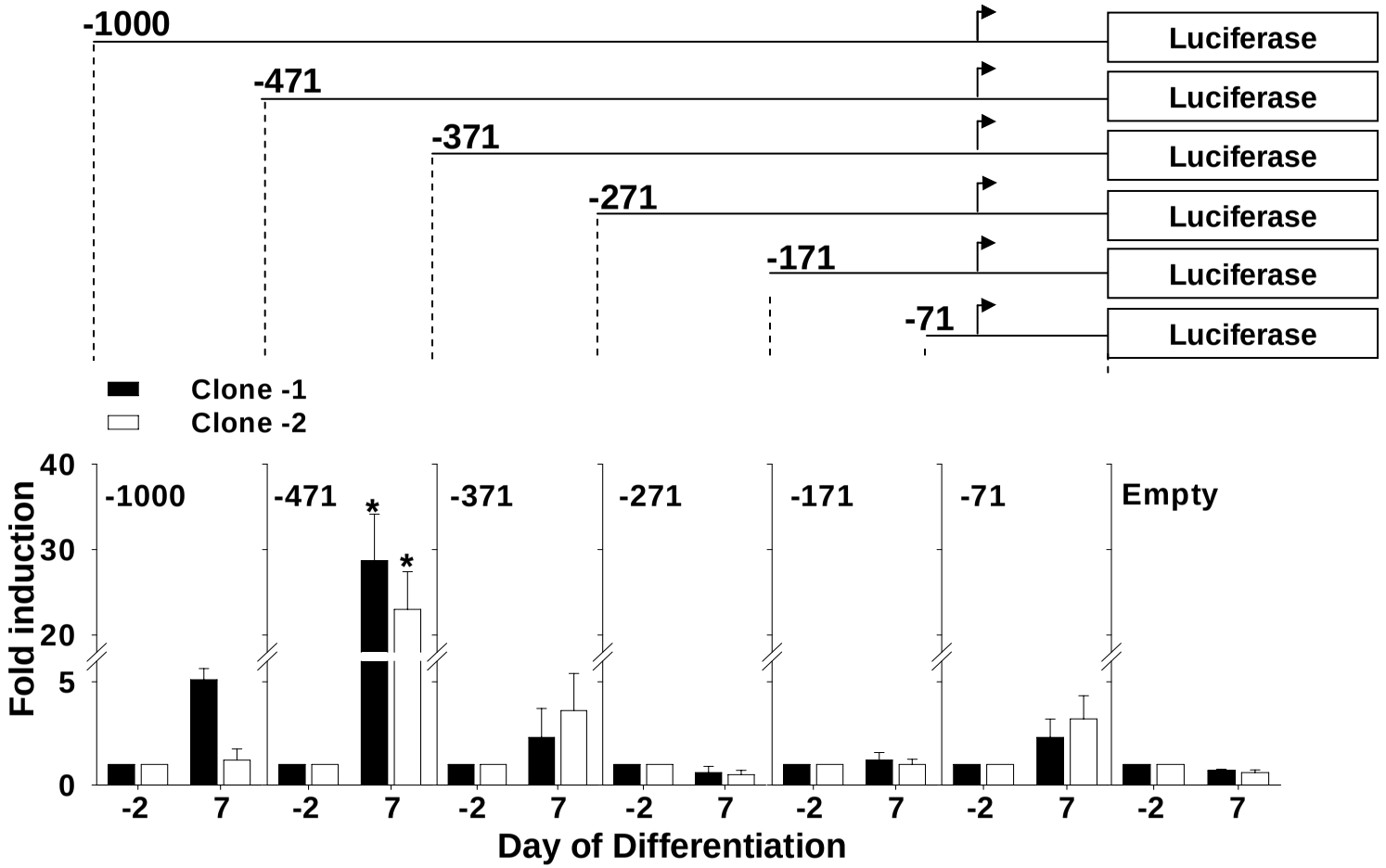
-1000
-471
-371
-271
-171
-71
Luciferase
Luciferase
Luciferase
Luciferase
Luciferase
Luciferase
Clone -1
Clone -2
Fold induction
40
30
20
5
0
-1000
-471
-371
-271
-171
-71
Empty
*
*
-2
7
Day of Differentiation

Figure 2.4. EMSA analysis of protein binding to the *Pemt* promoter using nuclear extract from 3T3-L1 cells.

Sections of the mouse *Pemt* promoter 40 bp in length were labelled with ^{32}P and incubated without (-) or with (+) nuclear extract (NE) isolated from 3T3-L1 adipocytes. The resulting DNA-protein complexes (a to c) were separated on 8% polyacrylamide gels and visualized by autoradiography. The results are representative of three independent experiments with similar results.

Figure 2.4

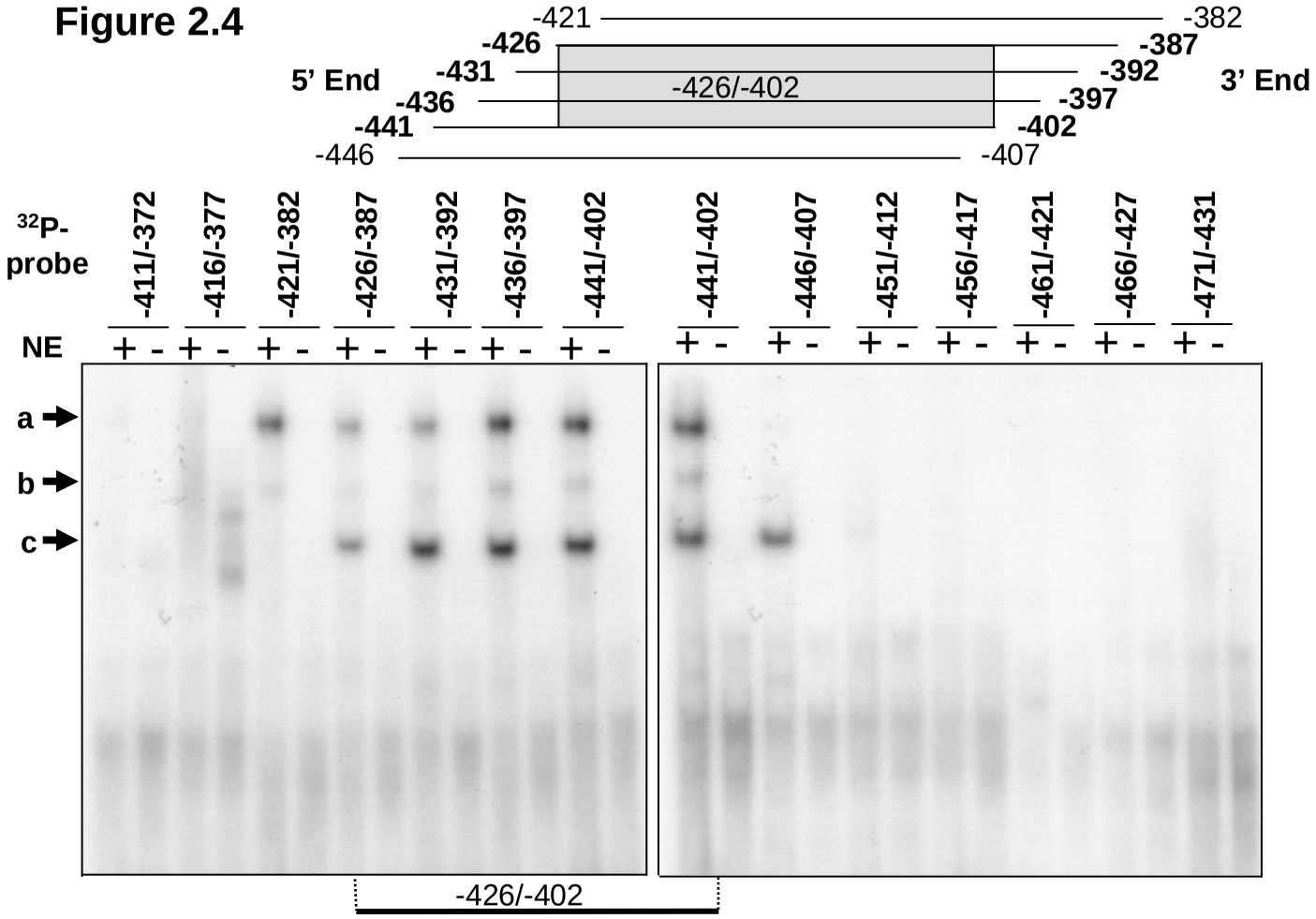
-421
-382
-426
-387
5' End
-431
-392
3' End
-426/-402
-436
-397
-441
-402
-446
-407
32P-probe
-411/-372
-416/-377
-421/-382
-426/-387
-431/-392
-436/-397
-441/-402
-441/-402
-446/-407
-451/-412
-456/-417
-461/-421
-466/-427
-471/-431
NE
+ - + - + - + - + - + - + - + - + - + - + - + - + -
a
b
c
-426/-402

Figure 2.5. EMSA analysis of protein binding to the *Pemt* promoter using nuclear extract from mouse liver.

Sections of the mouse *Pemt* promoter 40 bp in length were labelled with ^{32}P and incubated without (-) or with (+) nuclear extract (NE) isolated from mouse liver or 3T3-L1 adipocytes (A). The resulting DNA-protein complexes (a to f) were separated on 8% polyacrylamide gels and visualized by autoradiography. The results are representative of three independent experiments with similar results.

Figure 2.5

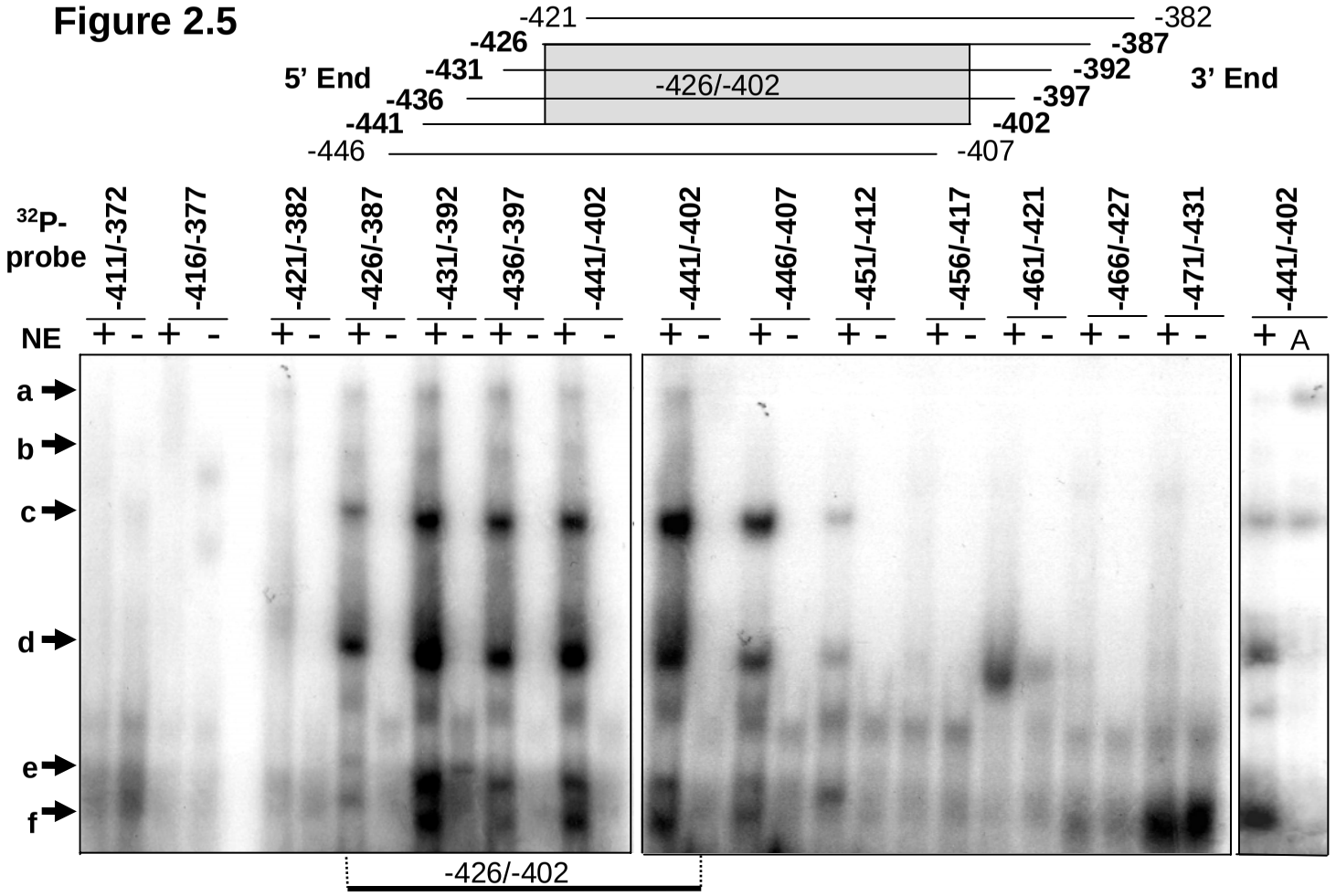
-421
-382
-426
-387
5' End
-431
-392
3' End
-426/-402
-436
-397
-441
-402
-446
-407
32P-probe
-411/-372
-416/-377
-421/-382
-426/-387
-431/-392
-436/-397
-441/-402
-441/-402
-446/-407
-451/-412
-456/-417
-461/-421
-466/-427
-471/-431
-441/-402
NE
+ - + - + - + - + - + - + - + - + - + - + - + - + - + - + - + - + A
a
b
c
d
e
f
-426/-402

Figure 2.6. Super-shift analysis of protein binding to the *Pemt* promoter using EMSA and nuclear extract from 3T3-L1 cells.

The -441/-402 section of the mouse *Pemt* promoter was labeled with ^{32}P and incubated without (-) or with (+) nuclear extract from 3T3-L1 cells. Unlabelled oligonucleotides containing the consensus sequence for YY1, the Sp family of transcription factors, or sterol response element binding protein (SREBP) were added to the binding reaction at 100-fold molar excess, as indicated. Antibodies raised against Sp1, Sp2, Sp3, YY1 or SREBP were used in binding reactions as indicated. Resulting DNA-protein complexes (a to f) and super-shifted (ss) complexes (indicated by arrowheads) were separated using 8% (left panel) or 7% (right panel) polyacrylamide gels and visualized by autoradiography. The results are representative of three independent experiments with similar results.

Figure 2.6 3T3-L1

Anti-SREBP	-	-	-	-	-	-	-	+	-	-		-	-	-	-	-	-	-	-	-
SREBP oligo	-	-	-	-	-	-	-	-	-	+		-	-	-	-	-	-	-	+	-
Anti-YY1	-	-	-	-	-	-	+	-	-	-		-	-	-	-	-	-	+	-	-
YY1 oligo	-	-	-	-	-	-	-	-	+	-		-	-	-	-	-	-	-	-	+
Anti-Sp3	-	-	-	+	-	-	-	-	-	-		-	-	-	+	-	-	-	-	-
Anti-Sp2	-	-	+	-	-	-	-	-	-	-		-	-	+	-	-	-	-	-	-
Anti-Sp1	-	+	-	-	-	-	-	-	-	-		-	+	-	-	-	-	-	-	-
Sp1 oligo	+	-	-	-	-	-	-	-	-	-		+	-	-	-	-	-	-	-	-
Nuclear Ext.	+	+	+	+	-	+	+	+	+	+		+	+	+	+	-	+	+	+	+
	1	2	3	4	5	6	7	8	9	10		11	12	13	14	15	16	17	18	19

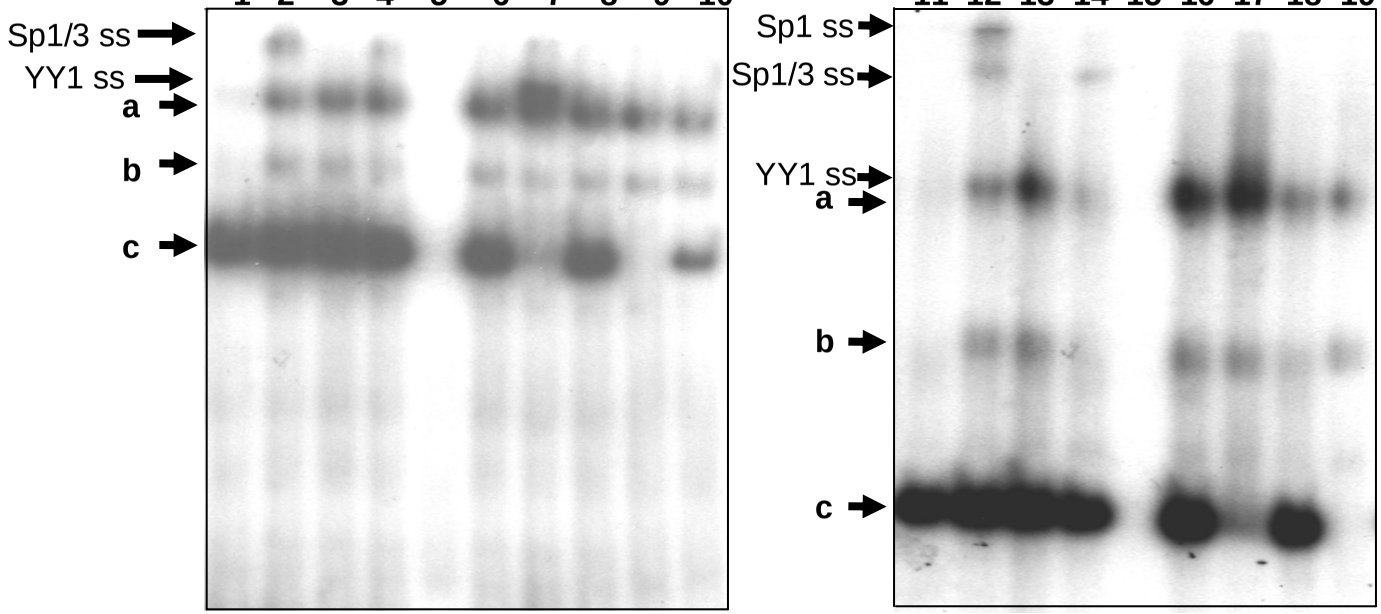

Figure 2.7. Super-shift analysis of protein binding to the *Pemt* promoter using EMSA and nuclear extract from mouse liver.

The -441/-402 section of the mouse *Pemt* promoter was labeled with ^{32}P and incubated without (-) or with (+) nuclear extract from mouse liver. Unlabelled oligonucleotides containing the consensus sequence for YY1, the Sp family of transcription factors, or sterol response element binding protein (SREBP) were added to the binding reaction at 100-fold molar excess, as indicated. Antibodies raised against Sp1, Sp2, Sp3, YY1 or SREBP were used in binding reactions as indicated. Resulting DNA-protein complexes (a to f) and super-shifted (ss) complexes (indicated by arrow heads) were separated using 8% (left panel) or 7% (right panel) polyacrylamide gels and visualized by autoradiography. The results are representative of three independent experiments with similar results.

Figure 2.7 Liver

	1	2	3	4	5	6	7	8	9	10		11	12	13	14	15	16	17	18	19	20
Anti-SREBP	-	-	-	-	-	-	-	+	-	-		-	-	-	-	-	-	-	+	-	-
SREBP oligo	-	-	-	-	-	-	-	-	-	+		-	-	-	-	-	-	-	-	-	+
Anti-YY1	-	-	-	-	-	-	+	-	-	-		-	-	-	-	-	-	+	-	-	-
YY1 oligo	-	-	-	-	-	-	-	-	+	-		-	-	-	-	-	-	-	-	+	-
Anti-Sp3	-	-	-	+	-	-	-	-	-	-		-	-	-	+	-	-	-	-	-	-
Anti-Sp2	-	-	+	-	-	-	-	-	-	-		-	-	+	-	-	-	-	-	-	-
Anti-Sp1	-	+	-	-	-	-	-	-	-	-		-	+	-	-	-	-	-	-	-	-
Sp1 oligo	+	-	-	-	-	-	-	-	-	-		+	-	-	-	-	-	-	-	-	-
Nuclear Ext.	+	+	+	+	-	+	+	+	+	+		+	+	+	+	-	+	+	+	+	+

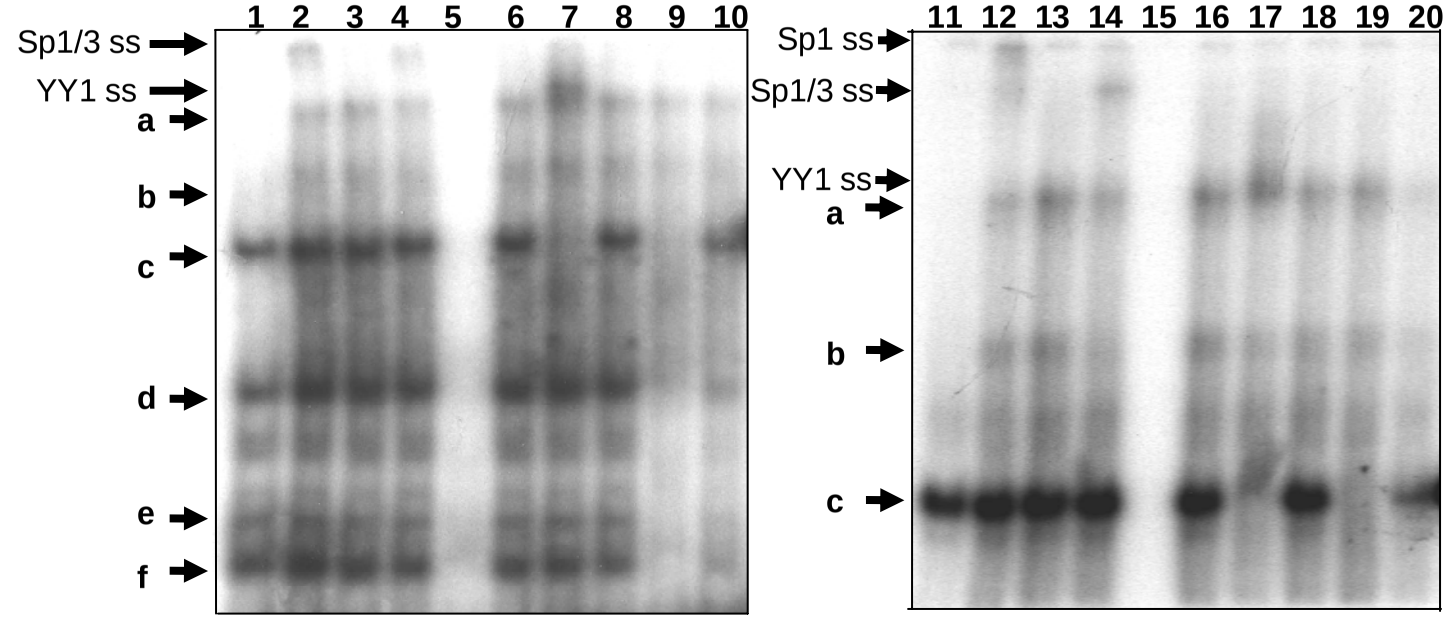

Figure 2.8. ChIP analysis of Sp1 and YY1 binding to the *Pemt* promoter.

(A) *In vivo* association of Sp1 with the *Pemt* promoter. Protein-DNA complexes were immunoprecipitated from lysates of 3T3-L1 pre-adipocytes (P) and adipocytes (A), without or with antibodies (AB) to IgG, or Sp1. The *Pemt* promoter was detected by PCR. DNA purified from sonicated cell lysates was used as a positive control (input). **(B)** Results of densitometric analysis of bands from three independent experiments using Sp1 antibody and are means ± SEM (*, $P<0.05$). **(C)** *In vivo* association of YY1 with the PEMT promoter. Protein-DNA complexes were immunoprecipitated from lysates of 3T3-L1 pre-adipocytes (P) and adipocytes (A), without or with antibodies (AB) to IgG, or YY1. The PEMT promoter was detected by PCR. DNA purified from sonicated cell lysates was used as a positive control (input). **(D)** Results of densitometric analysis of bands from three independent experiments using YY1 antibody are indicated as means ± SEM.

Figure 2.8

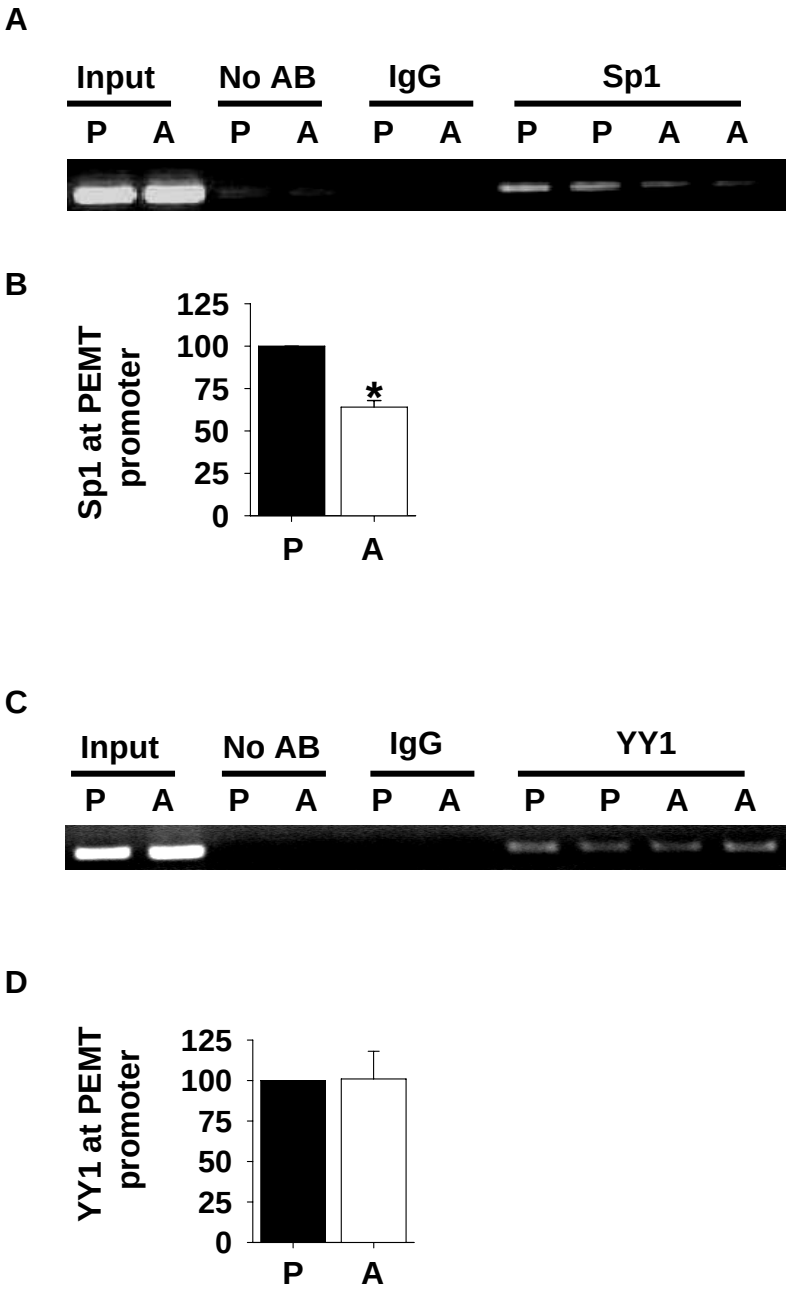
A
Input
No AB
IgG
Sp1
P A P A P A P P A A
B
Sp1 at PEMT promoter
125
100
75
50
25
0
*
P A
C
Input
No AB
IgG
YY1
P A P A P A P P A A
D
YY1 at PEMT promoter
125
100
75
50
25
0
P A

Figure 2.9. Analysis of mithramycin A-mediated inhibition of Sp1 binding to the *Pemt* promoter.

(A) 3T3-L1 stably expressing -471 Luc were differentiated to adipocytes and treated with the indicated concentration of mithramycin A (in 1% dimethylsulfoxide) or vehicle in 10% FBS, DMEM for 24 h. Luciferase activity was normalized to cellular protein. Values are means ± SEM of three independent experiments (*, $P<0.05$). **(B)** 3T3-L1 adipocytes were incubated with vehicle (V) or mithramycin A (M, 10 μM) for 24 h. Nuclear extract was obtained and incubated with ^{32}P-labeled *Pemt* promoter (-441/-402). DNA/protein complexes were separated on an 8% polyacylamide gel. A 100-fold molar excess of unlabeled DNA oligonucleotide containing the Sp family consensus sequence was added to the binding reaction as indicated. **(C)** Densitometric analysis of results of three independent EMSA experiments are shown as a ratio of intensity of complex a (Sp1) to complex c (YY1) (*, $P<0.05$). **(D)** *In vivo* association of Sp1 with the *Pemt* promoter. Protein-DNA complexes were immunoprecipitated from lysates of 3T3-L1 adipocytes treated with vehicle (V) or mithramycin A (M, 10 μM) for 24 h using antibodies (AB) to IgG, or Sp1. The *Pemt* promoter was detected by PCR. DNA purified from sonicated cell lysates was used as a positive control (input). **(E)** Results of densitometric analysis of bands from three independent experiments using Sp1 antibody are indicated as means ± SEM (*, $P<0.05$).

Figure 2.9

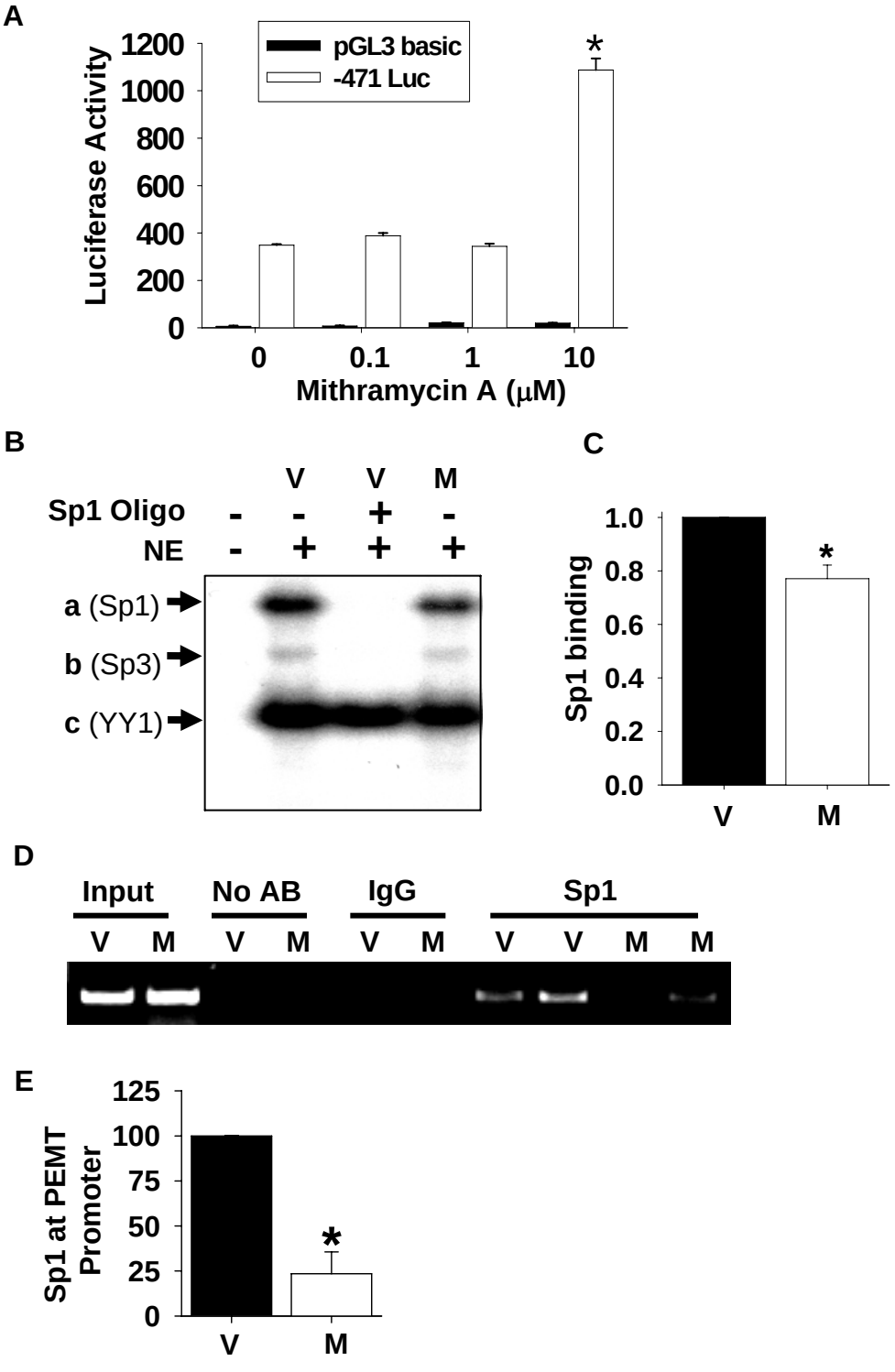
A
Luciferase Activity
1200
1000
800
600
400
200
0
pGL3 basic
-471 Luc
*
0
0.1
1
10
Mithramycin A (μM)
B
V
V
M
Sp1 Oligo
-
-
+
-
NE
-
+
+
+
a (Sp1)
b (Sp3)
c (YY1)
C
Sp1 binding
1.0
0.8
0.6
0.4
0.2
0.0
*
V
M
D
Input
No AB
IgG
Sp1
V
M
V
M
V
M
V
V
M
M
E
Sp1 at PEMT Promoter
125
100
75
50
25
0
*
V
M

Figure 2.10. Analysis of the influence of Sp1 on *Pemt* promoter/luciferase activity.

(A) 3T3-L1 pre-adipocytes stably expressing the pGL3 basic vector without (pGL3 basic) or with the *Pemt* promoter section -471 to +130 bp (-471 Luc) upstream of the luciferase reporter gene were treated with retrovirus generated from either an empty pBabe vector (Empty, black bars) or pBabe.puro containing cDNA encoding Sp1 (Sp1, white bars). Cell lysates from 3T3-L1 fibroblasts transduced with the indicated virus were immunoblotted with antibodies raised against Sp1 and PDI (protein disulfide isomerase). Densitometric analysis of immunoblots is shown below the immunoblot. Values represent means of three separate independent experiments. Luciferase activity was measured and normalized to cellular protein in 3T3-L1 pre-adipocytes **(B)** and adipocytes **(C)**. **(D)** 3T3-L1 pre-adipocytes stably expressing the pGL3 basic vector without (pGL3 basic) or with the *Pemt* promoter section -471 to +130 bp (-471 Luc) upstream of the luciferase reporter gene were transduced with retrovirus generated from either pSuper.retro containing scrambled- (Scrambled RNAi) or Sp1- (Sp1 RNAi) shRNA sequences. Luciferase activity measured in pre-adipocytes **(E)** and adipocytes **(F)** and normalized to cellular protein. Values are means ± SEM of three independent experiments (*, $P<0.05$).

Figure 2.10

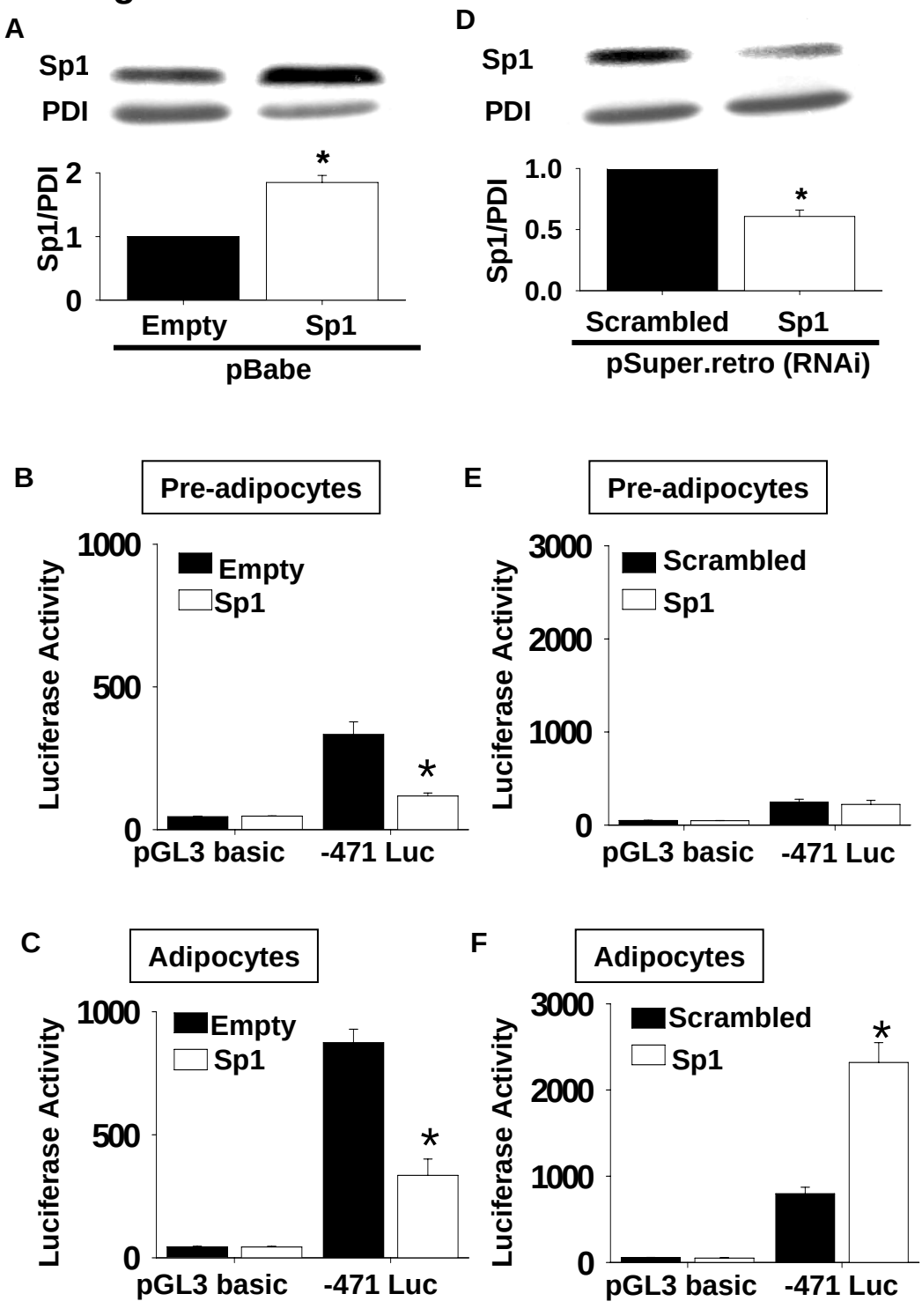
A
Sp1
PDI
Sp1/PDI
2
1
0
*
Empty
Sp1
pBabe
D
Sp1
PDI
Sp1/PDI
1.0
0.5
0.0
*
Scrambled
Sp1
pSuper.retro (RNAi)
B
Pre-adipocytes
Luciferase Activity
1000
500
0
Empty
Sp1
*
pGL3 basic
-471 Luc
E
Pre-adipocytes
Luciferase Activity
3000
2000
1000
0
Scrambled
Sp1
pGL3 basic
-471 Luc
C
Adipocytes
Luciferase Activity
1000
500
0
Empty
Sp1
*
pGL3 basic
-471 Luc
F
Adipocytes
Luciferase Activity
3000
2000
1000
0
Scrambled
Sp1
*
pGL3 basic
-471 Luc

Figure 2.11. Analysis of Sp1, Sp3, YY1, PEMT and TBP protein levels by immunobloting.

3T3-L1 fibroblasts were differentiated into adipocytes. Day 0 represents 2 days post-confluence and the starting point of the differentiation protocol. Cells were harvested at the indicated times (top row of numbers). 3T3-L1 homogenates (50 μg protein) were separated on 0.4% SDS/10% polyacrylamide gels, electroblotted on to PVDF membranes, and probed with antibodies raised against Sp1, Sp3, YY1, PEMT or TBP (TATA-box binding protein). The results are representative of three independent experiments. The numbers below each gel represent the mean of densitometric analysis of three immunoblots relative to the amount of TBP detected. HeLa whole cell lysate (50 μg, Santa Cruz Biotech.) was used as a positive control for the indicated nuclear proteins.

Figure 2.11

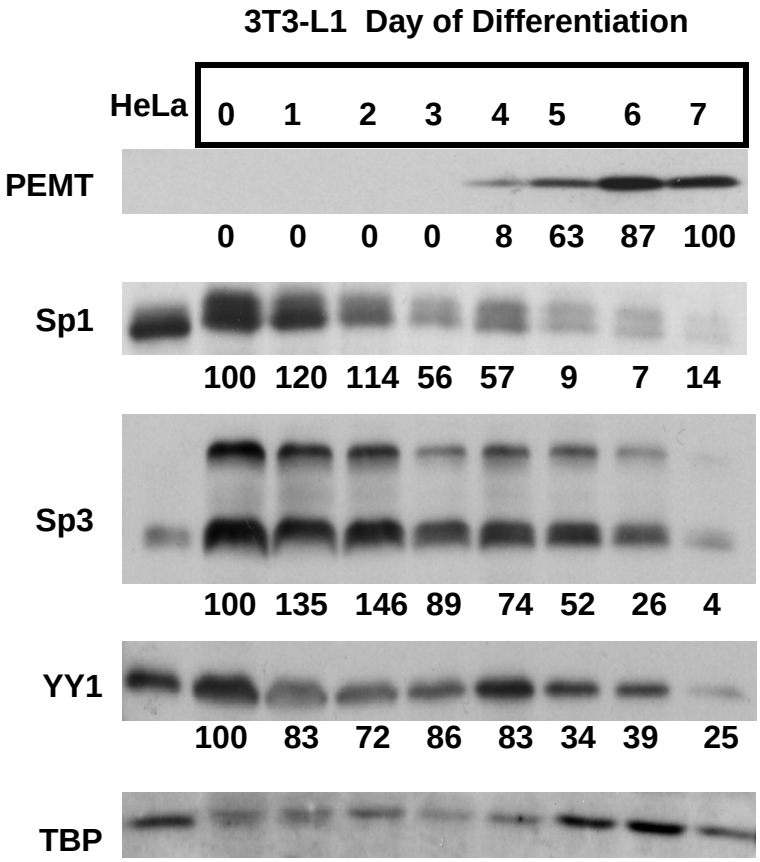
3T3-L1 Day of Differentiation
HeLa
0 1 2 3 4 5 6 7
PEMT
0 0 0 0 8 63 87 100
Sp1
100 120 114 56 57 9 7 14
Sp3
100 135 146 89 74 52 26 4
YY1
100 83 72 86 83 34 39 25
TBP

Figure 2.12. Tamoxifen inhibits *Pemt* gene expression

(A) Total RNA was extracted from the liver of adult male PEMT wild type mice injected subcutaneously with either tamoxifen (0.5mg/kg/day in sesame oil, 1% benzyl alcohol) or vehicle for 5 consecutive days. The RNA was reverse transcribed to cDNA, and *Pemt* mRNA levels were detected by qPCR. mRNA levels were normalized to cyclophilin using a standard curve. Data represents means ± SEM (*, $P<0.05$, n=5-7 mice). **(B)** 3T3-L1 stably expressing -471 Luc were differentiated to adipocytes and treated with the indicated concentration of tamoxifen (in 1% dimethylsulfoxide) or vehicle in 10% FBS, DMEM for 7 days. Luciferase activity was normalized to cellular protein. Values are means ± SEM of three independent experiments (*, $P<0.05$, ANOVA).

Figure 2.12

A

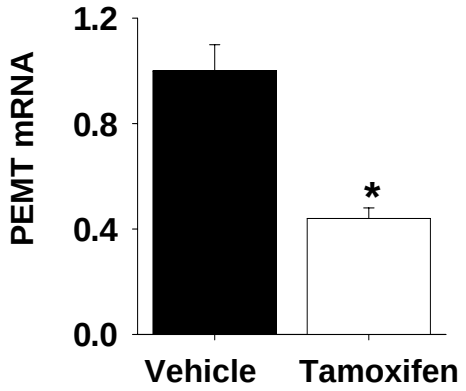

B

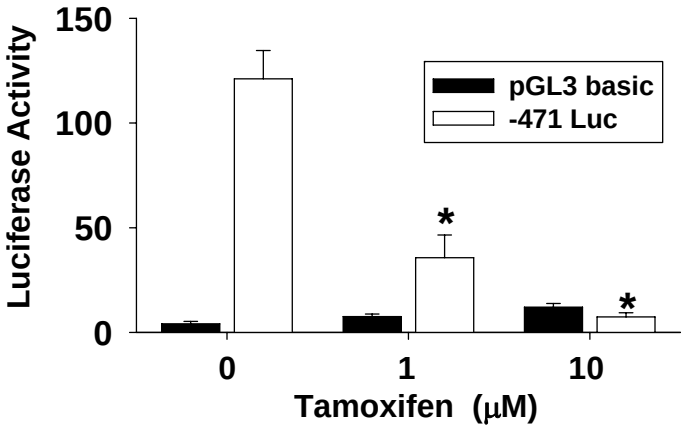

Figure 2.13. Tamoxifen inhibits *Pemt* gene expression by increasing Sp1 binding

(A) 3T3-L1 adipocytes were incubated with vehicle (V), or tamoxifen (T, 10 μM) for 7 days or mithramycin A (M, 10 μM) for 24 h. Cells were then washed twice with phosphate-buffered saline. Nuclear extract was obtained and incubated with ^{32}P-labeled *Pemt* promoter (-441/-402). DNA/protein complexes (a-c) were separated on an 8% polyacylamide gel. A 100-fold molar excess of unlabeled DNA oligonucleotide containing the Sp family consensus sequence was added to the binding reaction as indicated. **(B)** Densitometric analysis of the results of three independent EMSA experiments are shown as a ratio of intensity of complex a (Sp1) to the intensity of complex c (YY1) (*, P<0.05). **(D)** *In vivo* association of Sp1 with the *Pemt* promoter. Protein-DNA complexes were immunoprecipitated from lysates of 3T3-L1 adipocytes treated with vehicle (V) or tamoxifen (T, 10 μM) for 7 days using antibodies (AB) to IgG, or Sp1. The *Pemt* promoter was detected by PCR. DNA purified from sonicated cell lysates was used as a positive control (input). **(E)** Results of densitometric analysis of bands from three independent experiments using Sp1 antibody are indicated as means ± SEM (*, P<0.05).

Figure 2.13

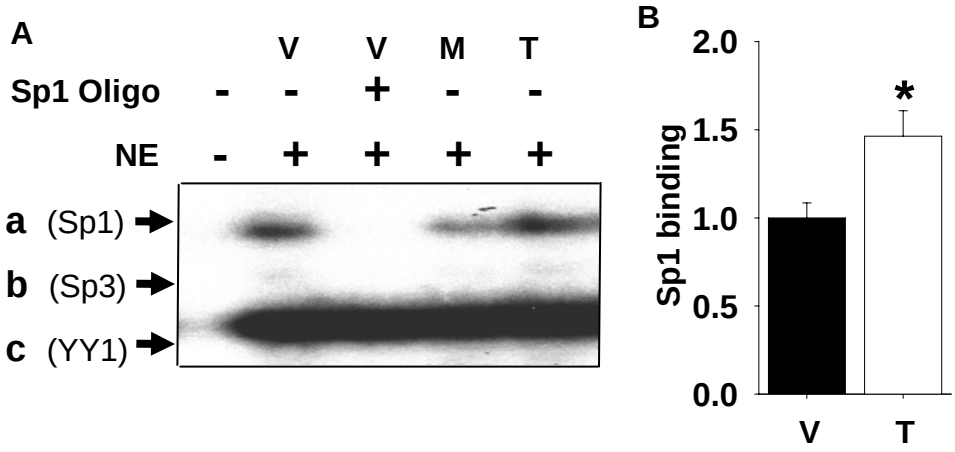
A
V V M T
Sp1 Oligo - - + - -
NE - + + + +
a (Sp1)
b (Sp3)
c (YY1)
B
Sp1 binding
2.0
1.5
1.0
0.5
0.0
*
V
T
C
Input
No AB
IgG
Sp1
V T V T V T V V T T
D
Sp1 at PEMT Promoter
200
150
100
50
0
*
V
T

Figure 2.14. Tamoxifen requires the Sp1 binding site to inhibit *Pemt* gene expression

(A) The -441/-402 section of the mouse promoter containing the wild-type GC-element (Wt) or the mutated GC-element (MSp1) was ^{32}P labelled and incubated without (-) or with nuclear extract from mouse liver (+). Resulting DNA-protein complexes (a to c) were separated using an 8% polyacylamide gel and visualized by autoradiography. The results are representative of three independent experiments. **(B)** 3T3-L1 adipocytes stably expressing -471 Luc or -471MSp1 Luc (containing a mutation in the Sp1 binding site) were differentiated to adipocytes and treated with 10 μm tamoxifen (in 1 % dimethylsulfoxide) or vehicle in 10 % FBS, DMEM for 7 days. Luciferase activity was normalized to cellular protein. Values are means ± SEM of three independent experiments (*, $P<0.05$ compared to 3T3-L1 adipocytes stably expressing -471 Luc treated with vehicle; #, $P<0.05$, compared to 3T3-L1 adipocytes stably expressing -471 Luc treated with vehicle or tamoxifen, ANOVA).

Figure 2.14

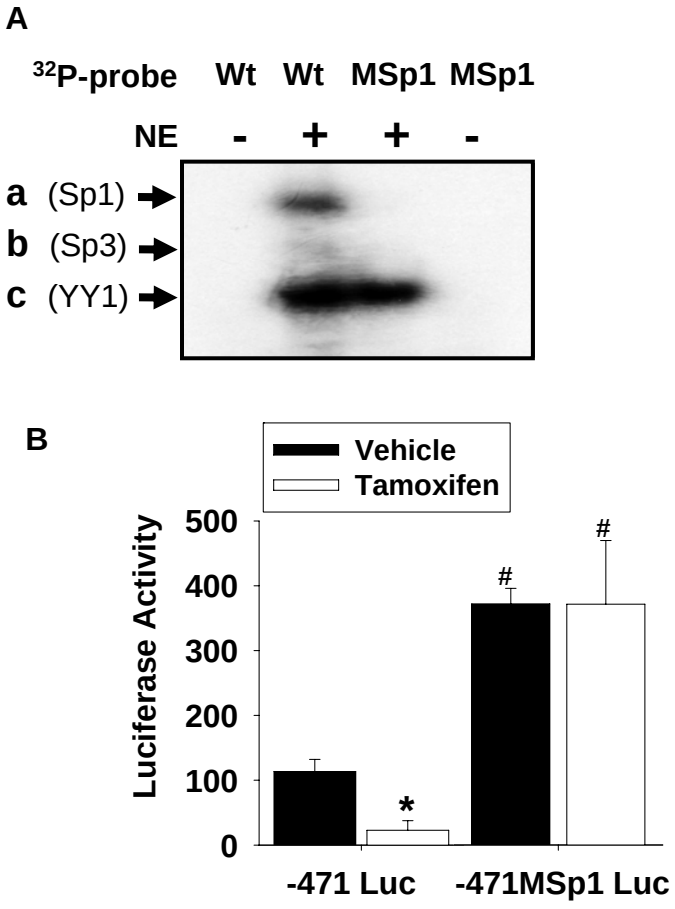
A
32P-probe Wt Wt MSp1 MSp1
NE - + + -
a (Sp1)
b (Sp3)
c (YY1)
B
Vehicle
Tamoxifen
Luciferase Activity
500
400
300
200
100
0
*
#
#
-471 Luc
-471MSp1 Luc

2.5 References

1. Vance, D. E., and Vance, J. E. (2008) Phospholipid biosynthesis in eukaryotes. In: Vance, D. E., and Vance, J. E. (eds). *Biochemistry of Lipids, Lipoproteins and Membranes (pp 213-244)*, 5 Ed., Elsevier, New York
2. Vance, D. E., and Ridgway, N. D. (1988) *Prog Lipid Res* **27**(1), 61-79
3. Bremer, J., and Greenberg, D. M. (1960) *Biochim Biophys Acta* **37**, 173-175
4. Cui, Z., Vance, J. E., Chen, M. H., Voelker, D. R., and Vance, D. E. (1993) *The Journal of biological chemistry* **268**(22), 16655-16663
5. Shields, D. J., Lehner, R., Agellon, L. B., and Vance, D. E. (2003) *The Journal of biological chemistry* **278**(5), 2956-2962
6. DeLong, C. J., Shen, Y. J., Thomas, M. J., and Cui, Z. (1999) *The Journal of biological chemistry* **274**(42), 29683-29688
7. Reo, N. V., Adinehzadeh, M., and Foy, B. D. (2002) *Biochim Biophys Acta* **1580**(2-3), 171-188
8. Sundler, R., and Akesson, B. (1975) *The Journal of biological chemistry* **250**(9), 3359-3367
9. Walkey, C. J., Yu, L., Agellon, L. B., and Vance, D. E. (1998) *The Journal of biological chemistry* **273**(42), 27043-27046
10. Noga, A. A., Zhao, Y., and Vance, D. E. (2002) *The Journal of biological chemistry* **277**(44), 42358-42365

11. Noga, A. A., and Vance, D. E. (2003) *The Journal of biological chemistry* **278**(24), 21851-21859

12. Saadeh, S. (2007) *Nutr Clin Pract* **22**(1), 1-10

13. Loria, P., Lonardo, A., and Targher, G. (2008) *Clin Sci (Lond)* **115**(1), 1-12

14. Glass, C. K., and Witztum, J. L. (2001) *Cell* **104**(4), 503-516

15. Li, Z., Agellon, L. B., and Vance, D. E. (2005) *The Journal of biological chemistry* **280**(45), 37798-37802

16. Li, Z., Agellon, L. B., Allen, T. M., Umeda, M., Jewell, L., Mason, A., and Vance, D. E. (2006) *Cell Metab* **3**(5), 321-331

17. Zhao, Y., Su, B., Jacobs, R.L., Kennedy, B., Francis, G.A., Waddington, E., Brosnan, J.T., Vance, J.E., and Vance, D.E. (2009) *Arteriosclerosis, Thrombosis, and Vascular Biology* **29**(9), 1349-1355

18. Walkey, C. J., Cui, Z., Agellon, L. B., and Vance, D. E. (1996) *J Lipid Res* **37**(11), 2341-2350

19. Ince, T. A., and Scotto, K. W. (1995) *The Journal of biological chemistry* **270**(51), 30249-30252

20. Cui, Z., Shen, Y. J., and Vance, D. E. (1997) *Biochim Biophys Acta* **1346**(1), 10-16

21. Resseguie, M., Song, J., Niculescu, M. D., da Costa, K. A., Randall, T. A., and Zeisel, S. H. (2007) *Faseb J* **21**(10), 2622-2632

22. Klaunig, J. E., Goldblatt, P. J., Hinton, D. E., Lipsky, M. M., Chacko, J., and Trump, B. F. (1981) *In Vitro* **17**(10), 913-925

23. Banchio, C., Schang, L. M., and Vance, D. E. (2004) *The Journal of biological chemistry* **279**(38), 40220-40226

24. Andrews, N. C., and Faller, D. V. (1991) *Nucleic Acids Res* **19**(9), 2499

25. Deryckere, F., and Gannon, F. (1994) *Biotechniques* **16**(3), 405

26. Jordan, M., and Wurm, F. (2004) *Methods* **33**(2), 136-143

27. Spencer, V. A., Sun, J. M., Li, L., and Davie, J. R. (2003) *Methods* **31**(1), 67-75

28. Baker, T. K., Carfagna, M. A., Gao, H., Dow, E. R., Li, Q., Searfoss, G. H., and Ryan, T. P. (2001) *Chem Res Toxicol* **14**(9), 1218-1231

29. Gregoire, F. M., Smas, C. M., and Sul, H. S. (1998) *Physiological reviews* **78**(3), 783-809

30. Shi, Y., Seto, E., Chang, L. S., and Shenk, T. (1991) *Cell* **67**(2), 377-388

31. Suske, G. (1999) *Gene* **238**(2), 291-300

32. Miller, D. M., Polansky, D. A., Thomas, S. D., Ray, R., Campbell, V. W., Sanchez, J., and Koller, C. A. (1987) *Am J Med Sci* **294**(5), 388-394

33. Lelliott, C. J., Lopez, M., Curtis, R. K., Parker, N., Laudes, M., Yeo, G., Jimenez-Linan, M., Grosse, J., Saha, A. K., Wiggins, D.,

Hauton, D., Brand, M. D., O'Rahilly, S., Griffin, J. L., Gibbons, G. F., and Vidal-Puig, A. (2005) *Faseb J* **19**(9), 1108-1119

34. Pugh, B. F., and Tjian, R. (1991) *Genes Dev* **5**(11), 1935-1945
35. Boyer, T. G., Krug, J. R., and Maquat, L. E. (1989) *The Journal of biological chemistry* **264**(9), 5177-5187
36. Lin, S. Y., Black, A. R., Kostic, D., Pajovic, S., Hoover, C. N., and Azizkhan, J. C. (1996) *Mol Cell Biol* **16**(4), 1668-1675
37. Kim, S., Kang, J. K., Kim, Y. K., Seo, D. W., Ahn, S. H., Lee, J. C., Lee, C. H., You, J. S., Cho, E. J., Lee, H. W., and Han, J. W. (2006) *Biochem Biophys Res Commun* **342**(4), 1168-1173
38. Doetzlhofer, A., Rotheneder, H., Lagger, G., Koranda, M., Kurtev, V., Brosch, G., Wintersberger, E., and Seiser, C. (1999) *Mol Cell Biol* **19**(8), 5504-5511
39. Banchio, C., Schang, L. M., and Vance, D. E. (2003) *The Journal of biological chemistry* **278**(34), 32457-32464
40. Roder, K., Kim, K. H., and Sul, H. S. (2002) *Biochem Biophys Res Commun* **294**(1), 63-70
41. Zhang, Y., Liao, M., and Dufau, M. L. (2006) *Mol Cell Biol* **26**(18), 6748-6761
42. Feng, D., and Kan, Y. W. (2005) *Proc Natl Acad Sci U S A* **102**(28), 9896-9900
43. Chang, Y. C., Illenye, S., and Heintz, N. H. (2001) *Mol Cell Biol* **21**(4), 1121-1131

44. Lee, J. S., Galvin, K. M., and Shi, Y. (1993) *Proc Natl Acad Sci U S A* **90**(13), 6145-6149

45. Zhang, Y., and Dufau, M. L. (2003) *Mol Cell Biol* **23**(19), 6958-6972

46. Douglas, D. N., Dolinsky, V. W., Lehner, R., and Vance, D. E. (2001) *The Journal of biological chemistry* **276**(27), 25621-25630

47. Aoyama, C., Ishidate, K., Sugimoto, H., and Vance, D. E. (2007) *Biochim Biophys Acta* **1771**(9), 1148-1155

48. Houweling, M., Cui, Z., Tessitore, L., and Vance, D. E. (1997) *Biochim Biophys Acta* **1346**(1), 1-9

49. Pelech, S. L., Power, E., and Vance, D. E. (1983) *Can J Biochem Cell Biol* **61**(11), 1147-1152

50. Sesca, E., Perletti, G. P., Binasco, V., Chiara, M., and Tessitore, L. (1996) *Biochem Biophys Res Commun* **229**(1), 158-162

51. Grinstein, E., Jundt, F., Weinert, I., Wernet, P., and Royer, H. D. (2002) *Oncogene* **21**(10), 1485-1492

52. Kutoh, E., Margot, J. B., and Schwander, J. (1999) *Cancer Lett* **136**(2), 187-194

53. Singh, M. N., Martin-Hirsch, P. L., and Martin, F. L. (2008) *Med Sci Monit* **14**(9), RA144-148

54. Levy, N., Tatomer, D., Herber, C. B., Zhao, X., Tang, H., Sargeant, T., Ball, L. J., Summers, J., Speed, T. P., and Leitman, D. C. (2008) *Molecular endocrinology (Baltimore, Md* **22**(2), 287-303

55. Safe, S., and Kim, K. (2008) *J Mol Endocrinol* **41**(5), 263-275

56. Zhang, D., and Trudeau, V. L. (2006) *Comparative biochemistry and physiology* **144**(3), 306-315

57. Dong, J., Tsai-Morris, C. H., and Dufau, M. L. (2006) *The Journal of biological chemistry* **281**(27), 18825-18836

58. Lai, K., Harnish, D. C., and Evans, M. J. (2003) *The Journal of biological chemistry* **278**(38), 36418-36429

59. Dong, S., Zhang, Z., and Takahara, H. (2007) *Molecular endocrinology (Baltimore, Md* **21**(7), 1617-1629

60. Qin, C., Samudio, I., Ngwenya, S., and Safe, S. (2004) *Molecular carcinogenesis* **40**(3), 160-170

61. Ngwenya, S., and Safe, S. (2003) *Endocrinology* **144**(5), 1675-1685

Chapter 3

Tamoxifen Induces Steatosis in Mouse Liver by Activation of Fatty Acid Synthesis

3.1 Introduction

Tamoxifen (TMX) was originally developed in 1973 as an inhibitor of the physiological effects of estrogens in the pathogenesis of breast cancer (1). According to the U.S. National Institutes of Health, approximately 190,000 women in the USA will be diagnosed with, and 40,000 will die from, breast cancer in 2009 (2). Tamoxifen reduces the reappearance (47%) and death (26%) due to breast cancer (3). Despite the introduction of new anti-neoplastic agents, TMX is widely used for the treatment of hormone-responsive breast cancer due to the significant advantage of being inexpensive and well-tolerated (4). In addition, there is evidence to suggest that bladder (5) and prostate cancers (6) could be treated with TMX (5,7). Tamoxifen is a selective estrogen receptor modulator which can act as either an estrogen-agonist or -antagonist depending on the tissue (4,8). For example, TMX acts as an estrogen agonist in bone (3,9) and female lower genital tract (10). The benefits associated with the pro-estrogen activity of tamoxifen are underscored by recent clinical trials designed to treat anovulatory infertility (11) and prevent bone loss among postmenopausal women (12).

Despite the multiple applications of TMX, one frequent side effect is the development of non-alcoholic fatty liver disease which includes a spectrum of chronic liver damage that ranges from fatty liver (steatosis), to non-alcoholic steatohepatitis (13). It has been reported that 43% of

women with breast cancer treated with tamoxifen develop steatosis within the first 2 years of treatment (14); steatohepatitis (15) and cirrhosis (16) can also develop, particularly in overweight women. To date, the mechanism of TMX-induced steatosis remains unclear.

A limited number of studies have investigated the effect of TMX on hepatic lipid metabolism. Both inhibition of fatty acid oxidation (17,18) and increased triacylglycerol (TG) biosynthesis (19) have been implicated in the process. One possible explanation for the apparently different conclusions in these studies is that TMX is an appetite suppressor yet the animals were not always pair-fed (17,19). Second, the duration of tamoxifen treatment varied between studies (5-28 days) such that lipid metabolism was investigated at different stages of TMX-mediated steatosis (17-19).

In the current study our aim was to elucidate the initial mechanism underlying the accumulation of hepatic TG following TMX-treatment. We investigated the primary actions of TMX that initiate fat deposition in the liver. Mice were pair-fed and injected subcutaneously with either TMX (0.5 mg/kg/day) or vehicle (sesame oil, 1% benzyl alcohol) for 5 consecutive days. We found increased incorporation of [^{3}H]-acetate (~50%) into TG in hepatocytes from TMX-treated mice compared to control mice. TMX did not significantly alter fatty acid uptake, TG secretion or fatty acid oxidation. Together our data indicate that increased *de novo* fatty acid synthesis is

the primary event which leads to the TMX-induced steatosis in mouse liver.

3.2 Experimental Procedures

3.2.1 Animal Care

All animal procedures were performed in accordance with the University of Alberta Animal Policy and Welfare Committee, which adheres to the principles for biomedical research involving animals developed by the Council for International Organizations of Medical Sciences. Male C57BL/6J mice (Jackson Laboratory, Bar Harbour, ME) and male C57BL/6 (backcrossed >7 generations*) Pemt*$^{-/-}$ mice were 8-12 weeks old and maintained on a standard chow diet containing 6% (w/w) fat and 0.02% (w/w) cholesterol (LabDiet). Tamoxifen (Sigma) was dissolved at a concentration of 0.2 mg/ml in sesame oil containing 1% benzyl alcohol. The mice were injected subcutaneously with either TMX (0.5 mg/kg of mouse weight) or 2.5 μl vehicle (sesame oil, 1% benzyl alcohol)/g of animal weight. Animals were pair fed such that the vehicle-injected group received an amount of diet (g/g mouse weight) corresponding to the average amount that the TMX-treated animals had eaten the day before. The mice were injected at the same time of day on five consecutive days and anaesthetized 4 h following the final injection.

3.2.2 Lipid and Lipoprotein Analyses

Mice were fasted overnight (~16 h) before blood was collected by cardiac puncture of anaesthetized animals. Tissues were harvested immediately, rinsed in ice-cold phosphate-buffered saline and flash frozen in liquid N_2. Plasma lipoproteins were separated according to size using fast-protein liquid chromatography (20) on an Agilent 1200 chromatography system with a Superose 6 column (Amersham Pharmacia Biotech). The content of total cholesterol (unesterified + esterified) and TG was quantified in each fraction with in-line enzymatic assay kits for cholesterol (unesterified + esterified) Thermo Infinity reagents, VWR) and TG (Thermo Infinity TG regents, VWR). Peaks were identified by comparison with lipoprotein standards (21). Total lipids were extracted (22) from plasma (100 μl) or liver homogenate (1 mg protein) in ice-cold phosphate-buffered saline. TG, unesterified cholesterol and cholesteryl ester (CE) were measured by gas-liquid chromatography (23); amounts of phosphatidylcholine (PC) and phosphatidylethanolamine (PE) were determined by phosphorus assay (24) following separation by thin-layer chromatography in a developing solvent of chloroform/methanol/acetic acid/water (25/5/4/2, v/v).

3.2.3 Tissue Preparation and Histology

Mice were euthanized and the liver excised, fixed in 10% buffered formalin, cryo-sectioned (10 μm) and stained with Oil Red O to reveal neutral lipid accumulation. Color photographs were taken with AxioCam (Zeiss) mounted on a stereomicroscope (Axioskop) with a 40 X objective lens.

3.2.4 Isolation of Hepatocytes

Primary cultures of adult mouse hepatocytes were isolated using the collagenase perfusion technique as previously described (25). The cells were plated at a density of 1 X 10^6 cells on collagen-coated 60-mm dishes in high-glucose Dulbecco's modified Eagles medium (DMEM) supplemented with 10% fetal bovine serum. The cells were allowed to adhere to the plates for 2 h at 37^{o}C then washed with serum-free DMEM prior to incubation with the indicated radiolabel diluted in DMEM.

3.2.5 Incubation of Primary Cultures of Hepatocytes with Radioisotopes

Primary cultures of hepatocytes were isolated from vehicle- and TMX-treated animals. Following a 2 h incubation at 37^{o}C, the cells were rinsed with serum-free DMEM and incubated with one of the following radiolabels: 5 μCi [^{3}H]ethanolamine, 2 μCi [^{14}C]acetate or 5 μCi [^{3}H]glucose per dish. The cells were harvested at the indicated time,

washed twice with ice-cold phosphate-buffered saline (pH 7.4), scraped and sonicated in 1 ml phosphate-buffered saline. For experiments with [^{3}H]oleate, hepatocytes were incubated with 5 μCi [^{3}H]oleate per dish in the presence of 0.4 mM oleate and 0.4% bovine serum albumin. At the indicated times, the medium was removed and centrifuged for 5 min at 2,500 x g to remove dead cells. Prior to harvest, the cells were washed twice with ice-cold phosphate-buffered saline. Pulse-chase experiments were conducted by a 2 h pulse with 5 μCi [^{3}H]oleate per dish in the presence of 0.4 mM oleate and 0.4% bovine serum albumin. The cells were then washed twice with serum-free DMEM and incubated for 4 h in fresh serum-free DMEM in the absence of oleate**.**

3.2.6 Lipid Extraction and Thin-layer Chromatography

Total lipids were extracted from hepatocytes (1 mg protein) or media (2 ml) (22). The lipids were resolved by thin-layer chromatography in the solvent system chloroform/methanol/acetic acid/water (25/15/4/2, v:v) until the solvent migrated half way up the plate. The plate was allowed to dry prior to separation of neutral lipids using the solvent system heptane/isopropylether/acetic acid (60/40/4, v:v). Bands corresponding to phosphatidylcholine (PC), phosphatidylethanolamine (PE), cholesterol, CE, TG and phosphatidylinositol/phosphatidylserine were scraped and radioactivity determined.

3.2.7 Measurement of Acid-soluble Metabolites

Medium conditioned by the hepatocytes was centrifuged for 5 min at 2,500 x *g* to remove dead cells, then 30 μl 20% bovine serum albumin was added to 200 μl medium followed by 16 μl of 70% perchloric acid. The medium was centrifuged at 21,000 x *g* for 5 min after which radioactivity was measured in an aliquot of the supernatant.

3.2.8 RNA isolation and PCR analysis

Total RNA was isolated from liver tissue or cultured cells using Trizol® reagent (Life Technologies, Inc.) according to the manufacturer's instructions. First-strand cDNA synthesis from 2 μg of total RNA was performed using SuperScript™ II reverse transcriptase (Invitrogen) primed by oligo$(dT)_{12\text{-}18}$. PCR was performed using gene specific primers indicated in Table 3.1. Amplicons were measured using real-time quantitative PCR using a Rotor-gene 3000 instrument (Montreal Biotech) and analysed with the Rotor-Gene 6.0.19 program (Montreal Biotech).

3.2.9 Immunoblot Analyses

Liver homogenates (30 μg) were heated for 10 min at 90^0C in 62.5 mM Tris-HCl (pH 8.3), 10% glycerol, 5% (v/v) 2-mecaptoethanol, 1% SDS, and 0.004% bromophenol blue. The samples were electrophoresed on SDS-polyacrylamide (5-10%) gels in 25 mM Tris-HCl (pH 8.5), 192 mM glycine buffer containing 0.1% SDS. The proteins were transferred to

polyvinylidene fluoride membranes by electroblotting in transfer buffer [125 mM Tris-HCl, pH 8.3), 960 mM glycine, 10% (v/v) methanol]. Following transfer, the membrane was incubated overnight at 4^{o}C with 5% skim milk in 10 mM Tris-HCl (pH 7.4), 100 mM NaCl, 0.1% Tween 20 followed by incubation for 1 h at room temperature or overnight at 4^{o}C with antibody raised against the protein indicated.

Anti-protein-disulfide isomerase (PDI, Stressgen Biotechnologies Corp.) antibody (1:4000), anti-fatty acid synthase (FAS) antibody (1:1000), anti-acetyl-Coenzyme A (ACC) antibody (1:1000), anti-phosphorylated ACC antibody (Ser-79) (1:1000), anti-AMP activated protein kinase (AMPK) total antibody (1:1000), anti-phosphorylated AMPK antibody (1:500) (Thr-172), were diluted in 3 % bovine serum albumin. Rabbit anti-rat PE *N*-methyltransferase (PEMT) antibody (26) was diluted (1:5000) in 1 % skim milk. Immunoreactive proteins were detected using enhanced chemiluminescence system (Amersham Biosciences) according to the manufacturer's instructions. All antibodies were polyclonal, raised in rabbit with reactivity for the indicated mouse protein and purchased from Cell Signaling Technology® unless otherwise indicated.

3.2.10 Phosphatidylethanolamine *N*-methyltransferase Assay

Liver homogenates (50 μg protein) were incubated with phosphatidylmonomethylethanolamine and *S*-adenosyl[*methyl*-

^{3}H]methionine, and the incorporation of radiolabel into PC was measured as previously described (27).

3.2.11 Statistical Analysis

Data are expressed as means ± standard error of the mean (SEM) unless otherwise stated. Comparisons between treatment groups were performed using the unpaired Student's two-tailed *t*-test for most analyses. Friedman repeated analysis of variance (ANOVA) on ranks was used to compare animal food intake and weights. One way analysis of variance (ANOVA) using Tukey post-hoc analysis was used to compare differences in experiments with primary cultures of hepatocytes. A probability value of <0.05 is considered significant. Between 3 and 8 samples were examined for each measurement.

3.3 Results

3.3.1 Body weight and food Intake During Tamoxifen Treatment

Tamoxifen is a known appetite suppressor causing reduced food intake and lack of weight gain in rodents (18). Therefore, to prevent extraneous factors from confounding our experimental data the mice were pair-fed. On each day of the 5 day treatment the vehicle group received the amount of diet (g food/g body weight) corresponding to the average amount that the TMX-treated animals had eaten *ad libitum* the day before. Consequently, there was no significant difference in the food intake

between the two experimental groups (Figure 3.1A). The body weights of the TMX and vehicle treated mice were also similar during the treatment period (Figure 3.1B).

3.3.2 Short-term Tamoxifen Treatment induces Hepatic Steatosis

To confirm that short-term TMX treatment induces hepatic steatosis in mice we measured lipid levels in the liver. Following TMX-treatment hepatic TG was 72% higher than in control mice (Figure 3.2A). There was no significant difference in the amount of hepatic cholesterol or CE between the experimental groups (Figure 3.2B). The accumulation of hepatic TG in TMX-treated mice was confirmed by greater Oil Red O staining of liver sections compared to the vehicle-treated group (Figure 3.2C). Thus, our animal model recapitulates the liver steatosis observed in breast cancer patients treated with TMX.

3.3.3 Tamoxifen Does Not Decrease Plasma TG

Two possible mechanisms that might account for TG accumulation in the liver are decreased hepatic lipoprotein secretion and increased lipid synthesis. We therefore determined if the accumulation of TG in the liver of TMX-treated mice were due to inhibition of lipoprotein secretion. Since the liver is a central organ in lipoprotein metabolism we first determined whether TMX altered plasma levels of lipids in high density lipoproteins and very low density lipoproteins. TMX did not significantly change total

plasma TG (Figure 3.3A). Comparison of the lipoprotein profiles between treatment groups confirmed that the amounts of TG (Figure 3.3B) in each lipoprotein fraction were not altered by TMX treatment of the mice. However, the level of plasma CE (Figure 3.3C) was 20% lower in TMX-treated mice than in vehicle-treated mice. This result correlated with a slight reduction in total cholesterol (unesterified + esterified cholesterol) from the high density lipoprotein fraction of TMX-treated mice (Figure 3.3D).

3.3.4 mRNAs in Livers of TMX-treated Mice

In order to gain insight into the mechanism responsible for TMX-induced fatty liver we determined whether a specific pattern of hepatic gene expression was altered in response to TMX (Figure 3.4). The mRNA levels of some lipogenic genes - including sterol regulatory element-binding protein-1C (SREBP-1C), liver X receptor (LXRα), peroxisome proliferator-activated receptor gamma (PPARγ), triacylglycerol hydrolase (TGH), acetyl-CoA carboxyase (ACC), and diacylglycerol acyltransferase (DGAT) 1 and 2 - were similar between the treatment groups. However, the levels of mRNAs encoding fatty acid synthase (FAS) and stearoyl-CoA desaturase 1 (SCD-1) were increased by 2-fold and reduced by 60%, respectively, by TMX.

Genes associated with fatty acid β-oxidation - peroxisome proliferator-activated receptor alpha (PPARα), malonyl-CoA

decarboxylase (MCD), long chain acyl-CoA dehydrogenase (LCAD) and carnitine palmitoyltransferase 1 (CPT1) were not different between treatment groups (Figure 3.4). Similarly the two animals groups had comparable mRNA levels of CTP:phosphocholine cytidylyltransferase (CTα), peroxisome proliferator-activated receptor delta (PPARδ), and scavenger receptor B1 (SRB1). The expression of uncoupling protein 2 (UCP2) was significantly up-regulated in response to TMX. Furthermore, TMX increased expression of the mRNA encoding fatty acid translocase CD36 and significantly reduced the mRNA level of the PC biosynthetic enzyme phosphatidylethanolamine *N*-methyltransferase (PEMT) (Figure 3.4). As expected, the amount of mRNA for the house-keeping gene, TATA-box binding protein (TBP), was not significantly different between the two animal treatment groups.

3.3.5 Inhibition of PEMT Does Not Contribute to TMX-mediated Steatosis

The qPCR analysis of hepatic mRNAs revealed that the level of PEMT mRNA was lower in the TMX-treated animals compared to the controls (Figure 3.4). PEMT synthesizes PC from PE in the liver (26) and approximately 30% of PC in mouse liver is made by this enzyme (28). Studies from our laboratory have shown that PEMT-deficient mice develop hepatic steatosis due to decreased secretion of TG from the liver (29-31). Therefore, we investigated whether the decrease in PEMT mRNA

contributed to the hepatic steatosis in TMX-treated mice. Figures 3.5A and 3.5B show that the amount of PEMT protein and activity in the livers of mice treated with TMX were significantly lower (40-60%) than in the control mice. However, this decrease was not sufficient to reduce the amount of hepatic PC or the PC/PE ratio (Figure 3.5C).

To determine whether or not the TMX-mediated inhibition of PEMT reduced hepatic TG secretion we used primary cultures of hepatocytes isolated from TMX-treated and vehicle-treated mice. Despite a significantly reduced formation of [^{3}H]PC from [^{3}H]ethanolamine in hepatocytes isolated from TMX-treated mice (Figure 3.5D), the amount of TG secreted into the culture medium was not altered by TMX treatment (Figure 3.5E). This result indicates that the TMX-induced decrease in PEMT activity is not sufficient to reduce hepatic lipid secretion. To confirm that inhibition of PEMT did not contribute to TMX-mediated hepatic steatosis by an alternative mechanism, we used *Pemt*$^{-/-}$ mice. Following TMX-treatment for 5 consecutive days *Pemt*$^{-/-}$ mice accumulated ~50% less hepatic TG than the vehicle-treated *Pemt*$^{-/-}$ mice with no change in cholesterol or CE (Figure 3.5F). The magnitude of the TMX-mediated increase in hepatic TG levels was similar after TMX treatment of *Pemt*$^{-/-}$ (Figure 3.5F) and *Pemt*$^{+/+}$ mice (Figure 3.2A).

3.3.6 Hepatic Fatty Acid Synthesis is Increased by TMX

The real-time qPCR analysis identified several candidate lipid pathways which may be targets of TMX action in the liver. We directly examined the involvement of each pathway using primary cultures of hepatocytes isolated from adult mice treated for 5 days with either vehicle or TMX. The mRNA level of the fatty acid translocase CD36 in the livers of TMX-treated mice was higher than in control mice (Figure 3.4). Therefore, we investigated whether hepatic fatty acid uptake was enhanced by TMX. Primary cultures of mouse hepatocytes isolated from vehicle- and TMX-treated mice were incubated with [^{3}H]oleate and the uptake of this fatty acid into the cells was evaluated. The rate of transport of [^{3}H]oleate into hepatocytes was similar in the two treatment groups (Figure 3.6) suggesting that increased fatty acid uptake is not responsible for the TMX-mediated lipid accumulation in the liver.

To ascertain whether TMX promotes hepatic TG accumulation by increasing *de novo* fatty acid synthesis, we incubated primary cultures of hepatocytes with [^{14}C]acetate. The incorporation of [^{14}C]acetate into TG was significantly (60%) higher in the hepatocytes from TMX-treated mice after 2 h and 4 h of incubation compared to the control hepatocytes (Figure 3.7A). Similarly, the incorporation of [^{14}C]acetate into PC, PE and phosphatidylinositol/phosphatidylserine was increased (50-75%) by TMX treatment (Figures 3.7B-D). In contrast, TMX did not alter the incorporation

of [^{14}C]acetate into cholesterol or CE (Figures 3.7E and F). The observed increased incorporation of acetate into TG and various phospholipids indicates that fatty acid synthesis is elevated in response to TMX.

To confirm that the TMX-induced increase in radiolabeling of glycerolipids from [^{14}C]acetate reflected an increase in fatty acid synthesis rather than an increase in glycerolipid synthesis, we incubated primary cultures of hepatocytes isolated from vehicle- and TMX-treated mice with [^{3}H]oleate. Figure 3.8A shows that the formation of [^{3}H]TG from oleate in the TMX-incubated hepatocytes was not significantly different from that in control hepatocytes. In addition, the incorporation of [^{3}H]oleate into PC, PE, and phosphatidylinositol/phosphatidylserine was similar in hepatocytes ± TMX (Figures 3.8B-D). Thus, the radiolabeling experiments with primary cultures of hepatocytes indicate that TMX enhances fatty acid synthesis which subsequently promotes hepatic steatosis.

3.3.7 TMX Decreases the Phosphorylation of ACC in the Liver

The rate-limiting enzyme in *de novo* fatty acid synthesis, acetyl-CoA carboxylase (ACC), is activated upon dephosphorylation at Ser-79 (32,33). To determine whether or not TMX activated ACC in the liver we monitored the level of ACC phosphorylation (Ser-79) by using an antibody that specifically recognizes phosphorylated Ser-79 (Figure 3.9A). ACC phosphorylation (Ser-79) was reduced to undetectable levels following

TMX treatment whereas there was no change in the total amount of ACC protein or fatty acid synthase (FAS) protein upon TMX treatment (Figure 3.9A). In an attempt to explain the decreased phosphorylation of ACC we monitored the activity of the upstream kinase, AMP-activated protein kinase (AMPK) (32,34). Phosphorylation of the AMPK catalytic subunit (AMPK-α) at Thr-172 is essential for AMPK activation (32); therefore we used an antibody that specifically recognized AMPK phosphorylation at Thr-172. The level of AMPK phosphorylation was significantly decreased by TMX (Figure 3.9B). Together, these results suggest that TMX-induced lipogenesis is due to attenuated inhibition of ACC by AMPK.

Reduced AMPK activity is associated with impaired fatty acid oxidation (32) However, when we measured the rate of oxidation of [^{3}H]oleate in hepatocytes from vehicle- and TMX-treated mice the same amount of acid soluble metabolites was released into the media (Figure 3.9C). Thus, TMX does not appear to inhibit fatty acid oxidation.

3.4 Discussion

We have examined the mechanism by which TMX causes hepatic lipid accumulation in mice. This is the first study to address the antecedent mechanisms by which TMX promotes hepatic lipid accumulation in mice that is not confounded by differences in food intake. The results demonstrate that a primary effect of TMX is to increase hepatic fatty acid synthesis via activation of AMPK and ACC.

3.4.1 Tamoxifen Activates Fatty Acid Synthesis

Primary cultures of mouse hepatocytes were used to determine whether TMX-mediated accumulation of hepatic TG was caused by one or more of the following factors: increased lipogenesis, increased lipid uptake, reduction in β-oxidation, and/or reduced lipid secretion. We found that initially TMX promotes hepatic steatosis by increasing lipogenesis at least in part by reducing the phosphorylation (Ser-79) of the rate-limiting enzyme of fatty acid synthesis, ACC. It is well established that reduced phosphorylation of ACC in the liver activates fatty acid synthesis (33,35). Consistent with an anti-estrogen effect of TMX, increased hepatic lipogenesis might also account for the observed steatosis in ovariectomized rats (36). In the current study, AMPK phosphorylation (at Thr-172) decreased in response to TMX indicating that AMPK kinase activity was reduced (32) consequently accounting for decreased phosphorylation of ACC (33). Interestingly, estrogen has been shown to reduce adiposity in pair-fed ovarectomized mice by activating AMPK (Thr-172) in myocytes (37). It is unclear how estrogen mediates this activation or how TMX antagonizes it although TMX might inhibit AMPK activity directly through the classical nuclear estrogen receptors (ESR), ESRα and ESRβ (38,39), or the more recently described G protein-coupled receptor 30 (GPR30) (40-42). Estrogen activates multiple cellular kinase pathways via ESR and GRP30 including those involving the epidermal growth factor receptor and protein kinase A (39-44). Both of these cell signalling

pathways have been recently implicated in regulating AMPK phosphorylation and activity (45,46).

Interestingly, SREBP-1C which is a determinant of the biosynthesis of FA, as it promotes the expression of lipogenic genes such as FAS and ACC (47-50), was not changed in response to TMX. This result is consistent with several other reports on TMX action (18,51) and might reflect the complex effects of TMX and its metabolites on gene expression and cell signalling (40-42).

3.4.2 Tamoxifen Does Not Inhibit Fatty Acid Oxidation

We found that TMX did not alter the oxidation of [^{3}H]oleate in hepatocytes (production of [^{3}H]acid soluble metabolites). We also found no difference in levels of hepatic mRNAs encoding enzymes involved in fatty acid oxidation including PPARα, LCAD, MCD and CPT1. These results strongly indicate that the accumulation of TG in the liver following TMX-treatment is not initially due to reduced fatty acid oxidation. Our results are consistent with those reported by Gudbrandsen et al., showing no change in palmitoyl-CoA oxidation or CPT1 activity in the livers of rats treated orally with TMX (40 mg/kg/day) compared to vehicle (19). The TMX-mediated inhibition of fatty acid oxidation previously reported by Larosche et al., may reflect the much larger oral dose of TMX (200 mg/kg/day) used (17). It is likely that inhibition of fatty acid oxidation does occur at a later stage of TMX-mediated steatosis since increased fatty acid

synthesis typically results in the inhibition of fatty acid oxidation (32). Furthermore, there is evidence that estrogen might regulate fatty acid oxidation. Mice deficient in estrogen, including aromatase knock-out mice (52) and ovariectomized-mice (36) have impaired hepatic fatty acid oxidation which can be prevented with 17β-estradiol replacement.

3.4.3 Tamoxifen Had no Effect on Plasma TG Levels

In our study the increase in hepatic TG following TMX-treatment for 5 days was not accompanied by a decrease in plasma TG levels. Lilliot et al. also found no change in plasma TG levels when rats were treated with TMX (0.5 mg/kg/d) for 5 days (18). On the other hand, several other publications have shown decreased serum TG after longer duration (14-84 days) of TMX- treatment (19,53) or with a larger dose of the drug (~370 mg/kg/d) (17). In addition, one study analyzed plasma TG under non-fasting conditions (19) and another indicated marked differences (21%) in body weight between animal groups (53) making interpretation of the results problematic. In contrast to the disparity between reports on the effect of TMX on plasma TG levels, a reduction in plasma total cholesterol has been more consistently observed in response to TMX-treatment in both rodents (18,19,53,54) and in humans (55,56). This reduction might be partially explained by the observation that TMX inhibits the activity of acyl-CoA:cholesterol acyltransferase in the liver (19,57). Indeed, despite the

TMX-mediated increase in hepatic fatty acid synthesis in the current study, we observed no increase in the incorporation of acetate into CE.

3.4.4 PEMT Does Not Play a Major Role in the Initial Accumulation of Hepatic TG

PC synthesis and availability are important regulators of the secretion of TG into very low density lipoproteins from the liver (21,29,58-60). Based on the TMX-mediated decrease in the mRNA, protein and activity of PEMT we anticipated that hepatic TG secretion would be decreased by TMX (29,30). However, we did not observe any difference between the two experimental groups in the amount of [^{3}H]TG secreted from hepatocytes. In addition, TG was similarly increased (by 75%) upon TMX treatment in livers of PEMT-deficient and wild-type mice. These results strongly suggest that the decrease in PEMT expression is not a major initial contributor to TMX-mediated hepatic steatosis. This result is likely explained by the absence of any significant decrease in hepatic PC levels following TMX treatment. Previously, it was shown that mice that are heterozygous for the *Pemt* gene are not susceptible to hepatic steatosis when fed a choline-deficient diet which induces hepatic TG accumulation in PEMT knock-out mice (61). It is possible, however, that the TMX-mediated decrease in PEMT activity might cause steatosis after long-term TMX treatment and/or in the reduction in plasma cholesterol levels (31,62).

In conclusion, we show that TMX causes hepatic steatosis in mice primarily by increasing fatty acid synthesis. We have identified activation of ACC as a primary target of TMX. We suggest that the inhibition of fatty acid synthesis may prove to be beneficial in reducing hepatic steatosis induced by TMX.

Table 3.1 PCR primer sequences

The abbreviations for the mRNAs are : ACC, acetyl-CoA carboxylase; CYC, cyclophilin; CPT, carnitine:palmitoyltransferase; CT, CTP;phosphocholine cytidylyltransferase: DGAT, diacylglycerol;acyl-CoA acyltransferase; FAS, fatty acid synthase; TGH, triacylglycerol hydrolase; LCAD, long chain acyl-CoA dehydrogenase; LXR, liver X receptor; MCD, malonyl-CoA decarboxylase; PEMT, phosphatidylethanolamine *N*-methyltransferase; PPAR, peroxisome proliferator activated receptor; SCD, stearoyl-CoA desaturase; SRB1, scavenger receptor class B1; SREBP, sterol response element binding protein; TBP, TATA-box binding protein, UCP, uncoupling protein.

Gene	Forward Sequence	Reverse sequence
Acc	‘5–AGGTGTCGATAAATGCGGTCC–3’	5’–AGGTGTCGATAAATGCGGTCC–3’
Cyc	5’–TTCAAAGACAGCAGAAAACTTTCG–3’	5’–TCTTCTTGCTGGTCTTGCCATTCC–3’
Cd36	5’–TGGCTAAATGAGACTGGGACC–3’	5’–ACATCACCACTCCAATCCCAAG–3’
Cpt1	5’–TGAGTGGCGTCCTCTTTGG–3’	5’–CAGCGAGTAGCGCATAGTCATG–3’
Ctα	5’–GCTAAAGTCAATTCGAGGAA–3’	5’–CATAGGGCTTACTAAAGTCAACT–3’
Dgat1	5’–GGATCTGAGGTGCCATCGT–3’	5’–CCACCAGGATGCCATACTTG–3’
Dgat2	5’–GGCTACGTTGGCTGGTAACTT–3’	5’–TTCAGGGTGACTGCGTTCTT–3’
Fas	5’–TTCCGTCACTTCCAGTTAGAG–3’	5’–TTCAGTGAGGCGTAGTAGACA–3’
Tgh	5’–GGAGGGCAGGTGCTCTCA–3’	5’–GCCTTCAGCGAGTGGATAGC–3’
Lcad	5’–GCGAAATACTGGGCATCTGAA–3’	5’–TCCGTGGAGTTGCACACATT–3’
Lxrα	5’–CAGAAGAACAGATCCGCTTGAAG–3’	5’–TGCAATGGGCCAAGGCGTGAC–3’
Mcd	5’–TTCTGCATGTGGCTCTGACTGGT–3,	–GGGTCAGGCTGATGGAGTAGA
Pemt	5’–CTGTATGAGCTGGCTGCTGGGTTAC–3’	5’–CCTGTCAGCTTCTTTTGTGCA–3’
Pparα	5’–GACCTGAAAGATTCGGAAACT–3’	5’–CGTCTTCTCGGCCATACAC–3’
Pparγ	5’–TTGACATCAAGCCCTTTACCA–3’	5’–GGTTCTACTTTGATCGCACTTT–3’
Pparδ	5’–AACATGGAATGTCGGGTGTGC–3’	–ACTGACACTTGTTGCGGTTCTTC–3’
Scd1	5’–GTTGCCAGTTTCTTTCGTG–3’	5’–GGGAAGCCAAGTTTCTACACA–3’
Srb1	5’–TGGCATTCAGAGCAGTGTAAC–3’	5’–CCGTTGGCAAACAGAGTATC–3’
Srebp-1C	5’–ATGGATTGCACATTTGAAGAC–3’	5’–CTCTCAGGAGAGTTGGCACC–3’
Tbp	–ACCCTTCACCAATGACTCCTATG–3’	5’–TGACTGCAGCAAATCGCTTGG–3’
Ucp2	5’–CATTGGCCTCTACGACTCTG–3’	5’–GCCTGGAAGCGGACCTTTAC–3’

Figure 3.1. Body weight and food intake of mice treated with vehicle or tamoxifen.

C57BL/6 mice (8/group) were injected subcutaneously with vehicle (sesame oil, 1 % benzyl alcohol) or TMX (0.5 mg/TMX/kg/day) for 5 consecutive days**. (A)** Food intake for the 24 h period following each daily injection. The mice were pair fed such that the vehicle group (black bars) were fed the same amount (g food/g body weight) as the TMX group (white bars) consumed *ad libitum* the day before. Food intake was not determined for day 5 as the animals were fasted and euthanized 4 h after the final injection. Data are expressed as means ± S.D. (**B**) Animal body weight at each day during the 5 day injection period. The mice were weighed just prior to treatment with either vehicle (closed circles) or TMX (open circles). Data are expressed as means ± S.D.

Figure 3.1

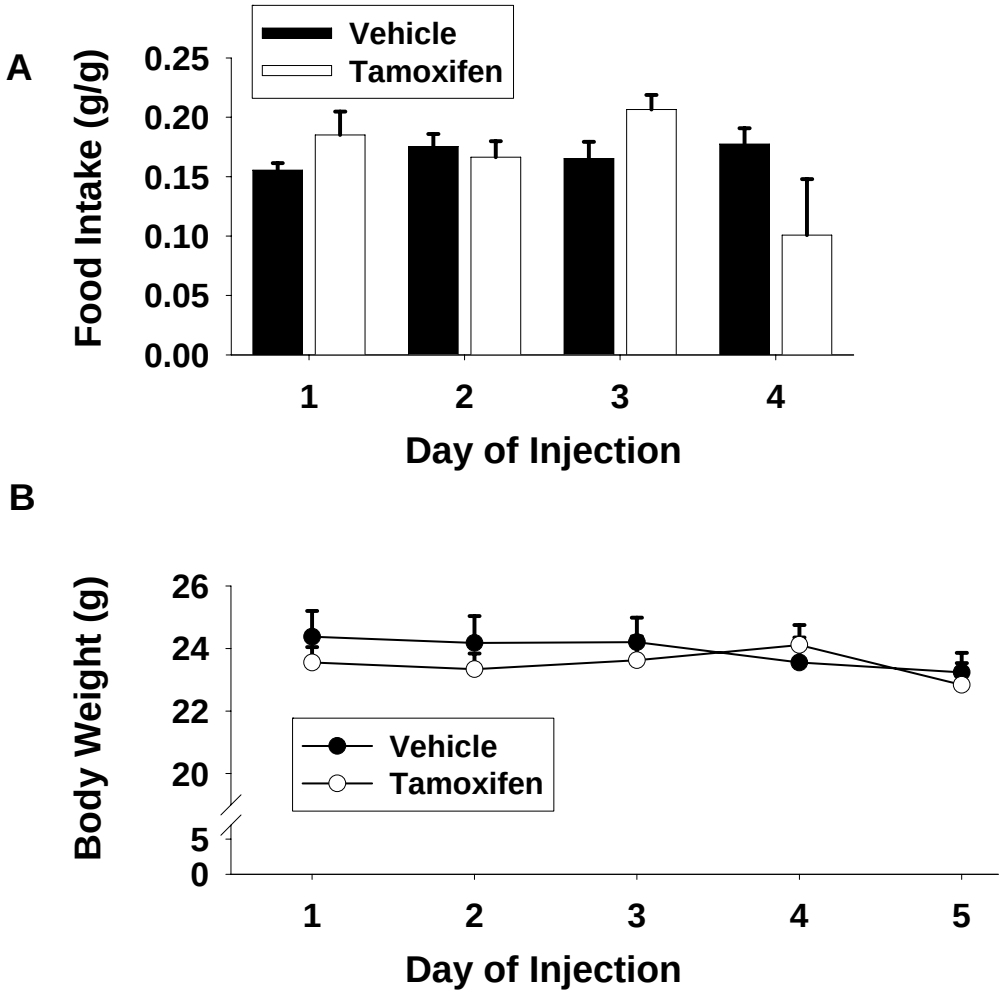
A
Vehicle
Tamoxifen
Food Intake (g/g)
0.25
0.20
0.15
0.10
0.05
0.00
1
2
3
4
Day of Injection
B
Body Weight (g)
26
24
22
20
5
0
Vehicle
Tamoxifen
1
2
3
4
5
Day of Injection

Figure 3.2. TMX induces lipid accumulation in liver.

Quantification of hepatic lipid in vehicle- (Veh, black bar) and tamoxifen- (TMX, white bar) treated mice. Lipids were extracted from liver homogenate (1 mg protein) and amounts of triacylglycerols (TG) (**A**), unesterified cholesterol and cholesteryl esters (CE) (**B**) were measured. Data are expressed as means ± SEM (* $P<0.05$, n = 7-8, student's *t* test). (**C**) Representative livers from vehicle- (Veh, left panel) and TMX- (TMX, right panel) treated mice (n = 4/group) were fixed in 10% buffered-formalin, cryosectioned (5 μm) and stained with Oil Red O to reveal neutral lipid (red, 40X objective magnification).

Figure 3.2

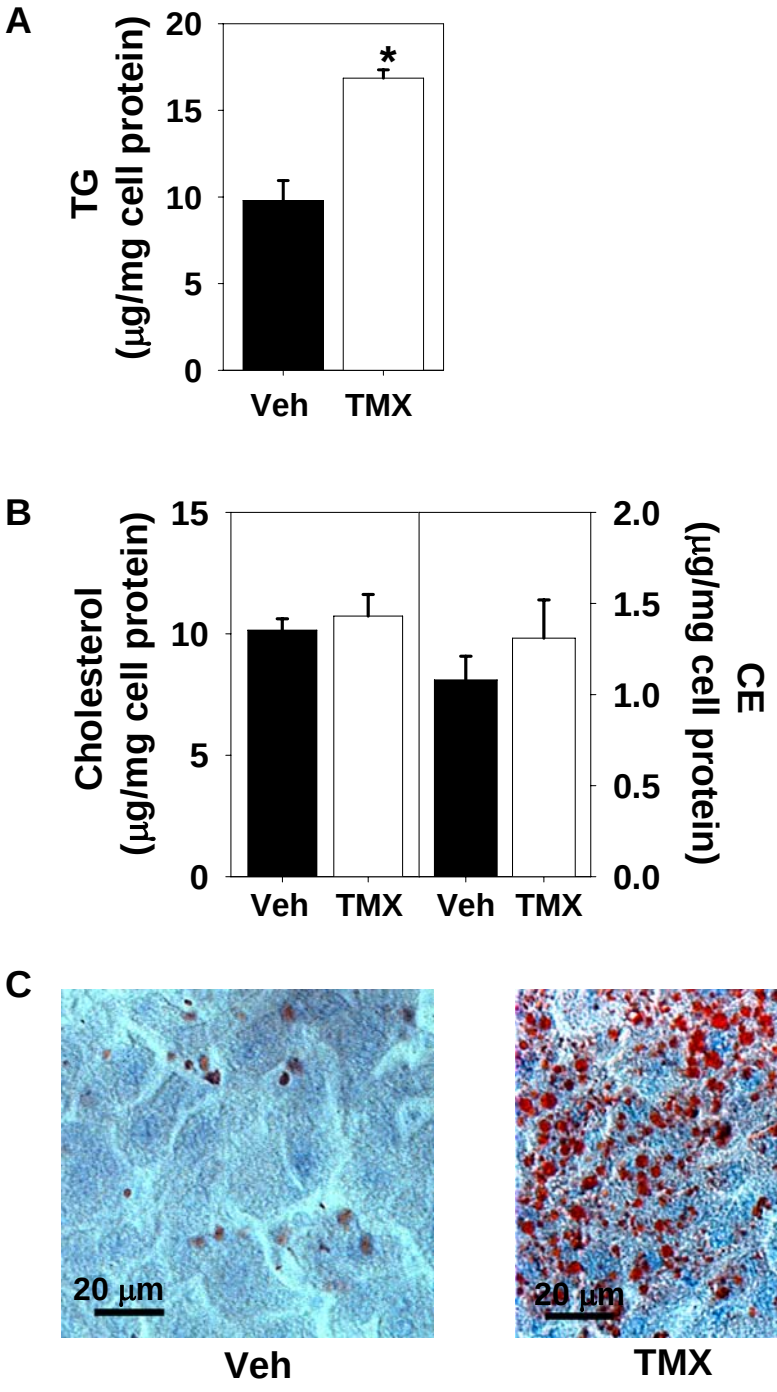
A
TG
(μg/mg cell protein)
20
15
10
5
0
*
Veh
TMX
B
Cholesterol
(μg/mg cell protein)
15
10
5
0
2.0
1.5
1.0
0.5
0.0
CE
(μg/mg cell protein)
Veh
TMX
Veh
TMX
C
20 μm
20 μm
Veh
TMX

Figure 3.3. TMX reduces plasma cholesterol.

(**A**) Plasma concentrations of TG were measured in samples from vehicle- (Veh, black bar) and tamoxifen- (TMX, white bar) treated mice following an overnight fast. Data are expressed as means ± SEM. (*, $P<0.05$, n = 7-8, student's *t* test). (**B**) Plasma lipoproteins from fasted mice treated with vehicle (solid line) or TMX (dashed line) were separated by gel filtration and the amount of TG was measured. Each curve represents mean values from 5 mice. (**C**) Plasma concentrations of cholesterol and CE were measured in samples from vehicle- (Veh, black bar) and tamoxifen- (TMX, white bar) treated mice following an overnight fast. Data are expressed as means ± SEM. (*, $P<0.05$, n = 7-8, Student's *t* test). (**D**) Plasma lipoproteins from fasted mice treated with vehicle (solid line) and TMX (dashed line) were separated by gel filtration and amounts of total cholesterol (unesterified + esterified) were measured. Each curve represents mean values from 5-8 mice.

Figure 3.3

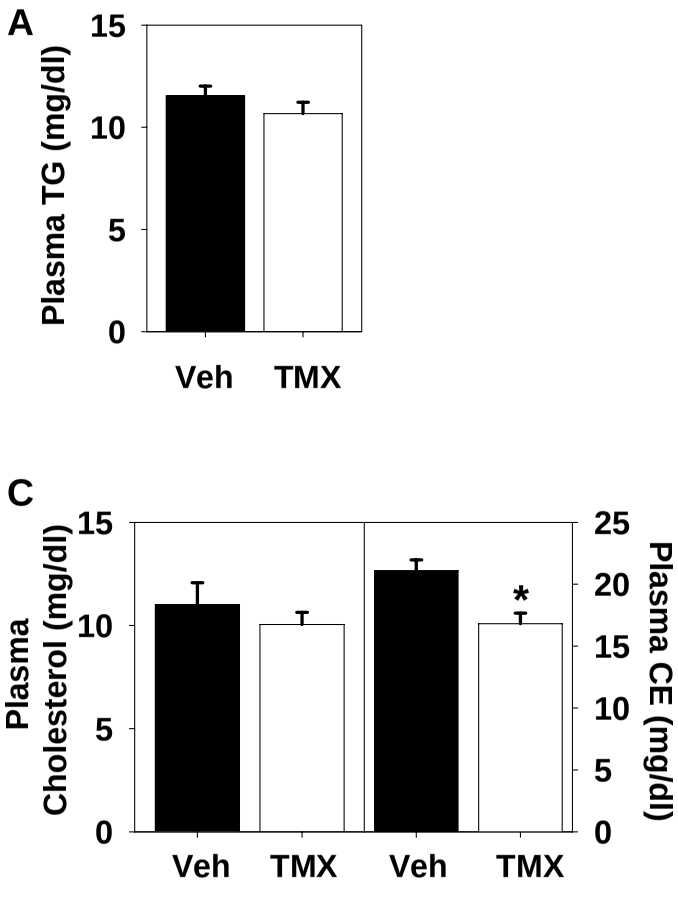
A
Plasma TG (mg/dl)
15
10
5
0
Veh
TMX
B
VLDL
LDL
HDL
Triacylglyceride (relative amount)
15
10
5
0
Vehicle
Tamoxifen
0
25
50
Retention Time (mins)
C
Plasma Cholesterol (mg/dl)
15
10
5
0
25
20
15
10
5
0
Plasma CE (mg/dl)
*
Veh
TMX
Veh
TMX
D
VLDL
LDL
HDL
Cholesterol (relative amount)
50
40
30
20
10
0
Vehicle
Tamoxifen
0
25
50
Retention Time (mins)

Figure 3.4. Hepatic mRNA levels

Mice treated with vehicle (black bars) or TMX (white bars) were euthanized and the livers harvested. Total RNA was isolated, reverse-transcribed to cDNA and mRNA levels of the indicated genes measured by qPCR. mRNA levels were normalized to cyclophilin using a standard curve. All data are means ± SEM (*, $P<0.05$, n = 3-6 animals, student's *t* test). The abbreviations for the mRNAs are presented in Table 3.1. FA, fatty acid; TG, triacylglycerol; PC, phosphatidylcholine.

Figure 3.4

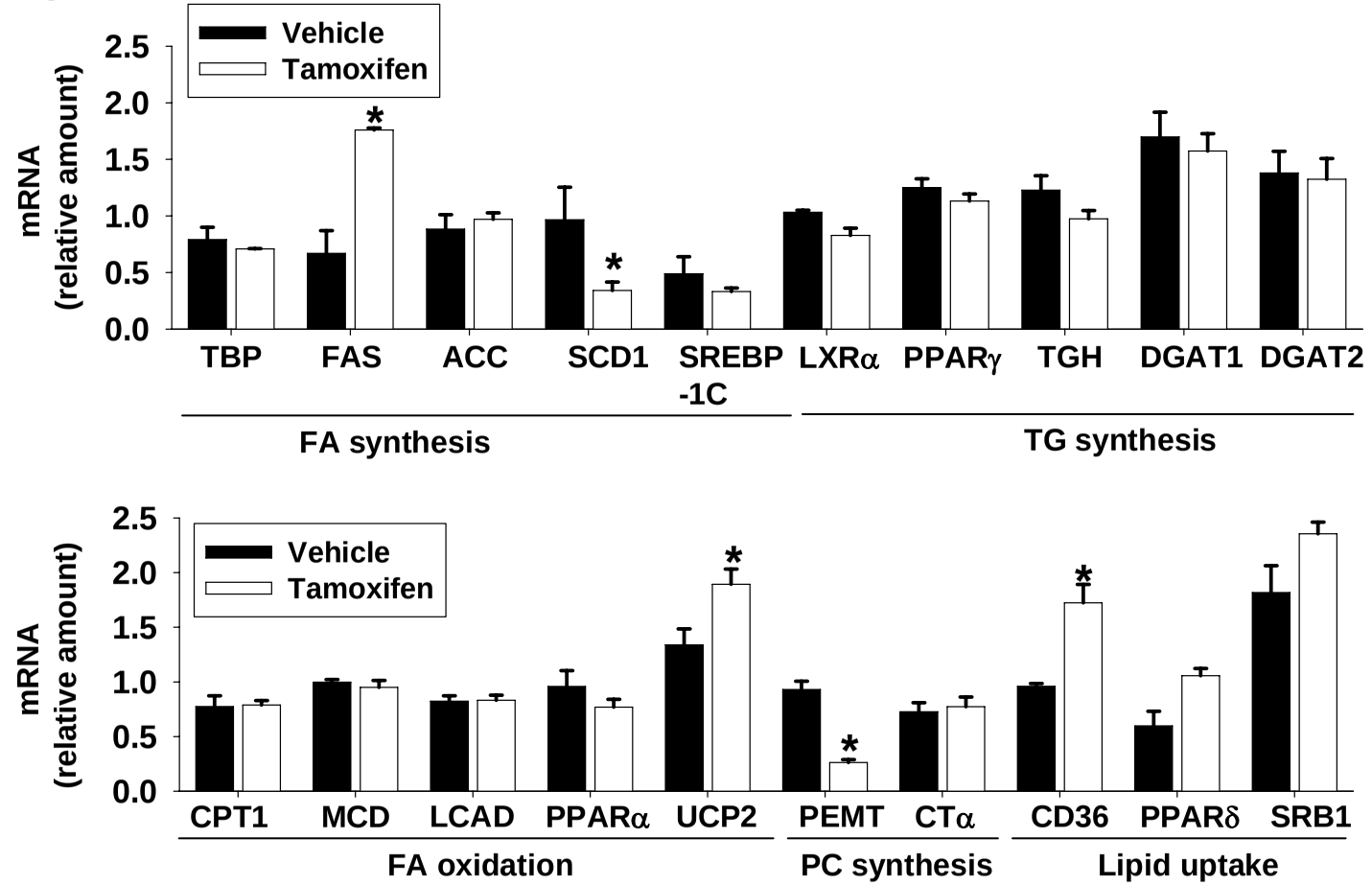
Vehicle
Tamoxifen
mRNA (relative amount)
2.5
2.0
1.5
1.0
0.5
0.0
*
*
TBP
FAS
ACC
SCD1
SREBP -1C
LXRα
PPARγ
TGH
DGAT1
DGAT2
FA synthesis
TG synthesis
Vehicle
Tamoxifen
mRNA (relative amount)
2.5
2.0
1.5
1.0
0.5
0.0
*
*
*
CPT1
MCD
LCAD
PPARα
UCP2
PEMT
CTα
CD36
PPARδ
SRB1
FA oxidation
PC synthesis
Lipid uptake

Figure 3.5. Tamoxifen-mediated inhibition of PEMT does not contribute to hepatic steatosis.

(**A**) Immunoblot analyses were performed on homogenates (30 μg protein) from livers harvested from mice treated with vehicle (Veh) or tamoxifen (TMX). Amounts of PEMT and protein disulfide isomerase (PDI) protein were determined by densitometric quantification of immunobots relative to PDI. (**B**) Phosphatidylethanolamine *N*-methyltransferase (PEMT) enzymatic assays were performed on liver homogenates (30 μg) from mice treated with vehicle (Veh, black bar) or tamoxifen (TMX, white bar). Data are means ± SEM. (*, $P<0.05$, n = 6 mice per group, student's *t* test). (**C**) Phospholipid [(PL): phosphatidylcholine (PC) and phosphatidylethanolamine (PE)] content was measured in liver homogenates (1 mg protein) from mice treated with vehicle (black bars) or TMX (white bar) by phosphorus assay. Data are means ± SEM, n= 4 mice/group. (**D**) Hepatocytes isolated from mice treated with either vehicle (Veh, black bar) or TMX (white bar) were incubated with [^{3}H]ethanolamine for 4 h and the radiolabel incorporated into PC was expressed as a percentage of radiolabel incorporated into (PC + PE). Data are means ± SEM of three independent hepatocyte preparations (*, $P<0.05$, student's *t* test). (**E**) Hepatocytes isolated from mice treated with either vehicle (black bars) or TMX (white bars) were incubated with [^{3}H]oleate for 2 h then washed and incubated in media without radiolabel for 4 h. The cells and media were collected and radiolabel incorporated into TG was measured. Values for vehicle group are set to 100. Data are means ± SEM of three independent hepatocyte preparations. (**F**) Quantification of hepatic lipids from pair-fed male *Pemt*$^{-/-}$ mice treated with either vehicle (black bars) or TMX (white bars) for 5 consecutive days. Lipids were extracted from liver homogenate (1 mg protein) and amounts of triacylglycerols (TG), unesterified cholesterol (C) and cholesteryl esters (CE) were determined. Data are means ± SEM (*, $P<0.05$, n = 6-8, student's *t* test).

Figure 3.5

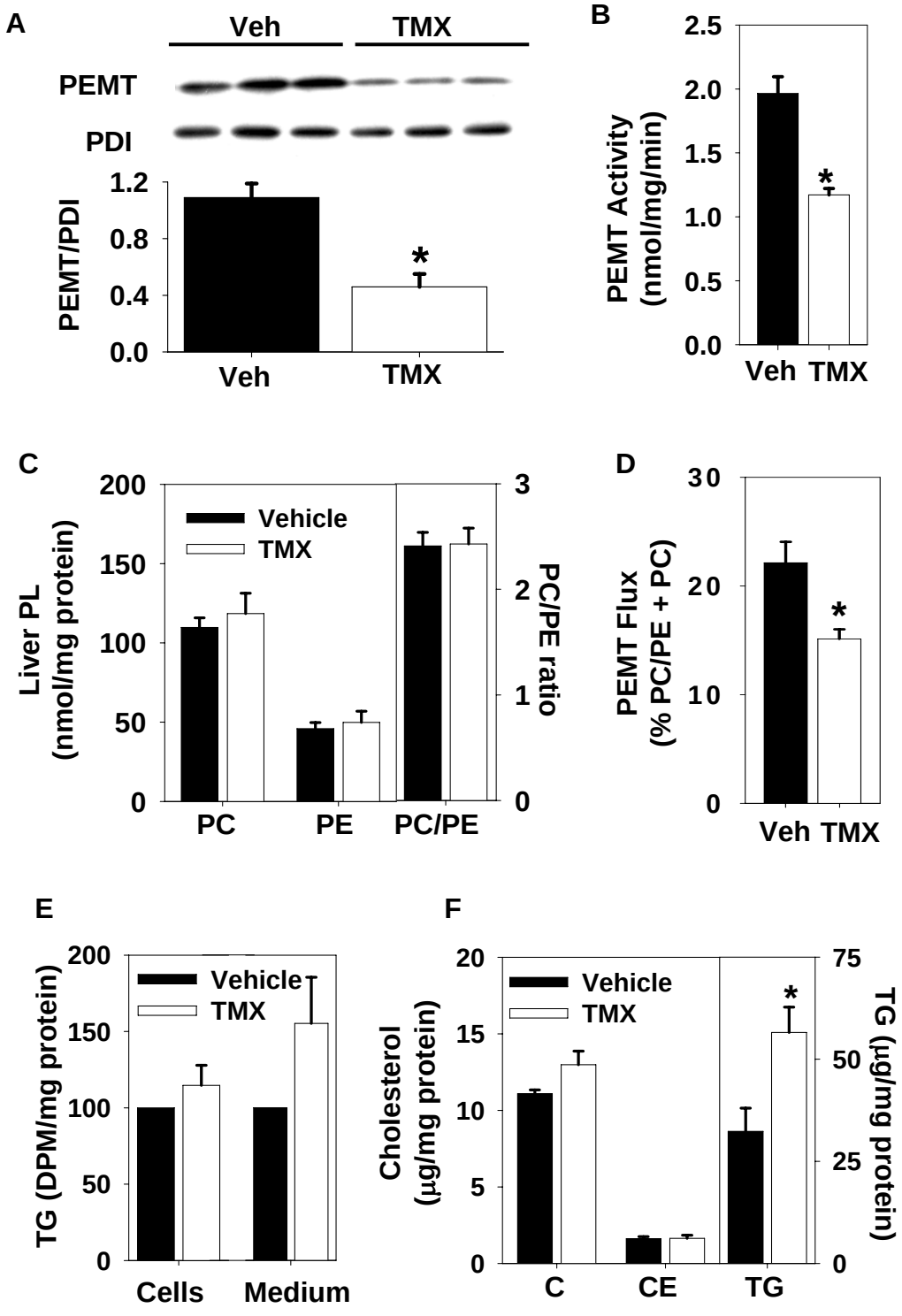
A
Veh
TMX
PEMT
PDI
PEMT/PDI
1.2
0.8
0.4
0.0
*
Veh
TMX
B
PEMT Activity
(nmol/mg/min)
2.5
2.0
1.5
1.0
0.5
0.0
*
Veh TMX
C
Liver PL
(nmol/mg protein)
200
150
100
50
0
Vehicle
TMX
PC/PE ratio
3
2
1
0
PC
PE
PC/PE
D
PEMT Flux
(% PC/PE + PC)
30
20
10
0
*
Veh TMX
E
TG (DPM/mg protein)
200
150
100
50
0
Vehicle
TMX
Cells
Medium
F
Cholesterol
(µg/mg protein)
20
15
10
5
0
Vehicle
TMX
TG (µg/mg protein)
75
50
25
0
*
C
CE
TG

Figure 3.6. Tamoxifen does not increase [^{3}H]oleate uptake by isolated mouse hepatocytes in primary culture

Primary cultures of hepatocytes were isolated from pair-fed male C57BL/6 mice (8-12 weeks) injected each day for 5 days with either vehicle (closed circles) or TMX (open circles). Cells were incubated with [^{3}H]oleate for the time indicated, then washed with phosphate-buffered saline and radiolabel in cell lysates was measured. Data are means ± SEM of three independent hepatocyte preparations.

Figure 3.6

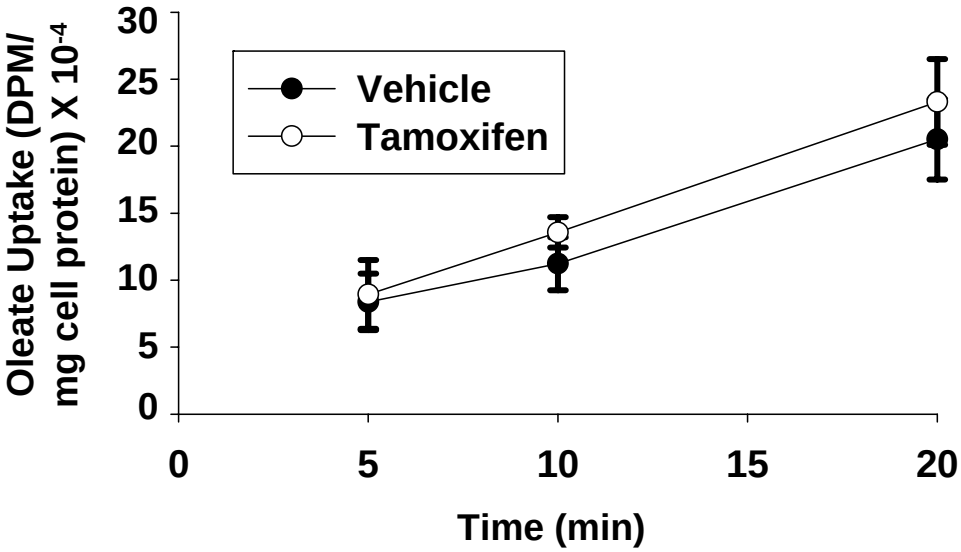
Oleate Uptake (DPM/ mg cell protein) X 10-4
30
25
20
15
10
5
0
Vehicle
Tamoxifen
0
5
10
15
20
Time (min)

Figure 3.7. Tamoxifen increases incorporation of [^{14}C]acetate into triacylglycerol and phospholipids.

Primary cultures of hepatocytes were isolated from pair-fed male C57BL/6 mice (8-12 weeks) injected each day for 5 days with either vehicle (closed circles) or TMX (open circles). Cells were incubated with [^{14}C]acetate for the time indicated, then washed, and radioactivity in (**A**) TG, (**B**) PC, (**C**) PE, (**D**) phosphatidylserine/phosphatidylinositol (PS/PI), (**E**) cholesterol and (**F**) CE was measured. Data are means ± SEM of three independent hepatocyte preparations (*, $P<0.05$ versus vehicle treatment, ANOVA).

Figure 3.7

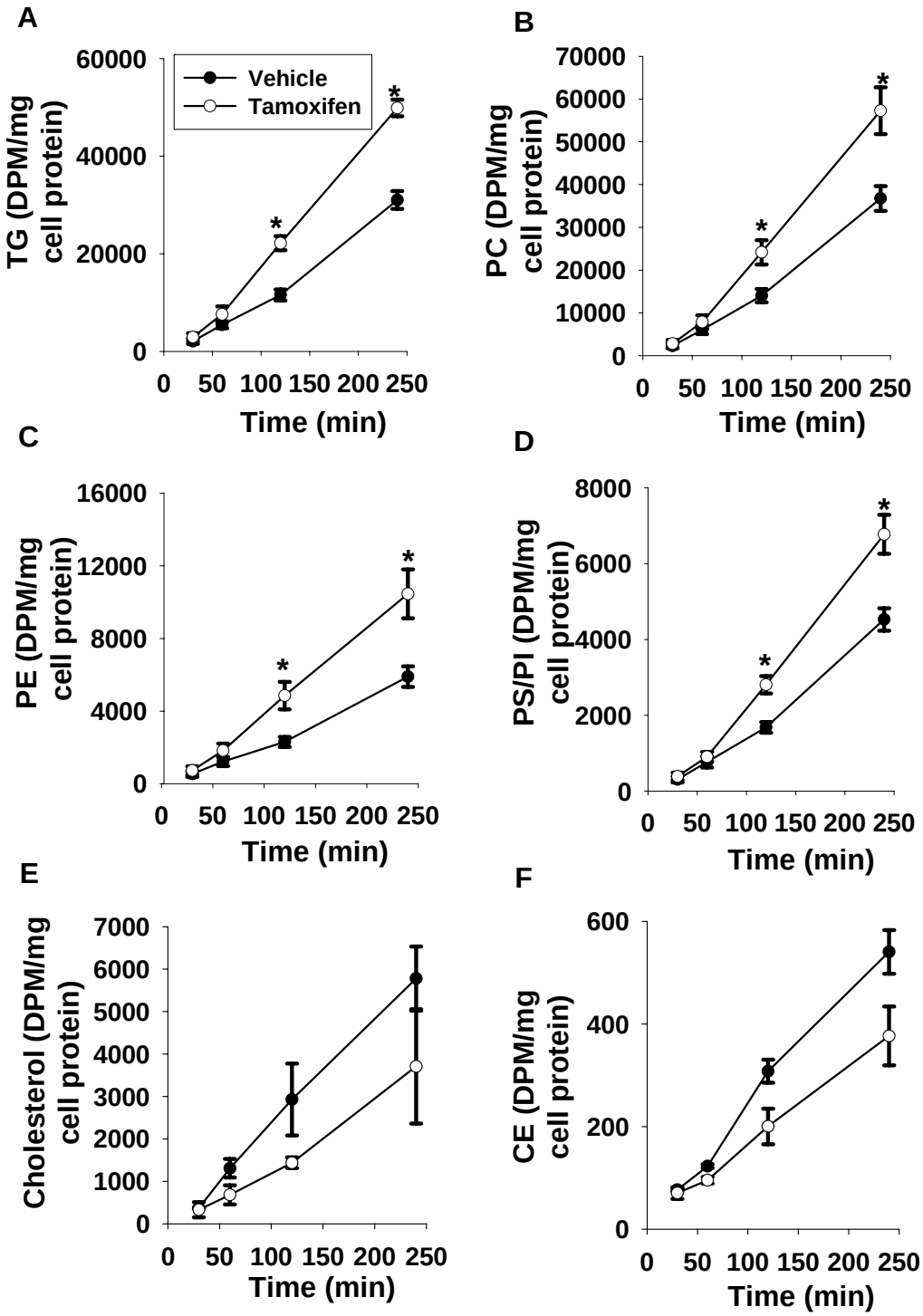
A
TG (DPM/mg cell protein)
Vehicle
Tamoxifen
Time (min)
B
PC (DPM/mg cell protein)
Time (min)
C
PE (DPM/mg cell protein)
Time (min)
D
PS/PI (DPM/mg cell protein)
Time (min)
E
Cholesterol (DPM/mg cell protein)
Time (min)
F
CE (DPM/mg cell protein)
Time (min)

Figure 3.8. Tamoxifen does not increase incorporation of [^{3}H]oleate into triacylglycerol.

Primary cultures of hepatocytes were isolated from pair-fed male C57BL/6 mice (8-12 weeks) injected for 5 days with either vehicle (closed circles) or TMX (open circles). Cells were incubated with [^{3}H]oleate for the time indicated, then washed with phosphate-buffered saline. Radioactivity in (**A**) TG, (**B**) PC, (**C**) PE, and (**D**) phosphatidylserine/phosphatidylinositol (PS/PI) was measured. Data are means ± SEM of three independent hepatocyte preparations.

Figure 3.8

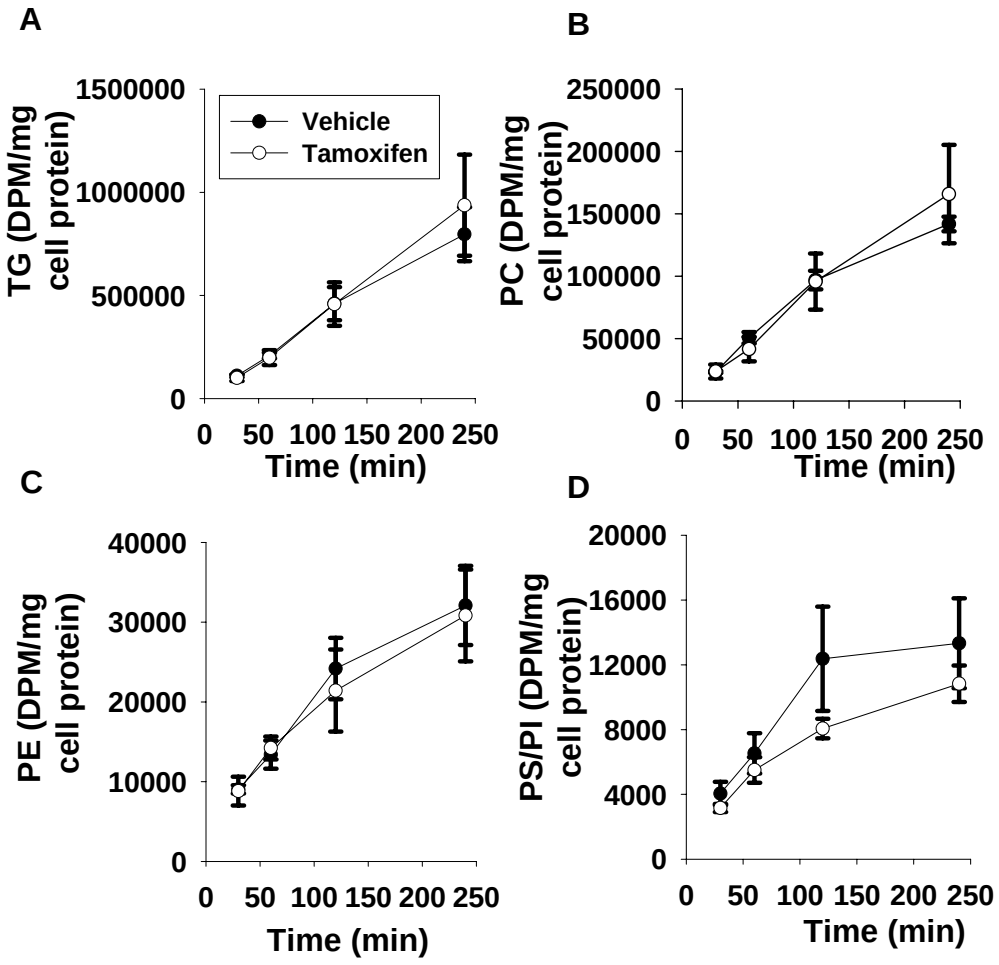
A
B
C
D
Vehicle
Tamoxifen
TG (DPM/mg cell protein)
PC (DPM/mg cell protein)
PE (DPM/mg cell protein)
PS/PI (DPM/mg cell protein)
Time (min)
0
50
100
150
200
250
500000
1000000
1500000
50000
100000
150000
200000
10000
20000
30000
40000
4000
8000
12000
16000

Figure 3.9. Tamoxifen decreases phosphorylation of acetyl-CoA carboxylase (ACC).

(**A**) Immunoblot analysis of homogenates (30 μg protein) from liver harvested from mice treated with vehicle (Veh) or tamoxifen (TMX). The levels of P-ACC, total ACC, and fatty acid synthase (FAS) were determined relative to protein-disulfide isomerise (PDI). At least three mice were used for each group. (**B**) Protein levels of AMP-dependent protein kinase (AMPK) and P-AMPK in liver homogenates (30 μg protein) from mice treated with vehicle (Veh) or TMX were assessed by immunoblotting and quantified by densitometry, normalized against total AMPK as a control for protein loading (*, $P<0.05$, n = 3-4). (**C**) Primary cultures of epatocytes were isolated from pair-fed male C57BL/6 mice (8-12 weeks) injected for 5 days with either vehicle (closed circles) or TMX (open circles). Cells were incubated with [^{3}H]oleate for the time indicated, medium was harvested and radiolabel in acid soluble metabolites measured. Data are means ± SEM of three independent hepatocyte preparations.

Figure 3.9

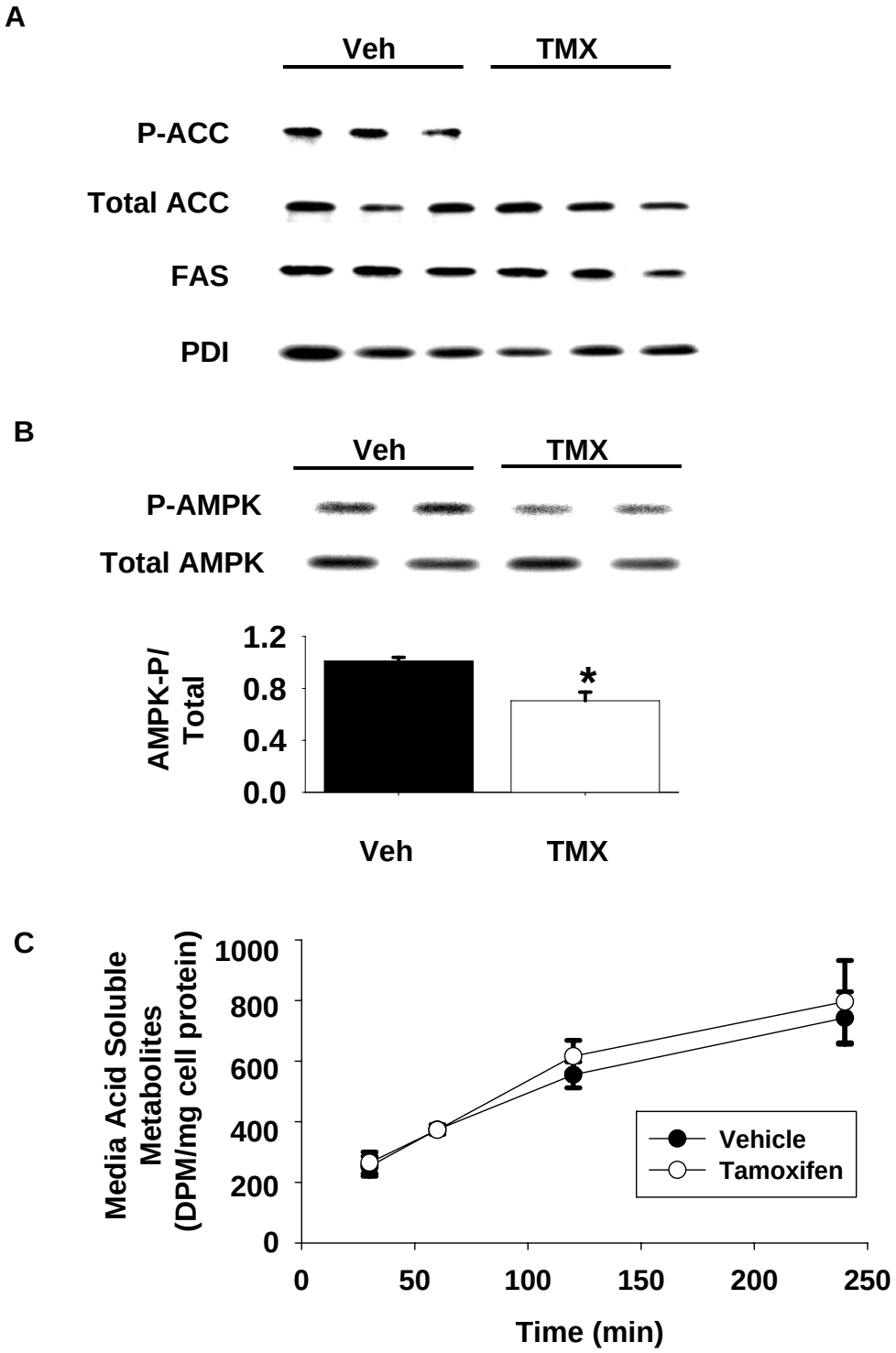
A
Veh
TMX
P-ACC
Total ACC
FAS
PDI
B
Veh
TMX
P-AMPK
Total AMPK
AMPK-P/ Total
1.2
0.8
0.4
0.0
*
Veh
TMX
C
Media Acid Soluble Metabolites (DPM/mg cell protein)
1000
800
600
400
200
0
0
50
100
150
200
250
Time (min)
Vehicle
Tamoxifen

3.5 References

1. Jordan, V. C. (1988) *Breast Cancer Res Treat* **11**(3), 197-209
2. Horner MJ, R. L., Krapcho M, Neyman N, Aminou R, Howlader N, Altekruse SF, Feuer EJ, Huang L, Mariotto A, Miller BA, Lewis DR, Eisner MP, Stinchcomb DG, Edwards BK (eds). SEER Cancer Statistics Review, 1975-2006, National Cancer Institiute. Bethesda, MD, . In. *http://seer.cancer.gov/csr/1975-2006/,based on November 2008 SEER data submission posted to the SEER web site, 2009.*
3. (1998) *Lancet* **351**(9114), 1451-1467
4. Singh, M. N., Martin-Hirsch, P. L., and Martin, F. L. (2008) *Med Sci Monit* **14**(9), RA144-148
5. Shen, S. S., Smith, C. L., Hsieh, J. T., Yu, J., Kim, I. Y., Jian, W., Sonpavde, G., Ayala, G. E., Younes, M., and Lerner, S. P. (2006) *Cancer* **106**(12), 2610-2616
6. Ragavan, N., Hewitt, R., Cooper, L. J., Ashton, K. M., Hindley, A. C., Nicholson, C. M., Fullwood, N. J., Matanhelia, S. S., and Martin, F. L. (2004) *Cancer Lett* **215**(1), 69-78
7. Glick, J. H., Wein, A., Padavic, K., Negendank, W., Harris, D., and Brodovsky, H. (1982) *Cancer* **49**(7), 1367-1372
8. Dhingra, K. (1999) *Invest New Drugs* **17**(3), 285-311
9. Eastell, R., Hannon, R. A., Cuzick, J., Dowsett, M., Clack, G., and Adams, J. E. (2006) *J Bone Miner Res* **21**(8), 1215-1223

10. Steiner, A. Z., Terplan, M., and Paulson, R. J. (2005) *Hum Reprod* **20**(6), 1511-1515

11. Wang, C. W., Horng, S. G., Chen, C. K., Wang, H. S., Huang, H. Y., Lee, C. L., and Soong, Y. K. (2008) *Reprod Biomed Online* **17**(1), 20-26

12. Rabaglio, M., Sun, Z., Price, K. N., Castiglione-Gertsch, M., Hawle, H., Thurlimann, B., Mouridsen, H., Campone, M., Forbes, J. F., Paridaens, R. J., Colleoni, M., Pienkowski, T., Nogaret, J. M., Lang, I., Smith, I., Gelber, R. D., Goldhirsch, A., and Coates, A. S. (2009) *Ann Oncol* **20**(9), 1489-1498

13. Saadeh, S. (2007) *Nutr Clin Pract* **22**(1), 1-10

14. Nishino, M., Hayakawa, K., Nakamura, Y., Morimoto, T., and Mukaihara, S. (2003) *AJR Am J Roentgenol* **180**(1), 129-134

15. Bruno, S., Maisonneuve, P., Castellana, P., Rotmensz, N., Rossi, S., Maggioni, M., Persico, M., Colombo, A., Monasterolo, F., Casadei-Giunchi, D., Desiderio, F., Stroffolini, T., Sacchini, V., Decensi, A., and Veronesi, U. (2005) *Bmj* **330**(7497), 932

16. Oien, K. A., Moffat, D., Curry, G. W., Dickson, J., Habeshaw, T., Mills, P. R., and MacSween, R. N. (1999) *Lancet* **353**(9146), 36-37

17. Larosche, I., Letteron, P., Fromenty, B., Vadrot, N., Abbey-Toby, A., Feldmann, G., Pessayre, D., and Mansouri, A. (2007) *J Pharmacol Exp Ther* **321**(2), 526-535

18. Lelliott, C. J., Lopez, M., Curtis, R. K., Parker, N., Laudes, M., Yeo, G., Jimenez-Linan, M., Grosse, J., Saha, A. K., Wiggins, D., Hauton, D.,

Brand, M. D., O'Rahilly, S., Griffin, J. L., Gibbons, G. F., and Vidal-Puig, A. (2005) *Faseb J* **19**(9), 1108-1119

19. Gudbrandsen, O. A., Rost, T. H., and Berge, R. K. (2006) *J Lipid Res* **47**(10), 2223-2232
20. Ordovas, J. M., and Osgood, D. (1998) *Methods Mol Biol* **110**, 105-111
21. Jacobs, R. L., Devlin, C., Tabas, I., and Vance, D. E. (2004) *The Journal of biological chemistry* **279**(45), 47402-47410
22. Bligh, E. G., and Dyer, W. J. (1959) *Can J Biochem Physiol* **37**(8), 911-917
23. Lohninger, A., Preis, P., Linhart, L., Sommoggy, S. V., Landau, M., and Kaiser, E. (1990) *Anal Biochem* **186**(2), 243-250
24. Bartlett, G. R. (1959) *The Journal of biological chemistry* **234**(3), 469-471
25. Klaunig, J. E., Goldblatt, P. J., Hinton, D. E., Lipsky, M. M., Chacko, J., and Trump, B. F. (1981) *In Vitro* **17**(10), 913-925
26. Cui, Z., Vance, J. E., Chen, M. H., Voelker, D. R., and Vance, D. E. (1993) *The Journal of biological chemistry* **268**(22), 16655-16663
27. Ridgway, N. D., and Vance, D. E. (1992) *Methods Enzymol* **209**, 366-374
28. Sundler, R., and Akesson, B. (1975) *The Journal of biological chemistry* **250**(9), 3359-3367
29. Noga, A. A., and Vance, D. E. (2003) *The Journal of biological chemistry* **278**(24), 21851-21859
30. Noga, A. A., Zhao, Y., and Vance, D. E. (2002) *The Journal of biological chemistry* **277**(44), 42358-42365

31. Zhao, Y., Su, B., Jacobs, R. L., Kennedy, B., Francis, G. A., Waddington, E., Brosnan, J. T., Vance, J. E., and Vance, D. E. (2009) *Arterioscler Thromb Vasc Biol* **29**(9), 1349-1355

32. Viollet, B., Guigas, B., Leclerc, J., Hebrard, S., Lantier, L., Mounier, R., Andreelli, F., and Foretz, M. (2009) *Acta Physiol (Oxf)* **196**(1), 81-98

33. Kim, K. H., Lopez-Casillas, F., Bai, D. H., Luo, X., and Pape, M. E. (1989) *Faseb J* **3**(11), 2250-2256

34. Dolinsky, V. W., and Dyck, J. R. (2006) *American journal of physiology* **291**(6), H2557-2569

35. Sul, H. S., Smith, S. (2008) Fatty acid synthesis in eukaryotes. In: Vance, D. E., Vance, J.E. (ed). *Biochemistry of lipid and lipoproteins (pp 155-190)*, 5 Ed., Elsevier, New York

36. Paquette, A., Wang, D., Jankowski, M., Gutkowska, J., and Lavoie, J. M. (2008) *Menopause* **15**(6), 1169-1175

37. D'Eon, T. M., Souza, S. C., Aronovitz, M., Obin, M. S., Fried, S. K., and Greenberg, A. S. (2005) *The Journal of biological chemistry* **280**(43), 35983-35991

38. Shiau, A. K., Barstad, D., Loria, P. M., Cheng, L., Kushner, P. J., Agard, D. A., and Greene, G. L. (1998) *Cell* **95**(7), 927-937

39. Zhang, D., and Trudeau, V. L. (2006) *Comparative biochemistry and physiology* **144**(3), 306-315

40. Prossnitz, E. R., Oprea, T. I., Sklar, L. A., and Arterburn, J. B. (2008) *J Steroid Biochem Mol Biol* **109**(3-5), 350-353

41. Prossnitz, E. R., Arterburn, J. B., Smith, H. O., Oprea, T. I., Sklar, L. A., and Hathaway, H. J. (2008) *Annual review of physiology* **70**, 165-190

42. Revankar, C. M., Cimino, D. F., Sklar, L. A., Arterburn, J. B., and Prossnitz, E. R. (2005) *Science (New York, N.Y* **307**(5715), 1625-1630

43. Filardo, E. J., Quinn, J. A., Frackelton, A. R., Jr., and Bland, K. I. (2002) *Molecular endocrinology (Baltimore, Md* **16**(1), 70-84

44. Song, R. X., Fan, P., Yue, W., Chen, Y., and Santen, R. J. (2006) *Endocrine-related cancer* **13 Suppl 1**, S3-13

45. Cao, C., Lu, S., Jiang, Q., Wang, W. J., Song, X., Kivlin, R., Wallin, B., Bagdasarian, A., Tamakloe, T., Chu, W. M., Marshall, J., Kouttab, N., Xu, A., and Wan, Y. (2008) *Cell Signal* **20**(10), 1830-1838

46. Omar, B., Zmuda-Trzebiatowska, E., Manganiello, V., Goransson, O., and Degerman, E. (2009) *Cell Signal* **21**(5), 760-766

47. Griffin, M. J., Wong, R. H., Pandya, N., and Sul, H. S. (2007) *The Journal of biological chemistry* **282**(8), 5453-5467

48. Latasa, M. J., Griffin, M. J., Moon, Y. S., Kang, C., and Sul, H. S. (2003) *Molecular and cellular biology* **23**(16), 5896-5907

49. Latasa, M. J., Moon, Y. S., Kim, K. H., and Sul, H. S. (2000) *Proceedings of the National Academy of Sciences of the United States of America* **97**(19), 10619-10624

50. Moon, Y. S., Latasa, M. J., Kim, K. H., Wang, D., and Sul, H. S. (2000) *The Journal of biological chemistry* **275**(14), 10121-10127

51. Mu, Y., She, R., Zhang, H., Dong, B., Huang, C., Lin, W., Li, D., and Li, X. (2009) *Hepatol Res* **39**(9), 910-920

52. Nemoto, Y., Toda, K., Ono, M., Fujikawa-Adachi, K., Saibara, T., Onishi, S., Enzan, H., Okada, T., and Shizuta, Y. (2000) *J Clin Invest* **105**(12), 1819-1825

53. Reckless, J., Metcalfe, J. C., and Grainger, D. J. (1997) *Circulation* **95**(6), 1542-1548

54. Grainger, D. J., Witchell, C. M., and Metcalfe, J. C. (1995) *Nat Med* **1**(10), 1067-1073

55. Gupta, S., Tandon, V. R., Kapoor, B., Gupta, A., Gupta, G. D., and Khajuria, V. (2006) *J Assoc Physicians India* **54**, 183-186

56. Bagdade, J. D., Wolter, J., Subbaiah, P. V., and Ryan, W. (1990) *J Clin Endocrinol Metab* **70**(4), 1132-1135

57. de Medina, P., Payre, B. L., Bernad, J., Bosser, I., Pipy, B., Silvente-Poirot, S., Favre, G., Faye, J. C., and Poirot, M. (2004) *J Pharmacol Exp Ther* **308**(3), 1165-1173

58. Verkade, H. J., Fast, D. G., Rusinol, A. E., Scraba, D. G., and Vance, D. E. (1993) *The Journal of biological chemistry* **268**(33), 24990-24996

59. Jacobs, R. L., Lingrell, S., Zhao, Y., Francis, G. A., and Vance, D. E. (2008) *The Journal of biological chemistry* **283**(4), 2147-2155

60. Fast, D. G., and Vance, D. E. (1995) *Biochim Biophys Acta* **1258**(2), 159-168

61. Walkey, C. J., Yu, L., Agellon, L. B., and Vance, D. E. (1998) *The Journal of biological chemistry* **273**(42), 27043-27046

62. Robichaud, J. C., Francis, G. A., and Vance, D. E. (2008) *The Journal of biological chemistry* **283**(51), 35496-35506

Chapter 4

Impaired Phosphatidylcholine Biosynthesis Reduces Atherosclerosis and Prevents Cardiac Dysfunction in ApoE $^{-/-}$ Mice

4.1 Introduction

Atherosclerosis is a progressive degenerative arterial disease characterized by obstructive plaque formation (1). Vascular lesions are initiated by accumulation of lipoprotein-derived lipid within artery walls. Elevated plasma levels of low density lipoproteins (LDLs) and its precursor, very low density lipoproteins (VLDLs) are well established risk factors for cardiovascular disease (1). The plasma concentrations of VLDL and LDL are determined by the rate of removal via receptor-mediated endocytosis and lipolysis as well as by the rate of VLDL secretion from the liver.

Generally, research investigating the role of lipoproteins in the progression of atherosclerosis focused on the metabolism of the core lipids triacylglycerol (TG) and cholesteryl ester (CE) (2). However, phospholipids (PLs) are fundamental in the assembly and secretion of VLDL from the liver (3-6). In addition, PLs on the surface of circulating VLDL and LDL come into contact with cell surface enzymes and receptors which may affect the rate of lipoprotein removal (7,8). Despite the importance of PLs for lipoprotein metabolism, the link between atherosclerosis and PLs has not been examined extensively.

Phosphatidylcholine (PC) is the predominant PL component of VLDL and LDL (9). PC is synthesized in the hepatic endoplasmic reticulum (ER) membrane where nascent lipoproteins are assembled, suggesting

that the process of hepatic PC synthesis and VLDL assembly and secretion may be coupled. The majority of PC is formed by the cytidine diphosphate (CDP)-choline pathway (9). This pathway requires choline and is regulated by the activity of CTP:phosphocholine cytidylyltransferase (CT). When the CDP-pathway is attenuated by feeding a choline-deficient (CD) diet to animals (10) or applying CD and methionine-deficient medium to cell culture (11) VLDL assembly was interrupted and secretion reduced (6,12). The importance of PC biosynthesis for VLDL secretion has also been demonstrated in mice lacking the major isoform of CT (CTα) in the liver (4).

The liver is a unique animal tissue since substantial amounts of PC can also be synthesized endogenously by phosphatidylethanolamine *N*-methyltransferase (PEMT) (13). PEMT generates approximately a third of total hepatic PC by catalyzing three sequential methylations of phosphatidylethanolamine (PE) using *S*-adenosylmethionine as a methyl donor (13-15). A specific role for PEMT in VLDL secretion has been demonstrated *in vivo* (16) and in experiments with hepatocytes (17). Targeted deletion of the *Pemt* gene in mice fed a high fat/high cholesterol diet reduced hepatic VLDL secretion (ApoB 100) and fasting plasma TG levels by 50% (16).

A well-established mouse model of atherosclerosis is the apolipoprotein E-knockout (apoE-KO) mouse (18,19). ApoE is a

glycoprotein which functions as a ligand for receptor-mediated lipoprotein removal from the blood. In the absence of apoE, the ability to clear lipoproteins is severely impaired resulting in elevated levels of LDL and VLDL. Unlike other mouse models which require high fat or western-type diet to promote plaque formation, apoE-deficient mice develop lesions spontaneously on a chow diet (18-21). The time-dependent formation and anatomical localization of lesions resembles the human disease more closely than other mouse atherosclerosis models (18-21). More recently, it has also been demonstrated that ~1 year old apoE-deficient mice develop changes in the left ventricular (LV) structure and function as a result of atherosclerotic lesions (22,23). To study the contribution of PEMT to atherosclerotic lesion formation and cardiac function, we combined the genetic model of PEMT deficiency with the apoE-KO mouse (18,19). These results establish that inhibition of PEMT prevents the development of atherosclerosis that leads to cardiac dysfunction.

4.2 Experimental Procedures

4.2.1 Animal Care

All animal procedures were performed in accordance with the University of Alberta Animal Policy and Welfare Committee, which adheres to the principles for biomedical research involving animals developed by the Council for International Organizations of Medical Sciences. Mice with genetic disruption of the *Pemt* gene (24) were backcrossed for seven

generations to obtain greater than 99.2% homogeneity in a C57BL/6J background strain (Jackson Laboratory, Bar Harbour, ME). *Pemt*$^{+/+}$*/Apoe*$^{-/-}$ and *Pemt*$^{-/-}$*/Apoe*$^{-/-}$ were then generated by interbreeding *Pemt*$^{-/-}$ mice with *Apoe*$^{-/-}$ mice (C57BL/6J Jackson Laboratory, Bar Harbour, ME). All mice were used in this study were male and maintained on standard chow diet containing 6 % (w/w) fat and 0.02% (w/w) cholesterol (LabDiet).

4.2.2 Lipid and Lipoprotein Analyses

Male mice were fasted overnight (~16 h) before blood was collected by cardiac puncture of anesthetized animals. Tissues were harvested immediately, rinsed in ice cold phosphate-buffered saline and flash frozen in liquid N_2. Plasma lipoproteins were separated by size using fast-protein liquid chromatography (25) on a Agilent 1200 with a Superose 6 column (Amersham Pharmacia Biotech). The content of choline-containing PLs, total cholesterol and TG was quantified in each fraction with in-line enzymatic assay kits (λ=500 nm) for choline (phospholipid c kit, Wako), total cholesterol (unesterified + esterified, Thermo Infinity reagents, VWR) and TG (Thermo Infinity TG regents, VWR). Peaks were identified by comparison with lipoprotein standards. Total lipids were extracted (26) from plasma (100 μl), liver homogenate (1 mg protein) or freshly isolated whole aortas (heart to the right renal artery) following removal of periadventital adipose tissue in ice cold phosphate buffered saline. TG, unesterified cholesterol and CE were measured by gas-liquid

chromatography (27) and amounts of PC and phosphatidylethanolamine were determined by phosphorus assay (28).

4.3.3 Tissue Preparation and Histology

Mice were euthanized and the heart and proximal aorta were excised, embedded in optimal cutting temperature compound (Tissue Tek) and quickly frozen in liquid N_2. Cryosections (10 μm) were prepared and stained with Oil Red O to reveal neutral lipid accumulation as well as hematoxylin to assist in tissue visualization (29). Atherosclerosis was quantitated by the *en face* technique (30). The entire aorta (heart to ileal bifurcation) was excised and fixed in 4% paraformaldehyde solution to aid in the removal of surrounding peri-adventitial adipose tissue prior to longitudinal dissection. To identify lipid-rich intimal lesions, the aortas were stained with 0.5% Sudan IV and color photographs were taken with AxioCam (Zeiss) mounted on a stereomicroscope (Axioskop) with a 5X objective lens. Image analysis was performed using MetaMorph 6.1 (Universal Image Corp.). The severity of atherosclerosis was calculated as the percentage of the Sudan IV-stained area relative to total aortic surface area.

For Masson's trichrome stain, freshly excised hearts were fixed in Bouin's solution (Sigma), embedded in paraffin and serial 5 μm cross-sections were taken. The sections were stained with Masson's trichrome stain (collagen, blue; muscle, red; nuclei, black), and color photographs

were taken with AxioCam (Zeiss) mounted on a stereomicroscope (Axioskop) with a 2.5X (whole heart) or 20X (myocardium/endocardium) objective lens.

4.2.4 *In Vivo* Assessment of Cardiac Function and Blood Pressure

Transthoracic echocardiography was performed on mildly anesthetized mice using a Vevo 770 High-Resolution Imaging System equipped with a 30-MHz transducer (RMV-707b; VisualSonics, Toronto). The mouse was placed on a heated electrocardiograph platform to acquire physiological parameters and maintain body temperature. To obtain aortic measurements the platform was tilted slightly to the right. The 30-MHz transducer was placed at the suprasternal notch. With this transducer position the ascending aorta, aortic arch, origin of the brachiocephalic vessels, descending thoracic aorta and right pulmonary artery can be visualized. In addition, the leaflets of the aortic valve in the aortic root can often be seen. Pulse Doppler flows were acquired from the ascending and descending arteries, as well as m-modes for the transverse arch. The transducer was placed just below the sternum using minimal pressure and angled toward the apex of the heart in order to obtain images for analysis of cardiac and aortic structures and function. Aortic diameter was measured at the level of the Valsalva sinus from the m-mode image. For transmitral recordings a depth setting of 4-7 mm was used and 6-9 mm was used for trans-aortic recordings. Aortic distensibility was calculated by

using the follow validated formula (31-33) (change in aortic diameter between systole and diastole)/ (diastolic aortic diameter) (pulse pressure). Pulse pressure was calculated by the equation (systolic blood pressure – diastolic blood pressure). Myocardial performance index was calculated using the equation (isovolumic contraction time + isovolumic relaxation time)/ejection time. Non-invasive blood pressure measurements were made using a tail cuff system (IITC Corp.).

4.2.5 Immunoblot Analyses

Liver homogenate (30 μg) or plasma (2 μl) were heated for 10 min at 90^{o}C in 62.5 mM Tris-HCl (pH 8.3), 10% glycerol, 5% (v/v) 2-mercaptoethanol, 1% SDS, and 0.004% bromophenol blue. The samples were electrophoresed on a SDS-polyacrylamide gel in 25 mM Tris-HCl (pH 8.5), 192 mM glycine, and 0.1% SDS buffer. The proteins were transferred to polyvinylidene fluoride membranes by electroblotting in transfer buffer (125 mM Tris-HCl, pH 8.3), 960 mM glycine, 10% (v/v) methanol). Following transfer, the membrane was incubated overnight at 4^{o}C with 5% skim milk in 10 mM Tris-HCl (pH 7.4), 100 mM NaCl, 0.1% Tween 20 (T-TBS) followed by 1 h at room temperature or overnight at 4^{o}C with antibody raised against the protein indicated. Anti-AMP activated protein kinase (AMPK) total antibody, anti-phosphorylated AMPK antibody (Thr-172), anti-acetyl-Coenzyme A carboxylase (ACC) antibody, anti-phosphorylated ACC antibody (Ser-79), hydroxymethylglutaryl-Coenzyme

A (HMG-CoA) reductase and anti-phosphorylated HMG-CoA reductase (Ser-872) were diluted (1:1000) in 3% bovine serum albumin, T-TBS. Anti-PDI antibody was diluted (1:4000) in 4% bovine serum albumin. Anti-apolipoprotein B antibody was diluted (1:7500) in 5% skim milk. Immunoreactive proteins were detected using enhanced chemiluminescence system (Amersham Biosciences) according to the manufacturer's instructions.

4.2.6 Statistical Analysis

Data are expressed as mean ± standard error of the mean (SEM). Comparisons between mouse strains were performed using the unpaired Student's two-tailed t-test. A probability value of <0.05 is considered significant.

4.3 RESULTS

4.3.1 Hepatic Phospholipid Composition

To determine whether the lack of PEMT on an apoE-KO background altered hepatic PL composition, we examined the PC and PE content of the liver. Consistent with previous findings in mice deficient in PEMT (7) we found that there was a small but significant ~8% decrease in hepatic PC levels and an 18% increase in PE content for *Pemt*$^{-/-}$/*Apoe*$^{-/-}$ mice at 6-months of age compared to *Pemt*$^{+/+}$/*Apoe*$^{-/-}$ controls (Figure 4.1A). Hepatic PC/PE ratios are important because they reflect the overall

PL membrane composition of the secretory system in which nascent VLDL are formed. Together, the changes in PL levels reduced the PC/PE ratio by 22% in the liver of PEMT deficient mice (Figure 4.1A). Similarly, we observed a significant decrease in both hepatic PC content (12%) and the PC/PE ratio (14%) in *Pemt*$^{-/-}$*/Apoe*$^{-/-}$ mice at 12-months of age (Figure 1B). These data indicate that the absence of PEMT is important for maintaining hepatic levels of PC in mice lacking apoE.

4.3.2 Liver Lipids are Decreased in the Absence of PEMT

PEMT deficiency has previously been associated with limiting hepatic PC for VLDL-TG secretion from the liver (7,16,17). In these studies decreased VLDL-TG secretion resulted in accumulation of hepatic TG. Therefore, we examined whether the absence of PEMT increased hepatic lipid content in apoE-KO mice. Interestingly, we determined that there was significantly less hepatic TG (39%, Figure 4.2A) in 6-month old *Pemt*$^{-/-}$*/Apoe*$^{-/-}$ mice relative to age-matched *Pemt*$^{+/+}$*/Apoe*$^{-/-}$ animals. At 12-months of age, *Pemt* $^{-/-}$*/Apoe* $^{-/-}$ mice had 37% lower hepatic CE as well as a 39% reduction in TG content (Figure 4.2B). The reduction in hepatic neutral lipids was accompanied by significant reductions in liver weight at both 6- (Figure 4.3A) and 12-months of age (Figure 4.3B).

4.3.3 AMPK is Activated in the Liver of PEMT Deficient Mice

In an attempt to explain the reduction of hepatic lipid levels in the absence of PEMT, we investigated whether hepatic fuel metabolism was altered. Since AMP-activated protein kinase (AMPK) regulates the energy status of the cell through inhibition of energy-consuming biosynthetic pathways, such as fatty acid and sterol synthesis, and stimulation of catabolic pathways such as fatty acid oxidation, we determined whether altered AMPK activity could account for the decreased hepatic lipids in *Pemt*$^{-/-}$*/Apoe*$^{-/-}$ mice (34,35). AMPK activity as judged by phosphorylation of the catalytic subunit at Thr-172, was increased modestly but significantly in the liver of 6-month-old *Pemt*$^{-/-}$*/Apoe*$^{-/-}$ mice relative to age-matched *Pemt*$^{+/+}$*/Apoe*$^{-/-}$ controls (Figures 4.4A and B). A similar increase in AMPK phosphorylation (Thr-172) was observed in the liver of PEMT deficient mice at 12-months of age (Figures 4.4C and D).

Since, AMPK activity was increased in the absence of PEMT we investigated the phosphorylation status of a physiological target of AMPK, acetyl-CoA carboxylase (ACC), that regulates fatty acid metabolism through the production of malonyl CoA (34,35). Phosphorylation of ACC (Ser-79) by AMPK leads to inhibition of ACC activity and reduced lipogenesis and increased fatty acid oxidation (34,35). The level of phosphorylated ACC (Ser-79) corresponded to the increase in AMPK

activity in the liver of *Pemt*$^{-/-}$*/Apoe*$^{-/-}$ mice relative to *Pemt*$^{+/+}$*/Apoe*$^{-/-}$ mice at both 6- (Figures 4.5A and B) and 12-months of age (Figures 4.5C and D).

AMPK also controls cholesterol synthesis via the phosphorylation and inhibition of HMG-CoA reductase at Ser-872 (34,35). The level of HMG-CoA reductase phosphorylation (Ser-872) was significantly higher in the liver of *Pemt*$^{-/-}$*/Apoe*$^{-/-}$ mice relative to *Pemt*$^{+/+}$*/Apoe*$^{-/-}$ mice at both 6- (Figure 4.6A and B) and 12-months of age (Figures 4.6 C and D). Thus, our results indicate that in the *Pemt*$^{-/-}$*/Apoe*$^{-/-}$ mouse, the activation of AMPK and consequent inhibition of its physiologic targets, ACC and HMG-CoA reductase, corresponds to the reduction in hepatic neutral lipid levels (Figure 4.2).

4.3.4 PEMT Deficiency in *Apoe*$^{-/-}$ mice Reduces Atherogenic Plasma Lipoproteins

The relationship between the availability of hepatic neutral lipids and VLDL secretion from the liver is well established (2). Thus, a reduced level of hepatic TG suggests that this may also attenuate VLDL-TG secretion in *Pemt*$^{-/-}$*/Apoe*$^{-/-}$ mice. After 6 months on a chow diet *Pemt*$^{+/+}$*/Apoe*$^{-/-}$ and *Pemt*$^{-/-}$*/Apoe*$^{-/-}$ mice had similar plasma levels of cholesterol and CE (Figure 4.7A). However, PEMT deficient animals had 24% less plasma TG (86.2 ± 5.8 mg/dl) compared to *Pemt* $^{+/+}$*/Apoe*$^{-/-}$ mice (112.9 ± 5.3 mg/dl) (Figure 4.7B). At 12-months of age *Pemt*$^{-/-}$*/Apoe*$^{-/-}$ mice had ~24% less plasma cholesterol and CE levels as well as a 45%

reduction in TG content compared to *Pemt*$^{+/+}$*/Apoe*$^{-/-}$ animals (Figures 4.7C and D).

In order to match the lipid reductions observed in the plasma of *Pemt*$^{-/-}$*/Apoe*$^{-/-}$ mice with specific lipoprotein fractions we used gel filtration chromatography. Comparison of the lipoprotein profiles between genotypes confirmed that the amount of cholesterol remained similar in each lipoprotein fraction at 6-months of age (Figure 4.8A). However, one year old *Pemt*$^{-/-}$*/Apoe*$^{-/-}$ mice had less cholesterol in the VLDL/intermediate density lipoprotein (IDL)/LDL fraction (Figure 4.8B) compared to *Pemt*$^{+/+}$*/Apoe*$^{-/-}$ animals. The amount of HDL-cholesterol did not change in the absence of PEMT. As expected, the reduction in plasma TG observed in the *Pemt*$^{-/-}$*/Apoe*$^{-/-}$ mice was due to a reduction in VLDL-TG at 6-months (Figure 4.8C) and 12-months (Figure 4.8D) of age. The distribution of choline-containing phospholipids was not different between genotypes for any of the lipoprotein fractions at 6-(Figure 4.8E) and 12-month age groups (Figure 4.8F).

To determine the number of VLDL/IDL/LDL particles in the plasma, we measured the amount of apoB 48 (Figures 4.9A and B). In the absence of PEMT, the level of apoB 48 was significantly reduced at 12-month-old compared to age matched *Pemt*$^{+/+}$*/Apoe*$^{-/-}$ animals. ApoB 100 was not detectable by immunoblot in either genotype since unlike wild-type mice the VLDL and LDL fractions of *Apoe*$^{-/-}$ mice contain

predominantly apoB 48 (36,37). These data indicate that PEMT deficiency in *Apoe*$^{-/-}$ mice results in an atheroprotective plasma lipoprotein profile. In the absence of PEMT plasma TG and CE are reduced in a pattern which mirrored the age-dependent reduction of hepatic lipid accumulation (TG and CE).

4.3.5 Plasma Phospholipid Composition

Plasma PC/PE ratios are important because they reflect the overall PL composition of circulating lipoproteins. A decrease in the PC/PE ratio of VLDL has been previously shown to increase uptake from the plasma and thereby reduce circulating levels of VLDL (8). Since the majority of plasma lipid is carried within VLDL particles in apoE-KO mice, we examined the PC/PE ratio in total plasma. Analysis of plasma samples from mice at 6-months of age revealed that there was no difference in PC/PE ratios between genotypes (Figure 4.10A). This was due primarily to a trend toward lower PE values as well as reduced PC content in plasma from *Pemt*$^{-/-}$*/Apoe*$^{-/-}$ mice. However, at 12-months of age plasma from *Pemt*$^{-/-}$*/Apoe*$^{-/-}$ mice had a 11% reduction in the PC/PE ratio compared to age-matched *Pemt*$^{+/+}$*/Apoe*$^{-/-}$ controls (Figure 4.10B). Thus, our findings suggest that the absence of PEMT on an apoE-KO background may increase the catabolism of VLDL at 12-months but not 6-months of age.

4.3.6 The Absence of PEMT Decreases Aortic Cholesterol Accumulation in *Apoe* $^{-/-}$ Mice

It is well established that apoE-KO mice spontaneously develop atherosclerotic lesions on a chow diet as they age (18,19). To determine if PEMT deficiency reduced atherosclerosis in *Apoe*$^{-/-}$ mice, we measured the development of aortic lesions in mice 12-months of age. In the aortic root, the size of the plaques stained by Oil Red O were smaller in *Pemt*$^{-/-}$*/Apoe*$^{-/-}$ mice compared to the *Pemt*$^{+/+}$*/Apoe*$^{-/-}$ mice (Figure 4.11A). Quantification of the lesion area along the entire aorta was determined by *en face* analysis (Figure 4.11B). Using computer assisted image analysis we determined that the percentage of the aorta surface area covered by atherosclerotic lesions was reduced by 28% in the *Pemt*$^{-/-}$*/Apoe*$^{-/-}$ mice compared to *Pemt*$^{+/+}$*/Apoe*$^{-/-}$ (Figure 4.11C). We also compared aortic cholesterol content between genotypes (Figure 4.11D). This parameter has been previously used as an independent parameter to quantify atherosclerosis in mice (38-40) and may be a more sensitive indicator of atherosclerosis since it accounts for lesion thickness which continues to increase when the area available for lesion development has been saturated (29,30) (41). We found that the amount of cholesterol and CE in the aorta of PEMT deficient mice was ~40% less than values obtained from aortas of age-matched *Pemt*$^{+/+}$*/Apoe*$^{-/-}$ controls (Figure 4.11D). Therefore, targeted deletion of PEMT in apoE-KO mice reduces both the size and cholesterol content of atherosclerotic lesions in the aortic wall.

4.3.7 *Pemt*$^{-/-}$/*Apoe*$^{-/-}$ mice are Resistant to Age-dependent Cardiac Dysfunction

The development of atherosclerosis in apoE-KO mice has been shown to contribute to age-dependent aortic stiffening (22,23,42), endothelial dysfunction (43-46), and hypertension (43). Furthermore, the resulting long-term increases in cardiac after-load associated with these pathologies have been linked to age-dependent cardiac dysfunction in apoE-KO mice (22,23,43,44). These studies prompted us to investigate whether PEMT deficiency also prevented consequences of atherosclerosis on cardiac function in apoE-KO mice. Aortic distensibility is a direct measure of arterial stiffness associated with vascular dysfunction and plaque formation (31,47-49). Therefore, the change in aortic diameter during the cardiac cycle was determined *in vivo* using echocardiographic assessment. We found that aortic distension was 2-fold larger in the *Pemt*$^{-/-}$*Apoe*$^{-/-}$ mice at 10-months of age compared to age-matched *Pemt*$^{+/+}$/*Apoe*$^{-/-}$ animals (Figure 4.11E). These observations suggested that PEMT deficiency reduces arterial stiffening associated with atherosclerosis. However, any improvement provided by the absence of PEMT in apoE-KO mice is not related to peripheral blood pressure since arterial pressures were similar between *Pemt*$^{+/+}$*Apoe*$^{-/-}$ and *Pemt*$^{-/-}$/*Apoe* $^{-/-}$ at 10-months of age (Table 1).

Analysis of cardiac structure by echocardiography indicated that Left Ventricle internal dimension in systole (LVIDs, Figure 4.12A) and diastole (LVIDd, Figure 4.12B) were both significantly decreased in 10-month-old *Pemt*$^{-/-}$*/Apoe*$^{-/-}$ mice compared to age-matched *Pemt*$^{+/+}$*Apoe*$^{-/-}$ mice. We found no difference in echocardiac measurements between genotypes at 6-months of age (data not shown). These results show that the absence of PEMT prevented age-dependent dilation of the LV cavity in apoE-KO mice. Dilatation of the LV was also accompanied by age-dependent impaired contractility of the LV in *Pemt*$^{+/+}$*Apoe*$^{-/-}$ mice. The LV isoventricular contraction time was significantly elevated in 10-month-old *Pemt*$^{+/+}$*Apoe*$^{-/-}$ mice compared to age matched *Pemt*$^{-/-}$*/Apoe*$^{-/-}$ animals (Figure 4.12C). The increased time required to increase ventricular pressure, a prerequisite to eject blood, indicates impaired LV function.

Other variables of systolic function including ejection fraction (Figure 4.12D) and fractional shortening (Figure 4.12E) were decreased in the apoE-KO mice, but were significantly improved in *Pemt*$^{-/-}$*/Apoe*$^{-/-}$ animals. In addition, a lower Myocardial performance index in *Pemt*$^{-/-}$*/Apoe*$^{-/-}$ compared to age-matched controls (P*emt*$^{+/+}$*/Apoe*$^{-/-}$) indicates markedly improved overall systolic and diastolic function in the absence of PEMT (Figure 4.12F). A reduction in atrial size was also observed in *Pemt*$^{-/-}$*/Apoe*$^{-/-}$ at 10-months of age (Table 1). Since an early indicator of dilated cardiomyopathy is enlarged atria, (50) these results demonstrate

that PEMT deficiency prevents the transition to cardiac dysfunction in apoE-KO mice.

Histological evaluation of cardiac cross-sections of 12-month old *Pemt*$^{+/+}$*/Apoe*$^{-/-}$ mice revealed severe cardiac fibrosis by Masson trichrome staining compared to *Pemt*$^{-/-}$*/Apoe*$^{-/-}$ control animals (Figures 4.13A and B). We observed fibrosis in the inner most layer of the heart, the endocardium, of *Pemt*$^{+/+}$*/Apoe*$^{-/-}$ (Figure 4.13C) which typically develops as a result of contact with thrombi (mural thrombi) (51). Mural thombi are frequently formed by reduced ejection fractions which are consistent with echocardiograph data for 10-month *Pemt*$^{+/+}$*/Apoe*$^{-/-}$ mice (Figure 4.12). In *Pemt*$^{-/-}$*/Apoe*$^{-/-}$ mice endocardial fibrosis was absent (Figure 4.13D). Other features associated with cardiomyopathy are fibrosis of the interstitum and myocardial disarray as attenuated and thickening myofibers intersect at various angles producing a whorled appearance (52). Both interstitial fibrosis and myocardial disarray were observed extensively through out the LV of *Pemt*$^{+/+}$*/Apoe*$^{-/-}$ mice (Figure 4.13E) but not in *Pemt*$^{-/-}$*/Apoe*$^{-/-}$ mice (Figure 4.13F). Finally, we found that the *Pemt*$^{-/-}$*/Apoe*$^{-/-}$ mice had lower heart mass compared to *Pemt* $^{+/+}$*/Apoe*$^{-/-}$ control animals (Table 2). Therefore, the improvement of several parameters of cardiac structure and function in *Pemt*$^{-/-}$*/Apoe*$^{-/-}$ mice indicate that PEMT deficiency can prevent the development of dilated cardiomyopathy which accompanies atherosclerosis in apoE-KO mice.

4.4 Discussion

Atherosclerosis and congestive heart failure is a significant clinical problem that results in the significant morbidity and mortality of aging populations (1,2,53,54). Our data provide evidence that deletion of the *Pemt* gene reduces atherosclerotic lesions by ~30% and prevents the associated development of dilated cardiomyopathy in apoE-KO mice. This beneficial effect is likely due to a reduction in plasma levels of atherogenic apoB-containing lipoproteins caused, at least in part, by decreased hepatic levels of TG and CE.

4.4.1 PEMT Deficiency Decreases Plasma Atherogenic Lipoproteins

In the absence of PEMT, a decrease in atherogenic lipoproteins in the circulation as well as reduced hepatic lipid accumulation is observed in apoE-KO mice at both 6- and 12-months of age. This alteration in lipid handling likely confers cardioprotection against the age-dependent lesion formation and cardiac dysfunction that is present in 10-month old apoE null mice.

It is well-established that the amount of hepatic TG exerts a strong influence on VLDL production (55,56). Thus, it is likely that the reduction in hepatic TG would be the primary contributing factor to the significant decreases in plasma VLDL-TG in *Pemt*$^{-/-}$/*Apoe*$^{-/-}$ mice at 6-months of age. In addition, the reduction in hepatic cholesterol and CE levels may also

reduce VLDL secretion from the liver of *Pemt*$^{-/-}$/*Apoe*$^{-/-}$ mice at 12-months of age (2,57). A chronic reduction in VLDL secretion from the liver of *Pemt*$^{-/-}$/*Apoe*$^{-/-}$ mice would tend to generate less LDL/IDL-cholesterol since the majority of VLDL particles are converted within the circulation to LDL (58). The conversion of VLDL to LDL would also potentially explain the time lag between the reduction in plasma TG at 6-months and the accompanying reduction in plasma CE and cholesterol at 12 months. In a recent study, mice deficient in PEMT reduced levels of atherogenic lipoproteins and aortic plaque formation due to decreased secretion and increased uptake of PE-enriched VLDL-particles (8).

Increased uptake is not likely the primary mechanism for plasma lipid lowering in *Pemt*$^{-/-}$/*Apoe*$^{-/-}$ mice as a significant decrease in plasma TG at 6-months of age was not accompanied by a reduction in the plasma PC/PE ratio. Thus, the interaction of apoE with lipoprotein receptors may be required for elevated uptake of VLDL with a reduced PC/PE ratio.

Our data provide evidence that PEMT deficiency reduces hepatic lipid levels on an apoE-KO background. This result was unexpected since PEMT deficiency has previously been shown to promote hepatic steatosis on both a chow (59) and high-fat diet (7,16). While the reason for the different effects of PEMT deficiency in different mouse genetic backgrounds remains unclear, we do provide clear evidence that PEMT-deficiency on an apoE-KO background beneficially affects whole body

energy metabolism. For example, PEMT deficiency reduced levels of hepatic cholesterol and triglyceride while at the same time lowering circulating levels of atherogenic lipoproteins. These metabolic changes are consistent with the activation of AMPK and consequent inhibition of ACC and HMG-CoA reductase, in the livers of *Pemt*$^{-/-}$*/Apoe*$^{-/-}$ mice. Though we have not established the underlying reason for increased AMPK activity impaired hepatic PC biosynthesis can alter whole body metabolism leading to increased energy expenditure and lack of weight gain (Jacobs R., unpublished data).

4.4.2 PEMT Deficiency Prevents the Development of Dilated Cardiomyopathy

Dilated cardiomyopathy is a disease associated with hypertrophy and systolic dysfunction of one or both ventricles which, if untreated, can progress to cardiac failure (50,54). Multiple causes exist though the primary causes are coronary artery disease, hypertension and cardiac ischemia (54). The apoE-KO mouse is a well characterized model of atherosclerosis that develops an age-dependent cardiac dysfunction (23,42,60). Therefore, we utilized the apoE null background to study the role of PEMT in the age-dependent progression of cardiovascular disease. The 10-month old apoE-KO mice clearly had a number of physical, functional and histological markers of dilated cardiomyopathy including increased internal dimension of the LV chamber, decreased ejection

fraction, and greater LV fibrosis (Figure 8 and 9) (50,52). Interestingly, the absence of PEMT prevented the development of this age-dependent dysfunction. *Pemt*$^{-/-}$*/Apoe*$^{-/-}$ animals at 10-months of age had cardiac physical and functional parameters within the normal range (61-63) (Figure 8, Table 1).

Several previous studies using *Apoe*$^{-/-}$ mice have linked the development of atherosclerosis to cardiac dysfunction (23,42,60). This is based on the well-established association between atherosclerosis and vascular stiffening (47,48,64). One effect of elevated arterial resistance is the development of peripheral hypertension. However, it seems unlikely that peripheral hypertension is a major contributor to cardiac dysfunction in 10-month apoE-KO mice since the blood pressure values are considered within the normal range (23,42,43,46). Yang et al., (43) have previously shown that *Apoe*$^{-/-}$ mice develop high peripheral blood pressure with age but this has not been observed in several more recent publications (23,42,46).

Alternatively, the development of cardiac dysfunction in *Apoe*$^{-/-}$ mice has been explained based on a chronic increase in aortic stiffness (22,23,42,60,65). In recent years it has become clear that decreased aortic elasticity has an adverse effect on cardiac function due to elevated systolic aortic (central) blood pressure (66,67). Increased aortic stiffness has been identified in normotensive patients with dilated cardiomyopathy

(68) and is a strong predictor of cardiovascular risk independent of systemic blood pressure (69-72). In animals, prolonged exposure (>3-months) to elevated aortic stiffness and central blood pressure (absence of peripheral hypertension) induced myocardial remodelling and interstitial fibrosis (73). This is consistent with the extensive length of time (≥10-months) required to observe significant cardiac dysfunction in the current and previous studies using *Apoe*$^{-/-}$ mice (22,23,60).

Due to the technical difficulty and invasive nature of directly measuring central blood pressure in mice this was not undertaken. However, aortic stiffness as determined by aortic distensibility (31) was elevated in *Apoe*$^{-/-}$ mice compared to *Pemt*$^{-/-}$/*Apoe*$^{-/-}$ animals (Figure 4.11E). Furthermore, it is well-known that atherosclerotic plaques significantly increase aortic stiffness in various animal models of cardiovascular disease (74-76) including apoE-KO mice (42,46,65,77). Since the absence of PEMT reduced the formation of aortic atherosclerotic plaques and improved distensibility, it is likely that less aortic stiffness over the long-term served as the major factor for the improved cardiac function and reduced fibrosis observed in *Pemt*$^{-/-}$/*Apoe*$^{-/-}$ mice. However, cardiac dysfunction may eventually occur in *Pemt*$^{-/-}$/*Apoe*$^{-/-}$ mice as the exposure time to aortic stiffness increases and severity of the lesions progress.

In conclusion, our results show that through the reduction of TG and cholesterol in circulation, PEMT deficiency in apoE-KO mice reduces

age-associated atherosclerosis and prevents the development of cardiac dysfunction. We suggest that inhibition of PEMT activity may prove to be a novel treatment for atherosclerosis.

Table 4.1 Peripheral blood pressure and echocardiographic parameters of 10- month old *Pemt* $^{+/+}$*/Apoe*$^{-/-}$ and *Pemt*$^{-/-}$*/Apoe*$^{-/-}$ mice.

Data are expressed as means ± SEM (p<0.05, n=9-14). * p<0.05 vs *Pemt*$^{+/+}$*/Apoe*$^{-/-}$ 10-months. Sys, systolic; Dia, diastolic ; HR, heart rate; SAP, systolic arterial blood pressure; DAP, diastolic arterial blood pressure; MAP, mean arterial blood pressure; LV, left ventricle; IVS, intraventricular septum thickness; LVPW, left ventricle posterior wall thickness; LA, left atrium inner diameter; IVRT, Isoventricular relaxation time; AV, aortic valve; SV, stroke volume; CO, cardiac output.

	Pemt$^{+/+}$*/Apoe*$^{-/-}$	*Pemt*$^{-/-}$*/Apoe*$^{-/-}$
HR (bpm)	434.2 ± 14.63	434.2 ± 17.33
SAP (mm Hg)	118.8 ± 3.97	111.4 ± 3.71
DAP (mm Hg)	93.6 ± 4.31	89.6 ± 5.12
MAP (mm Hg)	102.3 ± 3.98	96.1 ± 4.69
LV Vol (μl) Sys	34.1 ± 1.5	20.8 ±1.3*
LV Vol (μl) Dia	72.8 ± 1.4	57.2 ± 2.5*
IVS (mm) Sys	1.11 ± 0.02	1.13 ± 0.03
IVS (mm) Dia	0.80 ± 0.02	0.82 ± 0.03
LVPW (mm) Sys	1.08 ± 0.03	1.16 ± 0.03
LVPW (mm) Dia	0.77 ± 0.02	0.78 ± 0.02
LA (mm)	2.20 ± 0.10	1.80 ± 0.10*
IVRT (ms)	19.9 ± 0.6	17.8 ± 0.7*
AV SV	51.3 ± 2.2	47.57 ± 4.3
AV CO	19.3 ± 1.1	20.40 ± 2.3

Table 4.2 Physical characteristics of *Pemt*$^{+/+}$/*Apoe*$^{-/-}$ and *Pemt*$^{-/-}$/*Apoe* $^{-/-}$ mice 12-months of age

Data are expressed as means ± SEM (n = 45-50 for body weight, n = 8-10 for all other parameters). * indicates a significant difference (p<0.05) between *Pemt*$^{+/+}$/*Apoe*$^{-/-}$ and *Pemt*$^{-/-}$/*Apoe*$^{-/-}$ mice. WAT, white adipose tissue; BAT, brown adipose tissue.

	Pemt$^{+/+}$*/Apoe*$^{-/-}$	*Pemt*$^{-/-}$*/Apoe*$^{-/-}$
Body Weight (g)	28.0 ± 0.3	26.6 ± 0.3*
Body Length (cm)	10.2 ± 0.08	10.1 ± 0.05
Tibia Length (cm)	2.01 ± 0.07	2.10 ± 0.03
Heart Weight (mg)	164 ± 5	150 ± 6
Heart Weight (g) /Tibia Length(cm)	0.88 ± 0.03	0.72 ± 0.03*
Subcutaneous Fat Pad (g)	0.16 ± 0.02	0.13 ± 0.01
Gonadal Fat Pad (g)	0.34 ± 0.03	0.35 ± 0.03
Mesenteric Fat Pad (g)	0.18 ± 0.02	0.16 ± 0.01
Perirenal Fat Pad (g)	0.09 ± 0.01	0.14 ± 0.03
Intrascapular Fat Pad (g)	0.12 ± 0.02	0.13 ± 0.02
Total WAT (g)	0.90 ± 0.05	0.92 ± 0.08
BAT (g)	0.11 ± 0.01	0.11 ± 0.01

Figure 4.1 PL composition of liver

PL content was measured in liver from fasted 6- (**A**) and 12-month old (**B**) *Pemt*$^{+/+}$*/Apoe*$^{-/-}$ (black bar) and *Pemt*$^{-/-}$*/Apoe*$^{-/-}$ (white bar) mice. Lipids were extracted from liver homogenate (1 mg) and the amount of PC and PE were measured by phosphorus assay. Data are expressed as means ± SEM (*, p<0.05, 6-month animals n = 4-9, 12-month animals n = 6-11).

Figure 4.1

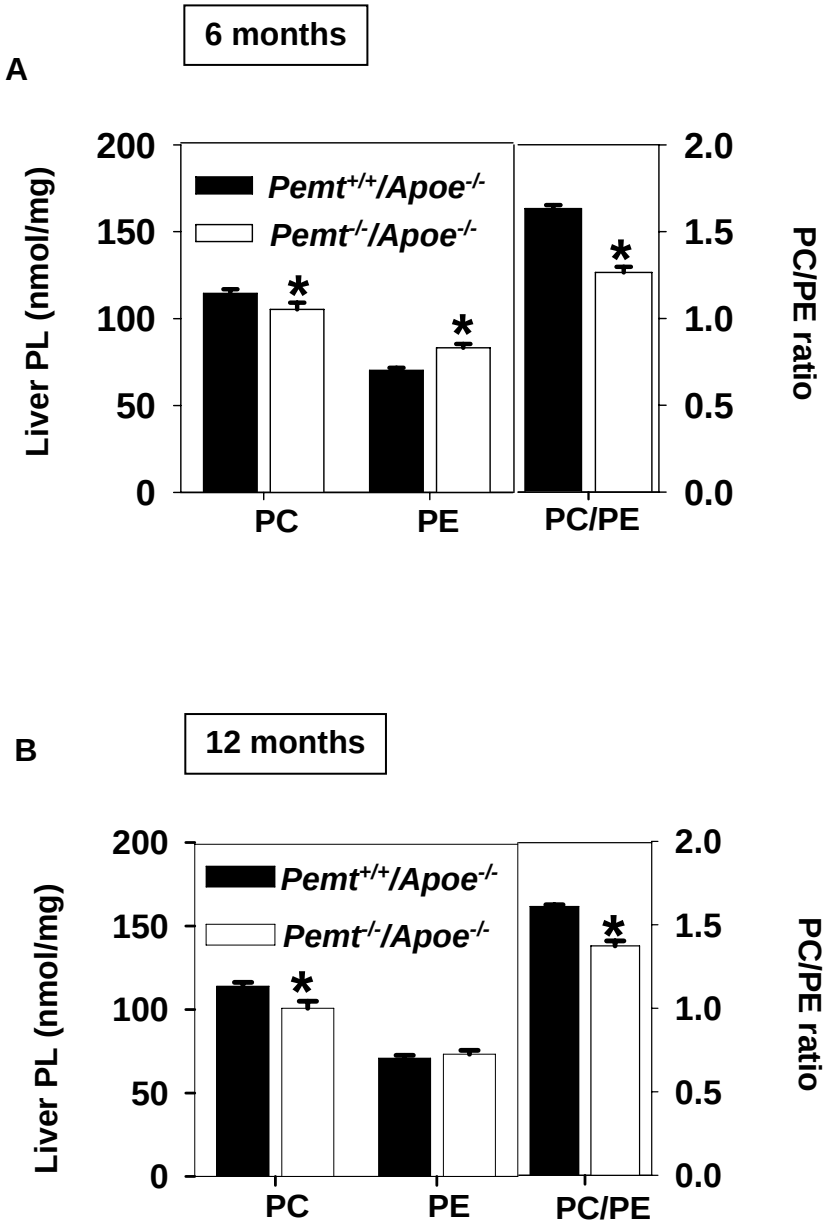
A
6 months
Liver PL (nmol/mg)
PC/PE ratio
Pemt+/+/Apoe-/-
Pemt-/-/Apoe-/-
200
150
100
50
0
2.0
1.5
1.0
0.5
0.0
PC
PE
PC/PE
*
B
12 months
Liver PL (nmol/mg)
PC/PE ratio
Pemt+/+/Apoe-/-
Pemt-/-/Apoe-/-
200
150
100
50
0
2.0
1.5
1.0
0.5
0.0
PC
PE
PC/PE
*

Figure 4.2. PEMT deficiency reduces hepatic lipid levels.

Quantitation of hepatic lipid levels from 6- (**A**) and 12-month old (**B**) *Pemt*$^{+/+}$/*Apoe*$^{-/-}$ (black bar) and *Pemt*$^{-/-}$/*Apoe*$^{-/-}$ (white bar) mice. Lipids were extracted from liver homogenates (1 mg protein) and amounts of TG, unesterified cholesterol and CE were measured. Data are expressed as means ± SEM (*, $p<0.05$, n = 6-9).

Figure 4.2

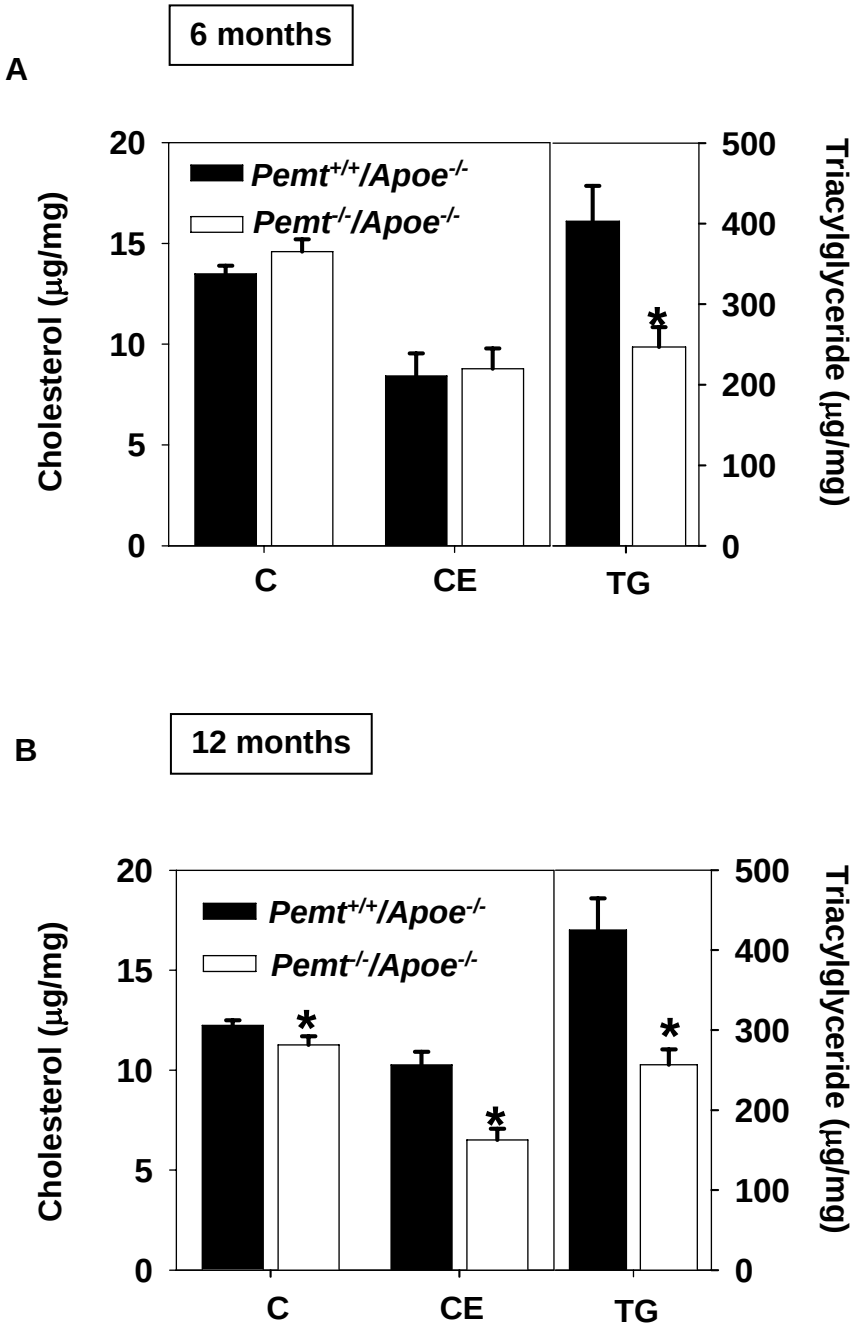
A
6 months
Pemt+/+/Apoe-/-
Pemt-/-/Apoe-/-
Cholesterol (μg/mg)
Triacylglyceride (μg/mg)
0
5
10
15
20
0
100
200
300
400
500
C
CE
TG
*
B
12 months
Pemt+/+/Apoe-/-
Pemt-/-/Apoe-/-
Cholesterol (μg/mg)
Triacylglyceride (μg/mg)
0
5
10
15
20
0
100
200
300
400
500
C
CE
TG
*
*
*

Figure 4.3. PEMT deficiency reduces hepatic weight.

Livers from 6- (**C**) and 12-month old (**D**) *Pemt*$^{+/+}$*/Apoe*$^{-/-}$ (black bar) and *Pemt*$^{-/-}$ */Apoe*$^{-/-}$ (white bar) mice were collected and weighed. Liver weights are expressed as total organ weight (g) and as a proportion of body weight (g/g). Data are expressed as means ± SEM (*, $p<0.05$, 6-month animals n = 9, 12-month old animals n = 6-7).

Figure 4.3

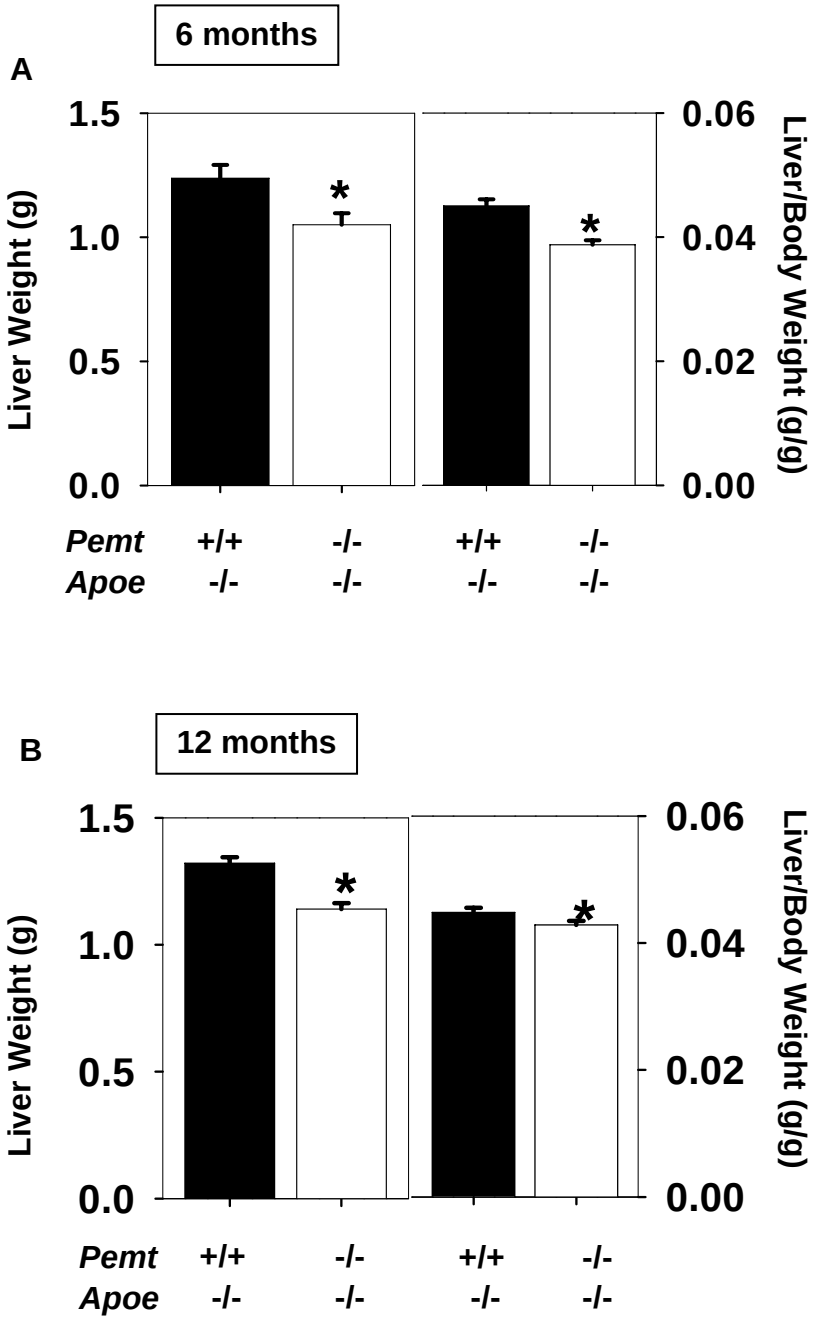
6 months
A
Liver Weight (g)
Liver/Body Weight (g/g)
1.5
1.0
0.5
0.0
0.06
0.04
0.02
0.00
*
*
Pemt +/+ -/- +/+ -/-
Apoe -/- -/- -/- -/-
12 months
B
Liver Weight (g)
Liver/Body Weight (g/g)
1.5
1.0
0.5
0.0
0.06
0.04
0.02
0.00
*
*
Pemt +/+ -/- +/+ -/-
Apoe -/- -/- -/- -/-

Figure 4.4. Analysis of AMPK activity in *Pemt* $^{+/+}$*/Apoe*$^{-/-}$ and *Pemt*$^{-/-}$*/Apoe*$^{-/-}$ mice.

Immunoblot analyses were performed on homogenates from livers harvested from *Pemt*$^{+/+}$*/Apoe*$^{-/-}$ and *Pemt*$^{-/-}$*/Apoe*$^{-/-}$ mice. Protein levels of AMPK, P-AMPK, and protein disulfide isomerase (PDI) in liver homogenates (30 μg) from 6-month (**A**) and 12-month old (**C**) *Pemt*$^{+/+}$*/Apoe*$^{-/-}$ and *Pemt*$^{-/-}$*/Apoe*$^{-/-}$ were determined by immunoblots and quantified by densitometry and normalized against total AMPK as a control for protein loading (**B, D,** *, $p < 0.05$, n = 3-4). PDI was used as an additional loading control.

Figure 4.4

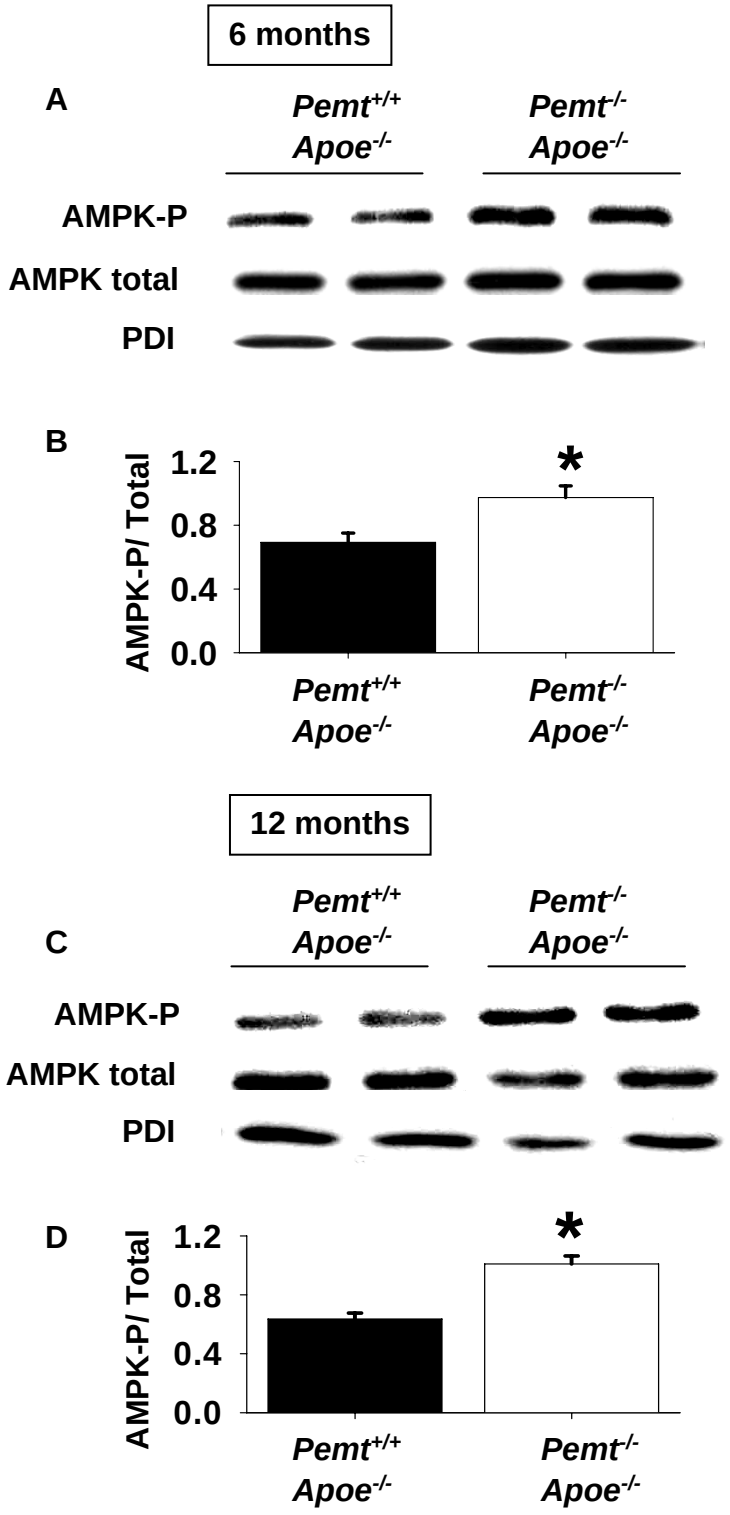
6 months
A
Pemt+/+ Apoe-/-
Pemt-/- Apoe-/-
AMPK-P
AMPK total
PDI
B
AMPK-P/ Total
1.2
0.8
0.4
0.0
*
Pemt+/+ Apoe-/-
Pemt-/- Apoe-/-
12 months
C
Pemt+/+ Apoe-/-
Pemt-/- Apoe-/-
AMPK-P
AMPK total
PDI
D
AMPK-P/ Total
1.2
0.8
0.4
0.0
*
Pemt+/+ Apoe-/-
Pemt-/- Apoe-/-

Figure 4.5. Analysis of ACC activity in *Pemt* $^{+/+}$*/Apoe*$^{-/-}$ and *Pemt*$^{-/-}$*/Apoe*$^{-/-}$ mice.

Immunoblot analyses were performed on homogenates from livers harvested from *Pemt*$^{+/+}$*/Apoe*$^{-/-}$ and *Pemt*$^{-/-}$*/Apoe*$^{-/-}$ mice. Protein levels of ACC, ACC-P and PDI in liver homogenates (30 μg) from 6-month (**A**) and 12-month old (**C**) *Pemt*$^{+/+}$*/Apoe*$^{-/-}$ and *Pemt*$^{-/-}$*/Apoe*$^{-/-}$ were determined by immunoblots and quantified by densitometry and normalized against total ACC as a control for protein loading (**B**, **D**, *, $p<0.05$, n = 3-4). PDI was used as an additional loading control.

Figure 4.5

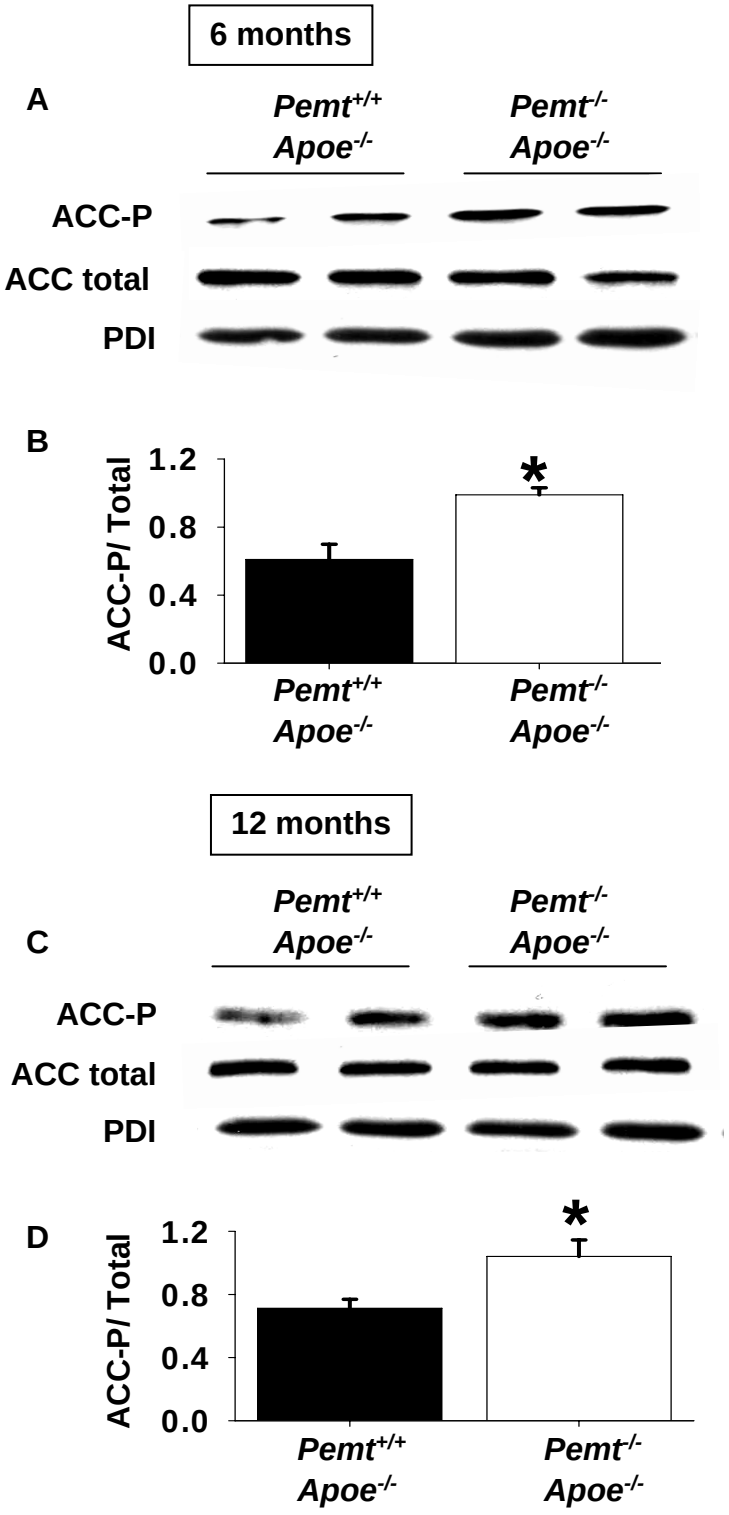
6 months
A
Pemt+/+ Apoe-/-
Pemt-/- Apoe-/-
ACC-P
ACC total
PDI
B
ACC-P/ Total
1.2
0.8
0.4
0.0
*
Pemt+/+ Apoe-/-
Pemt-/- Apoe-/-
12 months
C
Pemt+/+ Apoe-/-
Pemt-/- Apoe-/-
ACC-P
ACC total
PDI
D
ACC-P/ Total
1.2
0.8
0.4
0.0
*
Pemt+/+ Apoe-/-
Pemt-/- Apoe-/-

Figure 4.6. Analysis of HMG-CoA activity in *Pemt* $^{+/+}$*/Apoe*$^{-/-}$ and *Pemt*$^{-/-}$ */Apoe*$^{-/-}$ mice.

Immunoblot analyses were performed on homogenates from livers harvested from *Pemt*$^{+/+}$*/Apoe*$^{-/-}$ and *Pemt*$^{-/-}$*/Apoe*$^{-/-}$ mice. Protein levels of HMG-CoA reductase, P-HMG-CoA reductase, and PDI in liver homogenates (30 μg) from 6-month (**A)** and 12-month old (**C**) *Pemt*$^{+/+}$*/Apoe*$^{-/-}$ and *Pemt*$^{-/-}$*/Apoe*$^{-/-}$ were determined by immunoblots and quantified by densitometry and normalized against total HMG -CoA reductase as a control for protein loading. Data are expressed as means ± SEM (**B**, **D**, * , p<0.05, n = 3-4). PDI was used as an additional loading control.

Figure 4.6

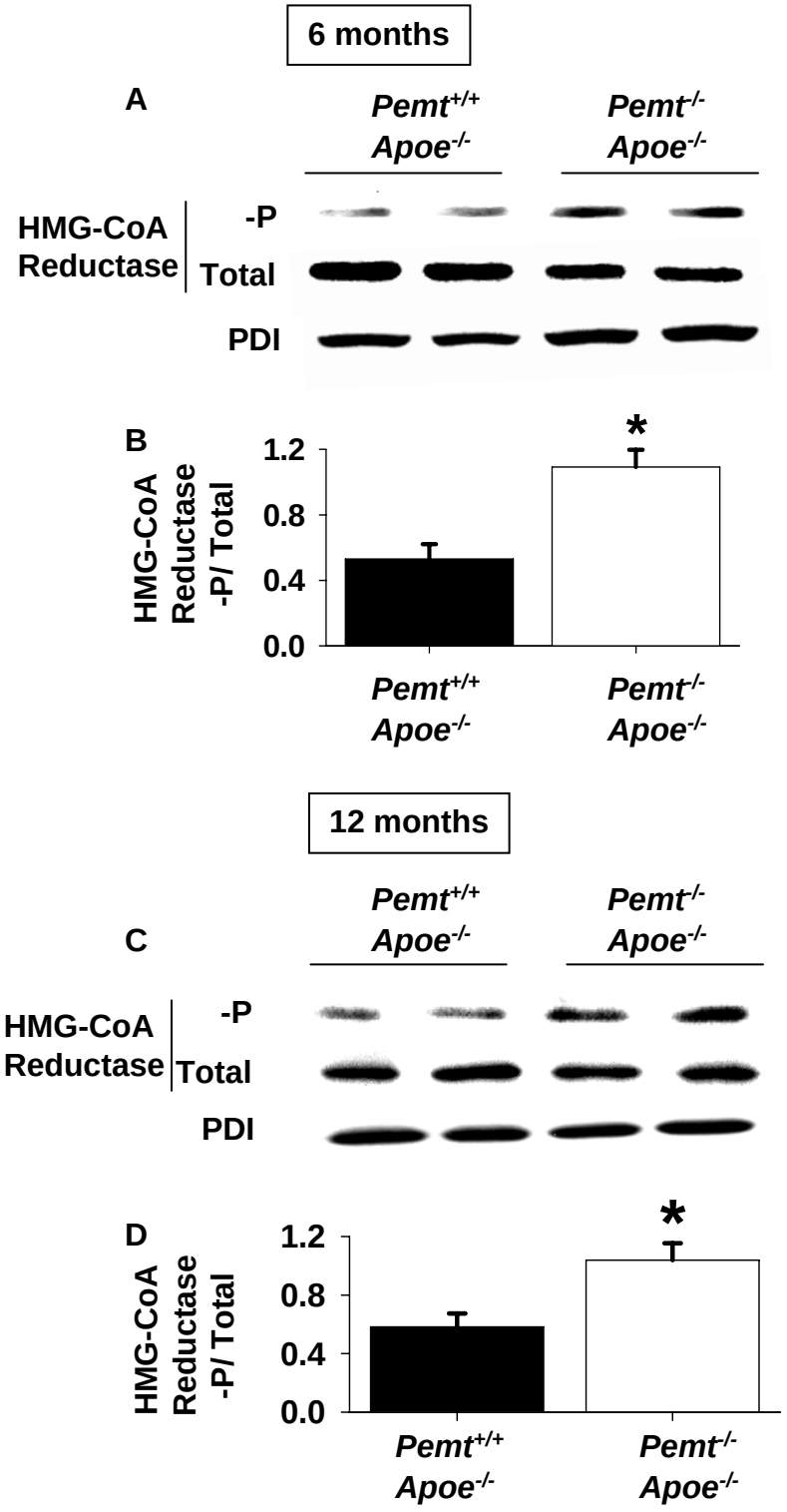
6 months
A
Pemt+/+ Apoe-/-
Pemt-/- Apoe-/-
HMG-CoA Reductase
-P
Total
PDI
B
HMG-CoA Reductase -P/ Total
1.2
0.8
0.4
0.0
*
Pemt+/+ Apoe-/-
Pemt-/- Apoe-/-
12 months
C
Pemt+/+ Apoe-/-
Pemt-/- Apoe-/-
HMG-CoA Reductase
-P
Total
PDI
D
HMG-CoA Reductase -P/ Total
1.2
0.8
0.4
0.0
*
Pemt+/+ Apoe-/-
Pemt-/- Apoe-/-

Figure 4.7. PEMT deficiency reduces atherogenic plasma lipoproteins in apoE null mice.

Plasma concentrations of cholesterol and TG were measured in samples from 6-month (**A, B**) and 12-month old (**C, D**) *Pemt*$^{+/+}$*/Apoe*$^{-/-}$ and *Pemt*$^{-/-}$*/Apoe*$^{-/-}$ mice following an overnight fast. Data are expressed as means ± SEM. (*, p<0.05, 6-month animals n = 3-5, 12-month animals n = 8-9).

Figure 4.7

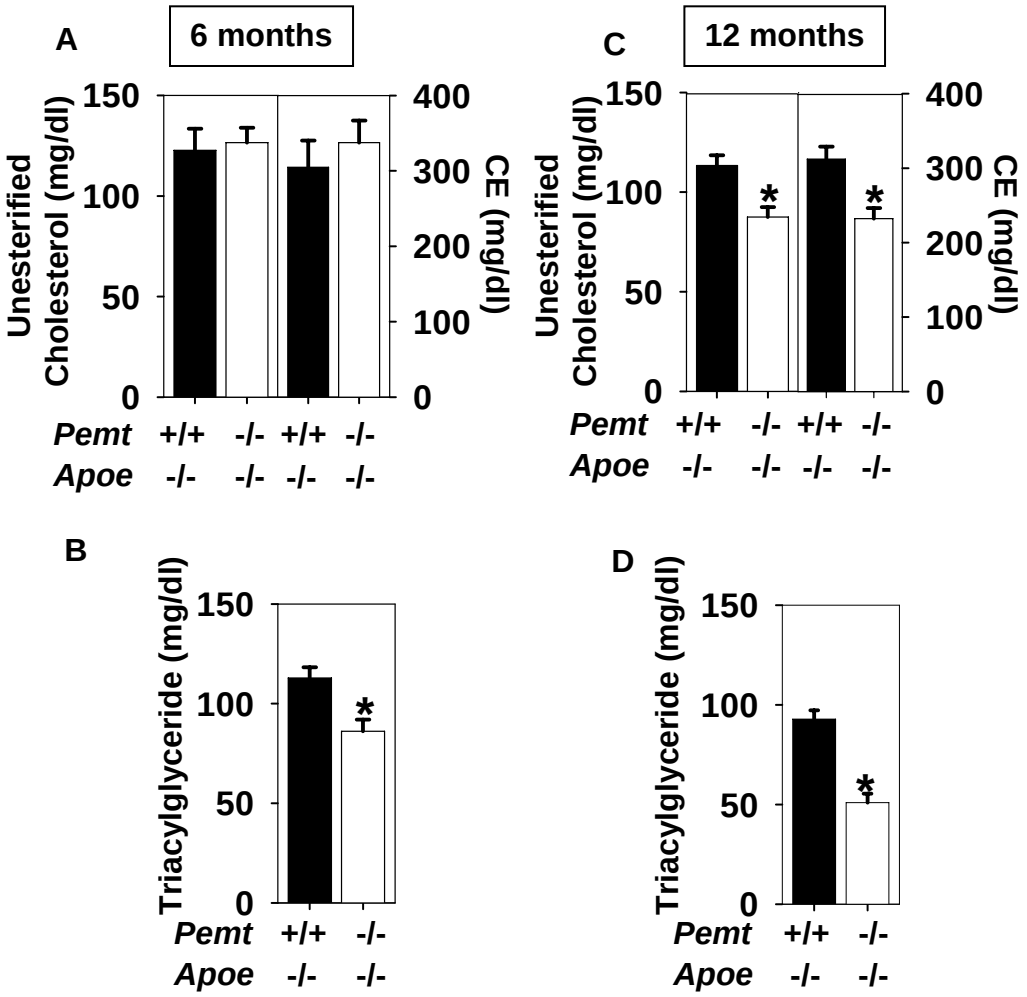
A
6 months
Unesterified Cholesterol (mg/dl)
CE (mg/dl)
150
100
50
0
400
300
200
100
0
Pemt +/+ -/- +/+ -/-
Apoe -/- -/- -/- -/-
C
12 months
Unesterified Cholesterol (mg/dl)
CE (mg/dl)
*
*
Pemt +/+ -/- +/+ -/-
Apoe -/- -/- -/- -/-
B
Triacylglyceride (mg/dl)
*
Pemt +/+ -/-
Apoe -/- -/-
D
Triacylglyceride (mg/dl)
*
Pemt +/+ -/-
Apoe -/- -/-

Figure 4.8. Lipoprotein protein profile of plasma from *Pemt*$^{+/+}$/*Apoe*$^{-/-}$ and *Pemt* $^{-/-}$/*Apoe*$^{-/-}$ mice.

Plasma lipoproteins from fasted *Pemt*$^{+/+}$/*Apoe*$^{-/-}$ (solid line) and *Pemt*$^{-/-}$/*Apoe*$^{-/-}$ (dotted line) were separated by gel filtration. Total cholesterol (unesterified + esterified), TG and choline-containing phospholipid concentrations were measured in each fraction from 6-month (**A, C**, and **E**) and 12-month old (**B, D,** and **F**) animals. Each curve represents mean values from 3-4 mice.

Figure 4.8

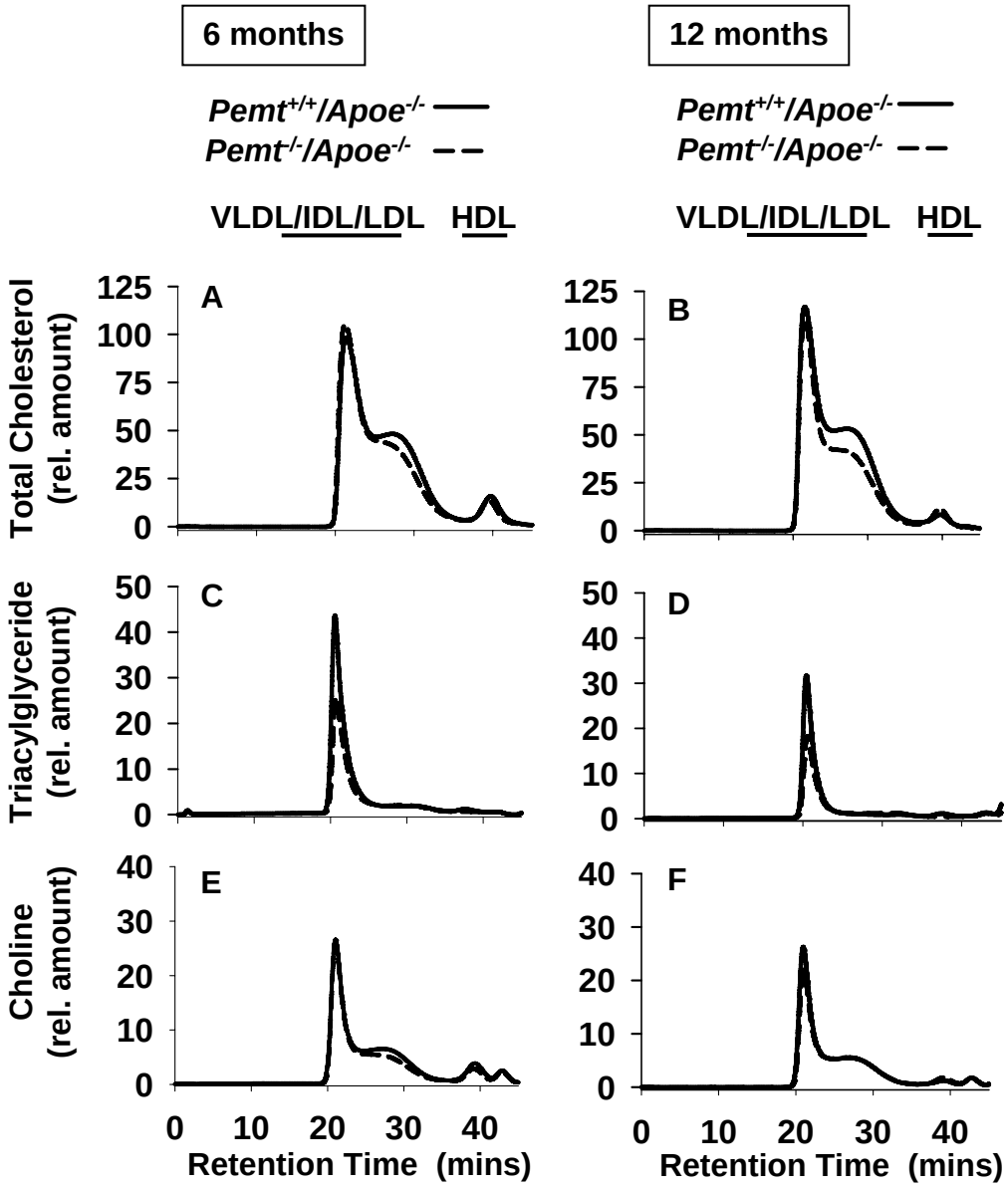
6 months
12 months
Pemt+/+/Apoe-/-
Pemt-/-/Apoe-/-
VLDL/IDL/LDL
HDL
Total Cholesterol (rel. amount)
Triacylglyceride (rel. amount)
Choline (rel. amount)
A
B
C
D
E
F
Retention Time (mins)

Figure 4.9. ApoB protein level of plasma from *Pemt*$^{+/+}$/*Apoe*$^{-/-}$ and *Pemt* $^{-/-}$ /*Apoe*$^{-/-}$ mice.

Plasma apoB (**A**) from fasted 12-month old mice was detected by immunoblot (upper panel). Proteins on the PVDF membrane were stained with Coomassie blue (lower panel). Numbers at left of lower panel indicate molecular mass (kDa). Protein levels of apoB 48 were quantitated by densitometry (**B**) and normalized against Coomassie blue stained protein. Data are expressed as means ± SEM (*, p<0.05, n = 3-4)

Figure 4.9

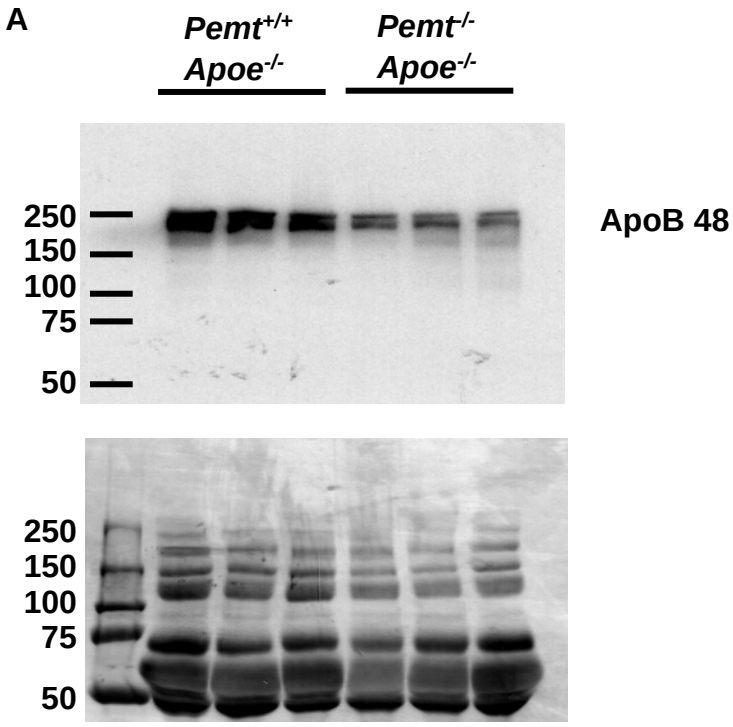
A
Pemt+/+
Apoe-/-
Pemt-/-
Apoe-/-
250
150
100
75
50
ApoB 48
250
150
100
75
50
B
ApoB 48
1.2
0.8
0.4
0.0
*
Pemt+/+
Apoe-/-
Pemt-/-
Apoe-/-

Figure 4.10. PL composition of plasma.

PL content was measured in plasma from fasted 6- (**A**) and 12-month old (**B**) *Pemt*$^{+/+}$*/Apoe*$^{-/-}$ (black bar) and *Pemt*$^{-/-}$*/Apoe*$^{-/-}$ (white bar) mice. Lipids were extracted from plasma (100 μl) and the amount of PC and PE were measured by phosphorus assay. Data are expressed as means ± SEM (*, $p<0.05$, 6-month animals n = 4-9, 12-month animals n = 6-11).

Figure 4.10

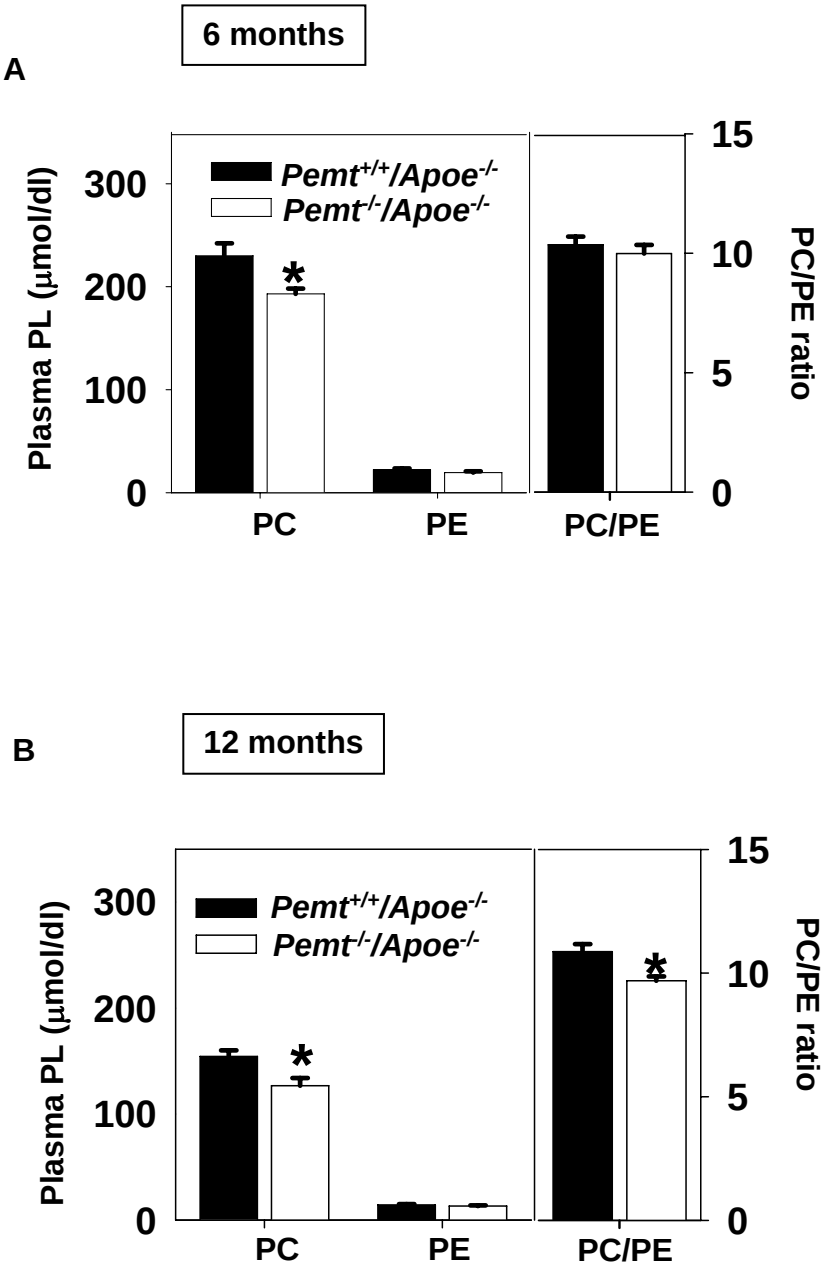
6 months
A
Pemt+/+/Apoe-/-
Pemt-/-/Apoe-/-
Plasma PL (μmol/dl)
300
200
100
0
15
10
5
0
PC/PE ratio
PC
PE
PC/PE
*
12 months
B
Pemt+/+/Apoe-/-
Pemt-/-/Apoe-/-
Plasma PL (μmol/dl)
300
200
100
0
15
10
5
0
PC/PE ratio
PC
PE
PC/PE
*
*

Figure 4.11. Reduced atherosclerotic lesions in 12-month old *Pemt*$^{-/-}$/*Apoe*$^{-/-}$ mice.

(**A)** Representative aortic roots sections from *Pemt*$^{+/+}$/*Apoe*$^{-/-}$ (upper panels) and *Pemt*$^{-/-}$/*Apoe*$^{-/-}$ (lower panels) 12-month old mice stained with Oil Red O (red) and hematoxylin (light blue). The scale bar represents 500 μm. (**B**) Representative *en face* preparations of aortas from *Pemt*$^{+/+}$/*Apoe*$^{-/-}$ (left panel) and *Pemt*$^{-/-}$/*Apoe*$^{-/-}$ (right panel) 12-month old mice stained with Sudan IV. (**C**) Quantification of lesion areas from Sudan IV stained aortas expressed as a percentage of total aortic surface area. Each point represents one mouse (*, $p<0.05$, n = 14-15). (**D**) Aortic cholesterol and CE content were measured in tissues obtained from 12-month old *Pemt* $^{+/+}$/*Apoe*$^{-/-}$ (black bar) and *Pemt*$^{-/-}$/*Apoe*$^{-/-}$ (white bar) mice. Data are expressed as means ± SEM (*, $p<0.05$, n = 7). (**E**) Aortic distensibility values for 10-month old *Pemt* $^{+/+}$/*Apoe*$^{-/-}$ (black bar) and *Pemt*$^{-/-}$/*Apoe*$^{-/-}$ (white bar) mice. Aortic distensibility was calculated using the equation (change in aortic diameter between systole and diastole)/ (diastolic aortic diameter) (pulse pressure). Data are expressed as means ± SEM (*, $p<0.05$, n = 9-10).

Figure 4.11

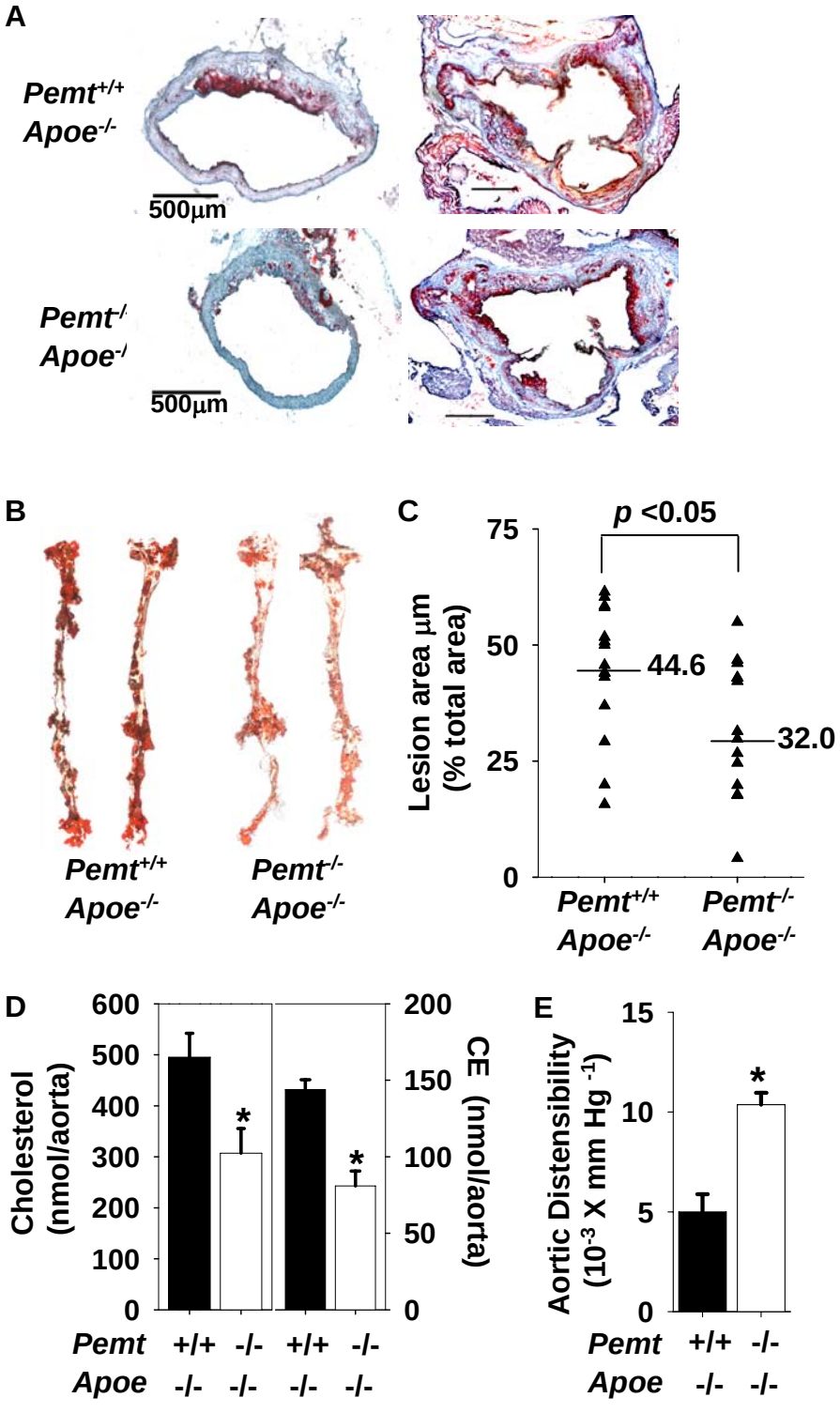
A
Pemt+/+
Apoe-/-
500μm
Pemt-/-
Apoe-/-
500μm
B
Pemt+/+
Apoe-/-
Pemt-/-
Apoe-/-
C
p <0.05
Lesion area μm
(% total area)
75
50
25
0
44.6
32.0
Pemt+/+
Apoe-/-
Pemt-/-
Apoe-/-
D
Cholesterol
(nmol/aorta)
600
500
400
300
200
100
0
CE (nmol/aorta)
200
150
100
50
0
*
*
Pemt +/+ -/- +/+ -/-
Apoe -/- -/- -/- -/-
E
Aortic Distensibility
(10-3 X mm Hg -1)
15
10
5
0
*
Pemt +/+ -/-
Apoe -/- -/-

Figure 4.12. PEMT deficiency improves age-dependent cardiac dysfunction.

Cardiac function was assessed in *Pemt*$^{+/+}$*/Apoe*$^{-/-}$ (black bars) and *Pemt*$^{-/-}$*/Apoe*$^{-/-}$ (white bars) mice at 10-months of age. Transthoracic echocardiography was performed to determine left ventricle internal dimension during diastole (LVIDd, **A**), and systole (LVIDs, **B**), isoventricular contraction time (IVCT, **C**), percentage ejection fraction (**D**) percentage fractional shortening (**E**) and myocardial performance index (**F**). Myocardial performance index is calculated using the equation (isovolumic contraction time + isovolumic relaxation time)/ejection time. Data are expressed as means ± SEM. (* $p<0.05$, n = 9-10).

Figure 4.12

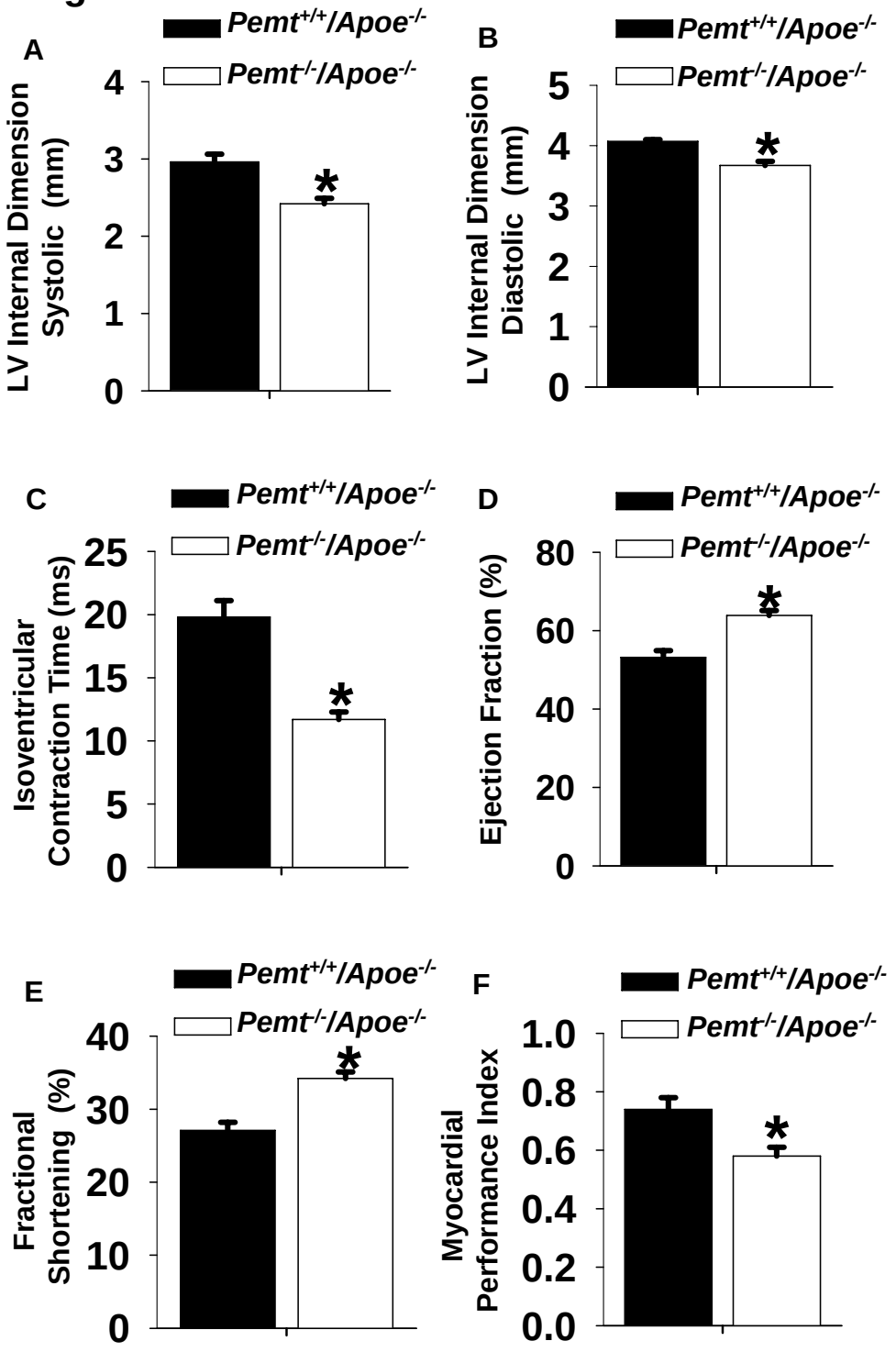
A
Pemt+/+/Apoe-/-
Pemt-/-/Apoe-/-
LV Internal Dimension Systolic (mm)
0
1
2
3
4
*
B
Pemt+/+/Apoe-/-
Pemt-/-/Apoe-/-
LV Internal Dimension Diastolic (mm)
0
1
2
3
4
5
*
C
Pemt+/+/Apoe-/-
Pemt-/-/Apoe-/-
Isoventricular Contraction Time (ms)
0
5
10
15
20
25
*
D
Pemt+/+/Apoe-/-
Pemt-/-/Apoe-/-
Ejection Fraction (%)
0
20
40
60
80
*
E
Pemt+/+/Apoe-/-
Pemt-/-/Apoe-/-
Fractional Shortening (%)
0
10
20
30
40
*
F
Pemt+/+/Apoe-/-
Pemt-/-/Apoe-/-
Myocardial Performance Index
0.0
0.2
0.4
0.6
0.8
1.0
*

Figure 4.13. PEMT deficiency decreases the severity of cardiac fibrosis and myofibril disorganization.

Representative cross-sections (5 μm) of hearts from *Pemt*$^{+/+}$*/Apoe*$^{-/-}$ (upper panels) and *Pemt*$^{-/-}$*/Apoe*$^{-/-}$ (lower panels) 12-month old mice stained for collagen (blue), muscle (red) and nuclei (black) with Masson's Trichrome. Cross-sections are representative of total cardiac fibrosis (**A, B**), endocardium fibrosis (**C, D**) and interstitial fibrosis **(E, F**). Magnifications: A and B 2.5X and C-F, 20X. Representative of 6 hearts per genotype. The scale bar represents the distance indicated (500 μm or 100 μm).

Figure 4.13

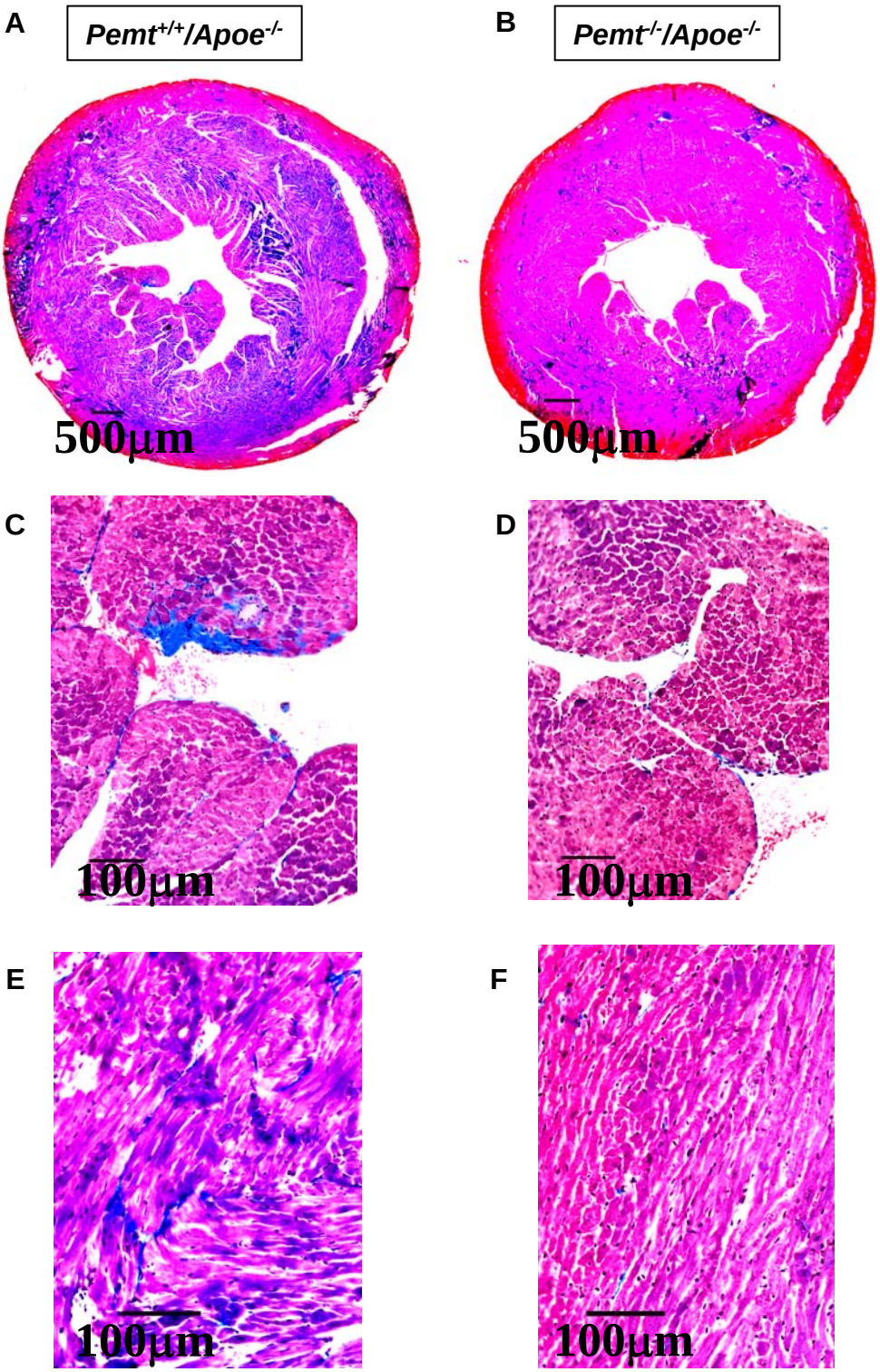
A
Pemt+/+/Apoe-/-
B
Pemt-/-/Apoe-/-
500µm
500µm
C
D
100µm
100µm
E
F
100µm
100µm

4.5 References

1. Glass, C. K., and Witztum, J. L. (2001) *Cell* **104**(4), 503-516
2. Davis, R. A., and Hui, T. Y. (2001) *Arteriosclerosis, thrombosis, and vascular biology* **21**(6), 887-898
3. Yao, Z. M., and Vance, D. E. (1989) *J Biol Chem* **264**(19), 11373-11380
4. Jacobs, R. L., Devlin, C., Tabas, I., and Vance, D. E. (2004) *J Biol Chem* **279**(45), 47402-47410
5. Vermeulen, P. S., Lingrell, S., Yao, Z., and Vance, D. E. (1997) *J Lipid Res* **38**(3), 447-458
6. Verkade, H. J., Fast, D. G., Rusinol, A. E., Scraba, D. G., and Vance, D. E. (1993) *J Biol Chem* **268**(33), 24990-24996
7. Zhao, Y., Su, B., Jacobs, R. L., Kennedy, B., Francis, G. A., Waddington, E., Brosnan, J. T., Vance, J. E., and Vance, D. E. (2009) *Arteriosclerosis, thrombosis, and vascular biology* **29**(9), 1349-1355
8. Zhao, Y., Su, B., Jacobs, R. L., Kennedy, B., Francis, G. A., Waddington, E., Brosnan, J. T., Vance, J. E., and Vance, D. E. (2009) *Arteriosclerosis, thrombosis, and vascular biology*
9. Vance, D. E., and Vance, J.E. . (2008) Phospholipid biosynthesis in eukaryotes. . In: Vance, D. E., Vance, J.E. (ed). *Biochemistry of Lipids, Lipoproteins and Membranes (5th Edn.)*, Elsevier B.V., San Diego, CA
10. Yao, Z. M., and Vance, D. E. (1990) *Biochem Cell Biol* **68**(2), 552-558
11. Yao, Z. M., and Vance, D. E. (1988) *J Biol Chem* **263**(6), 2998-3004

12. Fast, D. G., and Vance, D. E. (1995) *Biochim Biophys Acta* **1258**(2), 159-168

13. Vance, D. E., and Ridgway, N. D. (1988) *Prog Lipid Res* **27**(1), 61-79

14. Sundler, R., and Akesson, B. (1975) *J Biol Chem* **250**(9), 3359-3367

15. DeLong, C. J., Shen, Y. J., Thomas, M. J., and Cui, Z. (1999) *J Biol Chem* **274**(42), 29683-29688

16. Noga, A. A., and Vance, D. E. (2003) *J Biol Chem* **278**(24), 21851-21859

17. Noga, A. A., Zhao, Y., and Vance, D. E. (2002) *J Biol Chem* **277**(44), 42358-42365

18. Meir, K. S., and Leitersdorf, E. (2004) *Arteriosclerosis, thrombosis, and vascular biology* **24**(6), 1006-1014

19. Plump, A. S., and Breslow, J. L. (1995) *Annu Rev Nutr* **15**, 495-518

20. Reddick, R. L., Zhang, S. H., and Maeda, N. (1994) *Arterioscler Thromb* **14**(1), 141-147

21. Coleman, R., Hayek, T., Keidar, S., and Aviram, M. (2006) *Acta Histochem* **108**(6), 415-424

22. Onozuka, H., Fujii, S., Mikami, T., Yamada, S., Ishimori, N., Shimizu, T., Furumoto, T., Nakai, Y., Komuro, K., Nishihara, K., Okamoto, H., and Kitabatake, A. (2002) *Circ J* **66**(3), 272-276

23. Hartley, C. J., Reddy, A. K., Madala, S., Martin-McNulty, B., Vergona, R., Sullivan, M. E., Halks-Miller, M., Taffet, G. E., Michael, L. H., Entman, M. L., and Wang, Y. X. (2000) *Am J Physiol Heart Circ Physiol* **279**(5), H2326-2334

24. Walkey, C. J., Donohue, L. R., Bronson, R., Agellon, L. B., and Vance, D. E. (1997) *Proc Natl Acad Sci U S A* **94**(24), 12880-12885

25. Ordovas, J. M., and Osgood, D. (1998) *Methods Mol Biol* **110**, 105-111

26. Bligh, E. G., and Dyer, W. J. (1959) *Can J Biochem Physiol* **37**(8), 911-917

27. Lohninger, A., Preis, P., Linhart, L., Sommoggy, S. V., Landau, M., and Kaiser, E. (1990) *Anal Biochem* **186**(2), 243-250

28. Bartlett, G. R. (1959) *J Biol Chem* **234**(3), 469-471

29. Daugherty, A., and Whitman, S. C. (2003) *Methods Mol Biol* **209**, 293-309

30. Daugherty, A., and Rateri, D. L. (2005) *Methods* **36**(2), 129-138

31. O'Rourke, M. F., Staessen, J. A., Vlachopoulos, C., Duprez, D., and Plante, G. E. (2002) *American journal of hypertension* **15**(5), 426-444

32. Stacey, R. B., Bertoni, A. G., Eng, J., Bluemke, D. A., Hundley, W. G., and Herrington, D. *Hypertension* **55**(1), 26-32

33. Wilson, R. A., McDonald, R. W., Bristow, J. D., Cheitlin, M., Nauman, D., Massie, B., and Greenberg, B. (1992) *Journal of the American College of Cardiology* **19**(4), 733-738

34. Viollet, B., Guigas, B., Leclerc, J., Hebrard, S., Lantier, L., Mounier, R., Andreelli, F., and Foretz, M. (2009) *Acta Physiol (Oxf)* **196**(1), 81-98

35. Sul, H. S., Smith, S. (2008) Fatty acid synthesis in eukaryotes. In: Vance, D. E., Vance, J.E. (ed). *Biochemistry of lipid and lipoproteins (pp 155-190)*, 5 Ed., Elsevier, New York

36. Webb, N. R., de Beer, M. C., de Beer, F. C., and van der Westhuyzen, D. R. (2004) *J Lipid Res* **45**(2), 272-280

37. Ishibashi, S., Herz, J., Maeda, N., Goldstein, J. L., and Brown, M. S. (1994) *Proc Natl Acad Sci U S A* **91**(10), 4431-4435

38. Wu, K. K., Wu, T. J., Chin, J., Mitnaul, L. J., Hernandez, M., Cai, T. Q., Ren, N., Waters, M. G., Wright, S. D., and Cheng, K. (2005) *Atherosclerosis* **181**(2), 251-259

39. von Holt, K., Lebrun, S., Stinn, W., Conroy, L., Wallerath, T., and Schleef, R. (2009) *Atherosclerosis* **205**(1), 135-143

40. Wright, S. D., Burton, C., Hernandez, M., Hassing, H., Montenegro, J., Mundt, S., Patel, S., Card, D. J., Hermanowski-Vosatka, A., Bergstrom, J. D., Sparrow, C. P., Detmers, P. A., and Chao, Y. S. (2000) *J Exp Med* **191**(8), 1437-1442

41. Sparrow, C. P., Burton, C. A., Hernandez, M., Mundt, S., Hassing, H., Patel, S., Rosa, R., Hermanowski-Vosatka, A., Wang, P. R., Zhang, D., Peterson, L., Detmers, P. A., Chao, Y. S., and Wright, S. D. (2001) *Arteriosclerosis, thrombosis, and vascular biology* **21**(1), 115-121

42. Wang, Y. X., Halks-Miller, M., Vergona, R., Sullivan, M. E., Fitch, R., Mallari, C., Martin-McNulty, B., da Cunha, V., Freay, A., Rubanyi, G. M., and Kauser, K. (2000) *Am J Physiol Heart Circ Physiol* **278**(2), H428-434

43. Yang, R., Powell-Braxton, L., Ogaoawara, A. K., Dybdal, N., Bunting, S., Ohneda, O., and Jin, H. (1999) *Arteriosclerosis, thrombosis, and vascular biology* **19**(11), 2762-2768

44. Vincelette, J., Martin-McNulty, B., Vergona, R., Sullivan, M. E., and Wang, Y. X. (2006) *Transl Res* **148**(1), 30-36

45. Wikstrom, J., Gronros, J., and Gan, L. M. (2008) *Ultrasound Med Biol* **34**(7), 1053-1062

46. Johansson, M. E., Hagg, U., Wikstrom, J., Wickman, A., Bergstrom, G., and Gan, L. M. (2005) *Clin Sci (Lond)* **108**(6), 531-538

47. Dart, A. M., Lacombe, F., Yeoh, J. K., Cameron, J. D., Jennings, G. L., Laufer, E., and Esmore, D. S. (1991) *Lancet* **338**(8762), 270-273

48. van Popele, N. M., Grobbee, D. E., Bots, M. L., Asmar, R., Topouchian, J., Reneman, R. S., Hoeks, A. P., van der Kuip, D. A., Hofman, A., and Witteman, J. C. (2001) *Stroke; a journal of cerebral circulation* **32**(2), 454-460

49. Zieman, S. J., Melenovsky, V., and Kass, D. A. (2005) *Arterioscler Thromb Vasc Biol* **25**(5), 932-943

50. Bielecka-Dabrowa, A., Wierzbicka, M., Dabrowa, M., and Goch, A. (2008) *Cardiol J* **15**(4), 388-395

51. Stokman, P. J., Nandra, C. S., and Asinger, R. W. (2001) *Curr Treat Options Cardiovasc Med* **3**(6), 515-521

52. Herpel, E., Pritsch, M., Koch, A., Dengler, T. J., Schirmacher, P., and Schnabel, P. A. (2006) *Histopathology* **48**(6), 736-747

53. Lakatta, E. G., and Levy, D. (2003) *Circulation* **107**(1), 139-146

54. Gaddam, K. K., Verma, A., Thompson, M., Amin, R., and Ventura, H. (2009) *Med Clin North Am* **93**(3), 665-680

55. Olofsson, S. O., and Boren, J. (2005) *J Intern Med* **258**(5), 395-410

56. Adiels, M., Taskinen, M. R., Packard, C., Caslake, M. J., Soro-Paavonen, A., Westerbacka, J., Vehkavaara, S., Hakkinen, A., Olofsson, S. O., Yki-Jarvinen, H., and Boren, J. (2006) *Diabetologia* **49**(4), 755-765

57. Leon, C., Hill, J. S., and Wasan, K. M. (2005) *Pharm Res* **22**(10), 1578-1588

58. Karpe, F., Bickerton, A. S., Hodson, L., Fielding, B. A., Tan, G. D., and Frayn, K. N. (2007) *Biochem Soc Trans* **35**(Pt 3), 472-476

59. Zhu, X., Song, J., Mar, M. H., Edwards, L. J., and Zeisel, S. H. (2003) *Biochem J* **370**(Pt 3), 987-993

60. Wang, Y. X. (2005) *Neurobiol Aging* **26**(3), 309-316

61. Juan, F., Wei, D., Xiongzhi, Q., Ran, D., Chunmei, M., Lan, H., Chuan, Q., and Lianfeng, Z. (2008) *Int J Cardiol* **128**(1), 83-90

62. Du, J., Liu, J., Feng, H. Z., Hossain, M. M., Gobara, N., Zhang, C., Li, Y., Jean-Charles, P. Y., Jin, J. P., and Huang, X. P. (2008) *Am J Physiol Heart Circ Physiol* **294**(6), H2604-2613

63. Hinton, R. B., Jr., Alfieri, C. M., Witt, S. A., Glascock, B. J., Khoury, P. R., Benson, D. W., and Yutzey, K. E. (2008) *Am J Physiol Heart Circ Physiol* **294**(6), H2480-2488

64. Wilkinson, I. B., and Cockcroft, J. R. (1998) *Curr Opin Lipidol* **9**(3), 237-242

65. Herold, V., Wellen, J., Ziener, C. H., Weber, T., Hiller, K. H., Nordbeck, P., Rommel, E., Haase, A., Bauer, W. R., Jakob, P. M., and Sarkar, S. K. (2009) *Magma* **22**(3), 159-166

66. O'Rourke, M. F., and Nichols, W. W. (2005) *Hypertension* **45**(4), 652-658

67. Protogerou, A. D., Papaioannou, T. G., Blacher, J., Papamichael, C. M., Lekakis, J. P., and Safar, M. E. (2007) *J Hypertens* **25**(2), 265-272

68. Patrianakos, A. P., Parthenakis, F. I., Karakitsos, D., Nyktari, E., and Vardas, P. E. (2009) *Eur J Echocardiogr* **10**(3), 425-432

69. Blacher, J., Safar, M. E., Pannier, B., Guerin, A. P., Marchais, S. J., and London, G. M. (2002) *Curr Opin Nephrol Hypertens* **11**(6), 629-634

70. Blacher, J., Safar, M. E., Guerin, A. P., Pannier, B., Marchais, S. J., and London, G. M. (2003) *Kidney Int* **63**(5), 1852-1860

71. Lim, H. E., Park, C. G., Shin, S. H., Ahn, J. C., Seo, H. S., and Oh, D. J. (2004) *Blood Press* **13**(6), 369-375

72. Sutton-Tyrrell, K., Najjar, S. S., Boudreau, R. M., Venkitachalam, L., Kupelian, V., Simonsick, E. M., Havlik, R., Lakatta, E. G., Spurgeon, H., Kritchevsky, S., Pahor, M., Bauer, D., and Newman, A. (2005) *Circulation* **111**(25), 3384-3390

73. Lartaud-Idjouadiene, I., Lompre, A. M., Kieffer, P., Colas, T., and Atkinson, J. (1999) *Hypertension* **34**(1), 63-69

74. Hironaka, K., Yano, M., Kohno, M., Tanigawa, T., Obayashi, M., Konishi, M., Umemoto, S., and Matsuzaki, M. (1997) *Am J Physiol* **273**(3 Pt 2), H1142-1147

75. Hiromoto, M., Toma, Y., Tomochika, Y., Umemoto, S., and Matsuzaki, M. (1996) *Jpn Circ J* **60**(9), 691-698

76. Dalessandri, K. M., Bogren, H., Lantz, B. M., Tsukamoto, H., Bjorkerud, S., and Brock, J. (1990) *J Invest Surg* **3**(3), 245-251

77. Massberg, S., Brand, K., Gruner, S., Page, S., Muller, E., Muller, I., Bergmeier, W., Richter, T., Lorenz, M., Konrad, I., Nieswandt, B., and Gawaz, M. (2002) *J Exp Med* **196**(7), 887-896

Chapter 5

Summary and Future Directions

5.1 Conclusions

Significant advances have been made recently in identifying the physiological roles of PE methylation. PC derived from PEMT has been shown to contribute to hepatic lipid metabolism and lipoprotein secretion (1-4). The physiological importance of PEMT has been recently underscored in *Pemt*$^{-/-}$ mice which develop NAFLD (1,5) and are protected from cardiovascular disease (3). The experiments outlined in this thesis represent an attempt to identify factors which regulate *Pemt* gene expression and to further understand the contribution of PE methylation in the progression of liver and heart disease.

In our main study we identified 3T3-L1 adipocytes as an appropriate cell culture model for studying the expression of the mouse *Pemt* gene. This was based on the endogenous expression of both PEMT mRNA and protein when the 3T3-L1 fibroblasts were differentiated to adipocytes. Using classical promoter analysis techniques we determined that the -471 to +130 bp region of the mouse *Pemt* promoter contained important regulatory sites. One of these sites was identified as a Sp1 binding element. Sp1 binding to the *Pemt* promoter was inversely correlated with promoter activity. We also used RNA silencing and recombinant cDNA strategies to confirm that Sp1 was acting as a transcriptional repressor of *Pemt* gene expression in 3T3-L1 adipocytes. In addition, to being the first comprehensive investigation of regulatory

elements within the mouse *Pemt* promoter, this study prompted the re-examination of *Pemt* expression in adipose tissue. The physiological role of PEMT in adipose tissue is currently being investigated (Steyrer, E., personal communication)

The Sp1-mediated repression of *Pemt* transcription represents a mechanism where by gene expression can be regulated in the liver. We demonstrated that treatment with tamoxifen, an estrogen receptor modulator, decreased the hepatic level of PEMT mRNA, protein and activity in mice. The tamoxifen-induced decrease in *Pemt* promoter activity required the Sp1 binding site and increased Sp1 protein at the *Pemt* promoter.

Although we demonstrated that *Pemt* gene expression was repressed by Sp1, the contribution of additional regulatory proteins remains to be elucidated. Future studies should focus on identifying Sp1 binding partners as well as additional transcription factor binding sites within the mouse *Pemt* promoter. Additional studies are also required to determine the mechanism by which tamoxifen is reducing *Pemt* promoter activity. For example, to determine whether tamoxifen promotes direct physical interaction between Sp1 and the estrogen receptor and/or with some other nuclear factor(s). Since it was previously shown that estrogen treatment increases hepatic PEMT mRNA levels (6), it would be of interest to determine whether it is also mediated by Sp1.

Once, the repressive effect of tamoxifen on *Pemt* gene expression was identified, we attempted to characterize the role of PEMT during tamoxifen-induced hepatic steatosis. The absence of PEMT in mice has resulted in reduced secretion of VLDL-TG from the liver and hence the subsequent accumulation of hepatic TG (2,3,7). However, we determined that the reduction in PEMT activity does not contribute to tamoxifen-mediated hepatic steatosis in mice. Instead the repression of PEMT may reduce plasma HDL-cholesterol. In support of this hypothesis, preliminary studies demonstrated that tamoxifen does not reduce plasma HDL-cholesterol in *Pemt*$^{-/-}$ mice. These studies could be expanded by determining whether this effect is mediated directly by tamoxifen or indirectly via the inhibition of PEMT activity.

Incubation of primary cultures of hepatocytes with radio-labelled lipid precursors revealed that tamoxifen-treatment elevated *de novo* fatty acid synthesis. This was due to reduced phosphorylation and thus elevated activity of the rate-limiting enzyme in fatty acid synthesis, ACC. Although we determined that tamoxifen-treatment decreased the activity of the upstream kinase, AMPK, the specific mechanism remains to be identified. Initial studies in this area may focus on identifying the specific cell signalling pathway(s) activated in the liver by tamoxifen.

To gain insight into the role of PEMT in the progression of cardiac dysfunction we generated *Pemt*$^{-/-}$/*Apoe*$^{-/-}$ mice. Previous studies revealed

that the absence of PEMT is cardioprotective. This conclusion was based on dramatic reductions in atherosclerotic lesions in *Pemt*$^{-/-}$/*Ldlr*$^{-/-}$ mice compared to *Pemt*$^{+/+}$/*Ldlr*$^{-/-}$ controls (3). Currently, there is no evidence that *Ldlr*$^{-/-}$ mice develop changes in heart function as a result of hypercholesterolemia. In contrast, several groups have demonstrated age-dependent cardiac dysfunction in the *Apoe*$^{-/-}$ mouse (8-12). We demonstrated that the absence of PEMT reduced aortic atherosclerotic plaque formation and prevented the development of dilated cardiomyopathy in aged apoE null mice. Specifically, the absence of PEMT improved cardiac function by 50% compared to age-matched *Apoe*$^{-/-}$ controls.

Our investigation was the first to demonstrate that the absence of PEMT protects against heart dysfunction. A series of experiments should be conducted to further characterize the cardio-protective effect generated in *Pemt*$^{-/-}$*/Apoe*$^{-/-}$ mice. For example, heart function could be assessed in *Pemt*$^{+/+}$*/Apoe*$^{-/-}$ and *Pemt*$^{-/-}$*/Apoe*$^{-/-}$ mice following nutritional and physical challenges including dietary (high-fat diet, high-protein diet), exercise and *in vivo* occlusion of coronary arteries. This would provide additional insight into the mechanism involved and the specific conditions in which inhibition of PEMT may be suitable as a drug target.

This study was also the first to indicate that the absence of PEMT can significantly reduce hepatic TG levels. This is important since

reductions in the level of PC (PC/PE ratio) in the liver have been linked to hepatic steatosis and the progression to steatohepatitis (1,2) (Jacobs, R., unpublished results). Thus, our study provides a model in which targeted inhibition of PEMT could be advantageous for the prevention of both heart and liver diseases.

In our current study the decrease in hepatic TG and CE levels in the *Pemt*$^{-/-}$/*Apoe*$^{-/-}$ mice are likely due to reduced fatty acid and cholesterol synthesis respectively. However, it is unclear why the absence of PEMT reduces hepatic TG in *Apoe*$^{-/-}$ mice and not other mouse models. It is known that hepatic lipid metabolism is altered in the absence of apoE (13,14). Future initial studies should identify the differences in hepatic lipid metabolism and trafficking between the *Pemt*$^{-/-}$/*Apoe*$^{-/-}$ and *Pemt*$^{+/+}$/*Apoe*$^{-/-}$ animals. However, the majority of work in this field should focus on determining the link between PEMT-derived PC and energy metabolism in the liver. Recent preliminary studies in *Pemt*$^{-/-}$ mice have demonstrated that the exchange of information between the brain and liver (via the vagus nerve) regulates hepatic lipid metabolism (Jacobs, R., unpublished data). These experiments should be expanded to include the Apoe$^{-/-}$ mouse model and determining the link between PC metabolism and AMPK activity.

In conclusion, this thesis describes the first comprehensive investigation of regulatory regions involved in *Pemt* gene expression.

Furthermore, we have made significant developments in understanding the physiological role of PEMT in the progression of heart disease. These studies should provide a platform to identify nuclear factors which link *Pemt* gene expression with hepatic lipid metabolism and energy utilization.

5.2 References

1. Li, Z., Agellon, L. B., Allen, T. M., Umeda, M., Jewell, L., Mason, A., and Vance, D. E. (2006) *Cell metabolism* **3**(5), 321-331
2. Noga, A. A., and Vance, D. E. (2003) *The Journal of biological chemistry* **278**(24), 21851-21859
3. Zhao, Y., Su, B., Jacobs, R. L., Kennedy, B., Francis, G. A., Waddington, E., Brosnan, J. T., Vance, J. E., and Vance, D. E. (2009) *Arteriosclerosis, thrombosis, and vascular biology* **29**(9), 1349-1355
4. Robichaud, J. C., Francis, G. A., and Vance, D. E. (2008) *The Journal of biological chemistry* **283**(51), 35496-35506
5. Walkey, C. J. (1998) Evolutionary and nutritional importance of phospholipid methylation. In. *Biochemistry*, University of Alberta, Edmonton
6. Resseguie, M., Song, J., Niculescu, M. D., da Costa, K. A., Randall, T. A., and Zeisel, S. H. (2007) *Faseb J* **21**(10), 2622-2632
7. Noga, A. A., Zhao, Y., and Vance, D. E. (2002) *The Journal of biological chemistry* **277**(44), 42358-42365
8. Onozuka, H., Fujii, S., Mikami, T., Yamada, S., Ishimori, N., Shimizu, T., Furumoto, T., Nakai, Y., Komuro, K., Nishihara, K., Okamoto, H., and Kitabatake, A. (2002) *Circ J* **66**(3), 272-276
9. Wang, Y. X., Halks-Miller, M., Vergona, R., Sullivan, M. E., Fitch, R., Mallari, C., Martin-McNulty, B., da Cunha, V., Freay, A.,

Rubanyi, G. M., and Kauser, K. (2000) *American journal of physiology* **278**(2), H428-434

10. Wang, Y. X. (2005) *Neurobiology of aging* **26**(3), 309-316
11. Hartley, C. J., Reddy, A. K., Madala, S., Martin-McNulty, B., Vergona, R., Sullivan, M. E., Halks-Miller, M., Taffet, G. E., Michael, L. H., Entman, M. L., and Wang, Y. X. (2000) *American journal of physiology* **279**(5), H2326-2334
12. Herold, V., Wellen, J., Ziener, C. H., Weber, T., Hiller, K. H., Nordbeck, P., Rommel, E., Haase, A., Bauer, W. R., Jakob, P. M., and Sarkar, S. K. (2009) *Magma (New York, N.Y* **22**(3), 159-166
13. Mensenkamp, A. R., Jong, M. C., van Goor, H., van Luyn, M. J., Bloks, V., Havinga, R., Voshol, P. J., Hofker, M. H., van Dijk, K. W., Havekes, L. M., and Kuipers, F. (1999) *The Journal of biological chemistry* **274**(50), 35711-35718
14. Mensenkamp, A. R., Van Luyn, M. J., Havinga, R., Teusink, B., Waterman, I. J., Mann, C. J., Elzinga, B. M., Verkade, H. J., Zammit, V. A., Havekes, L. M., Shoulders, C. C., and Kuipers, F. (2004) *Journal of hepatology* **40**(4), 599-606